Emergent Matter of Quantum Geometry

by

Yidun Wan

A thesis
presented to the University of Waterloo
in fulfillment of the
thesis requirement for the degree of
Doctor of Philosophy
in
Physics

Waterloo, Ontario, Canada, 2009

AUTHOR'S DECLARATION

I hereby declare that I am the sole author of this thesis. This is a true copy of the thesis, including any required final revisions, as accepted by my examiners.

I understand that my thesis may be made electronically available to the public.

Abstract

This thesis studies matter emergent as topological excitations of quantum geometry in quantum gravity models. In these models, states are framed four-valent spin networks embedded in a topological three manifold, and the local evolution moves are dual Pachner moves.

We first formulate our theory of embedded framed four-valent spin networks by proposing a new graphic calculus of these networks. With this graphic calculus, we study the equivalence classes and the evolution of these networks, and find what we call 3-strand braids, as topological excitations of embedded four-valent spin networks. Each 3-strand braid consists of two nodes that share three edges that may or may not be braided and twisted. The twists happen to be in units of 1/3. Under certain stability condition, some 3-strand braids are stable.

Stable braids have rich dynamics encoded in our theory by dual Pachner moves. Firstly, all stable braids can propagate as induced by the expansion and contraction of other regions of their host spin network under evolution. Some braids can also propagate actively, in the sense that they can exchange places with substructures adjacent to them in the graph under the local evolution moves. Secondly, two adjacent braids may have a direct interaction: they merge under the evolution moves to form a new braid if one of them falls into a class called actively interacting braids. The reverse of a direct interaction may happen too, through which a braid decays to another braid by emitting an actively interacting braid. Thirdly, two neighboring braids may exchange a virtual actively interacting braid and become two different braids, in what is called an exchange interaction. Braid dynamics implies an analogue between actively interacting braids and bosons.

We also invent a novel algebraic formalism for stable braids. With this new tool, we derive conservation laws from interactions of the braid excitations of spin networks. We show that actively interacting braids form a noncommutative algebra under direction interaction. Each actively interacting braid also behaves like a morphism on non-actively interacting braids. These findings reinforce the analogue between actively interacting braids and bosons.

Another important discovery is that stable braids admit seven, and only seven, discrete transformations that uniquely correspond to analogues of C, P, T, and their products. Along with this finding, a braid's electric charge appears to be a function of a conserved quantity, effective twist, of the braids, and thus is quantized in units of 1/3. In addition, each CPT-multiplet of actively interacting braids has a unique, characteristic non-negative integer. Braid interactions turn out to be invariant under C, P, and T.

Finally, we present an effective description, based on Feynman diagrams, of braid dynamics. This language manifests the analogue between actively interacting braids and bosons, as the topological conservation laws permit them to be singly created and destroyed and as exchanges of these excitations give rise to interactions between braids that are charged under the topological conservation rules. Additionally, we find a constraint on probability amplitudes of braid interactions.

We discuss some subtleties, open issues, future directions, and work in progress at the end.

Acknowledgements

I am afraid that I can express my gratitude to just a few people of those who helped me in my 24 years of student life to obtain two Bachelor's, two Master's, and this PhD.

I first thank my parents, whose role in my education and life can never be overstated. My father, Renhui Wan, had a complex educational and professional background because of the war and instable political and economical circumstances in China during his childhood and juvenile years; however, his talent and persistence eventually led him to what he now is: an artist and connoisseur of Chinese cultural relics. Not only did he try his best to provide me a perfect environment to grow up and learn in, but also fostered all my extracurricular interests. My mother, Huarong Wang, is a wise woman. Movingly, she sacrificed her youth but used her wisdom to help her husband and children. My parents taught me a lot, in particular how to be an upright person. It is impossible to list here all that they have given to me, but I would like to thank them for their appreciation of my choice to be a physicist. Being traditional Chinese parents and because of their own life experience, they made a plan for my life and career. Therefore, it appeared an abrupt change to them when they heard that I had switched to physics after I obtained my Master's in Computer Science. Nonetheless, not only did they accept it, but also soon became excited and delighted about every one of my ideas, discoveries, and publications, although they did not understand any of them. This warm support full of love from the other side of the earth is an indispensable force propelling me to my PhD.

Another propelling force is the support from my wife, Zheng He. Zheng was a pharmacist in China. We met in the U.S., got married there, and then moved to Canada. To fully support me, she sacrificed her own career after having gone to graduate school at the University of Ottawa. My Research often drags me away from my family responsibilities; however, she has always been supportive and forbearing, which always touches me. Without a bit of complaint, she has drifted with me from Philadelphia to Ottawa, to Waterloo, and then to our next stop, Osaka, in the past eight years, and will probably keep drifting around the world. Words cannot describe my gratitude for her support and love. I know I do owe her a stable home. I also thank my son, Yitong, who was born in my most difficult year since I left China. He is still too young to understand how much excitement, happiness, color, and peace he has brought to me. He always tries his best not to interrupt me when he sees me working, which makes me guilty for having spent just a little time with him. To him I owe a lot too.

Chronologically, I now thank Mrs. Hongjun Zhao, my math teacher at junior high school. Honestly, my math scores were not good at all in my first high school year before she became my teacher. Magically, however, she foresaw that I would be good at math and selected me as the representative of math[1] for her class. It was she who first stimulated my talent in mathematics which eventually made me capable of doing theoretical physics. The other high school teachers I am grateful to are Mr. He Chen and Mr. De Pan, who taught me Mathematics and English. I also owe my gratitude to Prof. Shiqin Zhong at the South China University of Technology, where

---

[1]This was a typical Chinese thing. For each curricular course, a student, normally the best in a class, is selected by the teacher as the representative, with responsibilities for collecting/distributing assignments, assisting the teacher with marking, tutoring weaker students, etc.

Dedication

To my dearest *Zheng, Yitong, Yiqian, and parents*.
&
To my esteemed and beloved *grandmother* in Sukhavati.

Contents

List of Tables

List of Figures

Chapter 1

Introduction

1.1 An Invitation to emergent matter of quantum geometry[1]

What is space-time? What is matter? Physicists and philosophers have obsessed over these questions for centuries. In fact, an ultimate goal of modern physics is to find a unified answer for both questions. Although physicists have made numerous attempts, they are still far from the final answer. In this thesis, we are going to study a novel approach towards emergent matter degrees of freedom as topological excitations of quantum geometry, given several ansatzes inspired by background independent quantum gravity theories - in particular Loop Quantum Gravity.

The idea that matter is topological defects of space-time is an old dream that dates back to more than a century ago when Lord Kelvin proposed that atoms were knots in ether[1]. Kelvin's proposal failed due to its flawed setting and especially the limited knowledge people had about our universe at that time. Nevertheless, this dream was implanted in physicists thereafter. Various proposals of topological matter have arisen as physicists deepen and broaden their recognition of nature. An example is the topological Geon model due to Wheeler and others[2–6], but geons in this model were unstable and classical. To make stable geons[3], Finkelstein invented the notion of topological conservation laws that led to advances in condensed matter physics, e.g., topologically conserved excitations in $1 + 1$ condensed matter models such as sine-Gordon theory. Finkelstein's idea was not compatible with quantum gravity until the recent work by Markopoulou *et al.*[7–9] that motivated the work described in this thesis.

Analogously, certain condensed matter systems have quasi-particles as collective modes, e.g., phonons and rotons in superfluid He^4. A recent example in condensed matter physics is a unification scheme due to Wen, *et al.*[10, 11], where gauge theories and gravity[2] appear to be low energy effective descriptions of a new phase, the string-net condensate of lattice spin systems.

A main motivation of our approach in this thesis is also a topological matter model, the Helon model, proposed by Bilson-Thompson[12]. The Helon model, based on the Preon Model[13, 14],

---

[1]Here, by emergent we mean coexisting quantum geometry and matter because our approach will show that under certain ansatzes, a consistent theory of quantum gravity may automatically encodes matter degrees of freedom as topological excitations of the quantum geometry described by the theory.

[2]One should note that when we say gravity here we mean linearized gravity, not full Einstein gravity.

is more elementary than the Standard Model of elementary particles by interpreting the elementary particles as braids of three ribbons. In the Helon model, the integral twists of ribbons of braids give rise to the quantized electric charges of particles; the crossings of certain braids naturally account for the color charges of quarks and gluons. This model also has a nice scheme of the color interaction and the electro-weak interaction with lepton and baryon number manifestly conserved. It also explains why elementary particles fall into different generations. Nevertheless, this model has many issues as summarized in [12]. Most seriously, it lacks a formal theoretical framework that can promote it from a combinatoric game to a rigorous theory.

More recently, Markopoulou and Smolin noticed the possibility to realize the Helon model in certain background independent Quantum Gravity models such as Loop Quantum Gravity and Spin Foam models. They, together with Bilson-Thompson, then started to work on this possibility in [15] by identifying helons with emergent topological excitations of embedded spin networks that label the states in Loop Quantum Gravity. This brings us a new perspective: instead of promoting the Helon model to another theory of particles at merely a more elementary level, one can encode it in Loop Quantum Gravity and Spin Foam models to make a theory of both space-time and matter. In this setting, matter is emergent from, or more precisely, coexisting with, quantum space-time, and the corresponding low energy effective theories may give rise to general relativity coupled with quantum fields. To appreciate this, one needs to understand two other notions, namely spin networks and noiseless subsystems.

Let us briefly introduce the notion of noiseless subsystems first. Noiseless subsystems were first proposed in quantum information and computation for quantum error correction[16–19]. Noiseless subsystems are, in short, subsets of states of a quantum system that are protected from the evolution algebra of the system, and hence from any error in the algebra. Markopoulou *et al.*[8, 20, 21] first adopted the methods of noiseless subsystems in their attempt to resolve the issue of the low energy limit in background independent quantum gravity theories.

We pause to say a bit about background independence, on which [22] is a good review. A background independent theory is independent of the geometry of a background space-time. General Relativity is itself background independent, or in mathematical language, diffeomorphism invariant. This then naturally requires a consistent quantum theory of gravity to be background independent as well. Loop Quantum Gravity and Spin Foam Models[3] are two main background independent theories of quantum gravity. Other background independent approaches like Causal Dynamical Triangulations and Causal Sets are respectively reviewed in [23] and in [24, 25]. On the contrary, the Standard Model of elementary particles, a triumph of quantum physics, is defined in fixed flat space-time, and does not contain the gravitational interaction. The Standard Model is not a fundamental theory owing to its numerous free parameters and its lack of gravity. Therefore, if one is looking for a physical unification of gravity and matter, one should formulate the theory in a background independent way[4].

---

[3]In fact, Spin Foam models were first constructed as a covariant (path integral) formulation of Loop Quantum Gravity, but then became a rather independent approach.

[4]The community of theoretical physics has not agreed on how to interpret background independence. For example, String Theory, a major candidate for the theory of everything, has different interpretations of background independence (e.g., [26, 27]), which are still under debate (e.g., [22, 28]).

Nonetheless, background independence makes it difficult to take the low energy limit of a background independent theory of quantum gravity[9]. There have been different attempts in different approaches of quantum gravity. In Loop Quantum Gravity, [29–32] use methods of coherent states, which are, according to quantum physics, the quantum states closest to classical ones. In Spin Foam models, attempts using n-point correlations functions are made in[33–37], which is reasonable because all semiclassical observable are either correlation functions or their derivatives. The problem of the low energy limit remains a key open issue of quantum gravity with background independence, however. In view of this, Markopoulou and Kribs[8, 9, 20] proposed a new way to resolve this issue by looking for conserved quantities in background independent theories of gravity. Since the aforementioned noiseless subsystems are conserved states under the evolution algebra of a quantum system, there should be conserved quantities associated with them. This is why one can adapt the method of noiseless subsystems to find conserved quantities of quantum geometry in a large class of background independent theories.

The first application of noiseless subsystems in Loop Quantum Gravity[21] helps to explain the black hole entropy and how symmetries can emerge from a diffeomorphism invariant formulation of quantum gravity. Further efforts[15, 38, 39] to find conserved quantities in Loop Quantum Gravity and related models by noiseless subsystems have been fruitful. As mentioned, noiseless substructures of embedded 3-valent spin networks, which represent quantum geometry, appear to encode the helons in models of quantum gravity such as Loop Quantum Gravity. These noiseless substructures are braids whose associated conserved quantities are called reduced link invariants[15]. [39] even gives a mapping between some of these braids and the Standard Model particles. In Section 1.4, we will address the limitations of these discoveries. These limitations partly motivate [40–45], on which this thesis is based. We will come back to this point later.

1.2 Three Ansatz

The physical facts and observations introduced in the previous section encourage the author of the thesis to work towards a unification scheme in which matter emerges as topological excitations of the fundamental structure of space-time. It turns out that the results to be described in the thesis are based on the following three ansatz.

1. Space-time is pre-geometric and discrete at the fundamental scale.

2. A discrete space is represented by a set of framed, labeled graphs, embedded in a differential manifold. These graphs label orthonormal basis states of the discrete space.

3. These graphs evolve under a set of local moves.

Several remarks are in order. The first remark is that these ansatz do not assume a space-time dimension, such that one is free to work with any space-time dimension. Nevertheless, in this thesis we consider only 4-dimensional space-time that admits a (3+1)-foliation, which is consistent with our observable universe. These ansatz are essentially inspired by Penrose's idea and Loop Quantum Gravity and related theories, such as Spin Foam models, path integral formulations of

Loop Quantum Gravity. The framed, labeled graphs are what we call spin networks, to be defined shortly. These graphs evolve under a set of local moves, called adapted dual Pachner moves, which are generalized from the dual Pachner moves from Spin Foam models, which usually consider unembedded spin networks, to account for the embedding of our spin networks. Our spin networks and their evolution are different from those in Penrose's proposal and those in Loop Quantum Gravity and Spin Foam models in several respects. We shall address these these differences in more details, along with a brief introduction to spin networks in the next section. We hope that classical space-time would exist as certain limit of the pre-geometric history of the evolution of these graphs.

1.3   Spin networks

Penrose first invented spin networks as a fundamental discrete description of space-time[46, 47]; later, Rovelli and Smolin found a more generalized version of spin networks to label the states in Loop Quantum Gravity Hilbert space[48]. Although the context of spin networks in this thesis is mainly Loop Quantum Gravity and its path integral formulation, Spin Foam models, it will become clear that our results do not really depend on these models but find their natural home in the original proposal of spin networks[5], with the notion generalized.

1.3.1   Penrose's spin networks

Penrose proposed spin networks by noticing the fundamental incompatibility between General Relativity and Quantum Physics, the problem of the concept of continuum, and the divergences in quantum field theories. Penrose thinks that a discrete notion of space-time at and below the Planck scale is demanded to resolve this funamental incompatibility. In this new notion of space-time, the classical notion of space-time is no longer valid at the Planck level. As a consequence, the concept of time and space gives way to a more fundamental one - relation - which is the microscopic causal relation between quantum events[6]. According to quantum physics, the intrinsic, characteristic quantity of a quantum system, which also connects to space-time, is spin, or angular momentum. In view of this, Penrose uses combinatoric graphs, consisting of lines intersecting at vertices, to represent the fundamental states of space-time. Each line in a graph is labeled by a spin, an integer or half integer. Hence, such a graph is called a spin network. Later on, it was shown in [50] that the classical 3-dimensional angles of space can be recovered from 3-valent spin networks. Note that these spin networks are unembedded.

[46, 47] have all the details about Penrose's original proposal of spin networks. We now introduce a generalized version of spin networks that will be used in this thesis. An important remark is that Penrose's spin networks are a direct construction of fundamental quantum space-time, rather than obtained from quantizing space-time or General Relativity by any means. Nev-

---

[5]Note that Penrose's spin networks are unembedded, while those in Loop Quantum Gravity are embedded.

[6]The underlying philosophy is relationalism, as opposed to reductionism. [22, 28, 49] have review sections on it.

ertheless, the spin networks in Loop Quantum Gravity follows from quantizing General Relativity non-perturbatively.

1.3.2 Spin networks from Loop Quantum Gravity

Loop Quantum Gravity is a non-perturbative canonical quantization of General Relativity[7]. The background independence of General Relativity actually does not leave any room for perturbative quantization[22, 49, 51, 52]. Being a canonical background independent quantization of gravity, Loop Quantum Gravity assumes a $(d+1)$-dimensional differential manifold M, without metric but merely a differential structure with a Lie algebra[8] valued connection 1-form field; M is assumed to admit a foliation $M = \Sigma \times R$, where Σ is d-dimensional. For simplicity we take $d = 3$.

Because this thesis does not depend on any specific techniques and results of Loop Quantum Gravity but is only inspired by them, we do not review the technical settings and quantization procedure in Loop Quantum Gravity, which are nicely introduced in [32, 49].

In Loop Quantum Gravity, the states are graphs embedded in Σ with edges meeting on vertices (Fig. 1.1 shows a portion of a generic spin network). These edges are flux lines. Each edge e is labeled by an irreducible representation j_e of a Lie group (usually $SU(2)$ or $SO(3)$), and each vertex is labeled by an intertwiner that is the tensor product, invariant under gauge transformations, of the labels of the edges meeting at the vertex. The label on an edge determines the area quanta of the surface element intersecting the edge. The intertwiner on a vertex determines the volume quota of the region containing only the vertex. These graphs are called spin networks.
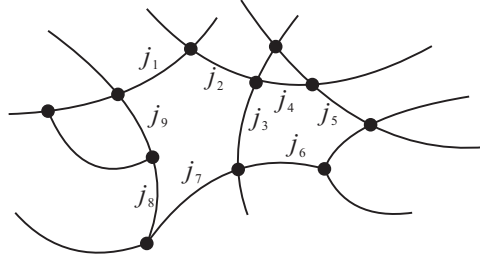
Figure 1.1: A portion of a generic spin network. Labels on nodes and some of the edges are neglected for simplicity.

Loop Quantum Gravity has produced many physical results, which are extensively reviewed in [28, 53, 54]. The result most relevant to this thesis is the evidence that space at the Planck scale is indeed discrete because spin network states are eigenstates of operators corresponding to geometric measurements such as area and volume. Take as an example the area operator $\hat{A}$ acting

---

[7]Other non-perturbative approaches to quantum gravity also exist; however, we focus here on Loop Quantum Gravity.

[8]Usually $\mathfrak{su}(2)$ or $\mathfrak{so}(3)$.

on a 2-dimensional surface S has the spectrum

$$\hat{A}[S]\,|\Gamma\rangle \propto \left(l_p^2 \sum_{i\in\{\Gamma\cup S\}} \sqrt{j_i(j_i+1)} \right) |\Gamma\rangle, \tag{1.1}$$

where l_p is the Planck length, and Γ is a spin network that has no vertices on S[9]. Therefore, the representation on an edge of a spin network indeed determines the quanta of area in the corresponding spin network state. Likewise, the intertwiners on the nodes of a spin network in a region determine the 3-volume of the region. This fundamental discreteness of space resolves the singularity problem and also eliminates ultraviolet divergences, as it provides a natural cutoff at the Planck scale to the physical spectrum of the theory.

In general, a vertex of a spin network can have any valence, the number of edges meeting at the vertex, as seen in Fig. 1.1. We may consider a basis of spin networks with definite valences, i.e., spin networks respectively with three, four, and higher valences. Hence, a generic Loop Quantum Gravity state is a linear combination of these basis states. Furthermore, one may think that 3-valent spin networks, which are the ones with the lowest valence, should be sufficient to provide a complete basis, such that all higher valent spin networks can be decomposed into 3-valent ones combinatorially. This is plausible and indeed suggested by Rovelli[48, 49] only in the case of $SU(2)$ and $SO(3)$. The 3-valent spin networks represent a basis of Loop Quantum Gravity state space. That is, associated with a spin network Γ is a state $|\Gamma\rangle$, and for two such states $|\Gamma\rangle$ and $|\Gamma'\rangle$, $\langle\Gamma|\Gamma'\rangle = \delta_{\Gamma\Gamma'}$. Spin network labels on edges and nodes are representations of the group elements, labeling the graphs in the classical configuration space, and the corresponding intertwiners.

Nevertheless, 3-valent spin networks have difficulty representing 3-space because a node of a 3-valent spin network gives rise to zero 3-volume. One can show that each node of a 4-valent spin network corresponds to a 3-volume[10][55, 56]. [57] also suggests that the intertwiner of a n-valent vertex determines a n-dimensional volume quantum.

Here comes a difference between the spin networks to be studied in this thesis and those conventionally used in Loop Quantum Gravity. That is, our spin networks are 4-valent, rather than trivalent, because we take it seriously that 4-valent nodes correspond to 3-volumes.

As representing the basis states in Loop Quantum Gravity, 3-valent spin networks acquire their dynamics by evolving under the action of the Hamiltonian constraint operator of Loop Quantum Gravity, which also helps to realize the 4D diffeomorphism invariance of the theory. The Hamiltonian constraint operator, in its well-accepted form given by Thiemann[58–60], acts only on vertices. Fig. 1.2 sketches the action of the Hamiltonian constraint on a node. Thus, one can view the Hamiltonian constraint as a local move that evolves a spin network state to another. In fact, Loop Quantum Gravity has a path integral formulation, Spin Foam models, casting the evolution of spin networks in a systematic, covariant way. Spin Foam Models receive their name because in these models quantum space-time as quantum histories of spin networks resembles a spin foam.

---

[9]If Γ has edges on S, a degeneracy arises and special regularization methods are needed to obtain the correct spectrum. See, for example, [49]

[10]This correspondence is at the Planck level. Whether it holds in a continuum limit is remains an open issue.
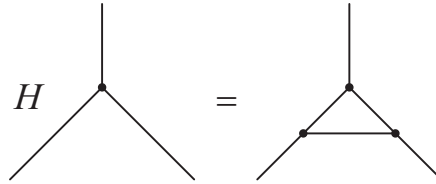
Figure 1.2: A sketch of the action of the Hamiltonian constraint on a vertex. Details such as coefficients and summing over are neglected because they are not used in this thesis.

Different Spin Foam models are available, such as the Barret-Crane model[61], Freidel-Krasnov model[62], and so on. In many studies of Spin Foam models, spin networks and their histories are taken to be unembedded, which are only combinatoric graphs. The key difference between embedded and unembedded spin networks is that the edges of an embedded spin network can knot, braid, and link together. The role of these knots, braids, and links has been a big open issue. Nevertheless, recently some of these topological structures of embedded spin networks are shown to correspond to matter degrees of freedom, which is the main topic of this thesis. A related work by the thesis's author also discusses another perspective of these structures[63].

According to Spin Foam models[49, 64–66], 3-valent spin networks evolve under two more moves, shown in Fig. 1.3(a) and (b), including the one in Fig. 1.2.
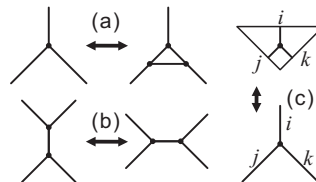
Figure 1.3: (a): expansion and contraction move. (b): exchange move. (c) duality between a triangle and a trivalent vertex.

One can actually understand these moves from the topological perspective in which 3-valent spin networks are the dual skeletons of triangulations of 2D surfaces. Fig. 1.3(c) shows this, where a node represents a triangle, and an edge represents a side of the triangle. This is fine because the vertices of trivalent spin networks have no volume, consistent with 2D. Then the evolution moves of trivalent spin networks are dual to the Pachner moves[67] relating different triangulations of the same surface. In this language, an expansion move becomes dual to a $1 \rightarrow 3$ Pachner move that splits one triangle into three. A contraction move and an exchange move then correspond to a $3 \rightarrow 1$ and a $2 \rightarrow 2$ Pachner move respectively (see Fig. 1.5).

This topological interpretation of spin networks indicates that summing over histories of the evolution of certain fundamental building blocks produces a quantum space-time. That is, one can build 3D, 4D, and $(n + 1)$D space-time from the evolution respectively of 2D triangles, 3D tetrahedra, and n-simplicies glued together. This picture is partly implemented in Spin Foam models and

fully implemented in another formulation of quantum gravity, Group Field theories, which we will briefly introduced in Section 8.2, where we discuss one of our future directions for formulating our approach of emergent matter of quantum geometry by means of Group Field Theories.

A subtlety exists, however. A spin network with line-like edges and point-like nodes, which are those under discussion so far, contains less information than an exact dual of a simplicial triangulation of a 2D surface. Here is the reason. Two triangles can be glued along a side in two opposite ways (Fig. 1.4(b) and (c)); hence, taking a line dual to a side of a triangle will fail to handle this information. One needs to fatten a trivalent spin network by framing edges to ribbons and vertices to disks to make an exact dual skeleton of a 2D triangulation. We call these framed spin networks 'ribbon spin networks'[11]. Fig. 1.4 shows this, and Fig. 1.5[12] depicts the corresponding evolution moves. The criteria for a legal 2D Pachner move is that the triangles before and after
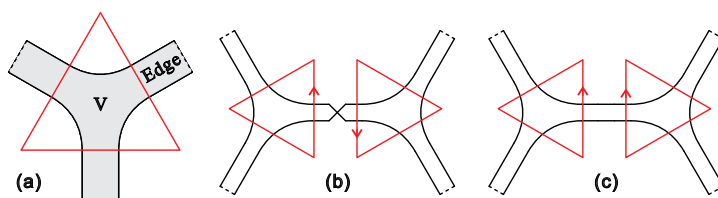
Figure 1.4: Duality between ribbon spin network and 2D triangulation.
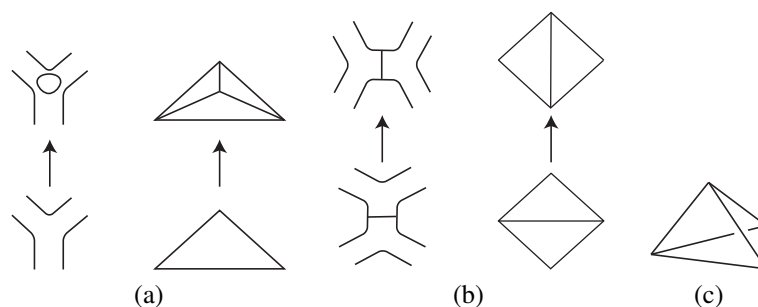
Figure 1.5: Pachner moves. (a) 1 → 3. (b) 2 → 2.

the move bounds a 3D tetrahedron, as is clear in Fig. 1.5. Interestingly, Major and Smolin[70–73] suggested that when Loop Quantum Gravity contains a non-zero cosmological constant, the corresponding spin networks become framed: edges and vertices become ribbons and disks in the

---

[11]For embedded spin networks, the duality is only local, i.e., restricted to a single simplex, in 3D and higher dimensions. In 2D, this restriction is unnecessary in 2D because an embedded ribbon spin network is dual to a topological manifold globally[68]. [68] does not directly study the embedded case; however, its results apply if we keep merely the permutation structure of the embedded spin networks and neglect other structures due to embedding.

[12]This figure is adopted from [69] with the author's permission.

trivalent case, and become tubes and spheres in the 4-valent case. Moreover, labels of framed spin networks turn out to be representations of the quantum group, e.g., $SU_q(2)$, corresponding to the original gauge group, e.g., $SU(2)$. In Group Field Theories, because the duality between simplices and spin network vertices is taken seriously, the spin networks arise therein are indeed framed, but unembedded.

It is time to remark again on the ansatz we posit. Our third ansatz requires the embedded 4-valent spin networks to evolve under adapted dual Pachner moves. These moves are adapted and are thus different from those in Spin Foam models. In many studies of spin foam models, the spin networks and spin foam histories are taken to be abstract, or unembedded. Our results do not directly apply to these models, as the topological structures our results concern arise from the embedding of the graphs in a topological three manifold. But neither do such models give dynamics for states of loop quantum gravity, which are embedded. A path integral formulation of loop quantum gravity must assign evolution amplitudes to embedded graphs, as those are the states found by quantizing diffeomorphism invariant gauge theories such as general relativity. [69] is a study of matter from unembedded spin networks in $(2 + 1)$-dimension. Therefore, the problem is how to build spin-foam like dynamics for embedded spin networks. The adapted dual Pachner moves to be defined in Section 2.6 for our framed and embedded 4-valent spin networks will resolve this problem.

1.3.3 Implications

All the above implies that spin networks are good representations of quantum space and that their evolution gives rise to quantum space-time. That said, we posit that spin networks are the most fundamental entities describing nature[13], going beyond Loop Quantum Gravity and Spin Foam Models. This is actually in accordance with Penrose's original proposal of spin networks, with, however, a great deal of generalization.

Nonetheless, none of the approaches to background independent quantum gravity we have discussed are able to produce the dimensionality of our physical space-time; rather, each model presupposes a dimensionality[14]. We do not address this issue in this thesis either. On the other hand, the topological interpretation of spin networks provides us a good reason to identify the valence of a spin network with the dimensionality of space. Consequently, to construct a theory of $(3 + 1)$-dimensional (or $2 + 1$) space-time, it is natural to base the theory on the evolution of 4-valent (or trivalent) spin networks.

Note that spin networks also arise in different contexts, such as in lattice gauge theories[75–78] and in topological field theories[79–82]; however, we do not discuss them here.

---

[13]An issue is again whether we should consider embedded or unembedded spin networks. Nevertheless, since all the information due to embedding can be characterized purely algebraically, as will be pointed out later in this thesis, embedded spin networks (or in other words, algebraic spin networks with embedding data) are more general objects than the unembedded ones.

[14]Why we live in 3-dimensional space and (3+1)-dimensional space-time remains a big open physical and philosophical issue. The earliest reasonable argument was due to Ehrenfest in 1917[74] that atoms are instable unless in 3D. Recently, anthropic arguments also arouse. Nevertheless, all these arguments sounds *a posteriori*, and a theory that naturally gives rise to our $(3 + 1)$ space-time is still missing.

1.4   Helon Model on trivalent spin networks

It is time to come back to the problem of unifying matter with gravity. Although Loop Quantum Gravity was not invented to be a unifying theory of matter and gravity or a theory of everything, there has been a large amount of work on coupling matter with gravity in the context of Loop Quantum Gravity and Spin Foam Models[83–88]. These approaches did not lead to the 4D semi-classical Einstein Equation, nor do they provide a fundamental unification, because they simply couple matter fields with gravity and quantizing the whole system in the way consistent with that of Loop Quantum Gravity or Spin Foam Models, leaving the issues of the Standard Model of particles unresolved.

In the rest of this thesis, we will show that assuming that quantum space-time arises from spin networks embedded in a topological 3-manifold and their evolution, topological excitations with dynamics inevitably emerge and can be a candidate for matter degrees of freedom. This indicates that a certain theory of spin networks may turn out to be a theory of everything. Recall that this is related to the old dream that matter is topological excitations of the geometry of space-time. Two questions delayed the realization of the dream. First, how do we identify an independent excitation or degree of freedom in a background independent quantum theory, where the semiclassical approximation is expected to be unreliable? Second, why should such excitations be chiral, as any excitations that give rise to the low mass observed fermions must be?

As previously explained, Markopoulou *et al.*[7–9] propose a solution to the first question by means of noiseless subsystems. The key point is that noiseless subsystems arise when a splitting of the Hilbert space of the whole system into system and environment reveals emergent symmetries that can protect subsystems from decohering as a result of inherently noisy interactions with the environment. The proposal raises the question of whether there are models of dynamical quantum geometry, in which this procedure reproduces at least some of the symmetries of the observed elementary particles.

This leads to an answer to the second question: why such excitations should be chiral, owing to the intrinsic chirality of these excitations in the recent work by Bilson-Thompson, Markopoulou, and Smolin[15] on implementing the previously mentioned Helon model[12] on framed trivalent spin networks embedded in a topological three manifold. They choose to work with trivalent spin networks for two reasons: 1) these conventionally label the basis states in Loop Quantum Gravity with a non-zero cosmological constant, and 2) helons are braids consisting of three ribbons. We have pointed out that trivalent spin networks have vertices corresponding to zero 3-volume and that they can only be made dual to 2D topologies. Bilson-Thompson *et al.* do notice this problem; that is why they directly treat the ribbon spin networks as 2D surfaces embedded in a topological 3-manifold. But it is unclear whether this set-up can indeed produce a $(3 + 1)$-dimensional picture. Let us introduce the trivalent approach in below.

[15] considers a theory with a basis of states labeled by framed trivalent spin networks embedded in a topological 3-manifold, which are called braided ribbon networks because topological structures like braids and knots arise through embedding. For two topologically distinct braided ribbon networks, Γ and Γ', their corresponding states satisfy $\langle \Gamma | \Gamma' \rangle = \delta_{\Gamma\Gamma'}$. A node of such a network is a trinion (Fig. 1.4(a)). The notion of trinion was first proposed in [89]. Since trinions,

with their edges connected trivially or in a braided way, comprise a braided ribbon network, they provide a decomposition of the state space represented by the braided ribbon networks. First of all, one can associate a finite dimensional Hilbert space, $\mathcal{H}_t$ with a trinion, t[15]. Hence, the Hilbert space associated with a braided ribbon network, Γ, is

$$\mathcal{H}_\Gamma = \bigotimes_{t \in \Gamma} \mathcal{H}_t. \tag{1.2}$$

In the equation above, t runs over all trinions in Γ and should be summed over the labels on their edges. Nevertheless, spin network labels play no role in obtaining the results in [15]; we thus neglect them. The overall state space of the theory of braided ribbon networks becomes a direct sum:

$$\mathcal{H} = \bigoplus_{\Gamma} \mathcal{H}_\Gamma, \tag{1.3}$$

where the sum runs only over topologically distinct braided ribbon networks.
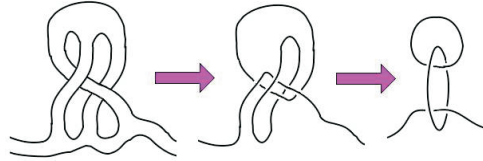
Figure 1.6: Obtaining the reduced link of the the braid on the left. The line at the bottom of the first figure is removed from the other ones by definition of reduced link invariants.

The basic moves of framed trivalent spin networks listed in Fig. 1.5 generate an evolution algebra that gives rise to the system's dynamics. It is then found that such a system bear topological excitations, which have characterizing topological invariants, as noiseless subsystems under the evolution algebra. These topological invariants are called reduced link invariants. Fig. 1.6 shows as an example of how to extract the reduced link of a topological structure, which is easily shown to be conserved under any evolution move[16]. One can understand a reduced link invariant as the eigenvalue of an operator, acting on sub states of braided ribbon network states, which commutes with the evolution algebra. Consequently, conserved quantum numbers emerge from dynamical quantum geometries. According to [7, 8, 20], the topological structure in Fig. 1.6[17] is indeed an excitation to be identified with a matter degree of freedom. In fact, a particular class of topological excitations carrying quantum numbers exists, which consists of capped 3-strand ribbon braids whose meaning is evident in Fig. 1.7(a).

---

[15]This association depends on the choice of quantum group in a specific Loop Quantum Gravity model with a non-zero cosmological constant.

[16]A $1 \to 3$ move adds a loop to a reduced link, but the loop should be dropped by definition[15], and hence does not impact the corresponding reduced link invariant.

[17]This figure is adopted from [15] with the author's permission.
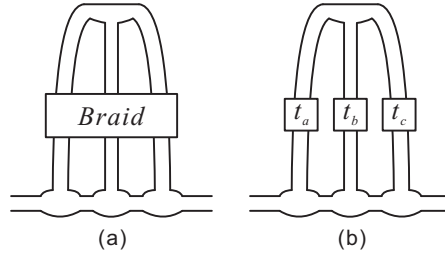
Figure 1.7: (a) Generic capped braids. (b) Unbraids with only twists t_a, t_b, and t_c, which are integers.

The capped braids are indeed the simplest systems in the trivalent model bound by the conservation of topological quantum numbers. These make contact with structures not only from topological quantum computing but also strikingly from classic results of knot theory from the 1980s. In both, chirality plays a key role because braids are chiral and topological invariants associated with braided ribbons are able to detect chirality and code chiral conservation laws. Indeed, [15] and two follow-ups[38, 90] have shown the following main results.

1. Many braid excitations are local, in the sense that they can be evolved by local moves to states, called isolated structures, which are attached by only a single edge to the rest of the graph representing the quantum geometry of space[38].

2. The braid excitations propagate on the ribbon network under the local evolution moves of the model[38].

3. Braid excitations admit discrete transformations that are thought to be Parity, Charge Conjugation, and Time Reversal of the braid states[15, 90].

4. There exists a dictionary between some braid excitations and the three generations of Standard Model particles and even more[90]. In this dictionary, twists of the ribbons of a braid are mapped to charges of particles. This actually encodes Bilson-Thompson's Helon model in the class of background independent quantum gravity theories whose basis states are labeled by embedded framed spin networks.

In making the above findings, the observation that any capped braid is topologically equivalent to a trivial braid with only integral twists on its three strands (see Fig. 1.7(b) for a generic example) plays a key role. That is, a capped braid is characterized by a triple of integral twists, $[t_a, t_b, t_c]$. One will see in Chapter 4 that a similar fact will arise in the case of 4-valent spin networks.

Many questions remain unanswered in the trivalent approach, however. We give an incomplete list of them in below.

1. Where does mass come from?

2. How does the quantum statistics arise to unambiguously identify a class of braid excitations with fermions and another class with bosons? Are there anyonic braid excitations?

3. How may an effective low energy dynamics emerge?

4. As a possible solution suggested by Markopoulou[7–9] to the low energy limit problem of background independent theories of quantum gravity, will semi-classical Einstein equations appear? If so, how?

5. What do the rest of the infinite number of braid excitations correspond to, as those mapped to Standard Model particles contribute a negligible small number to the total number of braid excitations?

6. Does there exist a (natural) mechanism, or a selection rule, such that only the correct number of low energy effective degrees of freedom will arise to reproduce the Standard Model, allowing predictions of certain new particles?

7. Given the definition of C, P, and T transformations in this approach, the braid states are all CP-invariant. Then how does the familiar CP-violation enter the theory?

Apart from these open questions, the trivalent approach has issues and limitations. First, as pointed out before, the trivalent ribbon networks do not have a 3D topological interpretation. Although they are embedded in a topological 3-manifold, whether their evolution will produce $(3 + 1)$-dimensional space-time in the continuum limit is unknown. Second, in mapping twists of braids to charges of particles, they put in by hand a factor of 1/3, to encompass the fractional quark charges. Third, to define C, P, and T for braid excitations, they assume $CPT = 1$ on massive particles at rest. The issue is two-fold. On the one hand, it is as yet unknown how a braid gives rise to mass. On the other hand, $CPT = 1$ is a symmetry of the S-matrix of Standard Model interactions rather than a symmetry for a single particle state. Another related issue is that the 3-strand capped braids admits the discrete symmetry group $S_3 \times \mathbb{Z}_2$, where S_3 is the permutation group of three objects. This group contains twelve elements, more than what we need for C, P, T, and their products, which is seven. To pick seven out of twelve discrete transformations, besides the aforementioned assumptions, they assume an interaction scheme of the capped braids, in accordance with the interactions between Standard Model particles. Nevertheless, as will be pointed out soon, interactions of braid excitations do not exist in their model yet.

Moreover, the dictionary between braids and Standard Model particles is incomplete: photons are still missing. More importantly, why should the braid excitations living on Planck level spin networks directly correspond to Standard Model particles after the symmetry breaking, which are rather low energy? One needs an effective description of these braid excitations showing that, in its low-energy limit, the known physics on the Earth arises. Given these open questions and issue, however, the 3-valent model does have very interesting results that urge one to look for solutions in alternative approaches.

The most serious limitation that the results of [15] suffer is: the conservation laws that preserve the excitations are exact, which means that creation and annihilation of particles do not exist. Indeed, [38] shows that the braided excitations of [15] are like solitons in integrable systems: they pass right through each other. This means that the interactions necessary to turn the trivalent approach into a theory of gravity and matter are missing from the approach. This is a

strong motivation for us to re-investigate the whole setup of the system in the case of 4-valent spin networks[18].

1.5   Braid excitations of 4-valent spin networks

The results obtained and issues encountered in the approach to encode the Helon model in the theories of trivalent spin networks motivate us to extend the study to 4-valent spin networks. One will see that the 4-valent theory described in this thesis, although its starting point was a modification of the original 3-valent approach, turns out to be a rich dynamical theory. The 4-valent approach will present a novel picture and perspectives of emergent matter in quantum geometry, and when combined with other mathematical tools, may lead to a unifying theory of matter and gravity, whose low energy limit is our familiar physics of gravity coupled with matter.

We consider mostly framed four-valent spin networks, also called tube graphs, embedded in a differential 3-manifold. We will also address unframed 4-valent spin networks in Chapters 2 and 3. Tube graphs and the corresponding dual Pachner moves, which are the evolution moves that naturally occur in spin foam models[49, 64–66] in 4D but with certain modifications adapted to the embedding of spin networks; hence, this extends the results on the existence of emergent, chiral degrees of freedom to that much-studied case.

As we did in the previous section for the 3-valent case, we consider a system whose basis states are labeled by tube graphs embedded in a topological three manifold, and decompose its state space by using the Hilbert space associated with each node. The dual Pachner moves to be described in Sections 2.6.1 and 2.6.2 generate the system's evolution algebra. As mentioned above, the evolution of 4-valent spin networks results in a (3 + 1)-dimensional picture.

We are interested in a type of topological excitations, namely 3-strand braids, each of which consists of two adjacent nodes with three common edges, possibly braided and twisted (see Fig. 2.3 for an example). As we will show in this thesis, certain 3-strand braid states are indeed noiseless subsystems, in the sense that the dual Pachner moves, with the restriction to the dual of triangulations of trivial regions, are exactly right to preserve the stability these braid states, while giving some propagation and interactions. That is, the default evolution moves of 4-valent spin networks in our theory endow the topological excitations with a dynamics.

One will see that most of the issues encountered in the 3-valent approach are resolved in our 4-valent approach. Some open questions are still there and will probably be long-standing; however, we will point out plausible routes to the answers. To these ends, we sketch in below our main results.

---

[18]As work in progress, in [91], Bilson-Thompson *et al.* are trying to fix the problem by inventing new set of evolution moves of trivalent spin networks. This is, however, somehow artificial and uncontrollable. In contrast, one will see that dynamics of topological excitations is naturally encoded in the evolution of 4-valent spin networks.

Main results

1. Adapted dual Pachner moves are defined to build a spin-foam like dynamics for embedded framed 4-valent spin networks.

2. The adapted dual Pachner moves on embedded four valent graphs may be restricted to those that are dual to Pachner moves on triangulations of regions of R^3, in such a way that some chiral braid states are locally stable, which means they cannot be undone by local moves involving the nodes that comprise them.

3. All stable braids can propagate in an induced way. Some of those stable chiral braids propagate actively, in the sense that under the local evolution moves they can exchange places with substructures adjacent to them in the graph. Results are found that limit the classes of actively propagating states.

4. Two types of braid interactions are found. The first is **direct interaction**: two neighboring braids in a spin network may merge under the action of the evolution moves. For this to happen one of them must be in a small class of states called actively interacting braids. We find examples of **actively interacting braids**, all of which are equivalent to trivial braids with twists. The second is **exchange interaction**: two adjacent braids may exchange a virtual actively interacting braid, resulting in another two adjacent braids.

5. A braid can also decay by radiating an actively interacting braid.

6. There exist conserved quantities associated with braids under interactions, with precise conservation laws.

7. The set of actively interacting braids forms a noncommutative algebra with direction interaction its binary product. It is also a set of morphisms taking non-actively interacting braids to one another.

8. Actively interacting braids are thus analogous to bosons, while non-actively interacting ones are analogous to fermions.

9. Constrained by braid dynamics, stable braid excitations admit seven, and only seven, discrete transformations, which are then identified with analogues of C, P, T, and their products.

10. Each CPT-multiplet of actively interacting braids is uniquely characterized by a non-negative integer.

11. Interactions of braids are invariant under C, P, and T separately, and are thus invariant under CPT.

12. The electric charge of a braid is quantized in units of 1/3, because it is directly related to the braid's twists that are naturally in units of 1/3.

13. **Braid Feynman diagrams** are proposed to represent braid dynamics.

14. A constraint on probability amplitudes of braid dynamics is obtained.

We shall leave the discussion on open issues for Chapter 8. We do not, in this thesis, investigate the correspondence with the Helon models of [12, 15]. The reason is that the structure of our theory is much richer than a direct identification of helons with braids. It is more reasonable to write down an action principle of our braid excitations at the Planck level and study its physical implications via its low energy effective theories.

We will not include the spin network labels because our results do not depend on spin network labels; nonetheless, we will discuss the possibility and necessity of incorporating them.

1.6   Summary

We summarize the content of this thesis as follows. Chapter 2 proposes a graphic notation of embedded 4-valent spin networks and describes the key topological structures of our study, namely 3-strand braids, using this notation. It then develops a graphic calculus of equivalence and evolutions moves of embedded 4-valent spin networks. This calculus is a major tool for our study of the dynamics of braids in the rest of the thesis. Chapter 2 is based on our work [40] and part of [41].

By the graphic calculus developed in Chapter 2, Chapter 3 discovers that some braids can propagate on its ambient spin network and can interact with each other. It discusses properties of braid propagation and interaction and finds an important class of braids, i.e., the actively interacting braids that will be shown analogous to bosons. Chapter 3 is based on our work [41].

Chapters 4 and 5 bring up, as another major tool, an algebraic calculus of 3-strand braids of embedded 4-valent spin networks. They make more findings of braid dynamics and capture the conserved quantities of braids under interactions in this new formalism. The former focuses on the actively interacting braids, while the latter provides a generalized approach. Chapters 4 and 5 are based on our work: [42] and [43].

In the algebraic formalism, Chapter 6 discovers seven and only seven discrete transformations of braids and make a unique analogy between them and the C, P, and T of particles. Chapter 6 is based on our work: [44].

Chapter 7 uses both the graphic calculus and algebraic calculus to discover braid decay and a new type of braid interaction, namely the exchange interaction. More interestingly, it represents braid interactions and decay in terms of braid Feynman diagrams, which suggests an effective theory of braid dynamics. Chapter 3 is based on our work: [45].

Chapter 8 discusses open issues and future directions, including work in progress.

Since the above summary makes a clear link between the chapters and the thesis author's papers they are based on, in the rest of the thesis, these papers will not be cited again.

Chapter 2

3-Strand Braids: A Graphic Calculus

In this chapter and the next, we study framed and unframed 4-valent embedded spin networks through their 2D projections in a new graphic notation. In a framed graph, edges are represented by tubes that meet at nodes that are punctured spheres[1]. If we take the limit where the tubes become lines, while the nodes remain punctured spheres we get the unframed case.

We are interested in a particular class of subgraphs of embedded spin networks. These subgraphs are what we call 3-strand braids (4-valent braids, or braids in short). Each 3-strand braid consists of two nodes that share three edges that may be braided. According to [7, 9, 15], these 3-strand braids are noiseless topological excitations of embedded 4-valent spin networks. To study these braid excitations, we shall develop a graphic calculus that describes 4-valent framed spin-networks embedded in 3-manifolds up to diffeomorphism and their evolution. In particular, as Chapter 3 will show, this graphic calculus enables one to study the dynamics of the 3-strand braids in a transparent way. Note that in this thesis, we consider only 3-manifolds homeomorphic to $\mathbb{R}^3$.

When using this notation, it is important to keep in mind the distinction between braids, which are diffeomorphism equivalence classes of embeddings of diagrams in three dimensional space, and the braid diagrams that represent them. Many braid diagrams will correspond to the same braid; they will be related by a set of equivalence moves. It will be important also to distinguish these equivalence moves from the dynamical moves to be introduced in the next section.

2.1   Notation

In the category of framed graphs, we discuss edges that are represented by tubes and nodes that are represented by 2-spheres with the incident edges attached at circles called punctures. We consider only 4-valent nodes that are rigid and dual to tetrahedra (Fig. 2.1). These nodes are non-degenerate, in the sense that no more than two edges of a node are co-planar. We will consider projections in which all nodes are in one of the configurations or states shown in Fig. 2.1.

---

[1]One may go further and consider the case in which the nodes are structureless points rather than punctured spheres. Nevertheless, in this case the dual Pachner moves are not well defined in the embedded case, such that spin foam models cannot be applied.
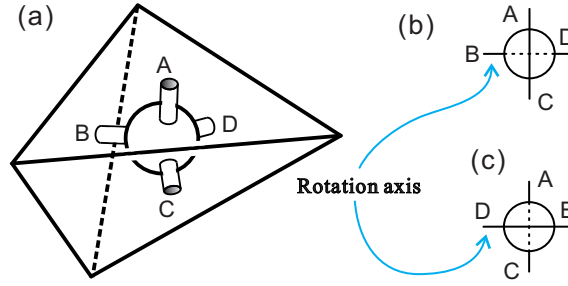
Figure 2.1: (a) is a tetrahedron and its dual node. A node can have two orientations in a diagram, (b) denotes the ⊕ state, while (c) denotes the ⊖ state.

Note that the duality between a 4-valent node and a tetrahedron is only considered local. That is, a 4-valent graph, formed by gluing 4-valent nodes along their tubular edges, is not guaranteed to be dual to a triangulation of a manifold. To glue two nodes along a piece of tube nontrivially, we assume that tubes have additional structures to record twists (Fig. 2.2).

If spin networks are not framed, we simply reduce tubes to lines but still keep spheres as nodes for convenience (to be explained in Section 2.1.1). To fully characterize the embedding of a spin network in $\mathbb{R}^3$, we assume that not only the nodes are rigid, i.e., they can only be rotated or translated, but also the positions on the node where the edges are attached to are fixed. That is, seen closely to a node, each attached edge is dual to a face of the tetrahedron dual to the node. This requirement and the local duality ensures the non-degeneracy of the nodes, although this may not be easily visualized in two dimensional projections of an embedded graph.

For calculational purposes, we simplify the tube-sphere notation in Fig. 2.1(a) to Fig. 2.1(b), in which 1) the sphere is replaced by a solid circle; 2) the two tubes in the front, A and C in (a), are replaced by a solid line piercing through the circle in (b); and 3) the two tubes in the back, B and D in (a) are substituted by B and D in (b) with a dashed line connecting them through the circle. There is no loss of generality in taking this simplified notation, because one can always arrange a node in the two states in Fig. 2.1(b) & (c) by diffeomorphism before taking a projection. Because of the local duality between a node and a tetrahedron and that all the four edges of a node are on an equal footing, if we choose one of the four edges of a node at a time, the other three edges are still on an equal footing, in respect to a rotation symmetry with the specially chosen edge as the rotation axis, e.g., the edge B in Fig. 2.1(b) & (c). This rotation symmetry will be discussed in detail in the next section.

Therefore, in a projection one can assign states to a node with respect to its rotation axis. If the rotation axis is an edge in the back, the node is in state ⊕, or is simply called a ⊕-node, e.g., Fig. 2.1(b) with edge B as the rotation axis. If the rotation axis is an edge in the back, the node is called a ⊖-node or in the state ⊖, e.g., Fig. 2.1(c) with edge D.

Nonetheless, if one wants to distinguish the other three edges of a node when one edge is fixed, a degeneracy of each state of the node arises. (This is indeed the case when we talk about the nodes of a braid, as will be seen shortly.) Taking Fig. 2.1(b) as an example, the node is in ⊕ w.r.t. edge

18

B; rotating the node about B produces permutations of the edges A, D, and C. Ignoring the twists and crossings that are created by rotations, which will be our next topic, it takes a full rotation for the node to roll back to its original configuration. It is easy to see that among all permutations, the results $(C, A, D)^2$, (D, C, A), and (A, D, C) keep the node in $\oplus$ w.r.t. B, whereas (A, C, D), (C, D, A), and (D, A, C) flip the node to $\ominus$ w.r.t. B. That is, each state has a 3-fold degeneracy; or in other words, each state is a triplet. The six sub-states in total record the configuration of the other three edges w.r.t. the rotation axis.

Because of the freedom to make a diffeomorphism transformation before projecting, this kind of rotations can be done without loss of generality. If we denote a full rotation by 2π, then the amount of rotation keeping a node within a state triplet is $2\pi/3$; however, a $\pi/3$ causes a node to jump back and forth between two state triplets. Note again that this type of rotations are not that with rigid metric but rather purely topological. Details of rotations will be studied in Section 2.3.2.

As aforementioned, twists can exist on edges, e.g., the $\pi/3$-twist on the edge B with respect to the solid red dot, shown in Fig. 2.2(a), the above discussion of rotations shows that the smallest distinguishable twist is $\pi/3$, and all higher twists distinguishable from each other in the projection must then be multiples of $\pi/3$.
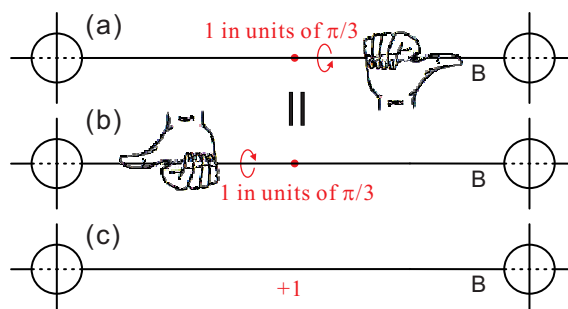
Figure 2.2: The 1 unit of twist (equivalent to a $\pi/3$ rotation) in (a) means cut to the right of the red dot and twist as shown. This is equivalent to the opposite twist on the opposite side of the red dot, as shown in (b). Thus, both may be represented as in (c), by a label of $+1$ of edge B.

One might be confused about how a twist is defined to be positive or negative, given two possible directions of a rotation of a node w.r.t. its rotation axis in a projection. Nevertheless, Fig. 2.2 presents an unambiguous resolution of this confusion. Because an edge is always between two nodes, and a rotation of a node creates/annihilates twists on its edges, one usually needs to specify the fixed point on an edge with respect to which a twist is counted, as in Fig. 2.2(a). In this manner, the one unit of twist in Fig. 2.2(a) is obviously equivalent to that in 2.2(b), which is the same amount of twist in the opposite direction on the other side of the fixed point. Interestingly, both twists in Fig. 2.2(a) and (b) are right-handed twists if one point his/her right thumb to the node on the same sides of the fixed point as that of the twists; therefore, we can unambiguously assign the same value to them, namely $+1$ (unit of $\pi/3$). This enables us to simply label an edge

---

[2]In this notation, e.g., (C, A, D) means $C \mapsto A$, $A \mapsto D$, and $D \mapsto C$.

with a (left-) right-handed twist a (negative) positive integer. For example, Fig. 2.2(a) and (b) can be replaced by 2.2(c) without ambiguity. Since the rotations are topological, one can normalize the π to one, such that twists are now in units of 1/3.

2.1.1 Framed and unframed spin networks

This thesis focuses on framed spin networks defined above. Nonetheless, loop quantum gravity without cosmological constant considers unframed graphs. Then, it is also useful to have results for unframed spin networks. The particular notation of unframed graphs is obtained from the framed case discussed here by shrinking tubes to lines, but keeping the nodes as rigid spheres, locally dual to tetrahedra. This is necessary so that the evolution moves are well defined for unframed embedded graphs, which will be explained in section 2.6.

In the rest of this thesis, we always consider the framed case, unless otherwise stated. Results for the unframed case will be understood from those for the framed case by neglecting the twists of the edges, unless we explicitly describe them.

2.2 Braids

Equipped with the notation in above, we found an interesting type of topological structures as subgraphs of embedded 4-valent spin networks, namely 3-strand braids, defined as follows.

Definition 2.1. *A 3-strand braid (or simply a braid) of a 4-valent spin network embedded in $\mathbb{R}^3$ consists of two nodes sharing three edges. We call the two nodes **end-nodes**, and their common edges **strands**. Each end-node of a braid also has an **external edge** that connects the braid to the rest of the spin network. The 2-dimensional projections of such a braid are what we call **braid diagrams**, a typical example of which is Fig. 2.3. This definition is subject to these conditions:*
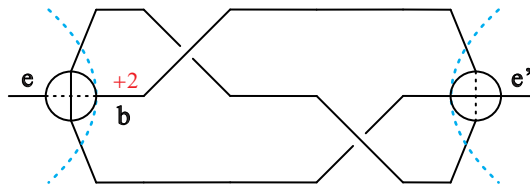
Figure 2.3: A typical braid diagram of a 3-strand braid consisting two end-nodes with three common edges. The region between the two dashed line satisfies the definition of an ordinary braid. Edges e and e' are called external edges. The strand in the middle also has a right handed twist of 2 units. In this figure, with respect to the middle strand, the left end-node is in a $\oplus$-state while the right end-node is in a $\ominus$-state.

1. *We can always arrange a braid diagram horizontally. In this way the (left) right external edge of a braid can always be the (left-) right-most edge of the (left) right end-node, and*

always stretches to the (left) right; external edges cannot tangle with the strands. Fig. 2.4(a) shows a violation of this condition.

2. *What is captured between the two end-nodes of a braid, e.g., the region between the two dashed lines in Fig. 2.3, should meet the definition of braid in the ordinary braid theory[3]. Fig. 2.4(b) shows a violation of this.*

3. *The three strands of a braid are never tangled with any other edge of the spin-net, as illustrated in right side of the braid diagram in Fig. 2.4(a) also show a violation of this.*
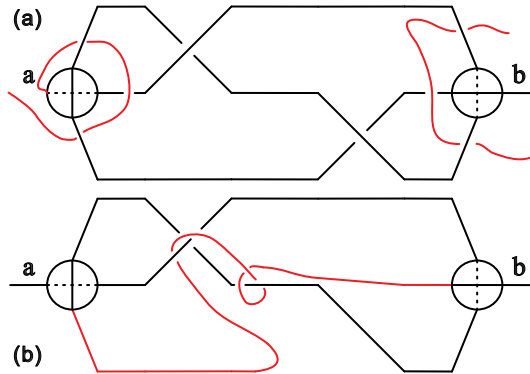
Figure 2.4: (a) is not a braid because of the tangle between the external edge *a* and the common edges of the two nodes, and/or the tangle between the common edges and another edge connecting elsewhere in the whole spin network. (b) is not a braid either because the region captured between the two nodes does not satisfy the ordinary definition of a braid.

Note that our braids are different from the braids in ordinary braid theory because the two end-nodes of such a braid are topologically significant to the state of the braid. Several important remarks are as follows.

We would like to emphasize that the braids defined above are 3D structures; they are sub-spinnets of embedded spin networks. We thus differentiated braids from their 2D projections, i.e., braid diagrams. Nonetheless, this differentiation admits two equivalent meanings. Here we focus on braids rather than the whole embedded spin network. On the one hand, one can directly work in 3D. For example, one can take two ambient isotopic braids due to two diffeomorphic embeddings, and project them in the same way to 2D, then the two braid diagrams must be equivalent to each other, in the sense that they can be transformed into each other by well-defined moves in the projected space (we will discuss these moves in Section 2.3). On the other hand, one can take a braid in 3D and project it to 2D in two different ways; the two braid diagrams are definitely equivalent. One can then lift these two braid diagrams to 3D in the same way, or one can deform

---

[3]Note that the exclusion of colinear and coplanar of the edges of a node mentioned in the beginning of Section 2.1 automatically prevents singular projections of the three strands of a braid, such that this condition can never be violated this way.

them by well-defined moves in the projected space and then lift them in the same way. In either case, the two different looking braids obtained in 3D must again be ambient isotopic to each other.

Therefore, any equivalent class of braids in 3D corresponds to an equivalence class of braid diagrams in 2D; the map between them is surjective[4]. Bearing this in mind, it is in fact unnecessary to distinguish braids from their braid diagrams. Nevertheless, in this thesis we prefer the second meaning explained in the last paragraph. That is, when we say a braid we mean all isotopic braids in 3D, and then we study this braid by its various braid diagrams. This is fine because we can always manipulate a braid in 3D before project it. In doing so, we suppress ambiguities. In the rest of this thesis we may use braids and braid diagrams interchangeably.

Let us put some further constraints on the equivalence class of braid diagrams. Equivalence relations of crossings exist on ordinary braids. These relations certainly hold for our braids as well because our braids have no difference from ordinary braids except for their end-nodes and twists . Nevertheless, we assume for each braid diagram of any of our braids these relations have been used such that the braid diagram has minimal number of crossings. We will give a symbolic version of this explanation in Section 5.1. Besides, we consider braid diagrams, which have the same number of crossings and equivalent crossing patterns up to braid relations, as a single braid diagram!

In Section 2.7, we will bring up a stability condition for the evolution of spin networks, which stabilizes some braid excitations. In the rest of this chapter, however, we shall first focus on the intrinsic properties of these braids in Section 2.3, or in other words the pure topological properties of the braids up to diffeomorphism, i.e., without dynamic evolution, and then move on to their evolution in Section 2.6.

We can also assign an integer, the **crossing number**[5], to a crossing according to its handedness, viz $+1$ for a right-handed crossing, -1 for a left-handed crossing, and 0 otherwise. Fig. 2.5 shows this assignment. Such a assignment scheme will become useful in the subsequent discussions.
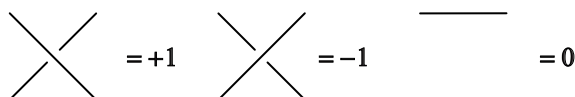
Figure 2.5: The assignments of right-handed crossing, left-handed crossing, and null crossing.

2.3   Equivalence Moves

As aforementioned, the tube diagrams of an embedded spin network belong to different equivalence classes. It is therefore obligatory to characterize these equivalence classes by equivalence relations. To do so, one needs to find the full set of local moves, operating on the nodes and edges,

---

[4]That is, braids mod ambient isotopy are equivalent to braid diagrams mod equivalence moves (to be defined in the next section). This is true because we claimed in the beginning of the chapter that we only consider 3-manifolds homeomorphic to $\mathbb{R}^3$.

[5]Not to be confused with the number of crossings of a braid.

which do not change the diffeomorphism class of the embedding of a diagram. In the discussion below, we work in the framed case. In the unframed case, one ignores the twists.

An obvious set of equivalence moves consists of the usual three Reidemeister moves[92], framed or unframed. The aforementioned braid relations are applications of Reidemeister moves. We will not repeat the details; these moves will be applied without further notice. More importantly, one can define two new kinds of equivalence moves on an embedded 4-valent spin-net. We consider two diagrams, in particular two braid diagrams, to be equivalent, if they are related by a sequence of equivalence moves. The first kind consists of translation moves. The second type of equivalence moves includes rotations defined on the nodes.
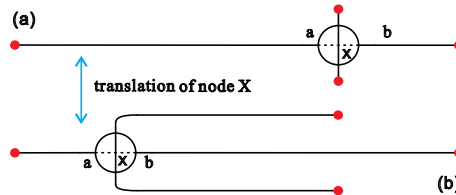
Figure 2.6: Red dots represent other nodes where edges *a* and *b* are attached to. (b) is obtained from (a) by translating node *X* from right to left, and vice versa.

2.3.1 Translations

We discuss translation moves first. Translation moves, which are in fact extended Reidemeister type of moves, involve not only the edges but also the nodes of an embedded spin-net; they reflect the translation symmetry of the embedded spin networks. Let us look at the simplest example first. Fig. 2.6(a) shows a node *X* connected to other places of the network via its four edges; red points represent attached points on other nodes. One can slide node *X* along its edge *a* to the left, which leads to Fig. 2.6(b); this does not change anything of the topology of the embedded spin-net. Fig. 2.7 illustrates more complicated cases where a crossing is taken into account.

In Fig. 2.7(a1) shows a node *X* and a crossing. Since the crossing is between the edge *a* of node *X* and the edge *e* of some other node, and because node *X* together with all its edges are above edge *e*, one can safely translate node *X* along edge *a* to the left passing the crossing, resulting in Fig. 2.7(a2), in which the crossing turns out to be between edge *e* and edge *b*. This is a symmetry of translation, which can be understood as a Reidemeister move[92].

Theses translation moves can apply all over an embedded spin network; however, we are going to use them only for studying braid propagation and interaction in Chapters 3 and 7. We also disallow any translation that may increase the number of crossings of a braid diagram because we assumed in Section 2.2 that the number of crossings of a braid diagram is kept minimum by braid relations.
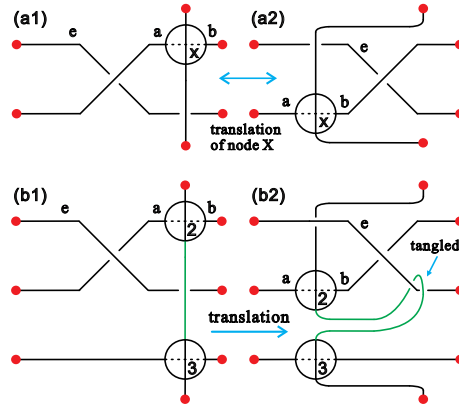
Figure 2.7: Red dots represent other nodes to which edges *a* and *b* are attached. (a1) and (a2) can be transformed into each other by translating node *X*. To transform (b1) into (b2) is not allowed because of the tangle produced by translating node *X*.
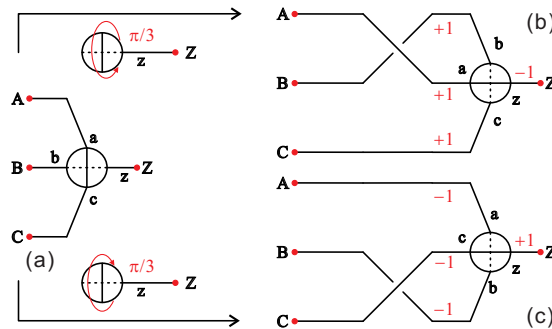
Figure 2.8: (b) & (c) are results of (a) by rotating the $\oplus$-node in (a) w.r.t. edge *z* in two directions respectively. Points *A*, *B*, *C*, and *Z* are assumed to be connected somewhere else and are kept fixed during the rotation. All edges of the node gain the same amount of twist after the rotation.

2.3.2   Rotations

Apart from the translation symmetry introduced in Section 2.1, a node also admits rotation symmetries with respect to any of its four edges. These rotations are purely topological rather than those with a rigid metric; they do not affect the diffeomorphism class of the embedding of the node.

$\pi/3$-Rotations: Generators of rotations

In Section 2.1 we pointed out that each of the two end-node states is in fact a triplet and that a $2\pi/3$ rotation preserve a triplet, whereas a $\pi/3$ rotation results in a jump from one triplet to the other. Because two consecutive $\pi/3$ rotations comprise a $2\pi/3$ rotation, $\pi/3$ rotations are generators of all possible rotations of node w.r.t. an edge of the node. To arrive at this conclusion only, we neglected

that a rotation of a node creates twists on the edges of the node and braid the edges. It is time to study these effects in detail: how does a rotation affect a subgraph consisting of a node and its four edges? We only show here the $\pi/3$ rotations because we can obtain the others by applying more $\pi/3$ ones; however, for future convenience we will illustrate $2\pi/3$ and π rotations in Appendix A.

In either of its states, i.e., $\oplus$ and $\ominus$, a node can be rotated in two opposite directions. Fig. 2.8 shows the case where the node is in a $\oplus$-state with respect to its rotation axis before the $\pi/3$ rotation is done, while Fig. 2.9 illustrates the other case.
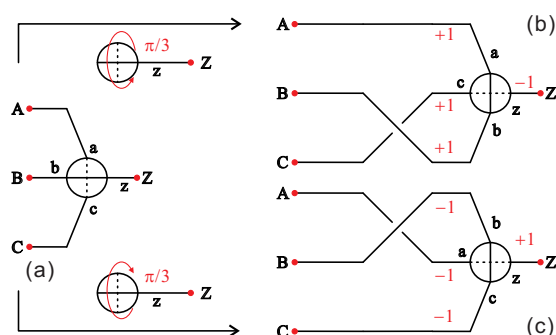
Figure 2.9: (b) & (c) are results of (a) by rotating the $\ominus$-node in (a) w.r.t. edge z in two directions respectively. Points A, B, C, and Z are assumed to be connected somewhere else and are kept fixed during the rotation. All edges of the node gain the same amount of twist after the rotation.

According to Fig. 2.8 and Fig. 2.9, a $\pi/3$ rotation always creates a crossing of two edges of the node and causes twists on all the four edges. Each twist is clearly of plus or minus $\pi/3$. The twist being created on the rotation axis of a node is always opposite to that of each of the other three edges of the node. That a $\pi/3$ rotation flips a node's state is also shown in Figures 2.8 and 2.9.

Recall that all the equivalence moves defined above are diffeomorphic operations on the embedded graphs. As an example, Fig. 2.10 depicts two equivalent braids that can be deformed into each other by a $\pi/3$ rotation of node 2 with respect to its external edge z.

Note that for an end-node of a braid, only its external edge is allowed to be the rotation axis. Otherwise, one may end up with a situation similar to Fig. 2.11, which does not satisfy Definition 2.1. Therefore, although sub-spin networks like Fig. 2.11 are equivalent to well-defined braids by rotations, they are not to be investigated because they complicate the clear structure of braids and do not have any new interesting property. Thus for simplicity we only allow the external edge of an end-node of a braid to be the rotation axis. If a node is not an end-node of a braid, any of its four edges can be chosen as a rotation axis.

By looking carefully at the rotations and the crossings and twists generated accordingly, one can find that the assignment of crossing numbers shown in Fig. 2.5 is consistent with the assignment of values to twists, as in Fig. 2.2. That is, A crossing and a twist of the same handedness acquire the same integral value.
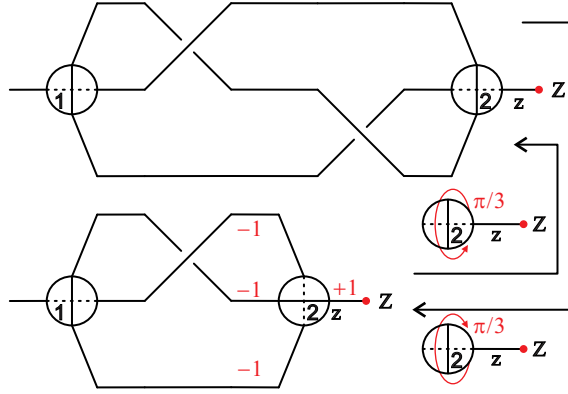
Figure 2.10: The two braids are equivalent because they can be transformed into each other by a $\pi/3$-rotation of node 2.
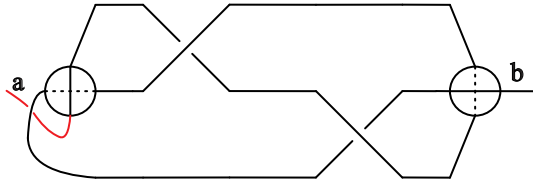
Figure 2.11: A sub-spinnet equivalent to a braid by rotations with respect to the strands of the braid; it does not satisfy our definition of a 3-strand braid any more.

2.3.3 Conserved quantity: effective twist number

Given that the rotations and translations are well-defined equivalence moves, there should be a conserved quantity, remaining the same before and after the moves. Rotations create or annihilate twist and crossings simultaneously, we thus define a composite quantity, christened **effective twist number of a rotation**,

$$\Theta_r = \sum_{e=1}^{4} T_e - 2 \times \sum_{\substack{\text{all Xings} \\ \text{created}}} X_i, \tag{2.1}$$

where T_e is the twist created by the rotation on an edge of the node, X_i is the crossing number of a crossing created by the rotation between any two edges of the node, and the factor of 2 is owing to that a crossing always involve two edges. One can easily check that the rotations in Fig. 2.8, Fig. 2.9, and Fig. A.1 through Fig. A.4 satisfy $\Theta_r \equiv 0$. That is, rotations have a zero effective twist number.

Therefore we can extend Θ_r to a more generalized quantity Θ_0, the **effective twist number** of a subdiagram of an embedded spin netork, by taking into account all the edges that are affected by

26

rotations on the nodes in the subdiagram. We define

$$\Theta_0 = \sum_{\substack{\text{all edges in a} \\ \text{subdiagram}}} T_e - 2 \times \sum_{\substack{\text{all Xings in a} \\ \text{subdiagram}}} X_i, \tag{2.2}$$

where T_e is the twist on an edge of the subdiagram, X_i is the crossing number of a crossing in the subdiagram. Since $\Theta_r \equiv 0$, Θ_0 is indeed a conserved quantity under rotations. In this thesis we are mostly interested in subdiagrams that are either braids or several braids next to each other.

The effective twist number Θ_0 in Eq. 2.2 is also found to be preserved under translation moves.

Note that the effective twist number is not defined in the unframed case, simply because the unframed case has no notion of twists. But then in the unframed case, the number of crossings of a braid is not an invariant and does not characterize the braid by itself.

2.4   Classification of Braids

With the help of equivalence moves - in particular the rotations - we can classify all possible 3-strand braid diagrams into two major types, namely reducible and irreducible braid diagrams. Details can be found in Appendix B. In this section we will just briefly repeat some key results Appendix B that will be used throughout this thesis. In classifying the braids, we treat them as isolated from their ambient spin networks, i.e., we consider a braid together with its two external edges. A remark is that the aforementioned restriction that only the external edge of an end-node of a braid can be the rotation axis of the node ensures the unambiguous assignments of states to the end nodes of a braid and keeps the classification of braids simple. Note also that twists on edges are irrelevant to this classification of braids. Nevertheless, the results are valid for both framed and unframed cases.

> Definition B.1: A braid diagram is **reducible** if it is equivalent to a braid diagram with fewer crossings; otherwise, it is **irreducible**.

The braid on top part of Fig. 2.10 is an example of a reducible braid diagram, while the bottom of the figure shows an irreducible one.

It is convenient to talk about the end-nodes of braids, with certain number of crossings taken into account. An N-crossing end-node is said to be a **reducible end-node** (Definition B.2), if it is equivalent to an M-crossing end-node with $M < N$, by equivalence moves acting on its node; otherwise, it is irreducible.

This gives rise to another definition of reducible braid diagram (Definition B.3). A braid diagram is **reducible** if it has a reducible end-node. If a braid diagram has a reducible left end-node it is called **left-reducible**. If it has both a left- and a right-reducible end node it is **two-way-reducible.** If a braid diagram B can be reduced to an trivial braid, i.e., a braid without crossings, B is a **completely reducible** (Definition B.4).

The following theorem states that it is unnecessary to investigate end-nodes with more than to crossings to see if they are irreducible.

Theorem B.1: An *N*-crossing end-node, $N > 2$, which has an irreducible 2-crossing sub end-node, is irreducible.

Recall the correspondence between an equivalence class of braids and an equivalence class of braid diagrams introduced in Section 2.2, the above classification of braid diagrams should directly apply to braids. That is, in the rest of the thesis we will often say that a braid is reducible or irreducible.

2.5 Representations of braids

Now that a braid stands for an equivalence class of braid diagrams, and the elements in a class transform into each other under equivalence moves, we desire the most convenient braid diagram in a class as the representative of the class. This choice of representative depends on the situation we are in.

According to our study, braids have two useful types of representatives. The first is a unique representative for each braid. In any class of braid diagrams, there is one, and only one, diagram[6] that has twist-free external edges. The reason goes like this: any rotation on an end-node of a braid creates twists on the external edge of the end-node; if there exist two braid diagrams with twist-free external edges in the same equivalence class, they must be related to each other by rotations, which is contradictory to that rotations create twists on external edges. Therefore, with a bit abusing of terminology, we say that a braid is in its **unique representation** when it is represented by its braid diagram without external twists. This representation will be convenient to our investigation of braid dynamics.

The second representation we are going to address is not unique. We know that braid diagrams in an equivalence class are either reducible or irreducible. The irreducible diagrams must all have the same number of crossings; otherwise, those with more crossings can be transformed into those with fewer crossings by rotations, namely they are not irreducible. Since one cannot reduce the number of crossings of an irreducible braid diagram, this number must be the smallest in the class. Following definition B.4, we call such an irreducible braid diagram an **extremum**. A braid has infinite number of extrema[7], which correspond to the infinite number of reducible braid diagrams in the class. Consequently, we say that a braid is in an **extremal representation** when it is represented by one of its extrema.

There is a special case of extremal representations. In Chapter 3 we will meet a special type of braids, the actively interacting braids, whose extrema are trivial braid diagrams with only twists. It is very handy to represent actively interacting braids by these trivial braid diagrams, as we will do in Chapters 4 and 5. In this case we rename an extremal representation a trivial representation.

---

[6]Note that this uniqueness is up to braid relations. But as explained in Section 2.2, a braid diagram strands for all braid diagrams that are equivalent to it by braid relations only!

[7]Lemma 5.3 presents a rigorous proof.

2.6 Evolution Moves

To define the models our results apply to, we have to choose a set of dynamical evolution moves. In spin-foams and other models of dynamics of spin networks, it is common to pick the dual Pachner moves[49, 65, 66]. To motivate the form of them, we posit here it is useful to recall how the Pachner moves arise in combinatorial topology. One defines the topology of a three manifold through operations on a simplicial triangulation. Many different simplicial complexes correspond to the same topological three manifold. Given two of simplicial complexes, one wants to know whether they correspond to the same topological three manifold. Pachner's theorem[67] gives the answer, it says they do if the two simplicial complexes can be connected by a finite sequence of local moves, which are called the Pachner moves. They are illustrated in Figures 2.12 and 2.16(a).

The dual to a simplicial complex is a framed four valent graph in which nodes are dual to tetrahedra and framed edges are dual to faces. One needs the framing of the graphs to preserve orientations. An edge between two nodes tells us that two tetrahedra, dual to those two nodes, share a triangular face. The framing is needed to tell us how to identify the two triangles.

Let us fix a non-singular topological manifold $\mathcal{M}$ and choose a triangulation of it in terms of tetrahedra embedded in $\mathcal{M}$ whose union is homeomorphic to $\mathcal{M}$. Any such simplicial triangulation of $\mathcal{M}$ has a natural dual that is a framed four valent graph embedded in that manifold, $\mathcal{M}$. If one makes a Pachner move on the triangulation, that results in a local move in the framed graph. These are the dual Pachner moves.

Nevertheless, not every embedding of a framed four valent graph in $\mathcal{M}$ is dual to a triangulation of $\mathcal{M}$. Examples of obstructions to finding the dual include the case of two nodes that share three edges that are braided (e.g., in Figure 2.3). This is an embedding of a graph that could not have arisen from taking the dual of a regular simplicial triangulation of $\mathcal{M}$. We note that these obstructions are local, in the sense that a subgraph of the embedded graph could be cut out and replaced by another subgraph that would allow the duality to a triangulation of $\mathcal{M}$.

This leads to the question how one defines the dual Pachner moves on subgraphs of embedded graphs which are not dual to any triangulation of $\mathcal{M}$. The answer is that we do not. We thus have the basic rule:

Basic rule:[8] The evolution rules on embedded framed four valent graphs are the dual Pachner moves and they are allowed only on subgraphs which are dual to a ball in R^3.

We now discuss in detail the moves that are allowed.

2.6.1 $2 \to 3$ and $3 \to 2$ moves

Fig. 2.12 depicts the $2 \leftrightarrow 3$ Pachner move on tetrahedra and the dual move on four valent graphs. One can see that as the result of the move, the 2 vertices together with the edge between in (a) are replaced by three new vertices and three new edges between them in (b), and vice versa.

The result of a $2 \to 3$ move on tetrahedra is unique up to equivalence moves (e.g., rotations). As a consequence the dual $2 \to 3$ move on framed graph embeddings is unique.

---

[8]This rule and other possible rules are discussed in detail in [69].
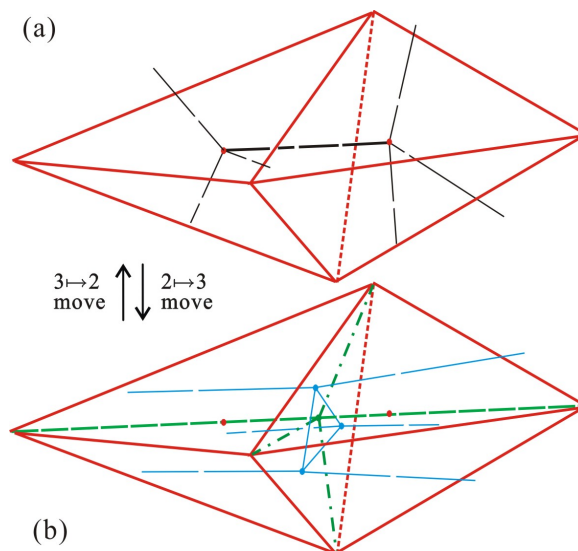
Figure 2.12: (a) shows two tetrahedra with a common face; the black lines represent the dual graph. (b) shows the three tetrahedra that result from a $2 \to 3$ Pachner move applied to the pair of tetrahedra in (a); the blue lines sketch the dual graph.

We now represent the allowed dual $2 \to 3$ move in our diagrammatic notation. This is done in Figures 2.13 and 2.14.

According to the basic rule, a $2 \to 3$ move is doable only on two neighboring nodes with one or more common edges in the case that that subgraph is dual to a triangulation of a ball in R^3. In terms of our diagrammatic notation this translates into the following conditions.

Condition 2.1. *A $2 \to 3$ move is doable on two nodes if and only if*

1. *the two nodes have one, and only one, common edge and can be arranged in either of the forms in Fig. 2.13(a) or Fig. 2.14(a);*

2. *(in the framed case) the common edge is twist-free; otherwise, one has to rotate either node to annihilate the twist);*

3. *the states of the two nodes with respect to the common edge are either both $\oplus$ or both $\ominus$.*

The reasoning for the above conditions is easily understood in terms of the local dual picture of tetrahedra. If Condition 2.1 holds for two neighboring nodes, the edges that form the loop generated by the $2 \to 3$ move are twist-free, as in above figures.

A $3 \to 2$ Pachner move is the reverse of a $2 \to 3$ Pachner move. It needs three tetrahedra, each pair of which share a face. By taking the dual of the simplicial picture, a $3 \to 2$ move on embedded framed four valent graphs is found to act on three nodes that are connected in pairs to make a triangle. The basic rule imposes conditions on a legal $3 \to 2$ move, which are as follows.

30
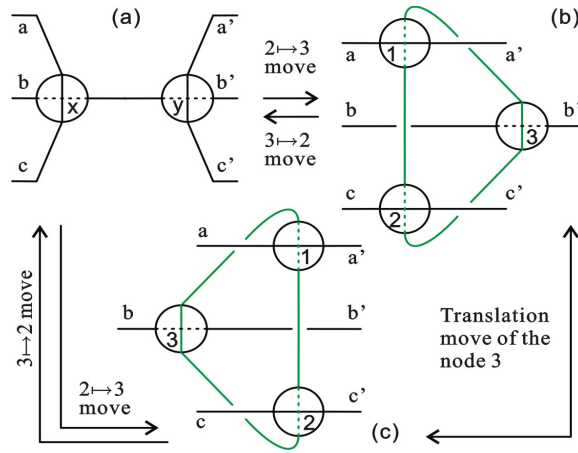
Figure 2.13: (a) is the original configuration of two nodes in $\oplus$-state, ready for a $2 \to 3$ move. (b) is the result of the $2 \to 3$ move from (a); it can also go back to (a) via a $3 \to 2$ move. The configuration of nodes X and Y in Fig. 2.13(a) is dual to the two tetrahedra with a common face in Fig. 2.12(a). By the dashed green lines, Fig. 2.12(b) shows how the two tetrahedra in (a) are decomposed into three tetrahedra, two of which are in the front and one is behind; such an operation is the $2 \to 3$ Pachner move. The dual picture of Fig. 2.12(b) is Fig. 2.13(b), in which a contractible loop is generated (see the green edges). One can also translate the node 3 in Fig. 2.13(b) to the left of the vertical green edge, which gives rise to Fig. 2.13(c). We can go back to Fig. 2.13(a) from (b) and (c) by a reversed move, viz the $3 \to 2$ move. One may notice that in Fig. 2.13(a), the nodes X and Y are all in $\oplus$ if the common edge of X and Y is the rotation axis.

Condition 2.2. *A $3 \to 2$ move is doable on three neighboring nodes if and only if*

1. *the three nodes with their edges can be arranged in one of the four proper configurations, namely Fig. 2.13(b), (c) and Fig. 2.14(b), (c);*

2. *the loop formed by the common edges of the three nodes is contractible (Figures. 2.15(a) & (b));*

3. *In the framed case, the edges forming the loop should be twist-free; Fig. 2.15(c) shows an example violating this condition.*

2.6.2 $1 \to 4$ and $4 \to 1$ Moves

A $1 \to 4$ Pachner move is a decomposition of a single tetrahedron into four tetrahedra contained in it. Its dual is a move that replaces a node by four nodes, connected as the dual of a tetrahedron (Fig. 2.16).

The result of a $1 \to 4$ move is unique up to equivalence moves. In Fig. 2.16(c), one can find four loops formed by the red edges, which are new edges generated by the move. Note that the
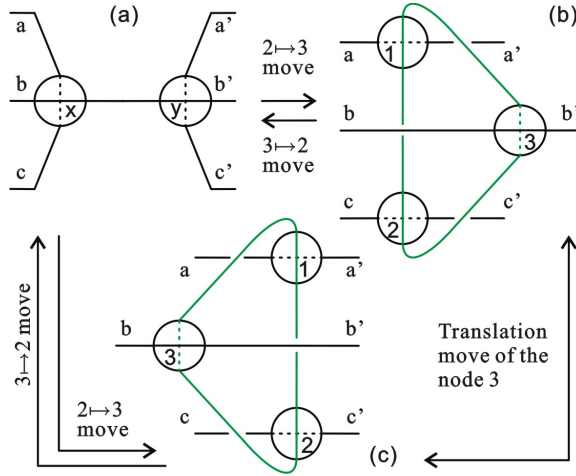
Figure 2.14: This is the case where the two nodes ready for a $2 \to 3$ move are both in ⊖-state with respect to their common edge. (a) is the original configuration of two nodes in ⊖-state, ready for a $2 \to 3$ move. (b) is the result of the $2 \to 3$ move on (a); it also goes back to (a) via a $3 \to 2$ move.

edges newly generated by the $1 \to 4$ move are all twist-free. Note also that since a node is always taken to be dual to a single tetrahedron, the basic rule is always satisfied, and hence a $1 \to 4$ move is not constrained.

A $4 \to 1$ Pachner move is the reverse of a $1 \to 4$ move; thus, it requires finding a configuration of four tetrahedra, in which any two tetrahedra share a face, with four faces left out. This configuration is dual to a tetrahedron that contains the original four. The dual $4 \to 1$ move hence also requires a special starting point: four nodes, each pair of which share an edge. As a result, we have the following conditions for a $4 \to 1$.

Condition 2.3. *A $4 \to 1$ move is doable on four neighboring nodes if and only if*

1. *the four nodes together with their common edges can be arranged as shown in Fig. 2.16(c) or its parity inverse;*

2. *the loops are all contractible, i.e., there does not exist any other edge that goes through the loop or tangled with the loop (e.g., Fig. 2.15);*

3. *closed loops in the initial diagram should be twist-free.*

Note that the dual Pachner moves defined in this section carefully record the relative positions of the edges and nodes (i.e., which is above and which is under)in a projection of the 3-dimensional graph. We have to do this because our graphs are embedded. The dual Pachner moves in Spin Foam models contain only the permutation relations of edges, which is sufficient for triangulations. Therefore, our Pachner moves are adapted to the embedded case and are able to endow embedded 4-valent spin networks a spin-foam like dynamics.
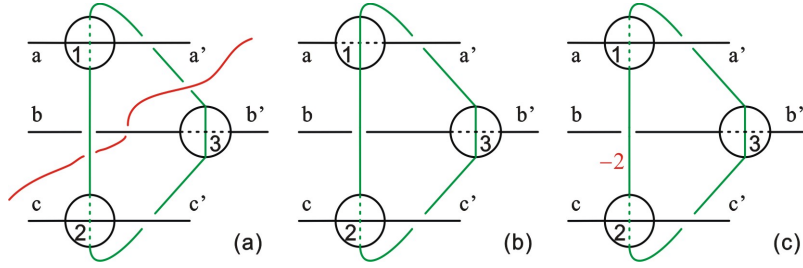
Figure 2.15: These are examples of configurations that do not allow a $3 \to 2$ move, owing to respectively the red edge and edge a' going through the green loops, which makes the latter incontractible; (c) is not either because of the $2\pi/3$-twist on a green edge.
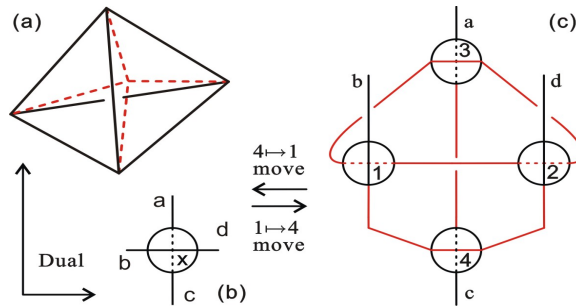
Figure 2.16: (a) shows how a $1 \to 4$ move is viewed with tetrahedra; dashed red lines illustrate the splitting of the big tetrahedron into four tetrahedra. (b) is the node dual to the big tetrahedron in (a). (c) comes from (b) via a $1 \to 4$ move; it can go back to (b) by a $4 \to 1$ move. Red lines in (c) are the edges generated by the move.

2.6.3 The unframed case and the role of internal twist

The same evolution moves apply to the unframed case, since the structure of nodes is sufficient to define the dual Pachner moves. One might posit an extension of the class of theories just described, such that internal twists are allowed on closed loops that are annihilated by a $3 \to 2$ move or a $4 \to 1$ move. In [41], one can see that this extension enlarges the class of actively propagating braids.

2.6.4 A conserved quantity

Eq. 2.2 defines a conserved quantity Θ_0, the effective twist of a sub-spinnet, which is invariant under equivalence moves. Now we show that we can generalize this Θ_0 to a quantity that is conserved also under the evolution moves, with the following modifications. Within a subdiagram $\mathcal{R}$, the edges and nodes of the diagram define continuous curves where the edges continue across the diagram as noted (that is each node projection gives a choice of the four incident edges into

two pairs, each of which is connected through the node). These curves are of two kinds, open, which end at two points on the boundary of $\mathcal{R}$ and closed. In addition, we define an *isolated substructure*[38] to be a subgraph which is attached to the rest of the graph by a single edge.

- Choose an arbitrary orientation of the open curves.

- Sum over the orientations of the closed curves.

- In the counting of crossings, all crossings of edges with edges in isolated substructures are to be ignored.

Then the following is conserved under all equivalence moves and evolution moves that act entirely within $\mathcal{R}$.

$$
\Theta_{\mathcal{R}} = \sum_{\text{Orientations of closed curves in } \mathcal{R}} \left[\sum_{\text{all edges in } \mathcal{R}} T_e - 2 \times \sum_{\text{all Xings in } \mathcal{R}} X_i \right] \tag{2.3}
$$

2.7 Stability of braids under the evolution moves

Consider a braid of the form of Figure 2.3. It is not difficult to show that the subgraph formed by the two nodes and the three shared edges is not dual to any triangulation of a ball in R^3. Hence a $2 \rightarrow 3$ move cannot be done on these two nodes. Nor can a $3 \rightarrow 2$ move be done on any three nodes that contain this pair for the same reason. Thus, the braid is stable under single moves.

We can extend this to the general observation that any braid whose graph is not dual to a triangulation of a ball in $\mathbb{R}^3$ is stable under single allowed moves. We believe that a stronger stability result for such braids exists, but postpone the consideration of this problem to future work.

The stable braid excitations satisfy the definition of noiseless subsystems in [15]. They are thus considered local excitations with conserved quantities. This locality has a subtlety, however, which will be discussed in Chapter 8.

2.8 Summary

In this chapter, we proposed a new notation, namely the tube-sphere notation, for embedded (framed) 4-valent spin-networks. With this notation, we discovered an interesting type of topological structures, the 3-strand braids, as sub-structures of embedded spin networks. We then developed a graphic calculus for local equivalence moves and local evolutions moves of embedded 4-valent spin networks, and hence for the braids. The equivalence moves are important and useful in two aspects. Firstly, by rotations, we classify 3-strand braids into two major types: reducible braids and irreducible braids; the former are further classified for the purpose of subsequent works. Secondly, by equivalence moves one is able to calculate braid propagation and interactions of embedded 4-valent spin networks in the next chapter. The local evolution moves govern the evolution of spin networks in time.

These results play a key role in the rest of this thesis and serve as a foundation of the whole dynamical theory of braids. In particular, in the next chapter we will see how these moves lead to propagation and interaction of braids on the network they are living.

Chapter 3

Braid Dynamics I: Propagation and Direct Interaction

Equipped with the graphic calculus of evolutions and equivalence moves, stable braids have rich dynamics: they can propagate on their ambient spin network, and some of them can join and become new braids. In this chapter, we are going to show part of this striking property of our braids. We will first study braid propagation and then a type of braid interactions called direct interaction, as opposed to another type called exchange interaction, which is a topic in Chapter 7. Before we reach Chapter 7, however, we may use interaction and direction interaction interchangeably.

3.1   Braid Propagation

We now come to the results on propagation of braids that follow from the evolution moves we have defined here. Because a braids can be considered an insertion in an edge, it makes sense to speak of them propagating to the left or to the right along that edge. To help visualize this in the diagrams we will always arrange a braid so that the edge of the graph it interrupts runs horizontally on the page. There are two types of propagation of braids, namely induced propagation and active propagation.

Under the evolution moves, in particular the $1 \rightarrow 4$ and $4 \rightarrow 1$ moves, some parts of a spin network may expand, while other parts may contract. Since a braid can be considered an insertion in an edge, if the ambient spin network of one end-node of the braid undergoes expansion and that of the other end-node of the braid undergoes contraction, the braid effectively moves towards the direction of contraction. We call this type of braid propagation *induced propagation* as it is induced by the evolutional change of the part of the spin network other than the braid itself. Because we can always arrange a braid diagram horizontally, when a braid propagates in an induced way, it may propagate to its right or its left. Since in an induced propagation of a braid, the braid is not involved in the action of evolution moves that cause this propagation, the braid remains the same.

As opposed to induced braid propagation, which can occur to any braid, there is *active braid propagation*, which occurs only to specific configurations and braids. In an active propagation

of a braid, the braid exchanges position with its adjacent structure under evolution moves; it is called active because the braid's structure undergoes intermediate changes in the process of the propagation. One can also the right and left active propagation of a braid. Nevertheless, active braid propagation needs some special settings that may bring changes to the overall setting in the thesis, we thus present it in Appendix C.

3.2   Direct Interaction
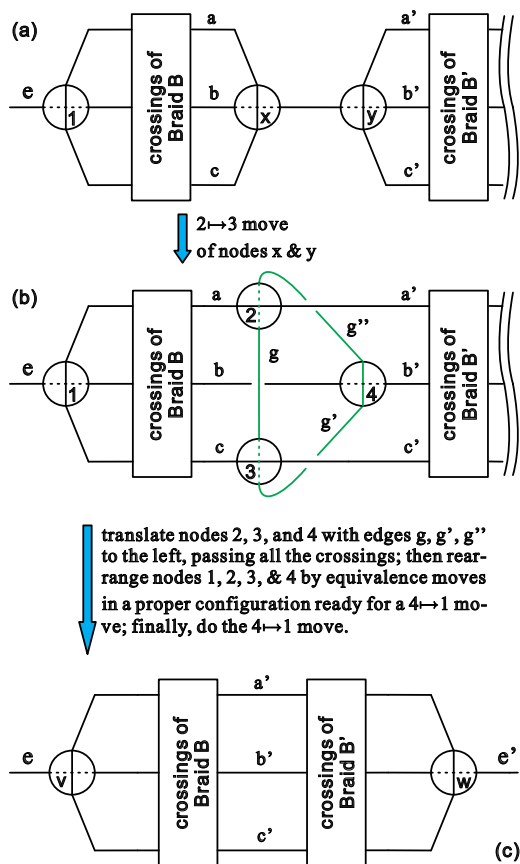
Figure 3.1: The direct interaction of two braids.

We show now that in a few circumstances braids can interact with each other, in the sense that two braids can meet and turn through a sequence of local moves into a single braid. We thus call this type of interactions **direction interaction**. This will be possible in the case that at least one of the braids are of a special class called *actively interacting*. As the moves are time reversal invariant, it is also possible for a single braid to decay to two braids, so long as one of the products is of this special class.

37

The initial state for a direct interaction has in it two braids adjacent to each other along an edge, which can be reached by either or both braids propagating along an edge. Certain series of evolution moves acting on such an initial state may result in a single braid (Fig. 3.1). The time reversed history will then give a case of a single braid decaying to two braids that can then propagate separately, which will be discussed in Section 7.3.

It turns out that braids may interact actively or passively. If a braid interacts actively, it can interact with any braid it encounters, and hence are called *actively interacting*. All other braids interact only passively, i.e., only if they encounter an actively interacting braid. We will see shortly how and when a braid can be actively interacting. We note also the possibility that braids may interact from the left or right, so we distinguish those two possibilities.

As in the case of active propagation, the **active right-interaction** of a braid B with a neighboring braid B' proceeds through a series of steps, indicated in Fig. 3.1. Each step must be a possible evolution or equivalence move for the interaction to take place.

1. Begin with the initial condition 3.1(a). As in the case of propagation first make a $2 \rightarrow 3$ move on nodes X and Y, leading to the configuration shown in Fig. 3.1(b).

2. If possible, without creating any tangles of the kind shown in Fig. C.2, translate nodes 2, 3, and 4 together with their common edge g, g', and g'' to the left, passing all crossings of B.

3. If possible, re-arrange nodes 1, 2, 3, and 4 with their edges, by equivalence moves into a configuration that allows $4 \rightarrow 1$ move.

4. If possible (see Condition 2.3), do the $4 \rightarrow 1$ move on nodes 1, 2, 3, and 4, resulting in Fig. 3.1(c).

The actively interacting braid is the one which the three nodes are pulled through, in this case it is braid B. We will see shortly that the class of such braids is very limited. The other braid, which may be arbitrary, is said to have passively interacted.

3.2.1 Examples of interacting braids

As we shall see in the next subsection, most braids do not actively interact. Because the last step of an interaction is a $4 \rightarrow 1$ move, the possibilities are limited because the initial step of a $4 \rightarrow 1$ move requires four nodes making up a tetrahedron. Here the issue raised above of how restrictive are the rules for a $4 \rightarrow 1$ move comes in. If we are less restrictive and allow internal twists, we get more actively interacting braids.

Even allowing moves that annihilate internal twists, all the examples we have so far found of actively interacting braids are equivalent to the trivial braid, made up of three strands with no crossings, but with twists on the edges.

Our first example of interaction is shown in Fig. 3.2. Fig. 3.2(a) depicts two braids: a 1-crossing braid B on the left of a braid B' with arbitrary crossings and twists. The right end-node W of braid B' is irrelevant, which can be either $\oplus$ or $\ominus$, here we assume it in the state $\ominus$ for the convenience of showing the left-interaction later. One may notice the $2\pi/3$-twist on edge c of
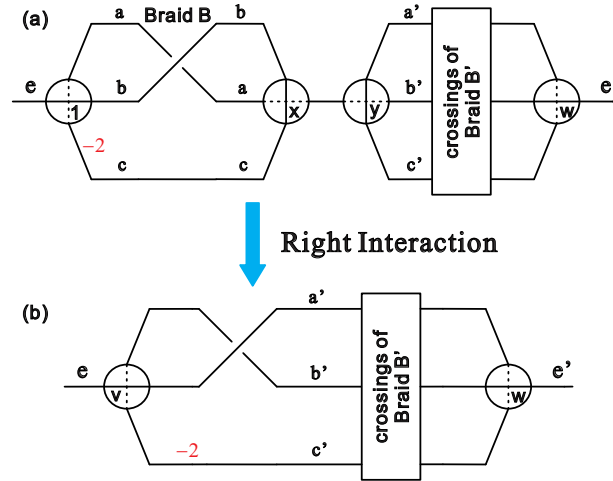
Figure 3.2: (a) contains a braid B on the left and a braid B' with arbitrary crossings & twists on the right. (b) is the resulted braid of the active right-interatction of B on B'.

braid B, the presence of which may be essential for the interaction to be done and will be explained shortly. The active right-interaction of braid B on B' results in the new braid shown in Fig. 3.2(b); one can see that the initial twist of braid B in Fig. 3.2(a) is preserved in Fig. 3.2(b) under the interaction.

The complete steps for the interaction are shown in Fig. 3.8 at the end of the chapter. In Fig. 3.8(f), the initial twist on strand c, -2, of braid B cancels the twist, $+2$, created by rotations, such that nodes 1, 2, 3, and 4 with their common edges are in a proper configuration for a $4 \to 1$ move, satisfying Condition 2.3. In addition, surprisingly, as already mentioned, the initial twists of braid B are preserved.

The same braid can interact to the left as well, as we show in Fig. 3.3.

Note that the braid B is completely reducible from either end; if we reduce it by a rotation of its right end-node, we get its equivalent braid, Fig. 3.4(b), which is a trivial braid with twists on all three strands and on its right external edge.

The second example of right interaction is shown in Fig. 3.5. This braid is also left-interacting, as can be easily checked. And it is also equivalent to a trivial braid with twists, from top to bottom the twists are 0, 0, +2, respectively, and a twist -2 on the right external edge. As for the first example, the initial twists in this example cancel the possible internal twists in the process of interaction, and they are individually conserved.

3.2.2 General results on direct interactions

Now we give some general results that limit the actively interacting braids.

Theorem 3.1. *A (left-) right-irreducible braid is not (left-) actively right-interacting. An irreducible braid is always inactive during an interaction. This also implies that only (left-) right-*

39
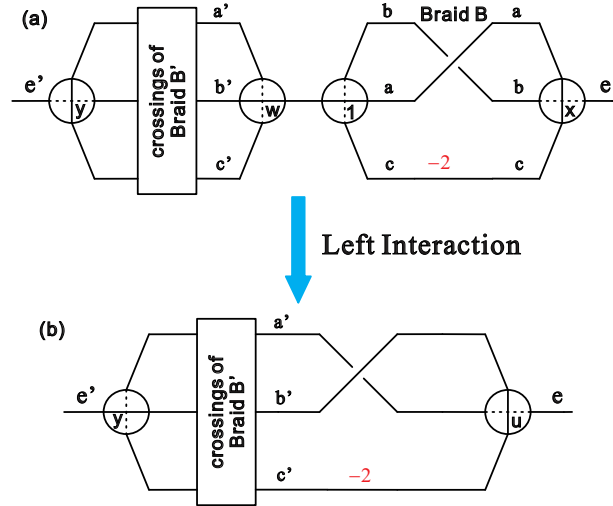
Figure 3.3: The braid in Fig. 3.2 can also interact from the left.
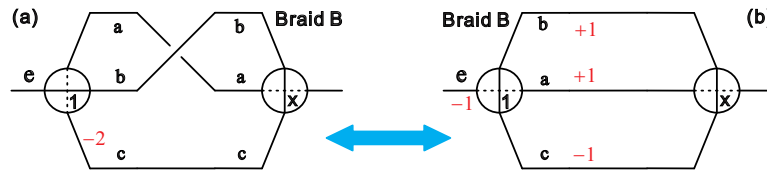
Figure 3.4: The braid in 3.2 is equivalent to a trivial braid with twists.

reducible braids can be actively (left-) right-interacting, which manifests the chirality of interactions.

Proof. As shown in Fig. 3.1, to complete a (left-) right-interaction requires the translation of nodes 2, 3, and 4 together with their common edges g, g', and g''. Nevertheless, as long as a braid is (left-) right-irreducible, if one assume that the braid is actively interacting and carries out the calculation, a tangle like that in Fig. Fig. C.2 arises and prevents the final $4 \to 1$ move according to Condition 2.3; hence, the right-interaction cannot be completed as desired. It is the same for a left-interaction. Therefore, is a braid is irreducible, i.e., both left- and right-irreducible, the braid can never actively interact onto anther braid; it always behaves inactively in any type of interactions. □

Theorem 3.2. *If the settings for active braid propagation described in Appendix C are allowed, a braid that is actively (left-/right-) two-way-interacting must also be actively propagating.*

Proof. The proof contains two parts. 1) We notice that in doing a direct interaction one needs to translate all the three nodes (say nodes α, β, and γ) and their common edges, obtained from the initial $2 \to 3$ move, all the way through the crossings of the active braid, say braid B. If braid

40
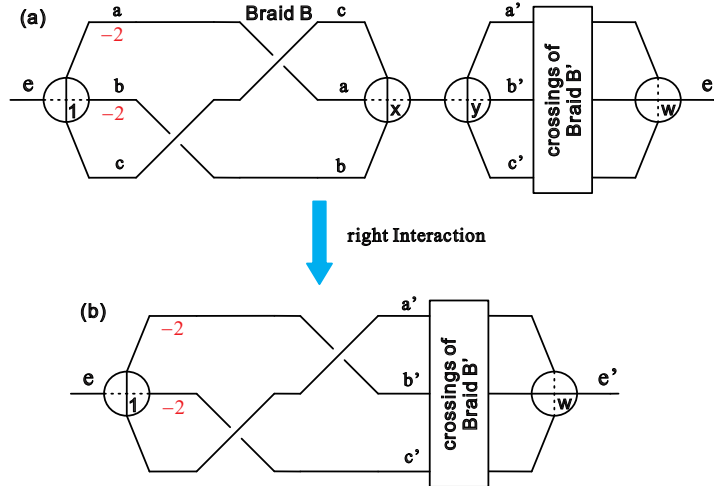
Figure 3.5: Second example of a right direct interaction.

B is to actively propagate in the same direction, however, two of the nodes α, β, and γ must be successfully translated. Therefore, if braid B is able to actively interact to the left (right), i.e., the translation of α, β, and γ does not cause any tanglement, the translation of any two of the three nodes should not lead to any tanglement either.

2) Given part 1), if braid B can actively interact, after being translated nodes α, β, and γ together with an end-node (say node 1) of braid B can be arranged in a proper configuration for a $4 \rightarrow 1$ move. There is no loss of generality to assume that we need to translate α and β for B to actively propagate in the same direction as its interaction; hence, after the translation we must demand that α, β, and node 1 can be rearranged in a proper configuration for a $3 \rightarrow 2$ move. So the question is, if α, β, γ and 1 can be configured for a $4 \rightarrow 1$ move, can we also configure α, β, and 1 for a $3 \rightarrow 2$ move?

Let us consider active right-interaction. In the proper configuration for a $4 \rightarrow 1$ move, we rename α, β, and γ by the permutation of 2, 3 and 4, since we don't know the relative positions of α, β, and γ after their translation over the crossings of an arbitrary braid B; the situation is shown in Fig. 3.6(a). We assumed the active propagation of braid B requires translating α and β; however, we don't know really know the renaming of α and β after their translation within an arbitrary braid B; they can be 2 and 3, or 2 and 4, or 3 and 4. Therefore, to prove that right-interaction implies right-propagation, it suffices to show that one can always re-arrange nodes 1, 2 and 3, or 1, 2, and 4, or 1, 3, and 4 in a proper configuration for a $3 \rightarrow 2$ move if 1, 2, 3 and 4 can be configured as in Fig. 3.6(a).

Fig. 3.6 clearly illustrates the procedure of re-arranging nodes 1, 3, and 4 in a proper configuration for a $3 \rightarrow 2$ move (compare the green loop in (c) with Fig. 2.14(b)), from the proper configuration of 1, 2, 3, and 4 for a $4 \rightarrow 1$ move. Interestingly and fortunately, all the equivalence moves taking 1, 3, and 4 in 3.6(a) to them in (c) do not result in any twist along the green loop, which satisfies Condition 2.2; this is a subtlety of the proof. As a consequence of symmetry,

41
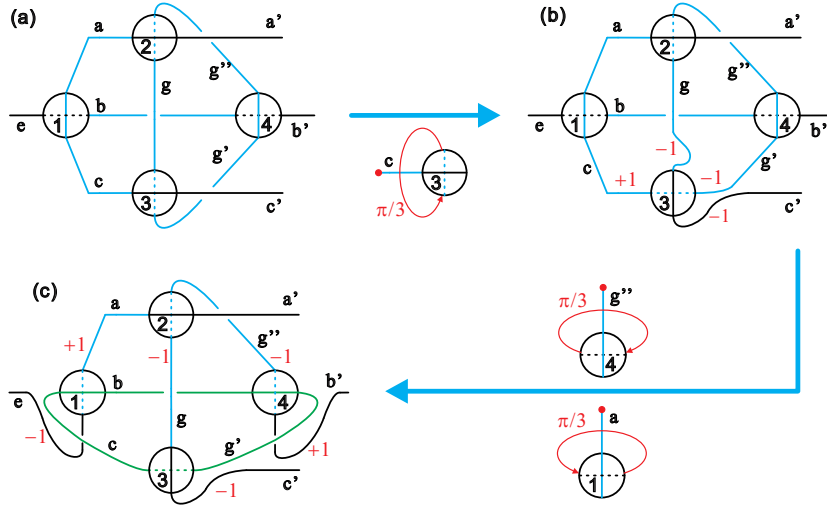
Figure 3.6: This figure shows the full procedure of re-arranging nodes 1, 3, and 4 in (a) in a proper configuration for a 3 → 2 move, as in (c). Note that the green loop in (c) is twist free after rotating nodes 1 and 4 from (b).

nodes 1, 2, and 4 in Fig. 3.6(a) can also be configured properly for a 3 → 2 move. The case of re-arranging nodes 1, 2, and 3 in Fig. 3.6(a) in a proper configuration for a 3 → 2 move is depicted in Fig. 3.7.

The proof in the case of an active left-interaction follows immediately by similarity and symmetry. Therefore, the theorem is proved.

As a closing remark, the validity of the theorem can also be seen if one looks at the local dual picture of a 4 → 1 move, in which four tetrahedra stick together forming a new tetrahedron; any three of them can form two tetrahedra by a 3 → 2 Pachner move. The above proof simply interpret this topological picture in a clear way with our notation of the embedded spinnets. In fact, the examples we have found of actively interacting braids are all reducible to a trivial braid with twists. This is consistent with these general results. □

3.3 Summary

We have considered here the interaction and propagation of locally topologically stable braids in four valent graphs of the kind that occur in loop quantum gravity and spin foam models. The dynamics is restricted to those coming from the dual Pachner moves, which includes the widely studied spin foam models. The graphs representing the states are embedded in a three manifold up to diffeomorphism. We considered both the framed and unframed cases. We also neglected the labels or colors on the spin networks as our results do not depend on them, nor do they depend on the precise amplitudes of the dual Pachner moves, so long as they are non-vanishing.

We studied braids made up of two 4-valent nodes sharing three edges and found three classes
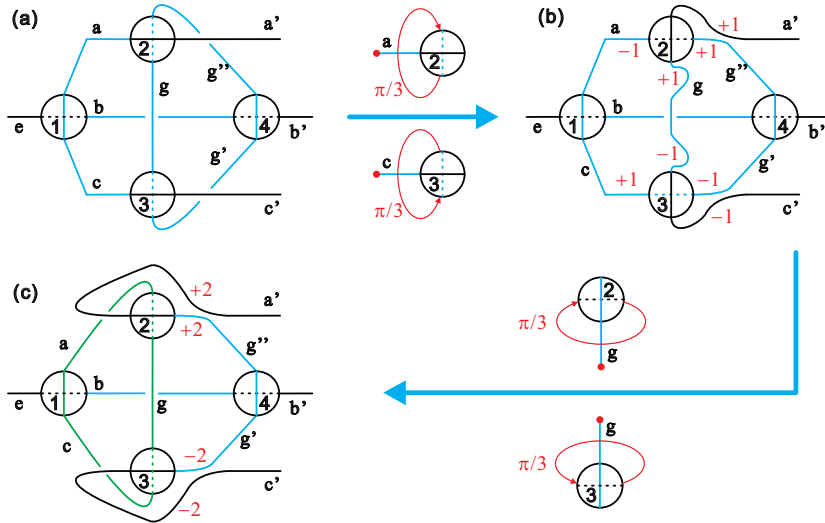
Figure 3.7: This figure shows the full procedure of re-arranging nodes 1, 2, and 3 in (a) in a proper configuration for a $3 \to 2$ move, as in (c). Note that the green loop in (c) is twist free after rotating nodes 2 and 3 from (b).

of them.

- Actively interacting braids, which also propagate. All the examples found so far are completely reducible to a trivial braid with twisted edges. This means that they are characterized by their end-node states and three integers that are the twists on the three edges.

- Braids that are not actively interacting. The possibilities for these are limited by general results we found.

- Braids that are neither actively interacting or actively propagating.

It is very interesting to note that the braids required in the three-valent case to realize Bilson-Thompson's Helon mode[12] also are classified by three integers representing twists on an unbraid[39]. This suggests that it may be possible to incorporate the Helon model with interactions within the dynamics of four-valent braids studied here. Moreover, combined with these results, in Chapter 7 we will show that actively interacting braids are analogous to bosons.

Other interesting research lines in this direction also exist. For example, in usual settings of Spin Foam models, Tensor models or Group Field Theories, graphs are unembedded and labeled by elements of the appropriate permutation groups, and are then called fat graphs. Whether the simplicial complex associated to a given fat graph as a Feynman diagram of a suitable field theory is a manifold or not can be explicitly determined[68]. It would be very interesting to clarify the relationship between the unembedded fat graphs and our embedded (framed) graphs and to see if our results also apply in the usual Spin Foam or Group Field Theory settings. Recently, Prémont-Schwarz has also obtained related results in the unembedded case[69].
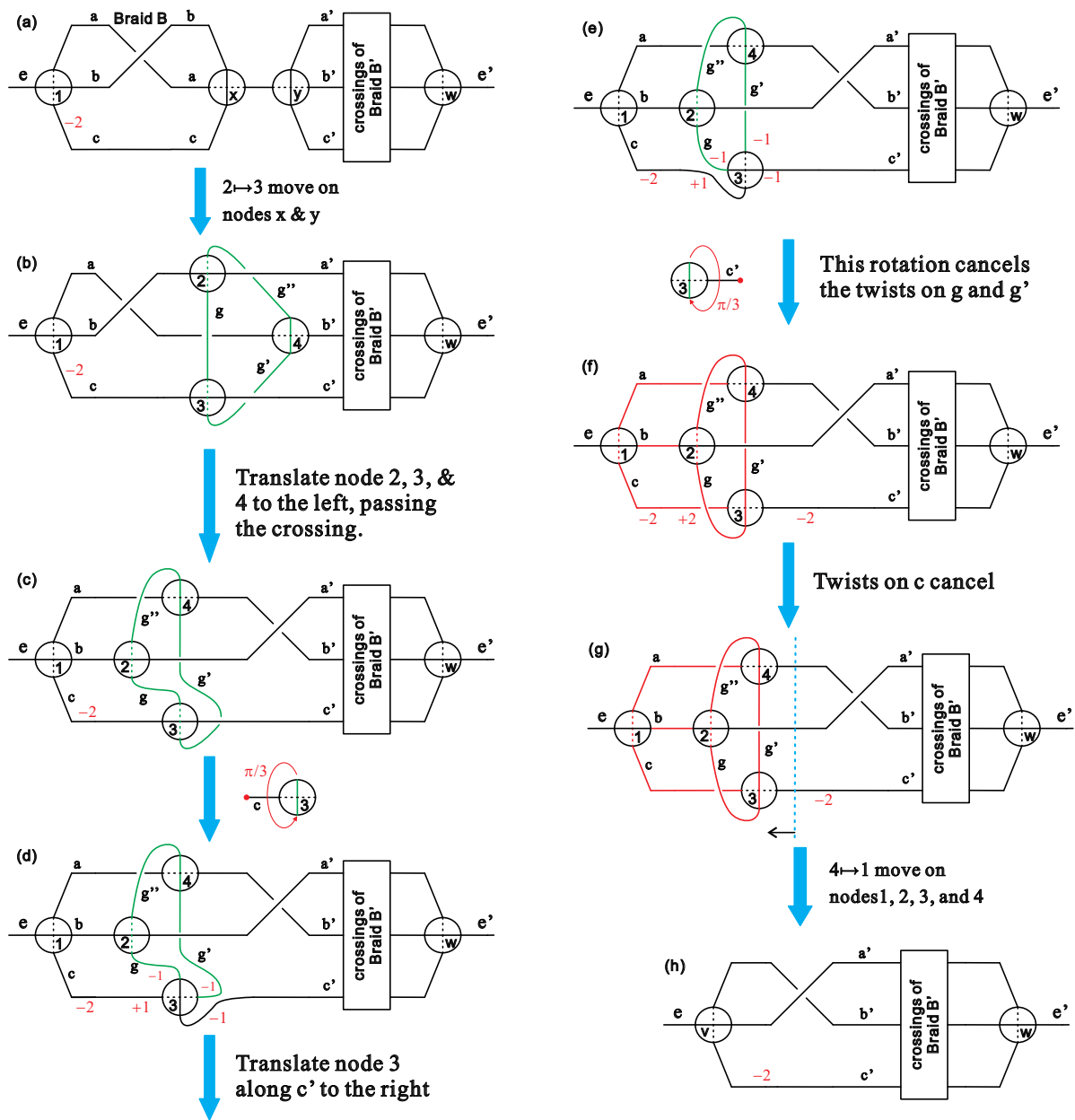
Figure 3.8: The detail of the first example of right direct interaction

Chapter 4

Algebraic Formalism: Actively Interacting Braids

Despite the power of the previously developed graphic calculus, a symbolic algebra would provide a concise tool, convenient for computation and more importantly more able to demonstrate conserved quantities as "quantum numbers". As the ultimate goal of this thesis is to interpret certain braid excitations as matter degrees of freedom in a physical way - particularly to see if the braid excitations can be mapped to Standard Model particles - we need a symbolic algebra that exhibits possible symmetries in a more transparent, lucid way.

Indeed, as a follow-up work of [15], [39] took a similar algebraic approach for three-valent spin networks; it characterizes each capped braid by only three integers, the Louis numbers, named after Louis Kauffman. In the 4-valent case, however, a braid is characterized by more integers, as one will see.

In this and the next chapter, we shall develop an algebraic formalism of 3-strand braids and their dynamics. In this new formalism, we will find many interesting properties of the braids, which were disguised in the graphic formalism. Because of the key role the actively interacting braids play in our approach, in this chapter we concentrate on these braids.

4.1   Notation

We decide to keep actively interacting braids in their trivial representations rather than unique representations, as opposed to what we did in Chapter 3. This choice will turn out to be extremely convenient in the algebraic formalism.

Let us first pin down the notation. We found that it is handy to denote a generic trivial braid in Fig. 4.1(a) algebraically with the notation in Eq. 4.1,

$$\begin{matrix} S_l \\ T_l \end{matrix}[T_a, T_b, T_c]\begin{matrix} S_r \\ T_r \end{matrix}, \tag{4.1}$$

where S_l, S_r, being '+' or '−', are respectively the states of the left and right end-nodes of a braid, T_l, T_r, called the **left** and **right external twists**, are respectively the twists on the left and right

external edges of a braid, and the triple $[T_a, T_b, T_c]$ records the twists on the three strands respectively in the order shown in Fig. 4.1(a), which are thus named the **internal twists**. The subscript a of an internal twist T_a is abstract and has no meaning before its position in the triple is fixed. So $[T_a, T_b, T_c] = [T_d, T_e, T_f]$ means $T_a = T_d, T_b = T_e$, and $T_c = T_f$. In the rest of the chapter, we will also consider the addition of two triple of twists, i.e., $[T_a, T_b, T_c] + [T_d, T_e, T_f] = [T_a + T_d, T_b + T_e, T_c + T_f]$.

All twists are valued in $\mathbb{Z}$ in units of $\pi/3$[40]. For example, we can denote the braid in Fig. 4.1(b) by $_{-1}^{+}[-1, 1, +2]_0^-$. Note that for a trivial braid diagram that interact actively, the set $\{T_l, S_l, T_a, T_b, T_c, S_r, T_r\}$ characterizing it is not completely arbitrary but rather has the following constraints.

1. $S_l \equiv S_r$. If a braid is actively interacting, each of its trivial braid diagrams must have both end-nodes in the same state (so the braid in Fig. 4.1(b) does not actively interact).

2. the triple $[T_a, T_b, T_c]$ is not arbitrary; however, the general pattern of them, ensuring active interaction, has not yet been found. Nevertheless, the algebra formulated in this chapter may turn out to be helpful to resolve this problem.
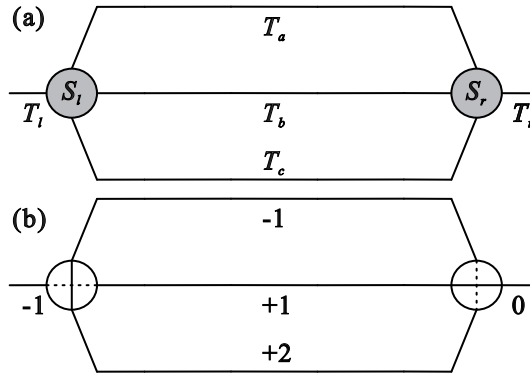
Figure 4.1: (a) is a trivial braid in general, in which the two unknown end-nodes are filled in grey. (b) is an instance of (a).

4.2 Algebra of equivalence moves: symmetries and relations

We are looking for a correspondence between our braids and particles, or matter degrees of freedom in general. If a trivial braid corresponds to a particle, its equivalent braids corresponding to the same particle. This fundamental degeneracy of a particle is a direct result of diffeomorphism invariance because equivalence moves do not change the diffeomorphism class of an embedding. Therefore, it is necessary to find out for any equivalence class of braid diagrams, in an algebraic way adapted to our new algebraic notation, how a trivial representation of a braid is related to

another trivial representation of the same braid, in particular how the set of quantities characterizing the representation changes, and more importantly what the conserved quantities are.
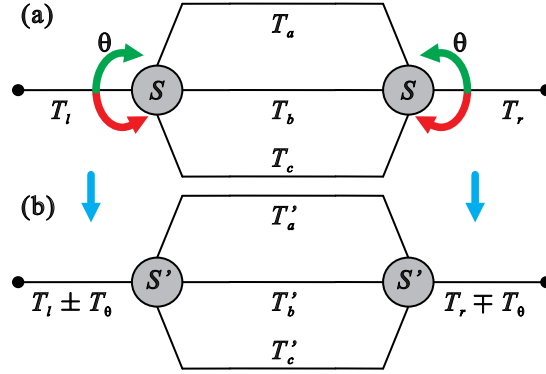
Figure 4.2: (a) is a actively interacting trivial braid in general; (b) is obtained from (a) by same amount of rotations respectively on both end-nodes of (a) in the same direction (either green or red) shown in the figure. $T_\theta \in \mathbb{Z}$ is the twist induced by the rotation θ. $[T'_a, T'_b, T'_c] = [P^S_\theta(T_a, T_b, T_c)]$, where P^S_θ is the permutation depending on both S and θ.

The tools we can utilize are the rotations introduced in Chapter 2. That is, we can use, e.g., $\pi/3$ rotations, to take a trivial braid to another. Concentrating on trivial braids only, however, we do not expect any crossing to appear because a single rotation on an end-node of a braid diagram creates/annihilates crossings, so we must apply rotations on both end-nodes of a trivial braid simultaneously, such that no crossing arises. The idea is illustrated in Fig. 4.2. A remark is that the "same direction" we mentioned in the caption of Fig. 4.2 is with respect to the surface the braid is projected on, i.e., this page; nonetheless, in our definition of rotation with respect to the rotation axis, i.e., the external edges, the rotation θ of the left end-node and the one of the right end-node are of opposite handedness. This has two immediate consequences: 1) in Fig. 4.2(b), while the resulted twist on the left external edge is $T_l \pm T_\theta$, the one on the right is $T_r \mp T_\theta$, a sign difference appears; and 2) this process creates no crossing and interestingly no extra twists on the three strands of the braid but rather results in the twists $[T'_a, T'_b, T'_c]$ in Fig. 4.2(b) as a permutation $[P^S_\theta(T_a, T_b, T_c)]$ of the three twists in Fig. 4.2(a). Note that P^S_θ depends also on S, the state of the end-nodes before being rotated, which is a special property of rotations in 4-valent case. We name a whole procedure of this type on a braid a **simultaneous rotation**.

We can describe the action of a simultaneous rotation on a trivial braid algebraically. We first define an operator for a simultaneous rotation that acts simultaneously on both end-nodes of braid. We denote the operator by $R_{n,-n}$, where n is the amount of rotation valued in units of $\pi/3$, i.e., $n \in \mathbb{Z}$, and the signs, which must be opposite in the first and the second subscripts, indicate respectively the handedness of rotations on left and right end-nodes. The second index of R seems a bit redundant; however, we keep it to make the rotation handedness explicit. Moreover, a state S is simply a sign, $+$ or $-$, so we let $-(+) = -$ and $-(-) = +$, i.e., $-S = \bar{S}$ both denoting the opposite

of S. Hence, in general we have

$$R_{n,-n}(^S_{T_l}[T_a, T_b, T_c]^S_{T_r}) = {}^{(-)^n S}_{T_l+n}[P^S_n(T_a, T_b, T_c)]^{(-)^n S}_{T_r-n},$$ (4.2)

where $(-)^n$ enters the equation because a $\pi/3$ rotation changes the end-node state once. When n is even, $R_{n,-n}$ does not change the end-node state of a braid, it is then christened an **even simultaneous rotation**, otherwise it is named an **odd simultaneous rotation**. The RHS of Eq. 4.2 clearly presents the three effects of a simultaneous rotation $R_{n,-n}$ on a trivial braid: the change of end-node state depending on n, the change of external twists depending on n, and the induced permutation P^S_n on the triple of internal twists, which is determined by the end-node state S before the action of R, n, and the handedness of the rotation on the left end-node.

In view of that $\pi/3$ rotations, corresponding to $n = \pm 1$, generate all possible rotations on the nodes of an embedded 4-valent spin network[40], R satisfies

$$R_{n,-n} = R^{(n)}_{1,-1},$$ (4.3)

where (n) means n-th power, e.g., $R^{(2)}_{1,-1} = R_{2,-2}$ and $R^{(-2)}_{1,-1} = R_{-2,2}$. Nevertheless, Eq. 4.3 is actually formal and is not as simple as it appears to be. The reason lies in that a simultaneous rotation induces a permutation depending on the end-node state before taking the rotation and that a $\pi/3$ inverses the end-node state. More precisely, for example, a rotation $R_{2,-2}$ is equal to two $R_{1,-1}$ in a row; the first $R_{1,-1}$ induces a permutation, flipping the end-node state from, say S, to $\bar{S}$, so the permutation induced by the second $R_{1,-1}$ now actually respects $\bar{S}$ rather than S. Mathematically, this reads

$$R_{2,-2}(^S_{T_l}[T_a, T_b, T_c]^S_{T_r}) = R_{1,-1}(^{\bar{S}}_{T_l+1}[P^S_1(T_a, T_b, T_c)]^{\bar{S}}_{T_r-1}) = {}^S_{T_l+2}[P^{\bar{S}}_1 P^S_1(T_a, T_b, T_c)]^S_{T_r-2}$$

In other words, the permutation induced by $R_{2,-2}$ is $P^{\bar{S}}_1 P^S_1$ but not $P^S_1 P^S_1$, we'll call this permutation P^S_2. This is readily generalized to higher rotations. Clearly, an induced permutation is an element of the permutation group $S_3 = Sym([T_a, T_b, T_c])$. In terms of disjoint cycles,

$$S_3 = \{\mathbb{1}, (1\ 2), (2\ 3), (1\ 3), (1\ 2\ 3), (1\ 3\ 2)\},$$

where for example, (1 2) means exchanging elements 1 an 2 in the triple $[T_a, T_b, T_c]$ and leaving the third one fixed, and (1 2 3) reads cyclically moving the first element in the triple to the second, the second to the third, and the third to the first. Moreover, for a product of permutations, the order of its action on a triple is, in our convention, from right to left.

It is then demanded but sufficient to study a simultaneous rotation of $\pi/3$ on both end-nodes of a trivial braid to fully understand how a general simultaneous rotation works and to obtain our desired algebraic relations in general. This is consistent to that $\pi/3$ rotations are generators of all rotations of braids. Fig. 4.3 illustrates this.

To obtain the exact algebraic form of this simultaneous rotation of $\pi/3$, we can split the rotation into two consecutive ones respectively on the two end-nodes of the braid in Fig. 4.3. Our choice is to first rotate the left and then the right end-nodes of the trivial braid in (a); it is obvious that
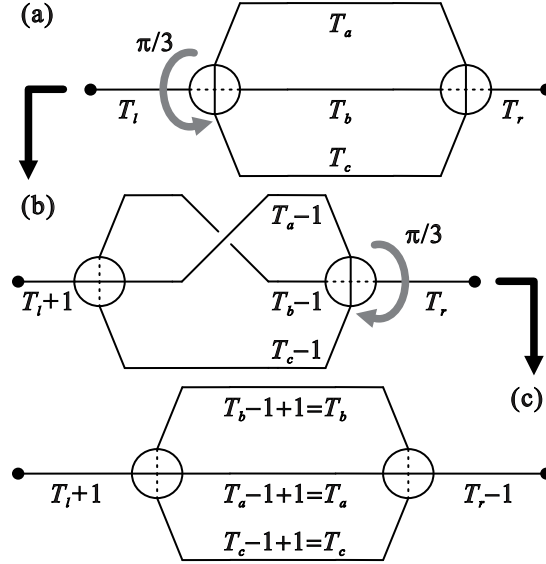
Figure 4.3: A simultaneous rotation of $\pi/3$ is split into two steps, namely two $\pi/3$ rotations respectively on the two end-nodes of the braid in (a). After a right-handed $\pi/3$ rotation on the left end-node, (a) gives rises to (b), in which all twists but T_r are modified from those in (a) accordingly, and a crossing is created. By another left-handed $\pi/3$ rotation on the right end-node of (b), however, a trivial braid appears again in (c). One sees that the induced permutation by this simultaneous rotation is $P_{+1}^+ = (1\ 2)$.

the order of this splitting does not matter, which guarantees that a simultaneous rotation is well-defined. This rotation gives an equivalence relation between the trivial braid in Fig. 4.3(a) and the one in (c), whose algebraic form is now clear:

$$R_{+1,-1}(^+_{T_l}[T_a, T_b, T_c]^+_{T_r}) = \ ^-_{T_l+1}[T_b, T_a, T_c]^-_{T_r-1} \ .$$

The permutation implied in this relation is $[P_{+1}^+(T_a, T_b, T_c)] = [T_b, T_a, T_c]$, i.e., $P_{+1}^+ = (1\ 2)$. Since each node has only two states and each rotation has only two directions, it is not hard to enumerate all possible simultaneous $\pi/3$ rotations on all possible actively interacting trivial braids, in a way similar to what we do in Fig. 4.3. For future convenience, we list all such relations in the following table.

From Table 4.1, one can see that the following quantities are invariant under these simultaneous rotations:

1. $T_l + T_r$;

2. T_a, T_b, and T_c are conserved individually modulo permutation;

3. S^2 (which additionally means that the interacting nature of braids is preserved under the simultaneous rotations).

49

$$R_{+1,-1}(^+_{T_l}[T_a, T_b, T_c]^+_{T_r}) = {}_{T_l+1}\bar{}[T_b, T_a, T_c]^-_{T_r-1} \qquad P^+_{+1} = (1\ 2)$$

$$R_{-1,+1}(^+_{T_l}[T_a, T_b, T_c]^+_{T_r}) = {}_{T_l-1}\bar{}[T_a, T_c, T_b]^-_{T_r+1} \qquad P^+_{-1} = (2\ 3)$$

$$R_{+1,-1}(^-_{T_l}[T_a, T_b, T_c]^-_{T_r}) = {}_{T_l+1}^+[T_a, T_c, T_b]^+_{T_r-1} \qquad P^-_{+1} = (2\ 3)$$

$$R_{-1,+1}(^-_{T_l}[T_a, T_b, T_c]^-_{T_r}) = {}_{T_l-1}^+[T_b, T_a, T_c]^+_{T_r+1} \qquad P^-_{-1} = (1\ 2)$$

Table 4.1: All possible simultaneous $\pi/3$ rotations on trivial braids that interact actively.

Furthermore, because of Eq. 4.3 this result applies to any simultaneous rotation. The above quantities help to derive two more conserved quantities: specifically $T_a + T_b + T_c$ and $T_{\text{total}} = T_l + T_a + T_b + T_c + T_r$. T_{total} is consistent to the effective twist found in Section 2.3.3: the sum of all twists and crossings of a subgraph - in particular a braid diagram - under any equivalent move. For a trivial braid no crossing exists and so the overall conserved quantity consists of twists only, this is T_{total}. All these conserved quantities are invariants under diffeomorphic embeddings.

Relations in Table 4.1 are generating relations for all possible simultaneous rotations, for example,

$$R_{+3,-3}(^+_{T_l}[T_a, T_b, T_c]^+_{T_r}) = R_{+2,-2}(_{T_l+1}\bar{}[T_b, T_a, T_c]^-_{T_r-1})$$
$$= R_{+1,-1}(_{T_l+2}^+[T_b, T_c, T_a]^+_{T_r-2})$$
$$= {}_{T_l+3}\bar{}[T_c, T_b, T_a]^-_{T_r-3},$$

where the π rotation is realized by three consecutive $\pi/3$ rotations. It is easy to check with our graphic calculus that the above calculation is indeed correct. One must be careful of performing an induced permutation at each step in such a calculation as permutation depends on both the end-node state before the rotation and the rotation handedness. In particular we will see three important identities regarding the induced permutations shortly. One can observe from Table 4.1 that

$$P^S_{\pm 1} P^{\bar{S}}_{\mp 1} = \mathbb{1}$$
$$P^S_{\pm 1} = P^{\bar{S}}_{\mp 1},$$
(4.4)

where S is the end-node state and $\bar{S}$ is its opposite. This can actually be generalized to the following lemma:

Lemma 4.1.

$$P^S_{2n} P^S_{-2n} \equiv \mathbb{1} \tag{4.5}$$
$$P^S_{2n+1} P^{\bar{S}}_{-(2n+1)} \equiv \mathbb{1} \tag{4.6}$$
$$P^S_n \equiv P^{\bar{S}}_{-n}, \tag{4.7}$$

where $n \in \mathbb{Z}$.

Proof. We shall begin by proving Eq. 4.5 (Eq. 4.6 follows similarly). First we have

$$P^S_{\pm 2} P^S_{\mp 2} = P^{\bar S}_{\pm 1} P^S_{\pm 1} P^{\bar S}_{\mp 1} P^S_{\mp 1} = P^{\bar S}_{\pm 1} \mathbb{1} P^S_{\mp 1} = \mathbb{1},$$

where the last two equalities hold by repeatedly applying Eq. 4.4, and $\bar S$ appears as a single $\pi/3$ rotation flips S. Using this we obtain

$$
\begin{aligned}
P^S_{\pm 2n} P^S_{\mp 2n} &= (P^S_{\pm 2})^n (P^S_{\mp 2})^n \\
&= (P^S_{\pm 2})^{n-1} \underbrace{P^S_{\pm 2} P^S_{\mp 2}}_{=\mathbb{1}} (P^S_{\mp 2})^{n-1} \\
&= (P^S_{\pm 2})^{n-1} (P^S_{\mp 2})^{n-1} \\
&= \mathbb{1},
\end{aligned}
$$

where the last line results from repeatedly performing the same expansion as in the second line. We then prove Eq. 4.7 by induction. It is already true for $n = \pm 1$ (Eq. 4.4). Assume it holds for $-(k-1) \le n \le k-1$ for some $k \in \mathbb{N}$, then we have for $|n| = k$

$$
P^S_{\pm k} = \begin{cases} P^{\bar S}_{\pm 1} P^S_{\pm(k-1)} = P^S_{\mp 1} P^{\bar S}_{\mp(k-1)} = P^{\bar S}_{\mp k} & \text{if } k \text{ is even,} \\ P^S_{\pm 1} P^S_{\pm(k-1)} = P^S_{\mp 1} P^{\bar S}_{\mp(k-1)} = P^{\bar S}_{\mp k} & \text{if } k \text{ is odd.} \end{cases}
$$

Thus Eq. 4.7 holds. The equations below are easy to derive; they are listed here for possible future use.

$$
\begin{aligned}
P^+_2 &= P^-_{-2} = (1\ 3\ 2) \\
P^+_{-2} &= P^-_2 = (1\ 2\ 3) \\
P^\pm_{6n+3} &\equiv (1\ 3) \\
P^\pm_{6n} &\equiv \mathbb{1},
\end{aligned}
\tag{4.8}
$$

where $n \in \mathbb{Z}$. $\qquad\qquad\qquad \square$

4.3 Algebra of interactions: symmetries and relations

Now that we consider trivial braids that interact actively, we may ask a question: do two actively interacting braids always interact to form another actively interacting braid? To answer this question, we need to first find out if two adjacent actively interacting braids, say B and B', always interact. One may feel this question somehow bizarre at first glance because how it is possible that two actively interacting braids do not interact.

Nevertheless, the reason to ask such a question is two-fold. Firstly, the first step of performing an interaction of B and B' is doing a $2 \to 3$ move about the two adjacent end-nodes of B and B' respectively; however, according to Condition 2.1 a $2 \to 3$ move is doable only if the two adjacent nodes are of the same state and their common edge is twist-free, as shown in Fig. 4.4. Secondly, in Chapter 3, we chose to represent a braid by its unique representative that has twist-free external edges, but in this chapter we represent a braid by its trivial braid diagrams whose external edges
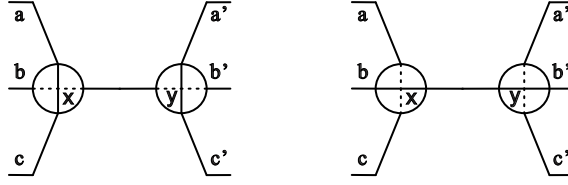
Figure 4.4: The only two possible configurations allowing a $2 \rightarrow 3$ move.

are not necessary twist-free. Therefore, when two trivial braids B and B' meet each other, to see if they interact we should first check if we can put their adjacent end-nodes in the same state and with a twist-free common edge in between, which constructs the **interaction condition**. In search of the answer to this question, an algebra of interactions between actively interacting braids will be naturally developed.
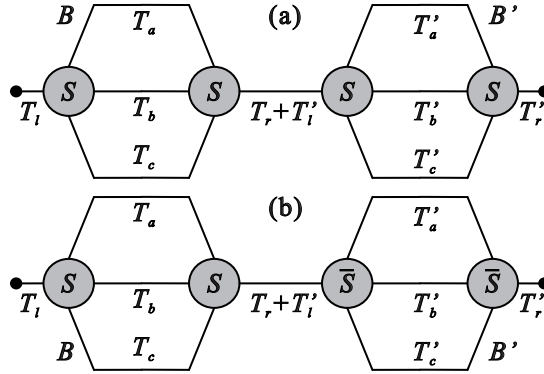
Figure 4.5: Two general cases in which two actively interacting braids B and B' meet each other: (a) B and B' have adjacent end-nodes in the same state; and (b) B and B' have adjacent end-nodes in opposite states. $\bar{S}$ stands for the opposite of S. The interaction condition in cases (a) and (b) are respectively $T_r + T'_l = 2n$ and $T_r + T'_l = 2n + 1$, $n \in \mathbb{Z}$.

For two actively interacting trivial braids B and B', with B on the left of B', two general cases deserve a study (Fig. 4.5). In Fig. 4.5(a), the right end-node of B and the left end-node of B' are already in the same state, so the task is not only to get rid of the overall twist $T_r + T'_l$ on the common edge but also to keep the adjacent end-nodes in the same state. We know that only multiples of $2\pi/3$ rotations do not change the state of the node being rotated, we thus demand that in this case $T_r + T'_l = 2n$, $n \in \mathbb{Z}$. For example, if $T_r + T'_l = 2$, we can perform a left-handed $2\pi/3$ rotation either on the right end-node of B or on the left end-node of B', such that the two adjacent end-nodes are still in state S and their common edge is now twist-free.

As to Fig. 4.5(b), the right end-node of B and the left end-node of B' are in opposite states, so we should rotate either of them to set them in the same state and annihilate the twist $T_r + T'_l$ at the mean time. Knowing that only odd multiples of $\pi/3$ rotations flip the state of the node under

rotation, we clearly must have in this case, $T_r + T'_l = 2n + 1, n \in \mathbb{Z}$.

Here is a good news. As long as the above interaction condition holds, such that a $2 \to 3$ move can be done on the two neighboring end-nodes of B and B', according to our definitions of interaction and of actively interacting braids, B and B' can definitely interact to form another braid, written as $B + B'$, which is also actively interacting. The reason is understood this way: the interaction, left or right, of $B + B'$ onto an arbitrary braid (actively interacting or not), say B'', can always be thought as a composite process of two interactions, namely $(B+B')+B'' = B+(B'+B'')$, in which B is the active braid in the second step, or $B'' + (B + B') = (B'' + B) + B'$, in which B' is the active one in the second step. In other words, an interaction is associative, with however, an active braid always playing the active role.

Nonetheless, how does $B + B'$ look like when it is represented by a trivial braid diagram? To perform the interaction, either B's right end-node or B'''s left end-node may be rotated before one can do a $2 \to 3$ move, which disguises the form of $B + B'$ from being guessed directly. Fortunately, this issue can be tackled as follows.

Let us take the case in Fig. 4.5(a) to study. Supposing the condition, $T_r + T'_l = 2n$, holds, we have two subcases. The first is the significantly easier to prove and so we shall address it first:

Lemma 4.2. *Given two actively interacting braids* $B = {}^S_{T_l}[T_a, T_b, T_c]^S_{T_r}$ *and* $B' = {}^{\pm S}_{T'_l}[T'_a, T'_b, T'_c]^{\pm S}_{T'_r}$ *satisfying the interaction conditions with* $T_r + T'_l = 0$, *the interaction of* B *and* B' *gives* $B^f = {}^S_{T_l}[(T_a, T_b, T_c) + (T'_a, T'_b, T'_c)]^S_{T'_r} = {}^S_{T_l}[T_a + T'_a, T_b + T'_b, T_c + T'_c]^S_{T_r}$

Proof. As $T_r + T'_l = 0$, no rotation is needed; hence, according to Section 3.2, $B + B'$ forms a connected sum of B and B', which reads, in our algebraic language,

$$B + B' \stackrel{T_r+T'_l=0}{=} B\#B' = {}^S_{T_l}[T_a, T_b, T_c]^S_{T_r} \# {}^S_{-T_r}[T'_a, T'_b, T'_c]^S_{T'_r}$$
$$= {}^S_{T_l}[(T_a, T_b, T_c) + (T'_a, T'_b, T'_c)]^S_{T'_r} = {}^S_{T_l}[T_a + T'_a, T_b + T'_b, T_c + T'_c]^S_{T'_r} . \tag{4.9}$$

$\square$

Before dealing with the other subcase, it is useful to prove another Lemma.

Lemma 4.3. *A simultaneous rotation commutes with a connected sum. In algebraic words, this means*

$$R_{n,-n}(B\#B') = R_{n,-n}(B)\#R_{n,-n}(B'), \ n \in \mathbb{Z}. \tag{4.10}$$

Proof. Let $B = {}^S_{T_l}[T_a, T_b, T_c]^S_{T_c}$ and $B' = {}^S_{-T_c}[T'_a, T'_b, T'_c]^S_{T_r}$. Note that B and B' have the same end-node state, and that the right external twist of B, T_c, cancels the left external twist of B', $-T_c$, which

is the most general situation in which a connected sum is viable. Hence, we have

$$
\begin{aligned}
R_{n,-n}(B) \# R_{n,-n}(B') &= R_{n,-n}(_{T_l}^{S}[T_a, T_b, T_c]_{T_c}^{S}) \# R_{n,-n}(_{-T_c}^{S}[T'_a, T'_b, T'_c]_{T'_r}^{S}) \\
&= {}_{T_l+n}^{(-)^n S}[P_n^S(T_a, T_b, T_c)]_{T_c-n}^{(-)^n S} \# {}_{-T_c+n}^{(-)^n S}[P_n^S(T'_a, T'_b, T'_c)]_{T'_r-n}^{(-)^n S} \\
\xrightarrow{T_c-n+(-T_c+n)=0} &= {}_{T_l+n}^{(-)^n S}[P_n^S(T_a + T'_a, T_b + T'_b, T_c + T'_c)]_{T'_r-n}^{(-)^n S} \\
&= R_{n,-n}(_{T_l}^{S}[T_a + T'_a, T_b + T'_b, T_c + T'_c]_{T'_r}^{S}) \\
\xrightarrow{Eq.4.9} &= R_{n,-n}(B \# B'),
\end{aligned}
$$

closing the proof. $\qquad\square$

If $T_r + T'_l = 2n \neq 0$, we are in the second subcase. We can choose to do a rotation of $-(T_r + T'_l)$ on either the right end-node of B or on the left end-node of B' to annihilate the twist $T_r + T'_l$ on the common edge. If we rotate the right end-node of B by $-(T_r + T'_l)$, we create crossings on B and change B's twists, but we want to stay with the trivial braid diagrams. To get around of this problem we simply need to perform a rotation of the opposite handedness on the left end-node of B as well, such that B is still in its trivial representation. In other words, we perform a simultaneous rotation of $T_r + T'_l$ on B. Likewise, if we rotate the left end-node of B' to cancel the twist $T_r + T'_l$, we should perform a simultaneous rotation of $-(T_r + T'_l)$ on B'. In either choice, we arrive at a situation legal for a connected sum. Nonetheless, each choice yields a result for $B + B'$, a natural question is whether the two results "the same", or to be precise, equivalent? The answer is "Yes", which is not only true for this case but also valid for the case in Fig. 4.5(b).

We now prove this statement as a theorem. Here is the setup of the theorem. For two actively interacting trivial braids B and B', with B adjacent to B' on the left, if the interaction condition holds, one may need to perform a simultaneous rotation on either B or B' to remove the twist on their common edge for the interaction to happen by a connected sum.

Theorem 4.1. *The resulting interaction $B + B'$ between two actively interacting braids does not depend on the choice of the braid being simultaneously rotated.*

Proof. Let $B = {}_{T_l}^{S}[T_a, T_b, T_c]_{T_r}^{S}$ and $B' = {}_{T'_l}^{\pm S}[T'_a, T'_b, T'_c]_{T'_r}^{\pm S}$, which considers both cases in Fig. 4.5: $T_r + T'_l = 2n, n \in \mathbb{Z}$ for $+S$, and $T_r + T'_l = 2n + 1, n \in \mathbb{Z}$ for $-S$. Then, $B + B' = {}_{T_l}^{S}[T_a, T_b, T_c]_{T_r}^{S} + {}_{T'_l}^{\pm S}[T'_a, T'_b, T'_c]_{T'_r}^{\pm S}$, and we have

$$
\begin{aligned}
B + B' &= {}_{T_l}^{S}[T_a, T_b, T_c]_{0}^{S} \# R_{-(T_r+T'_l), T_r+T'_l}\left({}_{T_r+T'_l}^{\pm S}[T'_a, T'_b, T'_c]_{T'_r}^{\pm S} \right) \\
&= {}_{T_l}^{S}[T_a, T_b, T_c]_{0}^{S} \# {}_{0}^{(-)^{T_r+T'_l}(\pm S)}[P_{-(T_r+T'_l)}^{\pm S}(T'_a, T'_b, T'_c)]_{T'_r+T_r+T'_l}^{(-)^{T_r+T'_l}(\pm S)} \\
\xrightarrow{(-)^{T_r+T'_l}(\pm S)=S} &= {}_{T_l}^{S}[T_a, T_b, T_c]_{0}^{S} \# {}_{0}^{S}[P_{-(T_r+T'_l)}^{\pm S}(T'_a, T'_b, T'_c)]_{T'_r+T_r+T'_l}^{S} \\
&= {}_{T_l}^{S}[(T_a, T_b, T_c) + (P_{-(T_r+T'_l)}^{\pm S}(T'_a, T'_b, T'_c))]_{T'_r+T_r+T'_l}^{S} , \quad (4.11)
\end{aligned}
$$

$$B + B' = R_{T_r+T'_l, -(T_r+T'_l)} \left({}^S_{T_l}[T_a, T_b, T_c]^S_{T_r+T'_l} \right) \# {}^{\pm S}_0[T'_a, T'_b, T'_c]^{\pm S}_{T'_r}$$

$$= {}^{(-)^{T_r+T'_l}S}_{T_l+T_r+T'_l}[P^S_{T_r+T'_l}(T_a, T_b, T_c)]^{(-)^{T_r+T'_l}S}_0 \# {}^{\pm S}_0[T'_a, T'_b, T'_c]^{\pm S}_{T'_r}$$

$$\xrightarrow{(-)^{T_r+T'_l}S = \pm S} = {}^{\pm S}_{T_l+T_r+T'_l}[(P^S_{T_r+T'_l}(T_a, T_b, T_c)) + (T'_a, T'_b, T'_c)]^{\pm S}_{T'_r} , \tag{4.12}$$

and

$$\begin{aligned}
&{}^S_{T_l}[(T_a, T_b, T_c) + (P^{\pm S}_{-(T_r+T'_l)}(T'_a, T'_b, T'_c))]^S_{T'_r+T_r+T'_l} \\
&\cong {}^{\pm S}_{T_l+T_r+T'_l}[(P^S_{T_r+T'_l}(T_a, T_b, T_c)) + (T'_a, T'_b, T'_c)]^{\pm S}_{T'_r} , \tag{4.13}
\end{aligned}$$

where $\cong$ means "equivalent to". Note that $\pm S$ stands for the two cases respectively.

It is sufficient to prove Eq. 4.13. In view of Lemma 4.3, we may apply a simultaneous rotation of $T_r + T'_l$ on the LHS of Eq. 4.13, but perform the rotation respectively on the two components of the connected sum and then take the connected sum. That is,

$$\begin{aligned}
&{}^S_{T_l}[(T_a, T_b, T_c) + (P^{\pm S}_{-(T_r+T'_l)}(T'_a, T'_b, T'_c))]^S_{T'_r+T_r+T'_l} \\
&\cong R_{T_r+T'_l, -(T_r+T'_l)} \left({}^S_{T_l}[T_a, T_b, T_c]^S_0 \# {}^S_0[P^{\pm S}_{-(T_r+T'_l)}(T'_a, T'_b, T'_c)]^S_{T'_r+T_r+T'_l} \right) \\
&\xrightarrow{Eq. 4.10} = R_{T_r+T'_l, -(T_r+T'_l)} \left({}^S_{T_l}[T_a, T_b, T_c]^S_0 \right) \\
&\quad \# R_{T_r+T'_l, -(T_r+T'_l)} \left({}^S_0[P^{\pm S}_{-(T_r+T'_l)}(T'_a, T'_b, T'_c)]^S_{T'_r+T_r+T'_l} \right) \\
&= {}^{(-)^{T_r+T'_l}S}_{T_l+T_r+T'_l}[P^S_{T_r+T'_l}(T_a, T_b, T_c)]^{(-)^{T_r+T'_l}S}_{-(T_r+T'_l)} \\
&\quad \# {}^{(-)^{T_r+T'_l}S}_{T_r+T'_l}[P^{(-)^{T_r+T'_l}S}_{T_r+T'_l} P^{\pm S}_{-(T_r+T'_l)}(T'_a, T'_b, T'_c)]^{(-)^{T_r+T'_l}S}_{T'_r} \\
&= {}^{(-)^{T_r+T'_l}S}_{T_l+T_r+T'_l}[P^S_{T_r+T'_l}(T_a, T_b, T_c)]^{(-)^{T_r+T'_l}S}_{-(T_r+T'_l)} \# {}^{\pm S}_{T_r+T'_l}[T'_a, T'_b, T'_c]^{\pm S}_{T'_r} \\
&= {}^{\pm S}_{T_l+T_r+T'_l}[P^S_{T_r+T'_l}(T_a, T_b, T_c)]^{\pm S}_0 \# {}^{\pm S}_0[T'_a, T'_b, T'_c]^{\pm S}_{T'_r} \\
&= {}^{\pm S}_{T_l+T_r+T'_l}[(P^S_{T_r+T'_l}(T_a, T_b, T_c)) + (T'_a, T'_b, T'_c)]^{\pm S}_{T'_r} ,
\end{aligned}$$

which is the very Eq. 4.13. The second to the last line holds because the right subscript of the first term, $-(T_r + T'_l)$, cancels the left subscript of the second term, $T_r + T'_l$, and $(-)^{T_r+T'_l} = \pm S$ respectively in the two cases. The third equality holds for that

$$P^{(-)^{T_r+T'_l}S}_{T_r+T'_l} P^{\pm S}_{-(T_r+T'_l)} = \begin{cases} P^S_{T_r+T'_l} P^S_{-(T_r+T'_l)} \xoverset{Eq.4.5}{=} \mathbb{1}, & T_r + T'_l = 2n \\[2mm] P^{-S}_{T_r+T'_l} P^{-S}_{-(T_r+T'_l)} \xoverset{Eq.4.5}{=} \mathbb{1}, & T_r + T'_l = 2n + 1 \end{cases}$$

This completes the proof. $\qquad\square$

Let us see an example. Fig. 4.6 shows two actively interacting trivial braids, algebraically they
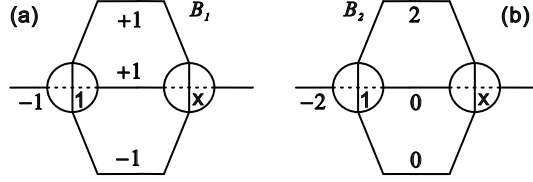
Figure 4.6: Two braids that interact actively.

are $B_1 = {}_{-1}^+[1,1,-1]_0^+$ and $B_2 = {}_{-2}^+[T+2,0,0]_0^+$. One sees that

$$
\begin{aligned}
B_1 + B_2 &= {}_{-1}^+[1,1,-1]_0^+ + {}_{-2}^+[2,0,0]_0^+ \\
&= {}_{-1}^+[1,1,-1]_0^+ \# R_{2,-2}({}_{-2}^+[2,0,0]_0^+) \\
&= {}_{-1}^+[1,1,-1]_0^+ \# {}_0^+[P_2^+(2,0,0)]_{-2}^+ \\
&= {}_{-1}^+[1,1,-1]_0^+ \# {}_0^+[0,0,2]_{-2}^+ \\
&= {}_{-1}^+[1,1,1]_{-2}^+.
\end{aligned}
$$

On the other hand,

$$
\begin{aligned}
B_1 + B_2 &= {}_{-1}^+[1,1,-1]_0^+ + {}_{-2}^+[2,0,0]_0^+ \\
&= R_{-2,2}({}_{-1}^+[1,1,-1]_{-2}^+) \# {}_0^+[2,0,0]_0^+ \\
&= {}_{-3}^+[-1,1,1]_0^+ \# {}_0^+[2,0,0]_0^+ \\
&= {}_{-3}^+[1,1,1]_0^+.
\end{aligned}
$$

Nonetheless, we have

$$
R_{2,-2}({}_{-3}^+[1,1,1]_0^+) = {}_{-1}^+[P_2^+(1,1,1)]_{-2}^+ = {}_{-1}^+[1,1,1]_{-2}^+,
$$

satisfying Theorem 4.3. Interestingly, $B_2 + B_1$ does not work because while B_2 and B_1 have the same end-node state, the common twist -1 is an odd number, which violates the condition of interaction.

Equipped with this algebra, we shall prove our primary result:

Corollary 4.1. *Given two actively interacting braids* $B = {}_{T_l}^S[T_a, T_b, T_c]_{T_r}^S$ *and* $B' = {}_{T_l'}^{\pm S}[T_a', T_b', T_c']_{T_r'}^{\pm S}$ *satisfying the interaction conditions, the resulting braid* $B^f = B + B'$ *conserves the quantities* $T_l + T_r + T_l' + T_r' = T_l^f + T_r^f$, $\sum_{i=a}^c (T_i + T_i') = \sum_{i=a}^c T_i^f$ *and* S^2.

Proof. We immediately use the result from the proof of the previous theorem:

$$
B^f = {}_{T_l+T_r+T_l'}^{\pm S}[(P_{T_r+T_l'}^S(T_a, T_b, T_c)) + (T_a', T_b', T_c')]_{T_r'}^{\pm S} \tag{4.14}
$$

By previous theorems, we know that this result is independent of the form of the braids in their interaction; hence, we need only to examine our final form. S^2 is conserved as our final result

56

shares the same value for S^2 of each of our initial states, and S^2 is invariant under the equivalence moves. We know that $T_l^f + T_r^f$ is conserved under the equivalence moves, and from our result we see that this conserved quantity is equal to $T_l + T_r + T_l' + T_r'$. Finally, $\sum_{i=a}^{c} T_i^f$ is the same regardless of the form of $P_{T_r+T_l'}^S$, this immediately has the form of $\sum_{i=a}^{c} (T_i + T_i')$. □

The three conserved quantities of this theorem have a clear meaning:

1. $T_l + T_r + T_l' + T_r' = T_l^f + T_r^f$, the total external twists before and after an interaction are the same;

2. $\sum_{i=a}^{c} (T_i + T_i')$, the total internal twists remains the same under interaction;

3. S^2, the interacting character of the braids is preserved.

4.4 Summary

Conservation laws are a valuable tool in gaining understanding of the underlying structure of a theory. Elucidating the actual content of a theory and revealing information that could otherwise remain inaccessible. Equipped with invariants and conserved quantities we are able to work to determine how the content of the theory relates to particle physics.

We have developed an algebraic notation for actively interacting braids, found a set of equivalence relations relating them, and developed conserved quantities associated with these relations. More importantly we discovered the relationship between these algebraic forms and the interaction of actively interacting braids. From this we wrote down quantities conserved under interaction. These are dynamically conserved quantities, which are also conserved under the equivalence moves.

This allows us to work towards a better understanding of and a classification of the complete set of these braids. As actively interacting braids interact with each other to produce actively interacting braids, we can generate an infinite set of such braids. The next step is to determine which of the conserved quantities found here may be mapped to quantum numbers characterizing fundamental particles.

It is worth noting that the algebraic calculus proposed in this chapter will be extended in the next chapter to that for all stable braids. Chapter 6 will then use this calculus to look for the discrete transformations of braids, which are analogous to C, P, T, and their combinations. To these ends, Chapter 7 will point out a route towards an effective theory of our braid excitations in terms of Feynman diagrams.

Chapter 5

Algebraic Formalism: General Braids

Although the graphic calculus has its own advantages - in particular in describing, e.g., the full procedure of the active propagation a braid, it is not very convenient for finding a braid's conserved quantities that are useful to characterize the braid as a matter-like local excitation. In view of this, we now continue our course of seeking a fully algebraic formalism of braids by generalizing the algebraic calculus developed in Chapter 4 to that of generic stable braids. In this algebraic formalism, we will define algebraic equivalence moves and conserved quantities and discuss the algebra of direct interactions between actively interacting braids and non-actively interacting braids. We list below the main results of this chapter, as they are important in subsequent studies:

1. There exist conserved quantities under interactions and we are able to show the form of these conservation laws.

2. Precise algebraic forms of braid interactions are presented.

3. The set of all stable braids form an algebra under braid interaction, in which the set of all actively interacting braids is the subalgebra.

4. This algebra is noncommutative because the left and right interactions of an actively interacting braid onto another braid are not the same in general. Conditions of commutative interactions are explicitly given.

5. Asymmetric interactions can be related by discrete transformation, such as P, T, CP, and CT.

5.1 Notation

We will extend the algebraic notation of actively interacting braids to the most general case, namely to actively propagating braids and in fact to all stable braids. In accordance to our graphic notation, a generic 3-strand braid is shown in Fig. 5.1(a).

In Section 2.5 we discussed two types of representations of braids that are useful in different situations. From then on, we found that trivial representations are suitable for actively interacting braids, while unique representations are good for non-actively interacting ones. Therefore, a
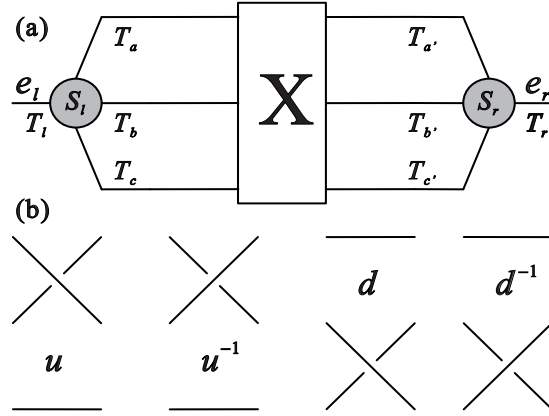
Figure 5.1: (a) is a generic 3-strand braid diagram. S_l and S_r are the states of the left and right **end-node**s respectively, valued in $\{+, -\}$. X represents a sequence of crossings, from left to right, formed by the three strands. (T_a, T_b, T_c) is the triple of the **internal twists** respectively on the three strands from top to bottom, on the left of X. T_l and T_r, called **external twists**, are respectively on the two external edges e_l and e_r. All twists are valued in $\mathbb{Z}$ in units of $\pi/3$. (b) shows the four generators of X, which are also generators of the braid group B_3.

generalized algebraic notation of a braid should take care of all possible choices of representations braids. Note that by definition the class of propagating braids excludes any actively interacting braid that is also propagating.

Let us now focus on the generic case depicted in Fig. 5.1(a). Since the crossing sequence X must satisfy the definition of ordinary braids, we can write X as a sequence of generators of the braid group B_3. The group B_3 has two generators and their inverses. Because we arrange a braid diagram horizontally, the generator and its inverse formed by the upper two strand of a braid are named u and u^{-1} respectively, while the one and its inverse formed by the lower two strand of a braid are d and d^{-1} respectively. Fig. 5.1(b) depicts this convention. We also assign an integral value, the crossing number, to each generator, i.e., $u = d = 1$ and $u^{-1} = d^{-1} = -1$, as consistent with Fig. 2.5.

For an arbitrary sequence X of **order** $n = |X|$, namely the number of crossings, we can write $X = x_1 x_2 \cdots x_i \cdots x_n$, where $x_i \in \{u, u^{-1}, d, d^{-1}\}$ represents the i-th crossing from the left. Therefore, each x_i in X has a two-fold meaning: on the one hand, it is an abstract crossing; on the other hand, it represents an integral value, 1 or -1. When a x_i appears in a multiplication it is usually understood as an abstract crossing, while in a summation it is normally an integer. Note that, as generators of the group B_3, the generators of X obey the following equivalence relations.

$$udu^{-1} = d^{-1}ud$$
$$u^{-1}du = dud^{-1} \tag{5.1}$$
$$udu = dud$$

We assume in any X, the above equivalence relations have been applied to remove any pair of

a crossing and its inverse[1]. For example, the sequence $udu^{-1}d^{-1}$ should have been written as $udu^{-1}d^{-1} = d^{-1}udd^{-1} = d^{-1}u$ by the first relation above. The crossing sequence X clearly induces a permutation, denoted by σ_X, of the three strands of a braid. It is obvious that the induced permutation σ_X takes value in S_3, the permutation group of the set of three elements. In terms of disjoint cycles,

$$S_3 = \{\mathbb{1}, (1\ 2), (1\ 3), (2\ 3), (1\ 2\ 3), (1\ 3\ 2)\}. \tag{5.2}$$

More precisely, the three internal twists in a triple (T_a, T_b, T_c) on the left of the X are permutated by the induced permutation into $(T_a, T_b, T_c)\sigma_X = (T_{a'}, T_{b'}, T_{c'})$, where $(T_{a'}, T_{b'}, T_{c'})$ is the triple of the internal twists on the right of X. Here σ_X is defined to be a *left-acting* function on the triple of internal twists for two reasons. Firstly, this is a convention of permutation group. Secondly, when another crossing sequence, say X', is appended to the right of X, which usually happens in interactions of braids, we naturally have $(T_a, T_b, T_c)\sigma_X\sigma_{X'} = (T_a, T_b, T_c)\sigma_{XX'}$, such that the induced permutation of the newly appended crossings is applied after the action of σ_X.

On the other hand, $(T_a, T_b, T_c) = \sigma_X^{-1}(T_{a'}, T_{b'}, T_{c'})$, where σ_X^{-1} is the inverse of σ_X and is a *right-acting* function of the triple. One should keep in mind that the indices of internal twists such as T_a and T'_a, a and a' are abstract and have no meaning until their values and positions in the triple of internal twists are fixed. So $(T_a, T_b, T_c) = (T_d, T_e, T_f)$ means $T_a = T_d, T_b = T_e$, and $T_c = T_f$. We will also consider the addition of two triples of twists, i.e., $(T_a, T_b, T_c) + (T_d, T_e, T_f) = (T_a + T_d, T_b + T_e, T_c + T_f)$. Therefore, we can denote a generic braid as Fig. 5.1(a) by

$$_{T_l}^{S_l}[(T_a, T_b, T_c)\sigma_X]_{T_r}^{S_r}, \tag{5.3}$$

or equally well by

$$_{T_l}^{S_l}[\sigma_X^{-1}(T_{a'}, T_{b'}, T_{c'})]_{T_r}^{S_r}. \tag{5.4}$$

In such a way, which side of the crossing sequence a triple of internal twists is on is transparent. For instance, the braid in Fig. **??**(a) can be written as $_0^+[(5, -1, 5)\sigma_{du^{-1}}]_0^-$ or $_0^+[\sigma_{du^{-1}}^{-1}(5, 5, -1)]_0^-$, where $\sigma_{du^{-1}} = (3\ 1\ 2)$ and $\sigma_{u^{-1}d}^{-1} = (2\ 3\ 1)$. Note that one should keep σ_X abstract rather than write down its explicit permutation value in a braid's expression, as it is there not only for indicating the permutation induced by X but also for recording the crossing sequence.

It is now clear that a generic braid is characterized by the 8-tuple, $\{T_l, S_l, T_a, T_b, T_c, X, S_r, T_r\}$. As mentioned before, S_l and S_r are just signs, $+$ or $-$, such that $-(+) = -$ and $-(-) = +$. Hence, for an arbitrary end-node state S, we may use both $-S$ and $\bar{S}$ for the inverse of S. In fact, this 8-tuple is not completely arbitrary for different type of braids. For a propagating braid B of n crossings represented by the braid diagrams with no external twists we have the following constraints.

1. $T_l = T_r = 0$.

2. The triple (S_l, X, S_r) is not arbitrary. If B is **actively propagating**, according to Section 3.1 and Appendix C, B must be at least reducible from either side, in particular its first crossing on the (left) right can be eliminated by the equivalence move, a $\pi/3$ rotation, which also flips the (left) right end-node. That is, letting $X = x_1x_2 \cdots x_{n-1}x_n$, then under a $\pi/3$

---

[1]This is the explanation to a remark of our definition of braids in Section 2.2.

rotation on the (left) right end-node, the triple (S_l, X, S_r) becomes $((\bar{S}_l, x_2 \cdots x_{n-1} x_n, S_r))$ $(S_l, x_1 x_2 \cdots x_{n-1}, \bar{S}_r)$.

3. The triple (T_a, T_b, T_c) is not arbitrary; however, the general pattern of them, ensuring the propagation of B, has not yet been found and is under investigation. But the algebra formulated and the conserved quantities to be found in this chapter may turn out to be helpful to resolve this problem.

Any braid whose characterizing 8-tuple violates the above constraints is not propagating

Although we prefer to write a propagating braid in its unique representation, it is sometimes useful to put it in an extremal representation. We shall leave the discussion of this representation to the next section after we defined rotations symbolically.

For an actively interacting braid, we choose a trivial representation for it. This has actually been carried out in the previous chapter. We thus will not repeat any detail here. It is good to see our notation of the generic case reduces to that of the actively interacting braids defined in Eq. 4.1. For trivial braid diagrams, the crossing sequence is trivial, and hence the induced permutation is the identity, i.e., $\sigma_X = \mathbb{1}$. The triple of internal twists on the left of X and the one on the right are the same. Moreover, we have $S_l = S_r = S$ in this case. As a result, the generic notation uniquely boils down to

$$ {}^{S}_{T_l}[T_a, T_b, T_c]^{S}_{T_r} , $$

which is the very notation introduced in Eq. 4.1 for actively interacting braids in their trivial representations.

5.2 Algebra of equivalence moves: symmetries and relations

Since an actively interacting braid can always be reduced to trivial braids with twists, it is sufficient to discuss the algebra of simultaneous rotations for these trivial braids. In Chapter 4, we have found general effects of simultaneous rotations on trivial braids, especially conserved quantities under this class of equivalence moves. For generic braids, however, we need to consider more generalized rotations of a braid, denoted by $R_{m,n}$ with $m, n \in \mathbb{Z}$, which is the combination of an $m\pi/3$ rotation on the left end-node and an $n\pi/3$ one of the right end-node of the braid. Let us record the algebraic form of such a rotation on a generic braid, and then explain it,

$$ R_{m,n}({}^{S_l}_{T_l}[(T_a, T_b, T_c)\sigma_X]^{S_r}_{T_r}) $$
$$ = {}^{(-)^m S_l}_{T_l+m}[(P^{S_l}_m(T_a - m - n, T_b - m - n, T_c - m - n))\sigma_{X_l(S_l,m)XX_r(S_r,n)}]^{(-)^n S_r}_{T_r+n} . \tag{5.5} $$

On the RHS of Eq. 5.5, the original end-node states, S_l and S_r, become $(-)^m S_l$ and $(-)^n S_r$. This is because a $\pi/3$ rotation of a node always flips the state of the node once, which means a $m\pi/3$ rotation should flip the state of a node m times. Besides, a rotation of the left (right) end-node of a braid creates a crossing sequence, appended to the left (right) of the original crossing sequence of the braid. In Eq. 5.5, the newly-generated sequence on the left is denoted by a function $X_l(S_l, m)$, depending on the original left end-node state and the amount of rotation, m. Likewise, the new

crossing sequence on the right is denoted by the function $X_r(S_r, n)$. We will elaborate these two functions shortly. As a consequence, the induced permutation by the crossing sequence changes accordingly, from σ_X to $\sigma_{X_l(S_l,m)XX_r(S_r,n)}$.

In addition, the left triple of internal twists is affected by the rotation of the left end-node, which induces a permutation $P_m^{S_l}$ on the triple, determined by the original end-node state and the amount of rotation m. This function, which obviously takes its value in the group S_3 shown in Eq. 5.2, is the same as the that induced by a simultaneous rotation on actively interacting braids, defined in Section 4.2. One may wonder why the similar permutation induced by the rotation on the right end-node does not appear in Eq. 5.5. This is owing to the advantage of our notation that needs the triple of internal twists on one side of a braid's crossing sequence, while the permutation σ takes care of the triple on the other side. If one indeed wants to have the triple of internal twists beside the right end-node explicit, one can use the alternative form of the rotation as follows instead.

$$R_{m,n}\left({}_{T_l}^{S_l}[\sigma_X^{-1}(T_{a'}, T_{b'}, T_{c'})]_{T_r}^{S_r}\right)$$
$$= {}_{T_l+m}^{(-)^m S_l}[\sigma_{X_l(S_l,m)XX_r(S_r,n)}^{-1}(P_{-n}^{S_r}(T_{a'} - m - n, T_{b'} - m - n, T_{c'} - m - n))]_{T_r+n}^{(-)^n S_r}, \tag{5.6}$$

Finally, the common increment of $-m - n$ of all internal twists, and the changes of the two external twists under the rotation $R_{m,n}$ in Eq. 5.5 and Eq. 5.6 are simple effects of the rotation.

We now explain more about these functions. Since the permutations P_m^S here are the same as those defined in Section 4.2, one should keep in mind Table 4.1, Eq. 4.8, and Lemma 4.1.

According to the graphic definitions of rotations in Section 2.3.2, we found that $X_l(S, m)$ and $X_r(S, n)$ have the following general algebraic forms.

$$X_l(+, m) = \begin{cases} (ud)^{-m/2} & \text{if } m \text{ is even,} \\ d(ud)^{(-1-m)/2} & \text{if } m \text{ is odd.} \end{cases} \quad X_l(-, m) = \begin{cases} (du)^{-m/2} & \text{if } m \text{ is even,} \\ u(du)^{(-1-m)/2} & \text{if } m \text{ is odd.} \end{cases}$$

$$X_r(+, n) = \begin{cases} (ud)^{-n/2} & \text{if } n \text{ is even,} \\ (ud)^{(1-n)/2}d^{-1} & \text{if } n \text{ is odd.} \end{cases} \quad X_r(-, n) = \begin{cases} (du)^{-n/2} & \text{if } n \text{ is even,} \\ (du)^{(1-n)/2}u^{-1} & \text{if } n \text{ is odd.} \end{cases} \tag{5.7}$$

where $n, m \in \mathbb{Z}$. If an exponent in Eq. 5.7 is positive, it means, for example, $(ud)^2 = udud$. We utilize part of Definition D.4: for a crossing sequence $X = x_1 \cdots x_i \cdots x_N$, $N \in \mathbb{N}$, $X^{-1} = x_N^{-1} \cdots x_i^{-1} \cdots x_1^{-1}$. Given this, the meaning of the negative exponents in Eq. 5.7 is clear. For instance, $(ud)^{-2} = d^{-1}u^{-1}d^{-1}u^{-1}$.

It is obvious that the number of crossings of either $X_l(S_l, m)$ or $X_r(S_r, m)$ does not depend on the end-node state,

$$|X_l(+, m)| = |X_l(-, m)| = |X_r(+, m)| = |X_r(-, m)| = |m|, \tag{5.8}$$

neither does the sum of crossing numbers of $X_l(S_l, m)$ or $X_r(S_r, m)$, namely

$$\sum_{i=1}^{|m|} x_i = \sum_{i=1}^{|m|} y_i = \sum_{i=1}^{|m|} z_i = \sum_{i=1}^{|m|} w_i = -m. \tag{5.9}$$

where, $x_i \in X_l(+, m)$, $y_i \in X_l(-, m)$, $z_i \in X_r(+, m)$, and $w_i \in X_r(-, m)$. In addition, Lemma 5.1 states a useful relation between $X_l(S, m)$ and $X_r(S, n)$.

Lemma 5.1. $X_l(S, m)X_r(S, -m) \equiv \mathbb{I}$. $\mathbb{I}$ *stands for no crossing.*

Proof. For m even,

$$X_l(+, m)X_r(+, -m) = (ud)^{-m/2}(ud)^{m/2} = \mathbb{I},$$
$$X_l(-, m)X_r(-, -m) = (du)^{-m/2}(du)^{m/2} = \mathbb{I};$$

for m odd,

$$X_l(+, m)X_r(+, -m) = d(ud)^{(-1-m)/2}(ud)^{(1+m)/2}d^{-1} = \mathbb{I},$$
$$X_l(-, m)X_r(-, -m) = u(du)^{(-1-m)/2}(du)^{(1+m)/2}u^{-1} = \mathbb{I}.$$

In conclusion, for any S and m, we have

$$X_l(S, m)X_r(S, -m) \equiv \mathbb{I}.$$

$\square$

The rotation $R_{m,n}$ is actually a generalization of the simultaneous rotation $R_{n,-n}$, defined in Eq. 4.2, as acting on actively-interacting braids in their trivial representations with $S_l = S_r = S$ and $X \equiv \mathbb{I}$, indicating $\sigma_X = \mathbb{1}$. Therefore, for consistency, our general rotation $R_{m,n}$ should reduce to the simultaneous rotation $R_{m,-m}$ on these braids, if we set $n = -m$. This is indeed so because

$$R_{m,-m}(^S_{T_l}[T_a, T_b, T_c]^S_{T_r}) =^{(-)^m S}_{T_l+m} [(P^S_m(T_a, T_b, T_c))\sigma_{X_l(S,m)\mathbb{I}X_r(S,m)}]^{(-)^m S}_{T_r-m};$$

however, Lemma 5.1 gives $X_l(S, m)\mathbb{I}X_r(S, m) \equiv \mathbb{I}$, such that

$$R_{m,-m}(^S_{T_l}[T_a, T_b, T_c]^S_{T_r}) =^{(-)^m S}_{T_l+m} [P^S_m(T_a, T_b, T_c)]^{(-)^m S}_{T_r-m},$$

which is the very simultaneous rotation defined in Eq. 4.2.

With these ingredients, we can proceed to find out conserved quantities of a generic braid under general equivalence moves, $R_{m,n}$. One can see that unlike trivial braids under simultaneous rotations, $T_l + T_r$ and the triple (T_a, T_b, T_c) are no longer conserved here for a generic rotation, only a combination of them with sum of crossing numbers, namely the effective twist[2] $\Theta = T_l + T_r + \sum_{i=a}^{c} T_i - 2\sum_{i=1}^{|X|} x_i$ is conserved under these general equivalence moves. Besides, the conserved quantities S^2 of actively interacting braids is generalized to the **effective state** $\chi = (-)^{|X|} S_l S_r$ for generic braids. These results are summarized by the following Lemma.

Lemma 5.2. *Under a general rotation $R_{m,n}$, a braid's effective twist number, Θ, and its effective state, χ, are conserved.*

---

[2]This is consistent with Eq. 2.3.

Proof. By Eq. 5.5, a general rotation $R_{m,n}$ can transform a generic braid

$$
{}^{S_l}_{T_l}[(T_a, T_b, T_c)\sigma_X]^{S_r}_{T_r},
$$

with $\Theta = T_l + T_r + \sum_{i=a}^{c} T_i - 2\sum_{i=1}^{|X|} x_i$ and $\chi = (-)^{|X|} S_l S_r$, into

$$
{}^{(-)^m S_l}_{T_l+m}[(P^{S_l}_m(T_a - m - n, T_b - m - n, T_c - m - n))\sigma_{X_l(S_l,m)XX_r(S_r,n)}]^{(-)^n S_r}_{T_r+n},
$$

with

$$
\Theta' = (T_l + m) + (T_r + n) + (\sum_{i=a}^{c} T_i - 3(m + n)) - 2(\sum_{i=1}^{|m|} y_i + \sum_{i=1}^{|X|} x_i + \sum_{i=1}^{|n|} z_i),
$$

where $y_i \in X_l(S_l, m)$ and $z_i \in X_r(S_r, n)$ and

$$
\chi' = (-)^{|X_l(S_l,m)|+|X|+|X_r(S_r,n)|}(-)^m S_l (-)^n S_r.
$$

Nonetheless, by Eq. 5.8 and Eq. 5.9, we obtain

$$
\Theta' = T_l + T_r + \sum_{i=a}^{c} T_i + \sum_{i=1}^{|X|} x_i + m + n - 3(m + n) - 2(-m - n) = \Theta,
$$

and

$$
\chi' = (-)^{|X|+|m|+|n|}(-)^m S_l (-)^n S_r = (-)^{|X|} S_l S_r = \chi.
$$

This establishes the proof. $\square$

As a direct consequence of Lemma 5.2, we have the following Theorem, which provides a character for actively-interacting braids.

Theorem 5.1. *The effective state of any actively-interacting braids is $\chi = 1$, and any braid with effective state $\chi = -1$ must be non-actively interacting.*

Proof. The proof of this theorem is very simple. Any actively-interacting braid has a trivial representation, whose effective state is $\chi \equiv S^2 = 1$. Hence, according to Lemma 5.2, the effective state of any actively-interacting braid must be $\chi = 1$. This implies, on the other hand, any stable braid with $\chi = -1$ is never actively-interacting. $\square$

All results we have obtained so far are valid for braids in any representation. Now we would like to consider the extremal representations of a braid. According to Chapter 4, we know that an actively interacting braid has infinite number of extrema, which are trivial braids related to each other by simultaneous rotations. Moreover, $T_l + T_r$, the triple (T_a, T_b, T_c) up to permutation, and S^2 are conserved under these simultaneous rotations. For non-actively interacting braids, the situation is more involved because their extrema are not trivial braids and that generic rotations (including generic simultaneous rotations) increase the number of crossings of an extremum, and hence take a braid away from their extremal representations. A non-actively interacting braid also has infinite number of extrema, however, according to the following Lemma.

Lemma 5.3. *Simultaneous rotations of the form $R_{3k,-3k}$ with $k \in \mathbb{Z}$ takes an extremum of a braid to another extremum of the braid.*

Proof. By definition, all extrema of the same braid have the same number of crossings. Thus we only need to prove that $R_{3k,-3k}$, $k \in \mathbb{Z}$ on an extremum preserves its number of crossings, then the resultant representation of braid must also be an extremum; otherwise the braid diagram undergoing the rotation should not be an extremum in the first place. Additionally, since $R_{3k,-3k} = R_{\pm 3,\mp 3}^{|k|}$ by Eq. 4.3, where the $\pm$ and $\mp$ depend on the sign of k. It is sufficient to prove the case of $k = \pm 1$, which are just simultaneous π rotations. We now prove that simultaneous π-rotations of a braid take the braid's crossing sequence, $X = x_1 \cdots x_i \cdots x_N$, $N \in \mathbb{N}$, to $\bar{X} = \bar{x}_1 \cdots \bar{x}_i \cdots \bar{x}_N$, $N \in \mathbb{N}$, where

$$\bar{x}_i = \begin{cases} d, & x_i = u \\ u, & x_i = d \end{cases},$$

and thus keep the number of crossings of the braid invariant. For one-crossing braids with arbitrary S_l and S_r, it is straightforward to see that $X_l(S_l, \pm 3)x_1 X_r(S_r, \mp 3) = \bar{x}_1$, for $x_1 = u, d, u^{-1}, d^{-1}$. We assume that the this is true for any braid with up to $N \in \mathbb{N}$ crossings, with arbitrary end-node states, namely

$$X_l(S_l, \pm 3)x_1 x_2 ... x_N X_r(S_r, \mp 3) = \bar{x}_1 \bar{x}_2 ... \bar{x}_N.$$

Hence, for any braid with $N + 1$ crossings and end-node states, say S_l' and S_r',

$$X_l(S_l', \pm 3)x_1 x_2 ... x_N x_{N+1} X_r(S_r', \mp 3)$$

$$\xrightarrow{X_r(S,\mp 3)X_l(S,\pm 3)=\mathbb{I}} = (X_l(S_l', \pm 3)x_1 x_2 ... x_N X_r(S, \mp 3))(X_l(S, \pm 3)x_{N+1} X_r(S_r', \mp 3)),$$

where we inserted a pair of crossing sequences, $X_r(S, \pm 3)$ and $X_l(S, \pm 3)$ with arbitrary S, whose product is trivial by Lemma 5.1, between the N-th and $(N + 1)$-th crossing. Note that these two crossing sequences inserted are not created by real rotations $R_{0,\pm 3}$ or $R_{\pm 3,0}$, but rather only equal to respectively the crossing sequences created by these two rotations. Hence, according to the assumption that the claim is valid for an N-crossing braid with arbitrary end-node states, and the validity for all one-crossing braids, we arrive at

$$X_l(S_l, \pm 1)x_1 x_2 ... x_N x_{N+1} X_r(S_r, \mp 1) = (\bar{x}_1 \bar{x}_2 ... \bar{x}_N)(\bar{x}_{N+1}) = \bar{x}_1 \bar{x}_2 ... \bar{x}_{N+1}.$$

Bearing in mind that $|X| = |\bar{X}|$, therefore by induction, simultaneous rotations, $R_{\pm 3,\mp 3}$ take a generic braid with crossing sequence X to an equivalent braid with sequence $\bar{X}$, which does not change the number of crossings. This certainly indicates that $R_{3k,-3k}$ with $k \in \mathbb{Z}$ rotates an extremum to another extremum of the same braid, which validates the proof. Furthermore, by Eq. 5.5, Eq. 5.6, and Eq. 4.8, and with a convenient redefinition: $\bar{X} = \bar{f}(X)$, we can pin down the algebraic form of the action of a $R_{3k,-3k}$, $k \in \mathbb{Z}$ on generic braids,

$$R_{3k,-3k}\left(^{S_l}_{T_l}[(T_a, T_b, T_c)\sigma_X]^{S_r}_{T_r}\right)$$
$$= ^{(-)^{3k}S_l}_{T_l+3k}[((1,3)^k(T_a, T_b, T_c))\sigma_{\bar{f}^k(X)}]^{(-)^{3k}S_r}_{T_r-3k}, \tag{5.10}$$

or equivalently,

$$R_{3k,-3k}({}^{S_l}_{T_l}[\sigma_X^{-1}(T_{a'}, T_{b'}, T_{c'})]^{S_r}_{T_r})$$
$$= {}^{(-)^{3k}S_l}_{T_l+3k}[\sigma_{\bar{f}^k(X)}^{-1}((1,3)^k(T_{a'}, T_{b'}, T_{c'}))]^{(-)^{3k}S_r}_{T_r-3k}, \tag{5.11}$$

where $(1,3)^k$ is the permutation induced by $R_{3k,-3k}$, and $\bar{f}^k(X) = X$ for k even, while $\bar{f}^k(X) = \bar{f}(X)$ for k odd. $\qquad\square$

Similar to the case of actively-interacting braids, generic braids also have conserved quantities under rotations in the form of $R_{3k,-3k}$, owing to the Lemma in below.

Lemma 5.4. $T_l + T_r$, $\sum_{i=a}^{c} T_i$, and $\sum_{i=1}^{|X|} x_i$ of an extremum of a braid are invariant under rotations of the form $R_{3k,-3k}$, $k \in \mathbb{Z}$. The triple (T_a, T_b, T_c) is invariant when k is even.

Proof. From Eq. 5.10 and Eq. 5.11, it is obvious that a rotation of the form $R_{3k,-3k}$, $k \in \mathbb{Z}$ takes $T_l + T_r$ to $T_l + 3k + T_r - 3k = T_l + T_r$, turns the triple (T_a, T_b, T_c) into $(1,3)^k(T_a, T_b, T_c)$, which is again (T_a, T_b, T_c) if k is even but does not affect $\sum_{i=a}^{c} T_i$ in any case, and changes $\sum_{i=1}^{|X|} X_i$ to $\sum_{i=1}^{|\bar{X}|} \bar{x}_i = \sum_{i=1}^{|X|} x_i$. $\qquad\square$

These conserved quantities imply that the previously defined Θ is also a conserved quantity under this class of equivalence moves, which is expected because in Lemma 5.2 we have shown that Θ is conserved under any rotations. That is, it is the same for any representation of a braid.

Now that we have found conserved quantities under rotations of the form $R_{3k,-3k}$, $k \in \mathbb{Z}$. The only issue left behind is that we have not proven that the simultaneous rotations of multiple of π are the only possible class of rotations under which the set of all extrema of a braid is closed. If this is true, then each conserved quantity in Lemma 5.4 is identical for all extrema of a braid. Strong evidences exist to show that this is indeed the case; however, we are lack of a rigorous proof. Therefore, we only state this observation as a conjecture.

Conjecture 5.1. *Any rotation that transforms an extremum to another extremum of the same braid must take the form of $R_{3k,-3k}$ with $k \in \mathbb{Z}$. Assuming this, all extrema of a braid share the same $T_l + T_r$, $\sum_{i=a}^{c} T_i$, and $\sum_{i=1}^{|X|} x_i$.*

5.3 Algebra of direct interactions: symmetries and relations

Chapter 4 shows that the interaction of any two actively interacting braids produces another actively interacting braid. Now that we are dealing with not only actively interacting braids but also other ones, one may ask what the outcome of the interaction of an actively interacting braid and a non-actively interacting braid, say a propagating braid, should be. To answer this question, we need sufficient preparation, divided into the following subsections.

5.3.1 Conserved quantities under interactions

We first repeat in words the interaction condition formulated in Chapters 3 and 4. This condition demands that one of the two braids, say B_1 and B_2, under an interaction must be active and that the two adjacent nodes, one of B_1 and the other of B_2, are either already in or can be rotated to the configuration where they have the same state and share a twist-free edge. The latter requirement is actually the Condition 2.1. The algebraic form of this condition is explicitly given in Chapter 4, and will be adopted directly.

As pointed out before, a convenient choice of the representative of the class is important. Whether a braid is propagating or not is most transparent when the braid is in its unique representation. On the other hand, an actively interacting braid can always be put in a trivial representation, which simplifies the calculation of interactions. Therefore, in this section we write actively interacting braids in their trivial representations, but non-actively interacting ones in their unique representations.

Now when an actively interacting braid, B, meets a non-actively interacting braid, B', say from the left of B' (the case where B is on the right of B' follows similarly), with the interaction condition fulfilled, what does the resulted braid $B + B'$ look like? Here, as in Chapter 4, we use a + for the operation of interaction. A special case is that B in its trivial form has no right external twist, and since B' is in the representation without external twist, one can directly apply a $2 \to 3$ move of the B's right end-node and the left end-node of B', then use the techniques introduced in Chapter 4 to complete the interaction. Let us address this simple case first.

Lemma 5.5. *Given an actively interacting braid $B = {}^{S}_{T_l}[T_a, T_b, T_c]^{S}_{T_r}$, with $T_r = 0$, and a non-actively interacting braid $B' = {}^{S_l}_{0}[(T'_a, T'_b, T'_c)\sigma_X]^{S_r}_{0}$, with $S_l = S$, the interaction of B and B' with B on the left of B' produces $B'' = {}^{(-)^{T_l}S_l}_{0}[(P^S_{-T_l}(T_a + T'_a + T_l, T_b + T'_b + T_l, T_c + T'_c + T_l))\sigma_{X_l(S, -T_l)X}]^{S_r}_{0}$.*

Proof. As $T_r = 0$ and $S = S_l$, the interaction condition is met and thus no rotation is needed; hence, according to Chapter 3, $B + B'$ forms a connected sum of B and B', which is, in our algebraic language,

$$
\begin{aligned}
B + B' &= {}^{S_l}_{T_l}[T_a, T_b, T_c]^{S_l}_{0} \ \# \ {}^{S_l}_{0}[(T'_a, T'_b, T'_c)\sigma_X]^{S_r}_{0} \\
&= {}^{S_l}_{T_l}[(T_a + T'_a, T_b + T'_b, T_c + T'_c)\sigma_X]^{S_r}_{0} \\
&\cong R_{-T_l, 0}\left({}^{S_l}_{T_l}[(T_a + T'_a, T_b + T'_b, T_c + T'_c)\sigma_X]^{S_r}_{0}\right) \\
&= {}^{(-)^{T_l}S_l}_{0}[(P^S_{-T_l}(T_a + T'_a + T_l, T_b + T'_b + T_l, T_c + T'_c + T_l))\sigma_{X_l(S, -T_l)X}]^{S_r}_{0} \,,
\end{aligned}
\tag{5.12}
$$

where a rotation $R_{-T_l, 0}$ is applied after the connected sum to put the resulted braid in its unique representation, which induces a permutation $P^S_{-T_l}$ on the left triple of internal twists, and a crossing sequence $X_l(S, -T_l)$, appended to the original X from left. $\qquad\square$

Nevertheless, in general the trivial diagram representing an actively interacting braid may have external twists on both external edges. If the interaction condition is satisfied when the trivial braid in this case meets a non-actively interacting braid, a rotation is usually required in order to perform the connected sum algebraically for them to interact. We now deal with this.

Lemma 5.6. *Given an actively interacting braid* $B = {}_{T_l}^{S}[T_a, T_b, T_c]_{T_r}^{S}$ *on the left of a non-actively interacting braid,* $B' = {}_0^{S_l}[(T_a', T_b', T_c')\sigma_X]_0^{S_r}$, *with the interaction condition satisfied by* $(-)^{T_r}S = S_l$, *the interaction of B and B' results in a braid*

$$B'' = {}^{(-)^{T_l}S}_0[((P^S_{-T_l}(T_a, T_b, T_c)) + (P^{(-)^{T_r}S}_{-T_l-T_r}(T_a', T_b', T_c')) + (T_l + T_r, \cdot, \cdot))\sigma_{X_l((-)^{T_r}S, -T_l-T_r)X}]_0^{S_r},$$

where $(T_l + T_r, \cdot, \cdot)$ *is the short for* $(T_l + T_r, T_l + T_r, T_l + T_r)$.

Proof.

$$B + B'$$

$$= {}_{T_l}^{S}[T_a, T_b, T_c]_{T_r}^{S} + {}_0^{S_l}[(T_a', T_b', T_c')\sigma_X]_0^{S_r}$$

$$\cong R_{T_r, -T_r}\left({}_{T_l}^{S}[T_a, T_b, T_c]_{T_r}^{S}\right) \# {}_0^{S_l}[(T_a', T_b', T_c')\sigma_X]_0^{S_r}$$

$$= {}^{(-)^{T_r}S}_{T_l+T_r}[P^S_{T_r}(T_a, T_b, T_c)]_0^{(-)^{T_r}S} \# {}_0^{S_l}[(T_a', T_b', T_c')\sigma_X]_0^{S_r} \tag{5.13}$$

$$= {}^{(-)^{T_r}S}_{T_l+T_r}[((P^S_{T_r}(T_a, T_b, T_c)) + (T_a', T_b', T_c'))\sigma_X]_0^{S_r} \quad \overset{(-)^{T_r}S = S_l}{\Longleftarrow} \tag{5.14}$$

$$\cong R_{-T_l-T_r, 0}\left({}^{(-)^{T_r}S}_{T_l+T_r}[((P^S_{T_r}(T_a, T_b, T_c)) + (T_a', T_b', T_c'))\sigma_X]_0^{S_r}\right)$$

$$= {}^{(-)^{T_l}S}_0[(P^{(-)^{T_r}S}_{-T_l-T_r}((P^S_{T_r}(T_a, T_b, T_c)) + (T_a', T_b', T_c')) + (T_l + T_r, \cdot, \cdot))\sigma_{X_l((-)^{T_r}S, -T_l-T_r)X}]_0^{S_r}$$

$$= {}^{(-)^{T_l}S}_0[((P^S_{-T_l}(T_a, T_b, T_c)) + (P^{(-)^{T_r}S}_{-T_l-T_r}(T_a', T_b', T_c')) + (T_l + T_r, \cdot, \cdot))\sigma_{X_l((-)^{T_r}S, -T_l-T_r)X}]_0^{S_r}, \tag{5.15}$$

where the simultaneous rotation $R_{T_r, -T_r}$ is applied to realize the interaction condition in order to do the connected sum, and the rotation $R_{-T_l-T_r, 0}$ is exerted such that the final result is in its unique representation, which induces a permutation $P^{(-)^{T_r}S}_{-T_l-T_r}$ and a crossing sequence $X_l((-)^{T_r}S, -T_l - T_r)$ concatenated to X from left. The above equation obviously reduces to Eq. 5.12 when $T_r = 0$. $\quad\square$

Nonetheless, each actively interacting braid has infinite number of equivalent trivial braid diagrams, in the sense that any two of them are related by a simultaneous rotation $R_{n,-n}$, $n \in \mathbb{Z}$. It is then naturally to ask if the choice of the trivial braid diagram representing a braid equivalence class influences the interaction of the braid and another braid. The answer is "No". The reason is obvious because of the equivalence of the trivial diagrams. Because of the necessity of realizing of the interaction condition in a concrete calculation of interaction, however, it is better to formulate this claim explicitly by our algebraic calculus as a Lemma.

Lemma 5.7. *For any actively interacting braid B, its interaction onto any other braid B', i.e.,* $B + B'$ *or* $B' + B$, *is independent of the choice of the trivial diagram representing B.*

Proof. We prove the case of $B + B'$. Let $B_0 = {}_{T_l}^{S}[T_a, T_b, T_c]_{T_r}^{S}$ be a trivial diagram representing an actively interacting braid B. Let $B' = {}_0^{S_l}[(T_a', T_b', T_c')\sigma_X]_0^{S_r}$ be the non-actively interacting braid on which B interacts. We assume the interaction condition is satisfied by $(-)^{T_r}S = S_l$. Any other trivial braid, say B_n, representing B can be obtained from B_0 by

$$B_n = R_{n,-n}(B_0) = {}^{(-)^nS}_{T_l+n}[P^S_n(T_a, T_b, T_c)]_{T_r-n}^{(-)^nS}.$$

$B_0 + B'$ has already been shown in Lemma 5.6, but we only need Eq. 5.13 therein, which is the configuration of the two braid after the interaction condition is realized. If we replace B_0 by B_n in the interaction, we have

$$
\begin{aligned}
B_n + B' &= {}^{(-)^n S}_{T_l+n}[P_n^S(T_a, T_b, T_c)]_{T_r-n}^{(-)^n S} + {}^{S_l}_0[(T'_a, T'_b, T'_c)\sigma_X]_0^{S_r} \\
&\cong R_{T_r-n,-T_r+n}\left({}^{(-)^n S}_{T_l+n}[P_n^S(T_a, T_b, T_c)]_{T_r-n}^{(-)^n S}\right) \# {}^{S_l}_0[(T'_a, T'_b, T'_c)\sigma_X]_0^{S_r} \\
&\xRightarrow{(-)^{2n}S=S} = {}^{(-)^{T_r}S}_{T_l+T_r}[P_{T_r-n}^{(-)^n S} P_n^S(T_a, T_b, T_c)]_0^{(-)^{T_r}S} \# {}^{S_l}_0[(T'_a, T'_b, T'_c)\sigma_X]_0^{S_r} \\
&\xRightarrow{P_{T_r-n}^{(-)^n S}=P_{T_r}^S P_{-n}^{(-)^n S}} = {}^{(-)^{T_r}S}_{T_l+T_r}[P_{T_r}^S P_{-n}^{(-)^n S} P_n^S(T_a, T_b, T_c)]_0^{(-)^{T_r}S} \# {}^{S_l}_0[(T'_a, T'_b, T'_c)\sigma_X]_0^{S_r} \\
&\xRightarrow{P_{-n}^{(-)^n S} P_n^S \equiv \mathbb{1} \text{ by Lemma 4.1}} = {}^{(-)^{T_r}S}_{T_l+T_r}[P_{T_r}^S(T_a, T_b, T_c)]_0^{(-)^{T_r}S} \# {}^{S_l}_0[(T'_a, T'_b, T'_c)\sigma_X]_0^{S_r} \,,
\end{aligned}
$$

which is exactly the same as Eq. 5.13. That is, if B_0 interacts with B', so does B_n, and they give rise to the same result. Likewise, this is also true for the case of $B' + B$. This closes the proof. $\square$

Now that we established Lemma 5.7, we may choose to always represent an actively interacting braid B by its trivial representative without right (left) external twist, in dealing with the interaction of B onto a non-actively interacting braid from the left (right). This should simplify the calculation and expression because Lemma 5.5 directly applies. Moreover, the result of Lemma 5.5, namely Eq. 5.12, is identical to the result when the actively interacting braid is in its unique representation. This again, together with Chapter 4, shows that the choice of representative of a braid does not affect the result of the interaction involving the braid, in accordance with Chapter 3. Examples can be found in Chapter 3, one just need to cast them in our new symbolic notation.

Equipped with this algebra, we shall prove one of our primary results.

Theorem 5.2. *Given an actively interacting braid, $B = {}^S_{T_l}[T_a, T_b, T_c]^S_{T_r}$, and a non-actively interacting braid, $B' = {}^{S_l}_0[(T'_a, T'_b, T'_c)\sigma_X]_0^{S_r}$, such that $B'' = B + B'$, the effective twist number Θ is an additive conserved quantity, while the effective state χ is a multiplicative conserved quantity, namely*

$$
\begin{aligned}
\Theta_{B''} &= \Theta_B + \Theta_{B'} \\
\chi_{B''} &= \chi_B \chi_{B'}.
\end{aligned}
\tag{5.16}
$$

Proof. We can readily write down

$$
\Theta_B = T_l + T_r + \sum_{i=a}^{c} T_i, \quad \chi_B = 1,
$$

and

$$
\Theta_{B'} = \sum_{i=a}^{c} T_i - 2\sum_{j=1}^{|X|} x_j, \quad \chi_{B'} = (-)^{|X|} S_l S_r.
$$

69

Hence, according to Eq. 5.15, we have

$$\Theta_{B''} = \sum_{i=a}^{c}(T_i + T_i') + 3(T_l + T_r) - 2\sum_{j=1}^{|X_l|} x_j - 2\sum_{k=1}^{|X|} x_k$$

$$= \sum_{i=a}^{c}(T_i + T_i') + (T_l + T_r) - 2\sum_{k=1}^{|X|} x_k$$

$$= \Theta_B + \Theta_{B'}, \tag{5.17}$$

where the second equality is a result of $\sum_{j=1}^{|X_l((-)^{T_r}S, -T_l-T_r)|} x_j = T_l + T_r$, by Eq. 5.9. Besides,

$$\chi_{B''} = (-)^{|T_l+T_r|+|X|}(-)^{T_l}S\,S_r = (-)^{|X|}(-)^{T_r}S\,S_r = (-)^{|X|}S_l S_r = \chi_{B'} = \chi_B \chi_{B'}. \tag{5.18}$$

□

This theorem demonstrates that the by far discovered two representative-independent conserved quantities, Θ and χ are also conserved under interactions, in the sense that the former is additive while the latter is multiplicative. This is consistent to Chapter 4 in which only interactions between actively interacting braids are discussed. In particular, χ becomes the S^2 in Chapter 4, whose conservation means that the interacting character of the braids is preserved. Furthermore, according to Theorem 5.1, the multiplicative conservation of χ shows that if the non-actively interacting braid involved in an interaction has $\chi = -1$, the resulted braid must also has $\chi = -1$, and is thus a non-actively interacting braid too.

5.3.2 Asymmetry between $B + B'$ and $B' + B$

It is important to note that Theorem 5.2 is also true for interactions where the actively interacting braids on the right of the non-actively interacting ones. In fact, all the discussion above can be equally well applied to this case. One must then ask a question: does an actively interacting braid gives the same result when it interacts on to a non-actively interacting braid from the left and from the right respectively? The answer is "No" in general. We now discuss this issue by considering an actively interacting braid, B, and a non-actively interacting braid, B'.

First of all, even if the interaction condition is met in the case $B + B'$, the case of $B' + B$ may not satisfy the interaction condition, such that $B' + B$ is an impossible interaction. If we assume the interaction condition can be realized in both cases, $B + B'$ and $B' + B$ still give rise to different results, i.e., inequivalent braids, in general. Let us explain this.

In the case of $B + B'$, by Lemma 5.7 we can represent B by its trivial braid diagram without T_r, viz $B \cong B_l = {}_{T_l}^{S}[T_a, T_b, T_c]_0^S$, which allows us to use Eq. 5.12. In the case of $B' + B$, however, we represent B by its trivial representation without the left external twist, which is obtained by a simultaneous rotation from B_l, i.e., $B \cong B_r = R_{-T_l, T_l}(B_l) = {}_0^{(-)^{T_l}S}[P_{-T_l}^S(T_a, T_b, T_c)]_{T_l}^{(-)^{T_l}S}$. Then for

$B' = {}^{S_l}_0[(T'_a, T'_b, T'_c)\sigma_X]^{S_r}_0$, the interaction condition in the latter case is $S_r = (-)^{T_l}S$. With also $S = S_l$, we conclude that the condition for both $B + B'$ and $B' + B$ doable is

$$S_l = (-)^{T_l}S_r. \tag{5.19}$$

Given this, by a similar calculation as that in Lemma 5.5, one can find

$$\begin{aligned}B' + B &= {}^{S_l}_0[((T'_a + T_l, T'_b + T_l, T'_c + T_l) + (\sigma_X^{-1}P^S_{-T_l}(T_a, T_b, T_c)))\sigma_{XX_r(S_r, -T_l)}]^{(-)^{T_l}S_r}_0 \\ &= {}^{S_l}_0[((T'_a + T_l, T'_b + T_l, T'_c + T_l) + (\sigma_X^{-1}P^S_{-T_l}(T_a, T_b, T_c)))\sigma_{XX_r(S_r, -T_l)}]^{S_l}_0 . \end{aligned} \tag{5.20}$$

To compare this to $B + B'$, we rewrite Eq. 5.12 as follows, taking Eq. 5.19 into account.

$$B + B' = {}^{S_l}_0[(P^S_{-T_l}(T_a + T'_a + T_l, T_b + T'_b + T_l, T_c + T'_c + T_l))\sigma_{X_l(S_l, -T_l)X}]^{S_r}_0 \tag{5.21}$$

It is important to notice that, by Eq. 5.20 and Eq. 5.21, both $B + B'$ and $B' + B$ are in their unique representations. Since we know such a representative is unique for each equivalence class of braids, $B + B'$ and $B' + B$ can never be equivalent. Nevertheless, $B + B'$ and $B' + B$ may simply be equal. For this to be true, braids B and B' are pretty strongly constrained.

Firstly, one obviously has to require $S_l = S_r$ and $T_l = 2k$, $k \in \mathbb{Z}$ in Eq. 5.20 and Eq. 5.21, such that $B + B'$ and $B' + B$ have the same end-node states. This, together with the interaction condition, also indicates $S_l = S_r = S$. Keeping this in mind, one must then demand that $B + B'$ and $B' + B$ have the same crossing sequence, namely $X_l(S, -T_l)X = XX_r(S, -T_l)$, which can also be written as $X_l(S, -T_l)XX_r^{-1}(S, -T_l) = X$. With Lemma 5.1, this can be put in the form, $X_l(S, -T_l)XX_l(S, T_l) = X$. Because Eq. 5.7 reads that $X_l(S, m) = X_r(S, m)$ for m even, this condition is better expressed as

$$X_l(S, -T_l)XX_r(S, T_l) = X,$$

which now appears to be the requirement that a simultaneous $(-T_l)$-rotation leaves the crossing sequence intact. Although it has been conjectured in the end of Section 5.2 that only simultaneous rotations of $6k$, $k \in \mathbb{Z}$ are able to achieve this condition, we would like to keep its current general format because the conjectured has not been proved. Interestingly, however, we will see an automatic input of $6k$, $k \in \mathbb{Z}$ shortly.

At this point, three possibilities will arise, each of which leads to a different condition on top of the conditions found above. The first possibility is that we do not put any constraint on the internal twists. Hence, according to Eq. 5.20 and Eq. 5.21, such that $B' + B$ equals $B + B'$ we have to demand $\sigma_X^{-1}P^S_{-T_l} = P^S_{-T_l} \equiv \mathbb{1}$. An immediate consequence is that $\sigma_X = \mathbb{1}$, which does not, however, constraint the pattern of X very much. Moreover, as we know that T_l is even, then by Eq. 4.8, $P^S_{-T_l} \equiv \mathbb{1}$ if and only if $T_l = 6j$, $j \in \mathbb{Z}$. With this T_l, Lemma 5.3 ensures the fulfillment of the condition, $X_l(S, -T_l)XX_r(S, T_l) = X$, which now becomes redundant in this case.

The second possibility is to relax the first one a little bit by only requiring $\sigma_X^{-1}P^S_{-T_l} = P^S_{-T_l}$. this requirement only means that $\sigma_X = \mathbb{1}$, without constraining $P^S_{-T_l}$. Then, we notice that while in Eq. 5.21 both of the triples (T_a, T_b, T_c) and (T'_a, T'_b, T'_c) are under the same permutation $P^S_{-T_l}$, in Eq. 5.20 only the triple (T_a, T_b, T_c) is permuted by $P^S_{-T_l}$. Therefore, the only way to make $B + B' = B' + B$ is

71

to mandate $P^S_{-T_l}(T'_a, T'_b, T'_c) = (T'_a, T'_b, T'_c)$. Note that this does not necessarily mean $P^S_{-T_l} = \mathbb{1}$, e.g., when $P^S_{-T_l} = (1, 2)$ and $T'_a = T'_b$.

The last possibility is to remove even the condition $\sigma_X = \mathbb{1}$. As a result, the constraint on internal twists turns out to be stronger than those in the previous two possibilities. It is not hard to see, we must have in general $T_a = T_b = T_c$ but still $P^S_{-T_l}(T'_a, T'_b, T'_c) = (T'_a, T'_b, T'_c)$ in the meanwhile.

We have now exhausted all conditions with the most general consideration. More importantly, although we restricted our discussion to the case where B' is a non-actively interacting braid, the conditions automatically applies to the case where B' is even an actively interacting braid in its unique representation. Let us summarize this in the following theorem as another primary result of this chapter.

Theorem 5.3. *Given an actively interacting braid $B = {}^S_{T_l}[T_a, T_b, T_c]^S_0$, and an arbitrary braid in its unique representation, namely $B' = {}^{S_l}_0[(T'_a, T'_b, T'_c)\sigma_X]^{S_r}_0$, for $B + B' = B' + B$ to be true, we demand*

$$
\begin{aligned}
S_l &= S_r = S \\
T_l &= 2k, \ k \in \mathbb{Z}
\end{aligned}
\tag{5.22}
$$

and

$$
X_l(S, -T_l)XX_r(S, T_l) = X
\tag{5.23}
$$

and any of the following three:

1.

$$
\begin{aligned}
\sigma_X &= \mathbb{1} \\
T_l &= 6k, \ k \in \mathbb{Z}
\end{aligned}
$$

$$
\sigma_X = \mathbb{1}
\tag{5.24}
$$
$$
T_l = 6k, \ k \in \mathbb{Z}
\tag{5.25}
$$

2.

$$
\sigma_X = \mathbb{1}
$$
$$
P^S_{-T_l}(T'_a, T'_b, T'_c) = (T'_a, T'_b, T'_c)
\tag{5.26}
$$

3.

$$
T_a = T_b = T_c
$$
$$
P^S_{-T_l}(T'_a, T'_b, T'_c) = (T'_a, T'_b, T'_c).
\tag{5.27}
$$

An important remark is that Theorem 5.3 is based on the assumption that Conjecture 5.1 may be incorrect. If Conjecture 5.1 happen to be correct (a strong evidence that it is indeed so exists), then the conditions in Theorem 5.3 should be modified as follows. The satisfaction of Eq. 5.23 indicates $T_l = 6k$, $k \in \mathbb{Z}$, which immediately ensures that Eq. 5.25 holds and that $P^S_{-T_l} \equiv \mathbb{1}$. Therefore, by simple logic the condition that $B + B' = B' + B$, if Conjecture 5.1 stands, is reduced to:

$$
\begin{aligned}
S_l &= S_r = S \\
T_l &= 6k, \ k \in \mathbb{Z}
\end{aligned}
\tag{5.28}
$$

and either

$$\sigma_X = \mathbb{1} \tag{5.29}$$

or

$$T_a = T_b = T_c. \tag{5.30}$$

The discussion above focuses on how $B + B'$ is equal to $B' + B$. Another possibility is that some asymmetric interactions are related by discrete transformations. Since discrete transformation is the topic of the next chapter, we will leave the discussion of this possibility there.

5.3.3 The algebraic structure

With the help of this notation and the algebraic method established on it we are able to show that the set of all stable braids, namely the actively interacting braids, actively propagating braids, and non-actively propagating braids, almost form an algebra under direct braid interaction. The set of stable braids is closed because any direct interaction of two stable braids never leads to an instable braid because the stability condition put forward in Section 2.7. But this set is not yet an algebra because a direct interaction does not happen between two non-actively interacting braids.

Nevertheless, the set of all actively interacting braids is indeed an algebra with direct interaction as its product, as we showed in Chapter 4 that a direct interaction between two actively interacting braids always results in another actively interacting braid. On the other hand, direct interactions between actively and non-actively interacting braids are more complicated and involved. Fortunately, provided with all the discussion in previous sections, we can try to answer the question raised at the beginning of Section 5.3. This question can be first partly answered by the following Theorem.

Theorem 5.4. *Actively interacting braids are morphisms on the set of non-actively interacting braids via direct interactions.*

Proof. This theorem can be rephrased; it simply states that an actively interacting braid behaves like a morphism, taking an non-actively interacting braid to another one via a direct interaction. That is, we need to show that any direct interaction between an actively interacting braid and a non-actively interacting one always leads to another non-actively interacting braid. Recalling Theorem 5.1 and Theorem 5.2, since the effective state χ is a multiplicative conserved quantity under interaction and an actively interacting braid must have $\chi = 1$, the interaction of an actively interacting braid and any non-actively interacting braid with $\chi = -1$ must leads to a non-actively interacting braid with $\chi = -1$.

Nonetheless, the above is not a complete proof because a non-actively interacting braid may also have $\chi = 1$. A full proof can be easily constructed by contradiction. For this purpose, we need the following facts, extracted from Chapter 3, of non-actively interacting braid:

1. A non-actively propagating braid is neither left nor right completely reducible.

2. An actively propagating braid is not completely-reducible from either end-node; otherwise it must be both left and right completely-reducible, which makes it an actively interacting braid if equipped with appropriate twists.

Now let us consider an actively interacting braid B in an arbitrary trivial representation and a non-actively interacting braid B' in its unique representation, with the interaction condition met, their interaction, say $B + B'$ (the case of $B' + B$, if possible, will follow similarly), results in, by Eq. 5.14, with internal twists ignored because they are irrelevant,

$$B + B' = \; {}^{S_l}_{T_l + T_r}[(\cdot, \because, \cdot)\sigma_X]^{S_r}_0 \qquad (5.31)$$

We do not apply a rotation of the left end-node of $B + B'$ because things will become less transparent otherwise. Note that according to Eq. 5.31, at this stage, the two end-nodes of $B + B'$ are in the same states respectively as those of B' before the interaction, and also that it has the same crossing sequence X as B' does. This means the irreducibility of $B + B'$ inherits that of B'.

We know that an actively interacting braid must be both left and right completely-reducible. Now that B' is non-actively interacting, it is never completely-reducible from both sides, which means $B + B'$ is not either by Eq. 5.31. Otherwise, B' should be two-way completely reducible in the first place, which is contradictory to any basic facts listed above of a non-actively interacting braid. Therefore, the theorem holds. $\qquad \square$

We still need to discuss if a direct interaction of an actively interacting braid and a non-actively interacting but actively propagating (non-actively propagating) braid creates an actively propagating (non-actively propagating) braid. The answer is: Not always. To illustrate this, we show two examples.

Let us consider an actively interacting braid, $B = {}^{+}_{-1}[1, 1, -1]^{+}_0$, and an actively propagating braid, $B_p = {}^{+}_0[(-5, -5, 1)\sigma_{ud^{-1}}]^{+}_0$, whose graphical presentations can be found in Appendix E. Hence, by Eq. 5.12 we have

$$B + B_p = {}^{-}_0[(P^{+}_1(-5, -5, -1))\sigma_{u^{-1}ud^{-1}}]^{+}_0$$
$$\xrightarrow{P^{+}_1 = (1,\ 2)} = {}^{-}_0[(-5, -5, -1)\sigma_{d^{-1}}]^{+}_0 \;, \qquad (5.32)$$

which is an irreducible braid according to Appendices B and C, and is thus non-actively propagating. This example shows the interaction of an actively interacting braid and an actively propagating braid can result in a non-actively propagating braid. The reason for such a situation to arise is that the pair cancelation of crossings and the change of the end-node state, as a consequence of the interaction, which is lucid in the example above.

On the other hand, An actively interacting braid and a non-actively propagating braid can also produce an actively propagating braid via their interaction. To show this, we can use the braid in Eq. 5.32 as the stationary one and name it B_s, and consider an actively interacting braid $B = {}^{-}_1[-1, -1, 1]^{-}_0$. Also by Eq. 5.12 we obtain

$$B + B_s = {}^{+}_0[(P^{-}_{-1}(-5, -5, 1))\sigma_{ud^{-1}}]^{+}_0$$
$$\xrightarrow{P^{-}_{-1} = (1,\ 2)} = {}^{+}_0[(-5, -5, 1)\sigma_{ud^{-1}}]^{+}_0 \;, \qquad (5.33)$$

which is the very B_p in the previous example.

Above all, the set of all stable braids is almost an algebra, with direct interaction as its associative binary operation. Stable braids are excitations of embedded spin networks, which are considered to be basis states describing the fundamental space-time. Consequently, a physical state is usually a superposition of these basis states. It is clear that braid interaction, as the binary operation of the set of stable braids, is bilinear. Within this almost algebra structure, the set of actively interacting braids is indeed an algebra. In addition, because of the asymmetry between left and right interactions elaborated in Section 5.3.2, this algebra is noncommutative.

5.4 Summary

Conservation laws play a pivotal role in revealing the underlying structure of a physical theory. By means of invariants and conserved quantities we are able to determine how the content of the theory relates to particle physics, or what kind of new mathematical and/or physical inputs are necessary so that the theory is meaningful.

We have generalized the algebraic calculus of actively interacting braids, proposed in the previous chapter, to all stable braids, found a set of equivalence relations relating them, and discovered conserved quantities associated with these relations. More importantly, by means of this calculus we studied the interaction between actively interacting braids and non-actively interacting braid, and found that the set of stable braids has a structure that is almost a noncommutative algebra, containing a noncommutative algebra of only actively interacting braids. Actively interacting braids behave like maps taking a non-actively interacting braid to another one. From this we found both additive and multiplicative conserved quantities of braids under interaction. These are not only dynamically conserved but also conserved under the equivalence moves.

The interaction relation between actively interacting braids and that between actively and non-actively interacting braids imply that actively interacting braids are analogous to bosons, whereas the non-actively acting ones are analogous to fermions, as we know that fermions usually do not directly interact with each other but rather can interact with (gauge) bosons. The evidence of this analogy will become stronger in Chapter 7 after the study of exchange interaction there.

A possible next step is to determine which of these conserved quantities may correspond to quantum numbers. This is exactly what we are going to do in the next chapter in which discrete transformations of our braids will be discovered and mapped to charge conjugation, parity, time reversal and their products.

Chapter 6

C, P, and T of Braids

One of our goals is to see whether some braid excitations of embedded 4-valent spin networks can eventually correspond to the standard model particles or are more fundamental matter degrees of freedom. Because CPT is a symmetry of quantum field theories, in this chapter we investigate the discrete transformations of 3-strand braids of embedded 4-valent spin networks and map them to C, P, and T transformations and their products. We will see that direct braid interaction respects CPT.

In fact, as a follow-up work of [15], in [39] a similar study of CPT-symmetry is being taken for reduced link invariants of three-valent spin networks. In the 3-valent case, however, the invariants cannot be created or annihilated. Consequently, the meaning of C, P, and T is unclear. Besides, the largest discrete symmetry in the 3-valent case is $S_3 \times \mathbb{Z}_2$, giving more than C, P, T, and their products. On the contrary, in the 4-valent case, we have dynamics that surprisingly and strongly constraints the number of possible discrete transformations to be exactly seven, excluding the identity, which are allowed on 3-strand braids. Moreover, the algebra developed and conserved quantities of braids found in the previous chapter also help finding and mapping discrete transformations of braids to C, P, and T. This will become clear soon in the sequel.

We expect the discrete transformations to be representation independent; therefore, in this chapter we do not restrict our discussion to any specific representation of braids, but study our braids in their generic forms, as seen in Fig. 5.1(a) and Eq. 5.3.

6.1 Discrete transformations

Though not separately, as a theorem the combined action of the three discrete transformations C, P and T, namely CPT, is a symmetry in any Lorentz invariant, local field theory. Being a concrete model of QFT, the Standard Model respects the CPT-symmetry too. We have examined the continuous transformations such as equivalence moves on the 3-strand braids of embedded 4-valent spin networks in the previous chapters; hence, it is natural to look for the possible discrete transformations of these local excitations and check their correspondence with C, P, and T transformations. If the braids in our model would eventually be mapped to the Standard Model particles, or even if

they are more fundamental entities on their own, which do not directly correspond to the Standard Model particles, they should be characterized by quantum numbers that have certain properties under the transformations of C, P, and T. In fact, investigating the action of discrete transformations on our braid excitations can help us to construct quantum numbers of a braid, such as spin, charge, and so on, from the characterizing 8-tuple of the braid. If the 8-tuple, which only contains topological information of the embedding and framing, is not sufficient to produce all necessary quantum numbers, we may have to take spin network labels into account. One will see that this is indeed the case.

The dynamics of the braids of embedded 4-valent spin networks, namely the propagation and interactions, exerts natural constraints on the discrete transformations that can be defined on braids. The reason is that, for example, we should not allow a discrete transformation to turn an actively interacting braid into a non-actively interacting one because QFT does not bear a transformation that magically changes a particle to something else, and vice versa. Similarly, we can obtain other necessary rules. As a guideline, all rules are listed in the following condition.

Condition 6.1. *A legal discrete transformation $\mathcal{D}$ on an arbitrary braid B must meet:*

1. *If B is actively interacting, then $\mathcal{D}(B)$ also actively interacts.*

2. *If B is not actively interacting, $\mathcal{D}(B)$ must remain so.*

3. *If B is actively propagating, $\mathcal{D}(B)$ must still be actively propagating.*

4. *If B is non actively propagating, $\mathcal{D}(B)$ is non actively propagating as well.*

6.1.1   The group of discrete transformations

It is more convenient to write all discrete transformations in a compact, algebraic form. This can be achieved by introducing the **atomic discrete operations** that act on the crossing sequence, the end-nodes, the triples of internal twists, and the pair of external twists separately. Each atomic transformations is not qualified as a legal discrete transformation on its own because of the violation of Condition 6.1. Nevertheless, one can write a legal discrete transformation as a unique combination of the atomic ones. All atomic transformations are defined and listed with sufficient details in Appendix D, we thus in the rest of the main text will directly use them without further explanation but only a reference to the definition of each of them upon its first appearance.

In view of the parity transformation in QFT, the first kind of discrete transformations one may come up with is the mirror imaging of a braid. A braid can have two different mirror images, however. One is to have the mirror perpendicular to the plane on which the braid is projected, whereas the other is to arrange the mirror parallel to and behind the plane. Let us study them in order.

Fig. 6.1 illustrates the former case. Although only two generators of the crossing sequence X of an arbitrary braid is shown in this figure, it is not hard to see that the order of the crossings of the original X on the left of the mirror must be reversed by the mirror, resulting an $\mathcal{R}(X)$ (Def. D.4) in the mirror image of the original braid. Besides, the mirror inverts every crossing in X, giving
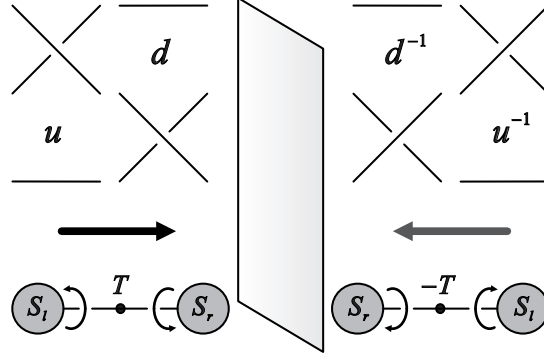
Figure 6.1: Shows how the crossing generators, end-nodes, twists, and propagation direction (indicated by the two thick arrows) of a braid (on the left) are mapped to their mirror images (on the right) via a mirror *perpendicular* to the plane on which the braid is projected.

rise to an $\mathcal{I}_X$ (Def. D.2). As a result, the mirror imaging takes the X to X^{-1}. Fig. 6.1 uses only one edge between the two end-nodes of a braid to demonstrate how the mirror changes the sign of the twist of the edge, which is sufficient to show that all twists of a braid should have a sign change via mirror imaging because the sign of a twist is unambiguously defined everywhere of an embedded spin network (recall Section 2.1). This means that the atomic operation $\mathcal{I}_T$ (Def. D.3) must be part of this mirror image transformation. In Fig. 6.1, the exchange of the two end-nodes implies the atomic operations $\mathcal{E}_S$ (Def. D.9) and $\mathcal{E}_{T_e}$ (Def. D.7), and an $\mathcal{R}$ also exists. Thus, the left triple of internal twists should be exchanged with the right triple of internal twists, i.e., an $\mathcal{E}_T$ (Def. D.6) is involved. These observations provide us an explicit definition of this mirror imaging as follows.

Definition 6.1. *The **perpendicular mirror imaging** is such a discrete transformation, denoted by $\mathcal{M}_\perp$, that*

$$\mathcal{M}_\perp = \mathcal{E}_S \mathcal{E}_{T_e} \mathcal{E}_T \mathcal{I}_T \mathcal{I}_X \mathcal{R},$$

and that for a generic braid $B = {}^{S_l}_{T_l}[(T_a, T_b, T_c)\sigma_X]^{S_r}_{T_r}$, with $(T_a, T_b, T_c)\sigma_X = (T_{a'}, T_{b'}, T_{c'})$

$$\mathcal{M}_\perp(B) = {}^{S_r}_{-T_l}[-(T_{a'}, T_{b'}, T_{c'})\sigma_{X^{-1}}]^{S_l}_{-T_r}, \tag{6.1}$$

with $-(T_{a'}, T_{b'}, T_{c'})\sigma_{X^{-1}} = -(T_a, T_b, T_c)$.

A important point to address is that $\mathcal{M}_\perp$ flips the propagation direction. That is, if a braid B is propagating, actively or in an induced way, to the right (left), then $\mathcal{M}_\perp(B)$ is propagating to the left (right), which is readily seen from Fig. 6.1 because a braid propagating towards the mirror from the left is mirrored to a braid towards the mirror from the right. This surely has no impact on a two-way propagating braid. Since $\mathcal{M}_\perp$ is simply a mirror image, an actively interacting braid stays so under this discrete transformation. Therefore, $\mathcal{M}_\perp$ fulfills Condition 6.1 and hence is indeed a legal discrete transformation of braids. Concrete graphic examples are shown in Appendix E.

Fig. 6.2 presents the second type of mirror imaging of a braid, where the mirror is parallel to and beneath the plane on which the braid is projected. In contrast to the mirror imaging of the

78
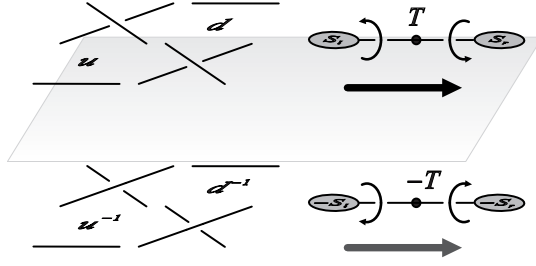
Figure 6.2: The crossing generators, end-nodes, twists, and the propagation direction of a braid (above the mirror) are mapped to their mirror images (below the mirror) via a mirror *parallel* to the plane on which the braid is projected.

first kind, the second kind does not reverse the order of the crossings and does not exchange the two end-nodes, which leads to no exchange of triples of internal twists. Fig. 6.2 makes clear that all crossings, twists, and the two end-node states are inverted, however, resulting in three atomic operations: $\mathcal{I}_X$, $\mathcal{I}_T$, and $\mathcal{I}_S$. As implied by the two thick arrows respectively above and below the mirror in Fig. 6.2, the propagation direction of a braid should not be reversed under this mirror imaging. This implies that a non-actively propagating braid remains so under this transformation. It is not hard to see that this type of mirror image of an actively interacting braid must still be actively interacting. Therefore, we have another legal discrete transformation of braids, as defined below.

Definition 6.2. *The parallel mirror imaging, $\mathcal{M}_\square$, is a discrete transformation in the form*

$$\mathcal{M}_\square = \mathcal{I}_X \mathcal{I}_T \mathcal{I}_S,$$

such that for a generic braid, $B = {}^{S_l}_{T_l}[(T_a, T_b, T_c)\sigma_X]^{S_r}_{T_r}$, *with* $(T_a, T_b, T_c)\sigma_X = (T_{a'}, T_{b'}, T_{c'})$

$$\mathcal{M}_\square(B) = {}^{\bar{S}_l}_{-T_l}[-(T_a, T_b, T_c)\sigma_{\mathcal{I}_X(X)}]^{\bar{S}_r}_{-T_r}, \tag{6.2}$$

with $-(T_a, T_b, T_c)\sigma_X = -(T_{a'}, T_{b'}, T_{c'})$.

After talking about reflections, it is now the turn to study other possibilities. The first is called a **vertical flip** (Fig. 6.3). Rather than showing the flip of a whole generic braid with respect to the axis (the thick grey horizontal line in the figure), Fig. 6.3 illustrates how the generators of a crossing sequence and a trivial braid diagram without crossings are transformed under such a flip, by which one can easily determine the corresponding transformation of an arbitrary braid. Note that this flip is not an equivalence rotation move, but rather a discrete operation, taking a braid, e.g., the one in the upper part of Fig. 6.3, directly to the one in the lower part of the same figure, without any continuous intermediate steps; hence, no extra twists or crossings are created or annihilated.

According to Fig. 6.3, the vertical flip neither reverses the order of crossings nor exchange the two end-nodes of a braid; however, it turns an upper crossing into a lower one and a lower one to an upper one, with their handedness unchanged, which gives rise to an $\mathcal{S}_c$ (Def. D.5), the chain
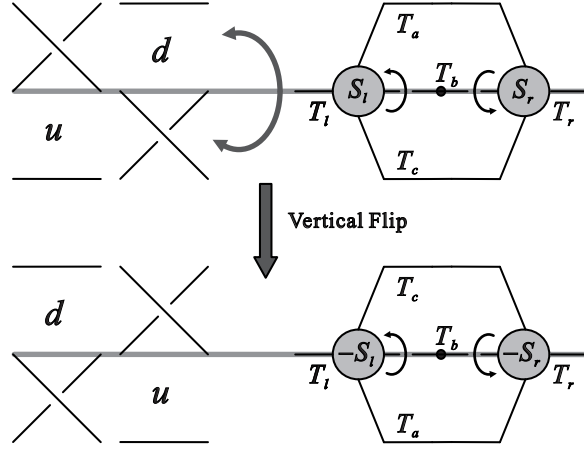
Figure 6.3: The discrete transformation, the **vertical flip**, as a flip of a braid diagram along the axis (the thick grey line) overlapped with the central strand of the braid. The transformation of crossing generators are shown on the left part.

shift of the crossing sequence X. From the figure an $\mathcal{I}_S$ is also obtained. An interesting property of the vertical flip is that it swaps the top and bottom internal twists of a braid, as seen in Fig. 6.3, leading to an $\mathcal{S}_T$ (Def. D.8). The last atomic operation involved in this rotation is seen from the figure to be an $\mathcal{I}_S$.

Obviously, a braid's propagation direction is intact under the vertical flip. Although each of it's end-node states is flipped, the crossing next to each end-node is shifted to its counterpart of the same handedness, which ensures a reducible end-node being again reducible after the transformation. Thus, a non-actively propagating braid is thus still non-actively propagating under this transformation. Likewise, an actively interacting braid remains actively interacting too after the transformation. Therefore, the vertical flip in Fig. 6.3 is indeed a legal discrete transformation. We now present its explicit definition.

Definition 6.3. *The **vertical flip**, $\mathcal{F}_V$, is a discrete transformation in the form*

$$\mathcal{F}_V = \mathcal{I}_S \mathcal{S}_T \mathcal{S}_c,$$

which for a generic braid $B = {}^{S_l}_{T_l}[(T_a, T_b, T_c)\sigma_X]^{S_r}_{T_r}$, with $(T_a, T_b, T_c)\sigma_X = (T_{a'}, T_{b'}, T_{c'})$, satisfies

$$\mathcal{F}_V(B) = {}^{\bar{S}_l}_{T_l}[(T_c, T_b, T_a)\sigma_{\mathcal{S}_c(X)}]^{\bar{S}_r}_{T_r}, \tag{6.3}$$

with $(T_c, T_b, T_a)\sigma_{\mathcal{S}_c(X)} = (T_{c'}, T_{b'}, T_{a'})$.

One may try to find out all other legal discrete transformations in a similar way. Nevertheless, our study shows that fortunately the aforementioned three discrete transformations and their products, seven altogether are the only allowable ones. In other words, $\mathcal{M}_\perp$, $\mathcal{M}_\square$, and $\mathcal{F}_V$ generate the largest group of legal discrete transformations, denoted by $G_\mathcal{D}$, which contains eight elements,

80

Discrete Transformation	Algebraic Form	Action on $B = \,^{S_l}_{T_l}[(T_a, T_b, T_c)\sigma_X]^{S_r}_{T_r}$	Prop-Direction
$\mathbb{1}$	$\mathbb{1}$	$\,^{S_l}_{T_l}[(T_a, T_b, T_c)\sigma_X]^{S_r}_{T_r}$	$+$
$\mathcal{M}_\perp$	$\mathcal{E}_S \mathcal{E}_{T_e} \mathcal{E}_T \mathcal{R} \mathcal{I}_X \mathcal{I}_T$	$\,^{S_r}_{-T_r}[-(T_{a'}, T_{b'}, T_{c'})\sigma_{X^{-1}}]^{S_l}_{-T_l}$	$-$
$\mathcal{M}_\square$	$\mathcal{I}_S \mathcal{I}_X \mathcal{I}_T$	$\,^{\bar{S}_l}_{-T_l}[-(T_a, T_b, T_c)\sigma_{\mathcal{I}_X(X)}]^{\bar{S}_r}_{-T_r}$	$+$
$\mathcal{F}_V$	$\mathcal{I}_S \mathcal{S}_c \mathcal{S}_T$	$\,^{S_l}_{T_l}[(T_c, T_b, T_a)\sigma_{\mathcal{S}_c(X)}]^{S_r}_{T_r}$	$+$
$\mathcal{F}_H = \mathcal{M}_\perp \mathcal{M}_\square$	$\mathcal{I}_S \mathcal{E}_S \mathcal{E}_{T_e} \mathcal{E}_T \mathcal{R}$	$\,^{\bar{S}_r}_{T_r}[(T_{a'}, T_{b'}, T_{c'})\sigma_{\mathcal{R}(X)}]^{\bar{S}_l}_{T_l}$	$-$
$\mathcal{M}_\perp \mathcal{F}_V$	$\mathcal{I}_S \mathcal{E}_S \mathcal{I}_T \mathcal{E}_{T_e} \mathcal{E}_T \mathcal{S}_T \mathcal{S}_c \mathcal{I}_X \mathcal{R}$	$\,^{\bar{S}_r}_{-T_r}[-(T_{c'}, T_{b'}, T_{a'})\sigma_{\mathcal{I}_X \mathcal{S}_c \mathcal{R}(X)}]^{\bar{S}_l}_{-T_l}$	$-$
$\mathcal{M}_\square \mathcal{F}_V$	$\mathcal{I}_T \mathcal{S}_T \mathcal{S}_c \mathcal{I}_X$	$\,^{S_l}_{-T_l}[-(T_c, T_b, T_a)\sigma_{\mathcal{I}_X \mathcal{S}_c(X)}]^{S_r}_{-T_r}$	$+$
$\mathcal{F}_V \mathcal{F}_H$	$\mathcal{E}_S \mathcal{S}_T \mathcal{E}_{T_e} \mathcal{E}_T \mathcal{S}_c \mathcal{R}$	$\,^{S_r}_{T_r}[(T_{c'}, T_{b'}, T_{a'})\sigma_{\mathcal{S}_c \mathcal{R}(X)}]^{S_l}_{T_l}$	$-$

Table 6.1: The group $G_\mathcal{D}$ and its action on a generic braid diagram. The last column shows whether the propagation direction of a braid changes under the corresponding transformations in the first column; a $-$ means flipped and a $+$ means unaffected.

including the identity transformation. $G_\mathcal{D}$ and its action on a generic braid is recorded in Table 6.1.

One can easily check that $G_\mathcal{D}$ is indeed a group. $G_\mathcal{D}$ is the largest group of legal discrete transformations of 3-strand braids because $G_\mathcal{D}$ exhausts all possible combinations of the atomic operations defined in Appendix D, which meet Condition 6.1, and because new atomic discrete operations cannot be constructed and combined with the current ones without violating Condition 6.1.

6.1.2 Conserved quantities

It is seen from Table 6.1 that each discrete transformation takes a braid to a new braid that is not equivalent to the original though they may be the same in some special cases. Focusing on the third column of Table 6.1, one readily finds that some characterizing quantities are invariant under some discrete transformations but are not under others. The characterizing 8-tuple of a braid also gives rise to composite quantities, which are conserved under certain and changed under other transformations. It is then necessary and helpful to explicitly demonstrate these quantities, as done in Table 6.2, not only for the purpose of mapping the discrete transformations to C, P, and T, but also for the task to sort out the physically meaningful quantum numbers of a braid. The reason to consider the quantities listed in Table 6.2, apart from their properties under discrete

$G_\mathcal{D}$	(S_l, S_r)	(T_l, T_r)	$[T_a, T_b, T_c]$	$\sum_{i=a}^{c} T_i$	$\sum_{i=1}^{|X|} x_i$	Θ'	$T_l + T_r$	Θ
$\mathcal{M}_\perp$	(S_r, S_l)	$-(T_r, T_l)$	$-[T_{a'}, T_{b'}, T_{c'}]$	$-$	$-$	$-$	$-$	$-$
$\mathcal{M}_\square$	$\left(\bar{S}_l, \bar{S}_r\right)$	$-(T_l, T_r)$	$-[T_a, T_b, T_c]$	$-$	$-$	$-$	$-$	$-$
$\mathcal{F}_V$	$\left(\bar{S}_l, \bar{S}_r\right)$	(T_l, T_r)	$[T_c, T_b, T_a]$	$+$	$+$	$+$	$+$	$+$
$\mathcal{F}_H$	$\left(\bar{S}_r, \bar{S}_l\right)$	(T_r, T_l)	$[T_{a'}, T_{b'}, T_{c'}]$	$+$	$+$	$+$	$+$	$+$
$\mathcal{M}_\perp \mathcal{F}_V$	$\left(\bar{S}_r, \bar{S}_l\right)$	$-(T_r, T_l)$	$-[T_{c'}, T_{b'}, T_{a'}]$	$-$	$-$	$-$	$-$	$-$
$\mathcal{M}_\square \mathcal{F}_V$	(S_l, S_r)	$-(T_l, T_r)$	$-[T_c, T_b, T_a]$	$-$	$-$	$-$	$-$	$-$
$\mathcal{F}_V \mathcal{F}_H$	(S_r, S_l)	(T_r, T_l)	$[T_{c'}, T_{b'}, T_{a'}]$	$+$	$+$	$+$	$+$	$+$

Table 6.2: Conserved quantities of a generic braid diagram under discrete transformations in $G_\mathcal{D}$. $|X|$ is the number of crossings. $\Theta = \sum_{i=a}^{c} T_i + T_l + T_r - 2 \sum_{i=1}^{|X|} x_i$ is the **effective twist**. $\Theta' = \Theta - (T_l + T_r)$ is called the **internal effective twist**. A $+$ means that the sign of a quantity is invariant, while a $-$ means the quantity is negated, under the corresponding transformation in the same row.

transformations, is their conservation under interactions. The **effective twist number** Θ, defined in Chapter 5, of a single braid is conserved under both equivalence moves and evolution moves. It is also an additive conserved quantity under interactions of two braids, in the sense that the Θ-value of the resulted braid of the interaction of two braids is equal to the sum of the Θ-values of the two braids before the interaction. This conservation law, though obtained in the unique representation of a braid, is independent of the choice of the representative of the braid.

In Chapters 4 and 5, however, we also studied braids in their extremal representation. An actively interacting braid has infinite number of extrema, namely their trivial braid diagrams. Fortunately, it is shown in Chapter 4 that all extrema of an actively interacting braid share the same value of the sum of the two external twists, i.e., $T_l + T_r$. Likewise, a propagating braid also has infinite number of extrema; however, Conjecture 5.1 indicates that all the extrema of an actively propagating braid have the same $T_l + T_r$, $\sum_{i=a}^{c} T_i$, and $\sum_{i=1}^{|X|} x_i$ as well. Thus, we may define another quantity, the **internal effective twist**, $\Theta' = \Theta - (T_l + T_r)$, which is the same for all extrema of a braid and is equal to Θ when the braid is in its unique representation.

Importantly, Chapters 4 and 5 showed that both $T_l + T_r$ and Θ', and hence Θ are additive conserved quantities under interactions. More precisely, for two braids, B_1 with Θ'_1 and B_2 with Θ'_2, the resulted braid $B_1 + B_2$ has $\Theta' = \Theta_1 + \Theta_2$.

In addition, all discrete transformations affect the end-nodes of a braid. Nevertheless, the only meaningful quantity, made of the end-node states of a braid, is the effective state, $\chi = S_l S_r (-)^{|X|}$,

which is a conserved quantity of braids under equivalence moves and also is a multiplicative conserved value under interactions of braids according to Theorem 5.2. Table 6.2 reads that none of the discrete transformations changes the number of crossings of a braid; therefore, all discrete transformations preserve the χ of a braid.

6.2 C, P, and T

Since a braid is a local excitation, regardless of whether it corresponds to a Standard Model particle or not one can at least make an analogy between it and a one-particle state. This is the main task of this section.

6.2.1 Finding C, P, and T

To map the discrete transformations found in the last section to C, P, T, and their products, it is helpful to recall how the latter ones act on single particle states in the context of quantum field theory. In Table 6.3, we chose to denote C, P, and T transformations in the Hilbert space by

	$|\mathbf{p}, \sigma, n\rangle$
$\mathcal{C}$	$\propto |\mathbf{p}, \sigma, n^c\rangle$
$\mathcal{P}$	$\propto |-\mathbf{p}, \sigma, n\rangle$
$\mathcal{T}$	$\propto (-)^{J-\sigma} |-\mathbf{p}, -\sigma, n\rangle$
$\mathcal{CP}$	$\propto |-\mathbf{p}, \sigma, n^c\rangle$
$\mathcal{CT}$	$\propto (-)^{J-\sigma} |-\mathbf{p}, -\sigma, n^c\rangle$
$\mathcal{PT}$	$\propto (-)^{J-\sigma} |\mathbf{p}, -\sigma, n\rangle$
$\mathcal{CPT}$	$\propto (-)^{J-\sigma} |\mathbf{p}, -\sigma, n^c\rangle$

Table 6.3: The action of $\mathcal{C}$, $\mathcal{P}$, $\mathcal{T}$, and their products on a one-particle state, where $\mathbf{p}$ is the 3-momentum, σ is the third component of the particle spin J, and n stands for the charge.

calligraphic letters $\mathcal{C}$, $\mathcal{P}$, and $\mathcal{T}$. For this reason we have already used calligraphic letters for the legal discrete transformations of braids as well because braids are topological excitations of embedded spin networks that are the states in the Hilbert space describing the fundamental spacetime.

Three remarks are in order. Firstly, so far we have not incorporated spin network labels, which are normally representations of gauge groups, and that our scheme in this section is to obtain the map between two groups of transformations mentioned above by trying to utilize topological characterizing quantities of a braid as much as possible, without involving spin network labels.

83

Secondly, for now we do not take into account the phase and sign factors in Table 6.3. Finally, all the transformations are restricted to local braid states, rather than a full evolution picture. Given these, surprisingly, the map between the discrete transformations on braids and those on single particle states turn out to be unique. We shall discuss these in the next section.

According to Table 6.3, the four transformations $\mathcal{P}$, $\mathcal{T}$, $\mathcal{CP}$, and $\mathcal{CT}$ reverse the three momentum of a one-particle state. But then, what do we mean by the momentum of a braid? In the case of Loop Quantum Gravity, there has not been a well-defined Hamiltonian yet but a Hamiltonian constraint that does not assign a well-defined energy and hence neither a momentum to a local excitation. In fact, the issue is more fundamental, in the sense that the meaning of a direction in space is unclear because we do not have a notion of space-time but only superposed spin networks, which may lead to a continuous space-time. In the case of spin networks as a concept of quantum geometry in general [46, 47], this problem of direction has not been solved either.

Nonetheless, we do not need an explicitly defined 3-momentum of a braid to pick out the discrete transformations that can flip the braid's momentum. Each braid is propagating in a direction, left or right. Propagation direction is a locally defined property of a braid with respect to its neighboring subgraph that can be projected horizontally on the plane one is looking at. This propagation direction is not the same as the propagation direction of the braid with respect to an external observer; the latter should be viewed with respect to the whole spin network embedded in a topological 3-manifold. Consequently a braid can actually propagate in any "direction" with respect to its spin network or to an external observer, regardless of its local propagation direction and how the semiclassical geometry is obtained. One may imagine looking at a braid that moves on a spin network along a "circle" and comes back to its original location.

Locally, i.e., within a sufficiently small subgraph containing a braid, however, a braid's local propagation direction coincides with its propagating direction w.r.t. the external observer hovering over the same side of the projection plane. An immediate result of this is that if the local propagation direction of a braid is flipped by a discrete transformation, so is its propagation direction w.r.t. the observer. The direction of the 3-momentum of braid, by any means it is defined, is associated with the braid's local propagation direction. Therefore, the discrete transformations reversing the 3-momentum of a braid are exactly those flipping the propagation direction of the braid, which are, according to Table 6.1, $\mathcal{M}_\perp$, $\mathcal{F}_H$, $\mathcal{M}_\perp \mathcal{F}_V$, and $\mathcal{F}_H \mathcal{F}_V$.

In other words, $\mathcal{M}_\perp$, $\mathcal{F}_H$, $\mathcal{M}_\perp \mathcal{F}_V$, and $\mathcal{F}_H \mathcal{F}_V$ are the only legal discrete transformations that may be identified with $\mathcal{P}$, $\mathcal{T}$, $\mathcal{CP}$, and $\mathcal{CT}$, and our task is to find precisely which is which. We know that $\mathcal{P}$ is the transformation that does not change any quantum number but the 3-momentum of a particle. Hence, the discrete transformation that reasonably corresponds to a $\mathcal{P}$ must have the fewest effects on the braid. From Tables 6.1 and 6.2 one can see that transformations $\mathcal{F}_H$ and $\mathcal{F}_V \mathcal{F}_H$ are the two candidates because they both reverse the 3-momentum without negating the twists, crossing values, and hence effective twists. Furthermore, $\mathcal{F}_H$ exchanges the left and the right triples of internal twists, but on top of this, $\mathcal{F}_V \mathcal{F}_H$ swaps the first and the third twists in the triple of internal twists of a braid. Therefore, $\mathcal{F}_H$ is the only candidate of a $\mathcal{P}$.

We need two more correspondences to pin down the complete mapping. For this we should find quantum numbers of a braid, which are, or analogous to, charge and spin. Among all the conserved quantities of a braid, composed of characterizing topological quantities of the braid, only the total

C	$\mathcal{P}$	$\mathcal{T}$	$C\mathcal{P}$	$C\mathcal{T}$	$\mathcal{P}\mathcal{T}$	$C\mathcal{P}\mathcal{T}$
$\mathcal{M}_\square$	$\mathcal{F}_H$	$\mathcal{F}_V\mathcal{F}_H$	$\mathcal{M}_\perp$	$\mathcal{M}_\perp\mathcal{F}_V$	$\mathcal{F}_V$	$\mathcal{M}_\square\mathcal{F}_V$

Table 6.4: The map between legal discrete transformations of braids and C, $\mathcal{P}$, $\mathcal{T}$, and their products.

effective twist number Θ is independent of the representative of the equivalence class of the braid. Other conserved quantities, e.g., Θ', are not. We know that charges, e.g., electric and color, are unambiguous quantum numbers of a particle. Consequently, representative-dependent conserved quantities of a braid, though maybe useful in other ways, should not be considered as charges. This means only Θ can be a candidate of determining certain charges of a braid.

Additionally, one can come up with two more reasons, which are more heuristic and physical. As we know, the electric charge of a particle is quantized to be multiples of 1/3. Now the interesting thing is that all our twists and hence the effective twists happen to be integers in units of 1/3 according to Section 2.1 too; the 1/3 arises naturally rather than being put in by hand. This is also an advantage of the 4-valent case because in the 3-valent case, in contrast, a factor of 1/3 must be set by hand[39]. On the other hand, the framing of our spin networks, which fattens an edge to a tube, is in fact a $U(1)$ framing; a tube coming from the framing of an edge is essentially an isomorphism from $U(1)$ to $U(1)$. If a tube is twist free, it simply means an identity map, whereas a twisted tube represents a non-trivial isomorphism. That is to say, a twist can be thought as characterizing the isomorphisms on $U(1)$ spaces. An interesting fact is that the electric charge is a result of a $U(1)$ gauge symmetry. These suggest that Θ or an appropriate function of it can be viewed as the "electric charge" of a braid, which may serve as an explanation of why electric charge is quantized so.

Bearing this in mind, Table 6.2 presents four discrete transformations, $\mathcal{M}_\perp$, $\mathcal{M}_\square$, $\mathcal{M}_\perp\mathcal{F}_V$, and $\mathcal{M}_\square\mathcal{F}_V$, which negate the Θ value of a braid and hence correspond to $C\mathcal{P}$, C, $C\mathcal{T}$, and $\mathcal{T}$ in certain manner. Our strategy is to find C first. Since a C does not flip the momentum, so does a $C\mathcal{P}\mathcal{T}$, the transformations $\mathcal{M}_\square$ and $\mathcal{M}_\square\mathcal{F}_V$ are candidates of C and $C\mathcal{P}\mathcal{T}$ for that they preserve the momentum, whereas $\mathcal{M}_\perp$ and $\mathcal{M}_\perp\mathcal{F}_V$ are possibly $C\mathcal{P}$ and $C\mathcal{T}$.

On a single particle state, a $C\mathcal{P}\mathcal{T}$ has one more effect than a C because it also turns σ, the z-component spin, to $-\sigma$. We notice that a $\mathcal{M}_\square\mathcal{F}_V$ affects a braids more than a $\mathcal{M}_\square$ does; it swaps the first and the third elements in the triple of internal twists of a braid besides adding a negative sign to Θ. As a result, although we do not know what of a braid behaves like the σ, we can now consider the transformation $\mathcal{M}_\square$ as C and the transformation $\mathcal{M}_\square\mathcal{F}_V$ to be $C\mathcal{P}\mathcal{T}$.

Given the three correspondences we now have, it is easy to track down all the rest. As a summary, we list the map between $G_\mathcal{D}$ and the group generated by C, $\mathcal{P}$, $\mathcal{T}$ in Table 6.4.

6.2.2 CPT multiplets of braids

With the C, P, and T we have found, one can see that certain diffeomorphism-inequivalent braids may not be totally different from each other, in the sense that they can belong to the same CPT-multiplet. It would be very interesting to see if a CPT-multiplet of braids has any characteristic property. It turns out that only actively interacting braids that belong to a CPT-multiplet have a clear and unique common topological property. We would like to formulate this claim as the theorem below.

Theorem 6.1. *Each CPT-multiplet of actively interacting braids is uniquely characterized by a non-negative integer, k - the number of crossings of all braids in the multiplet, when they are represented in the unique representation.*

Proof. This theorem has a two-fold meaning: that all actively interacting braids with the same number of crossings belong to the same CPT-multiplet, and that all actively interacting braids in a CPT-multiplet must have the same number of crossings. We prove the former first. As demonstrated in Chapter 3, a braid can interact actively if and only if it is completely reducible from both ends, and its end-nodes are in opposite states for odd number of crossings, and in the same state for even number of crossings. Bearing this in mind and by Appendix B, we can straightforwardly work out the forms of all actively interacting braids in the unique representation with k crossings for k even

$$
\begin{aligned}
B_1 &= {}^+[(T_{1a}, T_{1b}, T_{1c})\sigma_{(ud)^{k/2}}]^+ \\
B_2 &= {}^+[(T_{2a}, T_{2b}, T_{2c})\sigma_{(ud)^{-k/2}}]^+ \\
B_3 &= {}^-[(T_{3a}, T_{3b}, T_{3c})\sigma_{(du)^{k/2}}]^- \\
B_4 &= {}^-[(T_{4a}, T_{4b}, T_{4c})\sigma_{(du)^{-k/2}}]^-,
\end{aligned}
\tag{6.4}
$$

and for k odd,

$$
\begin{aligned}
B_1' &= {}^+[(T_{1a}', T_{1b}', T_{1c}')\sigma_{d(ud)^{(k-1)/2}}]^- \\
B_2' &= {}^+[(T_{2a}', T_{2b}', T_{2c}')\sigma_{d(ud)^{-(k+1)/2}}]^- \\
B_3' &= {}^-[(T_{3a}', T_{3b}', T_{3c}')\sigma_{u(du)^{(k-1)/2}}]^+ \\
B_4' &= {}^-[(T_{4a}', T_{4b}', T_{4c}')\sigma_{u(du)^{-(k+1)/2}}]^+,
\end{aligned}
\tag{6.5}
$$

where we have omitted all the external twists for that they are zero in the unique representation. For a braid to interact actively, in the braid's unique representation, the crossing sequence and end-node states of the braid uniquely determine the triple of internal twists of the braid, also according to Chapter 3. In addition, if an exponent in Eq. 6.5 or 6.6 is positive, it means, for example, $(ud)^2 = udud$. By adopting from Appendix I the definition of X^{-1} with respect to X, the meaning of the negative exponents in Eqs. 6.5 and 6.6 is clear: for instance, $(ud)^{-2} = d^{-1}u^{-1}d^{-1}u^{-1}$.

It is straightforward to see that if we apply $\mathcal{M}_\square$, $\mathcal{F}_V$, and $\mathcal{M}_\square\mathcal{F}_V$, or according to Table 6.3, C,

$\mathcal{PT}$ and $\mathcal{CPT}$ on B_1 for even k's and B_1' for odd k's, we get

$$
\begin{aligned}
C(B_1) &= {}^-[-(T_{1a}, T_{1b}, T_{1c})\sigma_{(du)^{-k/2}}]^- \\
\mathcal{PT}(B_1) &= {}^-[(T_{1c}, T_{1b}, T_{1a})\sigma_{(du)^{k/2}}]^- \\
\mathcal{CPT}(B_1) &= {}^+[-(T_{1c}, T_{1b}, T_{1a})\sigma_{(ud)^{-k/2}}]^+
\end{aligned}
\tag{6.6}
$$

for even k's, and

$$
\begin{aligned}
C(B_1') &= {}^-[-(T_{1a}', T_{1b}', T_{1c}')\sigma_{u(du)^{-(k+1)/2}}]^+ \\
\mathcal{PT}(B_1') &= {}^-[(T_{1c}', T_{1b}', T_{1a}')\sigma_{u(du)^{(k-1)/2}}]^+ \\
\mathcal{CPT}(B_1') &= {}^+[-(T_{1c}', T_{1b}', T_{1a}')\sigma_{d(ud)^{-(k+1)/2}}]^-
\end{aligned}
\tag{6.7}
$$

for odd k's. Comparing Eq. 6.5 with Eq. 6.7, and Eq. 6.6 with Eq. 6.8, one can see that the crossing sequence and end node states of $C(B_1)$, $\mathcal{PT}(B_1)$ and $\mathcal{CPT}(B_1)$ are exactly the same as that of B_4, B_3 and B_2 respectively, for even k's; similar observation holds for odd k's as well. As to the internal twists, since they are uniquely determined by crossing sequence and end node states, one must have

$$
\begin{aligned}
(T_{2a}, T_{2b}, T_{2c}) &= -(T_{1c}, T_{1b}, T_{1a}) \\
(T_{3a}, T_{3b}, T_{3c}) &= (T_{1c}, T_{1b}, T_{1a}) \\
(T_{4a}, T_{4b}, T_{4c}) &= -(T_{1a}, T_{1b}, T_{1c})
\end{aligned}
$$

for braids with even crossings, and similar relations for braids with odd crossings. Therefore, in the unique representation, all actively interacting braids with k crossings are related to each other by discrete transformations as following,

$$
\begin{aligned}
C(B_1) &= B_4 \\
\mathcal{PT}(B_1) &= B_3 \\
\mathcal{CPT}(B_1) &= B_2
\end{aligned}
\tag{6.8}
$$

for even k's, and

$$
\begin{aligned}
C(B_1') &= B_4' \\
\mathcal{PT}(B_1') &= B_3' \\
\mathcal{CPT}(B_1') &= B_2'
\end{aligned}
\tag{6.9}
$$

for odd k's.

Pointed out in the last section, none of the discrete transformations on a braid diagram is able to change the number of crossings of the braid diagram; hence, all braid diagrams in a CPT-multiplet must have the same number of crossings. This exhibits the latter meaning of the theorem. $\quad\square$

Since in the unique representation, for each number of crossings we have only four actively interacting braids, being related only by three discrete transformations, namely $C, \mathcal{PT}$ and $\mathcal{CPT}$,

applying the remaining four discrete transformations, viz $\mathcal{P}$, $\mathcal{T}$, $\mathcal{CP}$ and $\mathcal{CT}$ can not generate new braids with the same number of crossings, which means that their actions must be equivalent to, in certain order, those of C, $\mathcal{PT}$, $\mathcal{CPT}$, and the identity $\mathbb{1}$ on actively interacting braids.

As for braids that do not interact actively, we do not have a similar theorem. In fact, we can always find two non-actively interacting braids with m crossings ($m > 1$), in their unique representations, which are not related to each other by any discrete transformation in the unique representation. Here is an example with $m = 2$: for the braid, ${}^{S_l}[(T_a, T_b, T_c)\sigma_{ud^{-1}}]^{S_r}$, and the braid, ${}^{S'_l}[(T'_a, T'_b, T'_c)\sigma_{uu}]^{S'_r}$, whatever their internal twists and end-node states are, it is straightforward to see that the discrete transformations can never transform them into each other.

Nevertheless, it is still true for non-actively interacting braids that all braids in a CPT-multiplet have the same number of crossings when they are represented in the same type of representation. This is so simply because discrete transformations do not change the representation type and the number of crossings of a braid.

6.2.3   Interactions under C, P, and T

We have seen the effects of C, P, and T on single braid excitations, it is then natural and important to discuss the action of these discrete transformations on direct braid interactions. Braid interactions turn out to be invariant under CPT, and more precisely, under C, P, and T separately.

This type of interaction always involve two braids, one of which must be actively interacting. As pointed out in the previous chapter, in dealing with an interaction it is convenient to put the actively interacting braid, say B, in a trivial representation, and the other braid, say B', in its unique representation. Although Chapter 5 shows that the right-interaction of B on B', namely $B + B'$, and the left-interaction $B' + B$ are not equal in general, for the purpose here, we need only to consider either of the two cases because the other case follows similarly. Let us study $B + B'$.

Lemma 5.7 has proven that the interaction $B + B'$ is independent of the trivial braid diagram representing B, and suggests to choose the one with zero right external twist to represent B. Thus we let $B = {}^{S}_{T_l}[T_a, T_b, T_c]^{S}_0$, and $B' = {}^{S}_0[(T'_a, T'_b, T'_c)\sigma_X]^{S_r}_0$. Given this, we can adopt Eq. 5.21, the algebraic form of $B + B'$, as follows

$$B'' = B + B' = {}^{S_l}_{T_l}[(T_a + T'_a, T_b + T'_b, T_c + T'_c)\sigma_X]^{S_r}_0 \, , \tag{6.10}$$

where $S = S_l$, such that the interaction condition is satisfied. A subtlety is that the braid B'' in Eq. 6.10 is not the standard result that has zero external twist. To obtain the standard result, one should rotate the left end-node of B'' to remove the left external twist, T_l. We do so to reduce the complexity of this proof, which is fine because rotations, as equivalence moves, obviously commute with discrete transformations.

We now show that this interaction is invariant under a charge conjugation, i.e., to show $C(B) +$

$C(B') = C(B + B')$. By Tables 6.4 and 6.1, we readily obtain

$$
\begin{aligned}
C(B) &= C\left({}^{S}_{T_l}[T_a, T_b, T_c]^{S}_0\right) \\
&= {}^{-S}_{-T_l}[-T_a, -T_b, -T_c]^{-S}_0 \\
C(B') &= C\left({}^{S_l}_{0}[(T'_a, T'_b, T'_c)\sigma_X]^{S_r}_0\right) \\
&= {}^{-S_l}_{0}[-(T'_a, T'_b, T'_c)\sigma_{\mathcal{I}_X(X)}]^{S_r}_0 .
\end{aligned}
\tag{6.11}
$$

Hence, by the same token as how this kind of interaction is carried out in Eq. 6.10, we get

$$
\begin{aligned}
C(B) + C(B') &= {}^{-S}_{-T_l}[-T_a, -T_b, -T_c]^{-S}_0 + {}^{-S_l}_{0}[-(T'_a, T'_b, T'_c)\sigma_{\mathcal{I}_X(X)}]^{S_r}_0 \\
&= {}^{-S_l}_{-T_l}[-(T_a + T'_a, T_b + T'_b, T_c + T'_c)\sigma_{\mathcal{I}_X(X)}]^{-S_r}_0
\end{aligned}
\tag{6.12}
$$

Now we directly apply a C-transformation on the braid B'' in Eq. 6.10, which leads to

$$
\begin{aligned}
C(B'') &= C\left({}^{S_l}_{T_l}[(T_a + T'_a, T_b + T'_b, T_c + T'_c)\sigma_X]^{S_r}_0\right) \\
&= {}^{-S_l}_{-T_l}[-(T_a + T'_a, T_b + T'_b, T_c + T'_c)\sigma_{\mathcal{I}_X(X)}]^{-S_r}_0 ,
\end{aligned}
\tag{6.13}
$$

which is exactly the same as the RHS of Eq. 6.12. Therefore, because of the generality of B and B', all interactions are invariant under charge conjugation.

We now move on to the case of parity transformation. It is important to note that a discrete transformation acts on the whole process of an interaction - in particular the complete states before and after the interaction. As a result, in view of the fact from Table 6.1 that a P-transformation, i.e., the $\mathcal{F}_H$, exchanges the two end-nodes, reverses the crossing sequence, and exchanges the twists on the left and on the right of the crossing sequence of a braid, it should also switch the positions of the two braids involved in an interaction before the interaction happens. That is to say, to show the invariance of an right-interaction, say $B + B' = B''$ (the same braids as above), under P, one needs to prove that the left-interaction, $\mathcal{P}(B') + \mathcal{P}(B) = \mathcal{P}(B'')$, holds[1].

Applying a P-transformation on B and B' respectively brings us

$$
\begin{aligned}
\mathcal{P}(B) &= \mathcal{P}\left({}^{S}_{T_l}[T_a, T_b, T_c]^{S}_0\right) \\
&= {}^{-S}_{0}[T_a, T_b, T_c]^{-S}_{T_l} \\
\mathcal{P}(B') &= \mathcal{P}\left({}^{S_l}_{0}[(T'_a, T'_b, T'_c)\sigma_X]^{S_r}_0\right) \\
&= {}^{-S_r}_{0}[(T'_{a'}, T'_{b'}, T'_{c'})\sigma_{\mathcal{R}(X)}]^{-S_l}_0 ,
\end{aligned}
\tag{6.14}
$$

where $(T'_a, T'_b, T'_c)\sigma_X = (T'_{a'}, T'_{b'}, T'_{c'})$. Then according to Chapter 5, the left interaction of $\mathcal{P}(B)$ and

---

[1]The interaction condition is automatically satisfied in this way because the neighboring nodes of B' and B again are in the same state and have no twist on their common edge, after switching their positions. Please check [**?**] for details on the interaction condition.

$\mathcal{P}(B')$ reads

$$
\begin{aligned}
\mathcal{P}(B') + \mathcal{P}(B) &= {}^{-S_r}_{0}[(T'_{a'}, T'_{b'}, T'_{c'})\sigma_{\mathcal{R}(X)}]^{-S_l}_0 + {}^{-S}_{0}[T_a, T_b, T_c]^{-S}_{T_l} \\
&= {}^{-S_r}_{0}[((T'_{a'}, T'_{b'}, T'_{c'}) + \sigma^{-1}_{\mathcal{R}(X)}(T_a, T_b, T_c))\sigma_{\mathcal{R}(X)}]^{-S_l}_{T_l} \\
&\xRightarrow{Eq.D.3} = {}^{-S_r}_{0}[((T'_a, T'_b, T'_c)\sigma_X + (T_a, T_b, T_c)\sigma_X)\sigma_{\mathcal{R}(X)}]^{-S_l}_{T_l} \\
&= {}^{-S_r}_{0}[((T'_a + T_a, T'_b + T_b, T'_c + T_c)\sigma_X)\sigma_{\mathcal{R}(X)}]^{-S_l}_{T_l} .
\end{aligned}
\tag{6.15}
$$

Note that in the last line of the equation above, the σ_X and $\sigma_{\mathcal{R}(X)}$ should not be contracted by Eq. D.1, which we did not do, because the $\sigma_{\mathcal{R}(X)}$ is present there not only for denoting the permutation but also for recording the crossing sequence, namely $\mathcal{R}(X)$, of the resulted braid.

If we directly apply a P-transformation on B'' in Eq. 6.10, we attain

$$
\begin{aligned}
\mathcal{P}(B'') &= \mathcal{P}\left({}^{S_l}_{T_l}[(T_a + T'_a, T_b + T'_b, T_c + T'_c)\sigma_X]^{S_r}_0\right) \\
&= {}^{-S_r}_{0}[((T'_a + T_a, T'_b + T_b, T'_c + T_c)\sigma_X)\sigma_{\mathcal{R}(X)}]^{-S_l}_{T_l} ,
\end{aligned}
$$

for that the triple $(T'_a + T_a, T'_b + T_b, T'_c + T_c)\sigma_X$ is already the original triple of internal twists on the right of X, which should become the left one of $\mathcal{P}(B'')$, as the effect of parity transformation. This equation is precisely the one on the RHS of Eq. 6.15. Therefore, the invariance of braid interaction under parity transformation is established.

A subtlety arises in interactions under time reversal. The time reversal we have found is with respect to a single braid excitation; however, an interaction involves the time evolution of a spin network under dynamical moves. To apply our T-transformation to an interaction, one should reverse all the dynamical moves, e.g., a $1 \to 4$ move taken in the interaction becomes a $4 \to 1$ move under the time reversal, at the same time. In this sense, to show the invariance of the interaction, $B + B' \longrightarrow B''$, it suffices to show that $\mathcal{T}(B'') \longrightarrow \mathcal{T}(B') + \mathcal{T}(B)$, where the positions of B and B' are swapped as in the case of parity transformation. It is straightforward to prove the invariance of interactions under time reversal; the procedure is similar to that of the previous two cases, and is thus not explicitly presented here.

Consequently, all direct braid interactions are invariant under C, P, T, and any combination of them. This is not the case of the Standard Model of particles because of the absence of CP-violation. A possible reason is that all our current interactions are deterministic. Nonetheless, Chapter 5 suggested that one may consider superpositions of braids by taking spin network labels into account. This is to be discussed in the next section.

In the end of Section 5.3.2, we brought up the possibility that discrete transformations may provide a resolution of asymmetric direct interactions, i.e., they relate $B + B'$ and $B' + B$. Let us address this now. The transformations $\mathcal{P}$, $\mathcal{T}$, $\mathcal{CP}$, and $\mathcal{CT}$ swap the two braids undergoing a direct interaction. That is, for example, $\mathcal{P}(B + B') = \mathcal{P}(B') + \mathcal{P}(B)$. If B and B' happen to be invariant under $\mathcal{P}$, $B' + B$ is then equal to $\mathcal{P}(B + B')$. We list below the conditions for this to be true, based

on our studies above of direction interaction under discrete transformations.

$$B' + B = \begin{cases} \mathcal{P}(B + B'), & B = \mathcal{P}(B), \ B' = \mathcal{P}(B') \\ \mathcal{T}(B + B'), & B = \mathcal{T}(B), \ B' = \mathcal{T}(B') \\ C\mathcal{P}(B + B'), & B = C\mathcal{P}(B), \ B' = C\mathcal{P}(B') \\ C\mathcal{T}(B + B'), & B = C\mathcal{T}(B), \ B' = C\mathcal{T}(B'). \end{cases} \tag{6.16}$$

It is however necessary to remark that the current study of discrete transformations of braids would not be impact by just adding spin network labels in a straightforward way in to our scheme. A reason is that the discrete transformations found in this chapter do not change the spin network label of each existing edge of the network. One may try to construct discrete transformation that change the spin network labels on braids, but there could be many arbitrary ways of doing this, and one does not have a priori a reason to make a special choice.

6.3 Summary and discussion

In conclusion, we have found seven discrete transformations of 3-strand braids and mapped them to C, P, T, and their products. Along with this, the effective twist number of a braid has been demonstrated to be responsible for the electric charge of the braid. Interestingly, in their unique representation, all actively interacting braids with the same number of crossings form a CPT-multiplet. On the contrary, two non-actively interacting braids of the same number of crossings may not be related by any legal discrete transformation. This will help us to find a deeper correspondence between our braids and matter particles. Furthermore, braid interactions have been proven invariant under C, P, and T separately.

Nevertheless, the results we have obtained so far are purely based on the algebra of the action of discrete transformations on topological quantities characterizing braids. Although our braids live on embedded spin networks, spin network labels have yet not been incorporated along this research line; spin networks are treated as framed graphs with merely topological properties. For reasons that will be clear soon, however, it may be necessary to include spin network labels.

The mapping between the discrete transformations of braids and the C, P, and T were determined without referring to the definition of the spin of a braid. This is because our analysis indicates that spin cannot be constructed out of the conserved topological quantities we have in hand of braids. The reasons are as follows.

In our language, crossings of a braid and twists on the strands of the braid are on an equal footing because crossings and twists are interchangeable under equivalence moves, which leads to the effective twist number Θ of a braid, a conserved quantity independent of the representative of the braid. For the aforementioned reason, we may identify Θ or certain appropriate function of it as the charge of a braid. Θ cannot be associated with spin consistently. Furthermore, since in the context of particle physics, charge is a result of $U(1)$ gauge symmetry (and our twists are also related to $U(1)$ as previously explained), while spin results from Poincaré symmetry, a space-time symmetry, charge and spin thus could not be unified by superficially manipulating Θ.

Spin network labels are usually representations of a gauge group or of a quantum group. In both of the original spin network proposal[46, 47] and Loop Quantum Gravity, spin network labels are $SU(2)$ or $SO(3)$ representations. In the framed case, one uses, for example, the quantum $SU(2)$, namely $SU_q(2)$. Consequently, it is more reasonable to associate the spin of a braid with the spin network labels on the strands and/or external edges, and the intertwiners at the end-nodes of the braid. If one decorate the 4-valent spin networks by representations of gauge groups other than $SU(2)$ and $SO(3)$, say $SU(3)$, it may be possible to define color charges of braids as well.

If we agree on this, then Table 6.2 gives us a hint how we would find spin for braids. The time reversal is identified with the discrete transformation $\mathcal{F}_V \mathcal{F}_H$. Since a T-transformation flips the z-component of the spin of a single-particle state, and because external twists and internal twists of a braid are not separately conserved, by the last line of Table 6.2, the only effect of $\mathcal{F}_V \mathcal{F}_H$ on a braid, which may correspond to the change of spin under time reversal, is the exchange of the top and the bottom strands of the braid[2]. This implies that the spin network labels respectively on the top and the bottom strands are also subject to exchange under a $\mathcal{F}_V \mathcal{F}_H$, or simply a T-transformation. In other words, we would like to have a way of combining labels and/or intertwiners on a braid, which changes sign when the label on the top strand and the one on the bottom strand of the braid are exchanged. The sign factor of the action of any discrete transformation involving a time reversal, and other phase factors, in Table 6.3 will appear accordingly. Unfortunately, the precise form of this construction is unavailable for the moment; its discovery may require a complete and systematic approach that takes spin network labels into account.

Our observation that all interactions of braids are invariant under C, P, and T separately seems to indicate an issue that the interactions of braids we have studied so far are deterministic, in the sense that an interaction of two braids produces a definite new braid. Nevertheless, this may not be a problem at all because we have only worked with definite vertices of interactions. In terms of vertices we have definite result for an interaction as to the case in QFT; this is similar to what have been done in spin foam models or group field theories. Besides, one can certainly argue that if our braids are more fundamental entities, the CP-violation in particle physics does not necessarily exist at this level. Putting this CP-violation problem aside; however, a fully quantum mechanical picture should be probabilistic[3].

If we tend to take this as an issue, we may try to work with superpositions of braids and interactions of braids resulting in superposition of braids. A possible way out is to consider braids with the same topological structure but different sets of spin network labels as physically different. One may adopt from spin foam models the methods that can assign amplitudes to the dynamical moves, namely the dual Pachner moves restricted by the stability condition defined in Section 2.7 and discussed in [69], of the embedded 4-valent spin networks. A dynamical move such as a $2 \to 3$ and a $1 \to 4$ may then give rise to outcomes with the same topological configuration but different spin network labels; each outcome has a certain probability amplitude. As a result, an interaction of two braids may give rise to superposed braids, each of which has a certain probability to be observed, with the same topological content but different set of spin network labels. With this, CP-violating interactions may arise.

---

[2]This is implied by the exchange of the top and the bottom internal twists explicitly shown in the table

[3]One should note that a few theoretical physicists may not agree on this.

In Chapter 8 we will talk about a more elegant and unified way to resolve all the aforementioned issues once for all.

Chapter 7

Braid Dynamics II: Exchange Interaction and Feynman Diagrams

The goal of this chapter is to present an effective description of the braid excitations we have studied in previous chapters in the language of Feynman diagrams. As an analogy effective emergent degrees of freedom have been realized in condensed matter physics. For example, quasi-particles as collective modes can emerge in some condensed matter systems, such as phonons and rotons in superfluid He^4. Another example is the string-net condensation that gives rise to low energy effective gauge theories[10] and linearized gravity theories[11].

Chapter 5 shows that all actively interacting braids form a noncommutative algebra, in which the product (binary operation) is the direct braid interaction, and that an actively interacting braid behaves like a map, taking a non-actively interacting braid to another non-actively interacting one. Each direct braid interaction must always involve at least one actively-interacting braid. In this chapter we will investigate a new type of interaction that transforms two adjacent braids into another two adjacent braids, via exchanging a virtual actively interacting braid. This seems to imply that actively interacting braids behave like bosons whereas the others - in particular the chiral propagating braids - may be candidates for fermions.

Most importantly, an effective description of the braid dynamics exists, by representing the dynamics of braids in terms of Feynman diagrams. This also implies the existence of effective field theories of 3-strand braids of embedded spin networks. Main results of this chapter are summarized as follows.

1. Two neighboring braids may have an exchange interaction, i.e., they interact via exchanging a virtual actively interacting braid, resulting in two different adjacent braids.

2. Effective twists and effective states of braids are conserved under exchange interaction.

3. Exchange interaction is asymmetric in general; however, conditions for an exchange interaction to be symmetric are given.

4. Braids can radiate actively interacting braids.

5. Actively interacting braids behave analogously to bosons.

6. Braid Feynman diagrams representing braid dynamics are proposed.

7. A constraint on probability amplitudes of braid dynamics is obtained.

As before, in this chapter we do not take into account the labels that usually grace the edges and nodes of spin networks either because the braid excitations and their dynamics we study do not depend on them. Nonetheless, this chapter will urge the incorporation of spin network labels, in the traditional way or in a more generalized way, in future work, such that methods in certain spin foam models, in group field theories, or in tensor categories can be adapted.

7.1 Division of Braids

Having in hand all the previous results, it is time to cast our division of braids in a more formal way. We choose to denote the set of stable braids by $\mathfrak{B}_0^S$. Nevertheless, for reasons that will become transparent in the sequel we should enlarge $\mathfrak{B}_0^S$ by adding two more braids:

$$B_0^\pm = {}^\pm_0[0,0,0]_0^\pm , \tag{7.1}$$

which are completely trivial[1]. $B_0^\pm$ are actually unstable according to Section 2.7 because they are dual to a 3-ball. If we tolerate their instability they are obviously actively interacting. Bearing this in mind, let us still call the enlarged set the set of stable braids but use $\mathfrak{B}^S$ as its notation. According to Chapter 3, $\mathfrak{B}^S$ can be divided into the disjoint union of three subsets: the subset of all actively interacting braids (including $B_0^\pm$), the subset of all actively propagating braids that do not actively interact, and the subset of non-actively propagating braids that are passive in all direct interactions; they are denoted respectively by $\mathfrak{B}^b$, $\mathfrak{B}^f$, and $\mathfrak{B}^s$. Therefore, we have

$$\mathfrak{B}^S = \mathfrak{B}^b \sqcup \mathfrak{B}^f \sqcup \mathfrak{B}^s. \tag{7.2}$$

Because a new type of interaction will be introduced in this chapter, to get rid of any possible confusion we will hereafter denote a *direct interaction* by $+_d$, while name the new interaction **exchange interaction** for reasons will be clear when it is defined, and denote it by $+_e$. As a consequence, a bare + sign between two braids only means the adjacency of the braids. As pointed out in Chapters 4 and 5, $\mathfrak{B}^b$ is closed under the direct interaction, i.e., $\mathfrak{B}^b +_d \mathfrak{B}^b \subseteq \mathfrak{B}^b$.

This will help to make the algebraic structure of braids and the contact of our model with particle physics clearer.

---

[1]It is highly important to note again that at this point spin network labels have not been taken into account yet. Taking into account spin network labels has two immediate consequences. Firstly, $B_0^\pm$ are not just two braids, but infinite number of braids because they can be colored by different sets of spin network labels, so is any other braid in $\mathfrak{B}^S$. Secondly, $B_0^\pm$ are only trivial topologically but not algebraically and neither physically.

7.2 Exchange interaction

One of the two braids in a direct interaction must be an actively interacting braid. That is, we only have the following possible direct interactions: $\mathfrak{B}^b +_d \mathfrak{B}^b$, $\mathfrak{B}^b +_d \mathfrak{B} \setminus \mathfrak{B}^b$. Fortunately, there exists, as we are to show, another type of interaction, namely the exchange interaction, which can take two adjacent braids in $\mathfrak{B} \setminus \mathfrak{B}^b$ to another two neighboring ones in the same set. In fact, exchange interaction can be defined on the whole $\mathfrak{B}^S$ as a map, $+_e : \mathfrak{B}^S \times \mathfrak{B}^S \to \mathfrak{B}^S \times \mathfrak{B}^S$. It will be clear shortly that an exchange interaction always involves an exchange of a virtual actively interacting braid, which manifests the name of exchange interaction. It is useful to keep track of the direction of the exchange of the actively interacting braid during an exchange interaction. Therefore, we differentiate a *left* and a *right exchange interaction*, respectively denoted by $\overleftarrow{+}_e$ and $\overrightarrow{+}_e$. The arrow indicates the "flow" of the virtual actively interacting braid.

The graphic definition of right exchange interaction is illustrated in Fig. 7.1. The left one can be defined likewise. We now explain with the help of our algebraic notation the process in detail as follows.

1. We begin with the two adjacent braids, $B_1, B_2 \in \mathfrak{B}^S$ in Fig. 7.1(a). Their algebraic forms are: $B_1 = {}^{S_{1l}}[(T_{1a}, T_{1b}, T_{1c})\sigma_{X_{1A}X_{1B}}]^S$ and $B_2 = {}^{S}[(T_{2a}, T_{2b}, T_{2c})\sigma_{X_2}]^{S_{2r}}$. B_1's right end-node and B_2's left end-node are set in the same state, S, to satisfy the interaction condition. We also assume that B_1 is right-reducible (not necessarily fully right-reducible), such that the crossing sequence of B_1 has a maximal reducible segment, say X_{1B}, as shown in the figure. The reason for this will be clear soon. (Similarly, for left exchange interaction one should have B_2 left-reducible. If B_1 is right-reducible and B_2 is left-reducible, both left and right exchange interactions may occur but they lead to different results in general.)

2. A $2 \to 3$ move on the two nodes in the state S now leads to Fig. 7.1(b). The dashed lines simply means the crossing relation between the green lines and black ones can not be determined unless we know what exactly the state S is.

3. Because X_{1B} is the reducible part of the crossing sequence of B_1, according to Chapter 3 one can translate the three new nodes - one in state S and two in $-S$ - in (b) along with the edges g, g', and g'' to the left of X_{1B}, and rearrange them by equivalence moves into a proper configuration ready for a $3 \to 2$ move, as seen in Fig. 7.1(c). This is why we assume B_1 is right-reducible; otherwise, the translation is not viable. According to Chapter 3, in Fig. 7.1(c) the three nodes are shuffled by the translation and their states are related to S by $S' = (-)^{|X_{1B}|}S$. Nevertheless, because S is arbitrary dashed lines are also used in Fig. 7.1(c) for undetermined crossing relation between the green edges and the black ones. This procedure introduces twists in pair on the strands: $-(T_a, T_b, T_c)$ and (T_a, T_b, T_c), labeled in red in Fig. 7.1(c).

    Note that the triples (T_{1a}, T_{1b}, T_{1c}) and $-(T_a, T_b, T_c)$ are not existing on the strands separately. One should add $-(T_a, T_b, T_c)$ to (T_{1a}, T_{1b}, T_{1c}) with the permutation induced by X_{1A} taken into account, i.e., $(T_{1a}, T_{1b}, T_{1c}) - \sigma_{X_{1A}}^{-1}(T_a, T_b, T_c)$. The relation between (T_{2a}, T_{2b}, T_{2c}) and
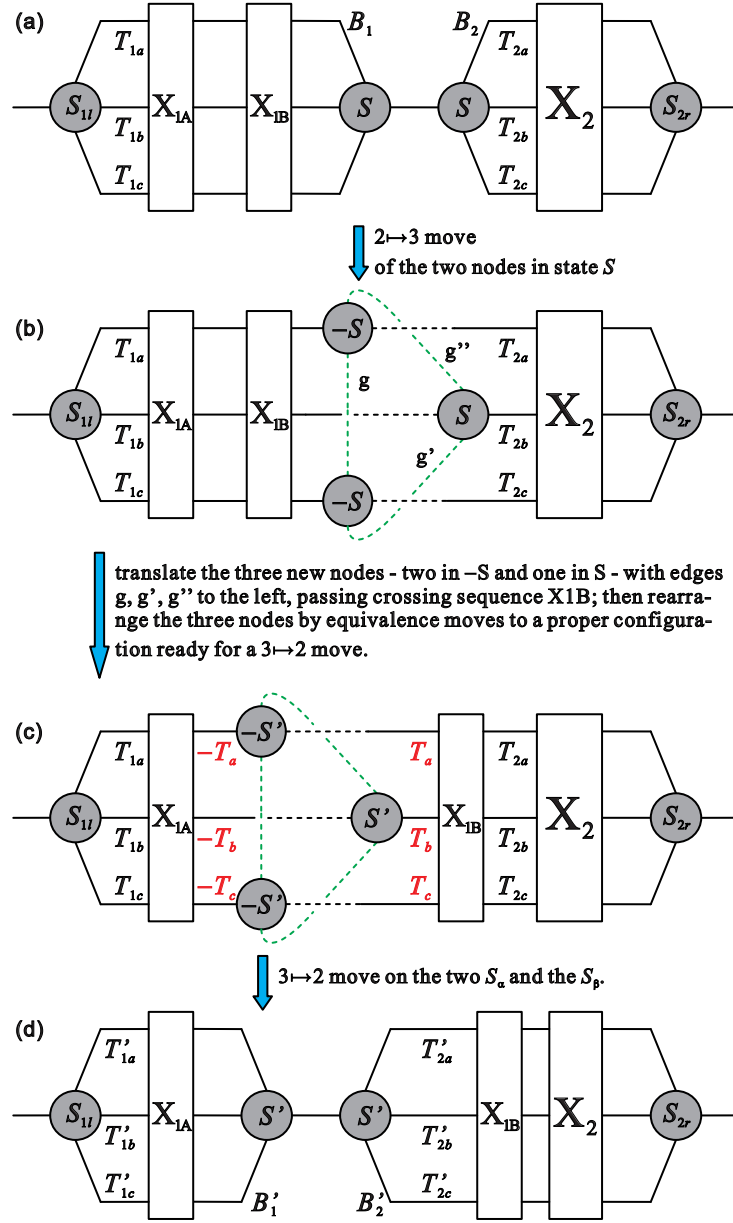
Figure 7.1: Definition of right exchange interaction: $B_1 \overset{\rightarrow}{+}_e B_2 \rightarrow B'_1 + B'_2$, $B_1, B_2, B'_1, B'_2 \in \mathfrak{B}^S$. In (b), the dashed lines emphasize the dependence of the $2 \rightarrow 3$ move on the state S of the two nodes on which the move is taken. In (c) and (d), $S' = (-)^{|X_{1B}|}S$. In (c), the dashed line means that the configuration depends on S'. In (d), $(T'_{1a}, T'_{1b}, T'_{1c})$ and $(T'_{2a}, T'_{2b}, T'_{2c})$ are the internal twists of B'_1 and B'_2 respectively, which are explained in the text.

(T_a, T_b, T_c) is likewise. This cannot be represented in the figure, which is a limitation of the graphic notation.

4. We then perform the $3 \to 2$ move and arrive at Fig. 7.1(c), which shows two new adjacent braids, B'_1 and B'_2, related to B_1 and B_2 by

$$(T'_{1a}, T'_{1b}, T'_{1c}) = (T_{1a}, T_{1b}, T_{1c}) - \sigma^{-1}_{X_{1A}}(T_a, T_b, T_c) \tag{7.3}$$

$$(T'_{2a}, T'_{2b}, T'_{2c}) = (T_a, T_b, T_c) + \sigma^{-1}_{X_{1B}}(T_{2a}, T_{2b}, T_{2c}). \tag{7.4}$$

This completes the right exchange interaction, $B_1 \vec{+}_e B_2 \to B'_1 + B'_2$.
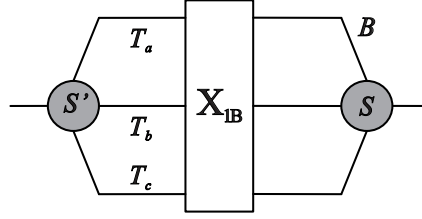
Figure 7.2: The actively interacting braid exchanged from B_1 to B_2, during their exchange interaction, in Fig. 7.1.

It can be shown, according to Chapters 3 and 5, that the only possible triple (T_a, T_b, T_c) in Fig. 7.1(c) is exactly the same as the triple of internal twists of the actively interacting braid, $B = {}^{S'}[(T_a, T_b, T_c)\sigma_{X_{1B}}]^S$, in Fig. 7.2. Note that as proved in Chapter 4, for an actively interacting braid of the form in Fig. 7.2, $S' = (-)^{|X_{1B}|}S$. Hence, B's left and right end-nodes are respectively in the same states as that of the left end-node of B'_2 in Fig. 7.1(d) and that of the right end-node of B_1 in Fig. 7.1(a). Thus, the form of braid B'_2 in Fig. 7.1(d), as a result of the final $3 \to 2$ move in the interacting process, must be precisely the result of the direct interaction of B and B_2. That is, Lemma 5.5 we have

$$B +_d B_2 = {}^{S'}[(T_a, T_b, T_c)\sigma_X]^S +_d {}^S[(T_{2a}, T_{2b}, T_{2c})\sigma_{X_2}]^{S_{2r}}$$
$$\to {}^{S'}[((T_a, T_b, T_c) + \sigma^{-1}_{X_{1B}}(T_{2a}, T_{2b}, T_{2c}))\sigma_{X_2}]^{S_{2r}} = B'_2,$$

which validates the relation in Eq. 7.4.

Therefore, the process of the right exchange interaction defined by Fig. 7.1 is as if B_1 gives out the actively interacting braid B in Fig. 7.2, which is then combined with B_2 by a direct interaction. In other words, B_1 and B_2 interact with each other via exchanging a virtual actively interacting braid B, and become B'_1 and B'_2. Or one may say that an exchange interaction is mediated by an actively interacting braid. This implies an analogy between actively interacting braids and bosons[2].

---

[2]More generally, this should imply the analogy between actively interacting braids and particles that mediate interactions, which should potentially include super partners of gauge bosons.

Note that in an exchange interaction, there does not exist an intermediate state in which only the virtual actively interacting braid is present because our definition of a braid requires the presence of its two end-nodes.

The following theorem summarizes the above as the first main result of this chapter. (The case of left exchange interaction is similar.)

Theorem 7.1. *Given two adjacent braids, $B_1, B_2 \in \mathfrak{B}^S$, $B_1 = {}^{S_{1l}}[(T_{1a}, T_{1b}, T_{1c})\sigma_{X_{1A}X_{1B}}]^S$ is on the left and is right-reducible with X_{1B} the reducible segment of its crossing sequence, and $B_2 = {}^S[(T_{2a}, T_{2b}, T_{2c})\sigma_{X_2}]^{S_{2r}}$, there exists a braid $B \in \mathfrak{B}^b$, $B = {}^{S'}[(T_a, T_b, T_c)\sigma_{X_{1B}}]^S$ with $S' = (-)^{|X_{1B}|}S$, such that it mediates the exchange interaction of B_1 and B_2 to create $B_1', B_2' \in \mathfrak{B}^S$, i.e.,*

$$
\begin{aligned}
& B_1 \vec{+}_e B_2 \\
& \rightarrow {}^{S_{1l}}[((T_{1a}, T_{1b}, T_{1c}) - \sigma_{X_{1A}}^{-1}(T_a, T_b, T_c))\sigma_{X_{1A}}]^{S'} + {}^{S'}[((T_a, T_b, T_c) + \sigma_{X_{1B}}^{-1}(T_{2a}, T_{2b}, T_{2c}))\sigma_{X_2}]^{S_{2r}} \\
& = B_1' + B_2'.
\end{aligned}
$$

(7.5)

It is important to remark that the reducibility of either braid in an exchange interaction is not necessary if we have included braid $B_0^{\pm}$ in Eq. 7.1. For example, two neighboring irreducible braids may still allow the steps in Fig. 7.1(a) and (b); however, Fig. 7.1(c) should be skipped because neither braid has a reducible crossing segment to be translated through; then, step in Fig. 7.1(d) is directly taken. Such a procedure is still dynamical because of the action of evolution moves, and thus can be considered a special case of exchange interaction. Needless to say, the actively interacting braid being exchanged in such an interaction is one of the two trivial braids $B_0^{\pm}$. This ensures that exchange interaction is a map on $\mathfrak{B}^S \times \mathfrak{B}^S$.

Another important remark is that two braids can have exchange interactions in different ways, in contrary to direct interaction. The occurrence of an exchange interaction on two braids does not have to exhaust the maximal reducible crossing segment of the reducible braid. For example as in Fig. 7.1, since X_{1B} is the maximal reducible crossing segment, we may take it to be the concatenation of two reducible crossing segments, i.e., $X_{1B} = X_{1B}'X_{1B}''$, then the translation taking Fig. 7.1(b) to (c) is allowed to terminate after passing through X_{1B}'', which becomes the crossing sequence of the virtual actively interacting braid in this new process. This certainly leads to two braids different from those in Fig. 7.1(d). In an ideal scenario, each possible way of the exchange interaction of two braids should have certain probability to occur.

This has an analogy in particle physics. Since quarks have both electric and color charges, both photons and gluons can mediate forces on quarks. The relation between actively interacting braids and bosons is yet not an actual identification, however. In fact, if each actively interacting braid corresponded to a boson, there would be too many "bosons". The underlining physics of that two braids can have exchange interactions in different ways deserves further studies.

It should be emphasized that each individual exchange interaction is a process giving rise to a unique result[3]. For preciseness, an expression like $B_1 \vec{+}_e B_2$ is only formal. Only when the exact

---

[3]With spin network labels the result is not unique any more because two topologically equal braids can be decorated by different sets of labels, and an interaction should result in a superposition of braids labeled differently.

forms of B_1 and B_2, in which their reducible segments are explicitly present, are given, $B_1 \vec{+}_e B_2$ acquires a precise and unique meaning. In computing an exchange interaction, we have to specify explicitly our choice of the reducible crossing segment of the braid that gives out the virtual actively interacting braid that depends on this choice. For any such choice Theorem 7.1 holds.

We have shown two representative-independent conserved quantities of stable braids, namely the effective twist Θ and the effective state χ, the former of which is additively conserved under direct interaction while the latter is multiplicatively conserved. Because of the representative-independence of these two quantities, we can write down their expressions for an arbitrary braid $B \in \mathfrak{B}^S$ in its unique representation, say $B = {}^{S_l}[(T_a, T_b, T_c)\sigma_X]^{S_r}$, as $\Theta_B = \sum_{i=a}^{c} T_i - 2 \sum_{j=1}^{|X|} x_j$ and $\chi_B = (-)^{|X|} S_l S_r$. These two quantities are important. The previous chapter has shown that Θ or certain function of Θ of a braid can be accounted for the "electric" charge of the braid. That is, braids can be charged. On the other hand, for actively interacting braids χ is a characteristic quantity because $\chi \equiv 1$ for any such braid. The following theorem presents that exchange interaction also preserves these two quantities in the same way as direct interaction does.

Theorem 7.2. *Given two neighboring stable braids, $B_1, B_2 \in \mathfrak{B}^S$, such that an exchange interaction (left or right or both) on them is doable, i.e., $B_1 +_e B_2 \rightarrow B_1' + B_2'$, $B_1', B_2' \in \mathfrak{B}^S$, the effective twist Θ is an additive conserved quantity, while the effective state χ is a multiplicative conserved quantity, namely*

$$\Theta_{B_1'} + \Theta_{B_2'} \overset{+_e}{=} \Theta_{B_1} + \Theta_{B_2}$$

$$\chi_{B_1'} \chi_{B_2'} \overset{+_e}{=} \chi_{B_1} \chi_{B_2}$$

(7.6)

This conservation law is independent of the virtual actively interacting braid being exchanged during the exchange interaction.

Proof. It is sufficient to prove this in the case of right exchange interaction, the other cases follow similarly. One can assume B_1 and B_2 are in the form as they are in Theorem 7.1. Hence, according to Theorem 7.1 one can readily write down

$$\Theta_{B_1} = \sum_{i=a}^{c} T_{1i} - 2 \sum_{j=1}^{|X_1|} x_{1j}, \quad \Theta_{B_2} = \sum_{i=a}^{c} T_{2i} - 2 \sum_{k=1}^{|X_2|} x_{2k}, \quad \chi_{B_1} = (-)^{|X_1|} S_{1l} S, \quad \chi_{B_2} = (-)^{|X_2|} S S_{2r},$$

where $X_1 = X_{1A} X_{1B}$, and

$$\Theta_{B_1'} = \sum_{i=a}^{c} (T_{1i} - T_i) - 2 \sum_{j=1}^{|X_{1A}|} x_{1Aj}, \quad \chi_{B_1'} = (-)^{|X_{1A}|} S_{1l} S',$$

$$\Theta_{B_2'} = \sum_{i=a}^{c} (T_i + T_{2i}) - 2 \sum_{m=1}^{|X_{1B}|} x_{1Bm} - 2 \sum_{k=1}^{|X_2|} x_{2k}, \quad \chi_{B_2'} = (-)^{|X_{1B} X_2|} S' S_{2r},$$

100

Hence, we have the following:

$$\Theta_{B_1'} + \Theta_{B_2'} = \sum_{i=a}^{c}(T_{1i} - T_i) - 2\sum_{j=1}^{|X_{1A}|} x_{1Aj} + \sum_{i=a}^{c}(T_i + T_{2i}) - 2\sum_{m=1}^{|X_{1B}|} x_{1Bm} - 2\sum_{k=1}^{|X_2|} x_{2k}$$

$$= \sum_{i=a}^{c}(T_{1i} + T_{2i}) - 2\sum_{j=1}^{|X_1|} x_{1j} - 2\sum_{k=1}^{|X_2|} x_{2k}$$

$$= \Theta_{B_1} + \Theta_{B_2},$$

$$\chi_{B_1'}\chi_{B_2'} = (-)^{|X_{1A}|}S_{1l}S'(-)^{|X_{1B}X_2|}S'S_{2r} = (-)^{|X_{1A}X_{1B}|}S_{1l}(-)^{|X_2|}S_{2r} = \chi_{B_1}\chi_{B_2},$$

where the use of $\sum\limits_{j=1}^{|X_{1A}|} x_{1Aj} + \sum\limits_{m=1}^{|X_{1B}|} x_{1Bm} = \sum\limits_{j=1}^{|X_1|} x_{1j}$, $S'^2 = S^2 \equiv +$, and $X_{1A}X_{1B} = X$ has been made. □

Therefore, exchanges of actively interacting braids give rise to interactions between braids that are charged under the topological conservation rules. The conservation of Θ is analogous to the charge conservation in particle physics.

7.2.1 Asymmetry of exchange interaction

As in the case of direct interaction, exchange interaction is not symmetric either. The asymmetry of exchange interaction is two-fold. On the one hand, given $B_1, B_2 \in \mathfrak{B}^S$, which are both right-reducible (left-reducible), in general $B_1 \vec{+}_e B_2 \neq B_2 \vec{+}_e B_1$ ($B_1 \overleftarrow{+}_e B_2 \neq B_2 \overleftarrow{+}_e B_1$). This is henceforth called the *asymmetry of the first kind*. On the other hand, if B_1 and B_2 are respectively right- and left-reducible, then in general $B_1 \vec{+}_e B_2 \neq B_1 \overleftarrow{+}_e B_2$, which is christened the *asymmetry of the second kind*. Most likely, the interactions on either side of these inequalities simply does not occur because they do not meet the interaction condition. Even when these interactions do occur, the inequalities hold in general. We now show that an exchange interaction can be symmetric in some cases.

An issue is that two braids may have several different exchange interactions. It is then impossible for, say $B_1 \vec{+}_e B_2$, to be equal to $B_2 \vec{+}_e B_1$ for all possible ways of how B_1 and B_2 may interact. The only precise question we can answer is actually, taking right exchange interaction as an example: For any B_1 and B_2, among all possible ways of $B_1 \vec{+}_e B_2$ and $B_2 \vec{+}_e B_1$, does there exist a way in which the reducible crossing segments of B_1 and B_2 are chosen, such that in this way $B_1 \vec{+}_e B_2 = B_2 \vec{+}_e B_1$?

We first study the the asymmetry of the first kind. It suffices to check the right exchange interaction and the left one follows likewise. We assume $B_1 = {}^{S_{1l}}[(T_{1a}, T_{1b}, T_{1c})\sigma_{X_1 X_1'}]^{S_{1r}}$ and $B_2 = {}^{S_{2l}}[(T_{2a}, T_{2b}, T_{2c})\sigma_{X_2 X_2'}]^{S_{2r}}$, with X_1' and X_2' certain choices of the reducible crossing segments of respectively B_1 and B_2. That both $B_1 \vec{+}_e B_2$ and $B_2 \vec{+}_e B_1$ are assumed to be legal requires that $S_{1r} = S_{2l} = S$ and $S_{2r} = S_{1l} = S'$ for some S and S'. Hence, we have $B_1 = {}^{S'}[(T_{1a}, T_{1b}, T_{1c})\sigma_{X_1 X_1'}]^{S}$ and $B_2 = {}^{S}[(T_{2a}, T_{2b}, T_{2c})\sigma_{X_2 X_2'}]^{S'}$. With this, Theorem 7.1 immediately gives us

$$B_1 \vec{+}_e B_2$$
$$\to {}^{S'}[((T_{1a}, T_{1b}, T_{1c}) - \sigma_{X_1}^{-1}(T_a, T_b, T_c))\sigma_{X_1}]^{S''} + {}^{S''}[((T_a, T_b, T_c) + \sigma_{X_1'}^{-1}(T_{2a}, T_{2b}, T_{2c}))\sigma_{X_1' X_2 X_2'}]^{S'}$$

$$B_2 \vec{+}_e B_1$$
$$\rightarrow {}^S[((T_{2a}, T_{2b}, T_{2c}) - \sigma_{X_2}^{-1}(T_a', T_b', T_c'))\sigma_{X_2}]^{S'''} + {}^{S'''}[((T_a', T_b', T_c') + \sigma_{X_2'}^{-1}(T_{1a}, T_{1b}, T_{1c}))\sigma_{X_2' X_1 X_1'}]^S \ ,$$

where $S'' = (-)^{|X_1'|}S$ and $S''' = (-)^{|X_2'|}S'$; (T_a, T_b, T_c) and (T_a', T_b', T_c') are the triples of internal twists of the two virtual actively interacting braids being exchanged in the two interactions respectively. Requiring that the RHS of the two interaction equations are equal term by term gives rise to

$$\begin{cases} S = S', & S'' = S''' \\ X_1 = X_2, & X_1' X_2 X_2' = X_2' X_1 X_1' \end{cases} , \tag{7.7}$$

and

$$\begin{cases} (T_{1a}, T_{1b}, T_{1c}) - \sigma_{X_1}^{-1}(T_a, T_b, T_c) = (T_{2a}, T_{2b}, T_{2c}) - \sigma_{X_2}^{-1}(T_a', T_b', T_c') \\ (T_a, T_b, T_c) + \sigma_{X_1'}^{-1}(T_{2a}, T_{2b}, T_{2c}) = (T_a', T_b', T_c') + \sigma_{X_2'}^{-1}(T_{1a}, T_{1b}, T_{1c}) \end{cases} . \tag{7.8}$$

Eq. 7.7 also implies $X_1' = X_2'$. We can then rewrite S' as S, S''' as S'', and both $X_1 X_1'$ and $X_2 X_2'$ as XX'. As a result, the two triples (T_a, T_b, T_c) and (T_a', T_b', T_c') must be equal, which is understood by recalling the steps in Fig. 7.1. Thus, Eq. 7.8 becomes

$$\begin{cases} (T_{1a}, T_{1b}, T_{1c}) - \sigma_X^{-1}(T_a, T_b, T_c) = (T_{2a}, T_{2b}, T_{2c}) - \sigma_X^{-1}(T_a, T_b, T_c) \\ (T_a, T_b, T_c) + \sigma_{X'}^{-1}(T_{2a}, T_{2b}, T_{2c}) = (T_a, T_b, T_c) + \sigma_{X'}^{-1}(T_{1a}, T_{1b}, T_{1c}) \end{cases} ,$$

whose only solution is

$$(T_{1a}, T_{1b}, T_{1c}) = (T_{2a}, T_{2b}, T_{2c}).$$

Therefore, B_1 and B_2 must be exactly the same. By the same token, this should be true for the case of left exchange interaction too.

We now investigate the asymmetry of the second kind. We assume a right-reducible braid $B_1 = {}^{S_{1l}}[(T_{1a}, T_{1b}, T_{1c})\sigma_{X_1 X_1'}]^S$ with X_1' the choice of its reducible crossing segment, and $B_2 = {}^S[(T_{2a}, T_{2b}, T_{2c})\sigma_{X_2' X_2}]^{S_{2r}}$ with X_2' the choice of its reducible crossing segment. Note that the right end-node of B_1 has already been made the same as the left end-node of B_2 such that $B_1 \vec{+}_e B_2$ and $B_1 \overleftarrow{+}_e B_2$ are both allowed.

By Theorem 7.1 we get

$$B_1 \vec{+}_e B_2 \rightarrow$$
$${}^{S_{1l}}[((T_{1a}, T_{1b}, T_{1c}) - \sigma_{X_1}^{-1}(T_a, T_b, T_c))\sigma_{X_1}]^{S'} + {}^{S'}[((T_a, T_b, T_c) + \sigma_{X_1'}^{-1}(T_{2a}, T_{2b}, T_{2c}))\sigma_{X_1' X_2' X_2}]^{S_{2r}} \ ,$$

where $S' = (-)^{|X_1'|}S$, and (T_a, T_b, T_c) the triple of internal twists of the virtual actively interacting braid in the interaction. Analogously we also have

$$B_1 \overleftarrow{+}_e B_2 \rightarrow$$
$${}^{S_{1l}}[((T_{1a}, T_{1b}, T_{1c}) + \sigma_{X_1 X_1' X_2'}^{-1}(T_a', T_b', T_c'))\sigma_{X_1 X_1' X_2'}]^{S''} + {}^{S''}[((T_{2a}, T_{2b}, T_{2c})\sigma_{X_2'} - (T_a', T_b', T_c'))\sigma_{X_2}]^{S_{2r}} \ ,$$

where $S'' = (-)^{|X_2'|}S$, and (T_a', T_b', T_c') the triple of internal twists of the virtual actively interacting braid in the interaction. The term-by-term equality of the RHS of the above two equations now

helps us to pin down the conditions on B_1 and B_2. Firstly, we must have $S' = S''$, which requires $|X_1'| = |X_2'| + 2n, n \in \mathbb{Z}$ and keeping $|X_1'| \geq 0$. Secondly, we demand $X_1 = X_1 X_1' X_2'$ and $X_1' X_2' X_2 = X_2$. The only solution of this is readily $X_1' X_2' = \mathbb{I}$. Or equivalently, we obtain $X_1' = X_2'^{-1}$. This sets $|X_1'| = |X_2'|$ and hence guarantees $S' = S''$. These results now turn the constraint on the triples of internal twists of B_1 and B_2 to be

$$
\begin{aligned}
(T_{1a}, T_{1b}, T_{1c}) - \sigma_{X_1'}^{-1}(T_a, T_b, T_c) &= (T_{1a}, T_{1b}, T_{1c}) + \sigma_{X_1'}^{-1}(T_a', T_b', T_c') \\
(T_a, T_b, T_c) + \sigma_{X_1'}^{-1}(T_{2a}, T_{2b}, T_{2c}) &= (T_{2a}, T_{2b}, T_{2c})\sigma_{X_2'} - (T_a', T_b', T_c')
\end{aligned}
\tag{7.9}
$$

Surprisingly, Eq. 7.9 actually puts no more constraint on B_1 and B_2 because it is automatically satisfied. The reason is as follows.

In both cases, namely $B_1 \vec{+}_e B_2$ and $B_1 \overset{\leftarrow}{+}_e B_2$, the configurations obtained by the first $2 \rightarrow 3$ move are the same, which has three new nodes and three new edges (like the dashed green ones in Fig. 7.1(b)). We call this configuration, Δ. In the case of $B_1 \vec{+}_e B_2$, one needs to translate the Δ to the left, passing through X_1', then rearrange Δ by equivalence moves into another configuration, say Δ', which is a proper for a $3 \rightarrow 2$ move. The equivalence moves taking Δ to Δ' equips Δ' with two opposite triples of twists, viz $-(T_a, T_b, T_c)$ on the left of Δ' and (T_a, T_b, T_c) on the right. (T_a, T_b, T_c) is the very triple of internal twists of the virtual actively interacting braid exchanged by B_1 and B_2 in this interaction. In the case of $B_1 \overset{\leftarrow}{+}_e B_2$, one translates Δ to the right, passing the crossing sequence X_2', and reforms it by equivalence moves into another one, say Δ'', which is also ready for a $3 \rightarrow 2$ move. Likewise, Δ'' is equipped with (T_a', T_b', T_c') on its left and $-(T_a', T_b', T_c')$ on its right. (T_a', T_b', T_c') is the very triple of internal twists of the virtual actively interacting braid exchanged in the process of $B_1 \overset{\leftarrow}{+}_e B_2$. Nevertheless, because of $X_2' = X_1'^{-1}$, according to Chapter 6, Δ' and Δ'' happen to be related to each other by a discrete transformation that is considered as a CP transformation. By the action property of a CP (see Chapter 6 for details), we have precisely

$$
(T_a', T_b', T_c') = -(T_a, T_b, T_c).
\tag{7.10}
$$

Putting this aside first, we have another useful identity from Eq. D.2:

$$
\sigma_X^{-1}(\cdot, \cdot, \cdot) = (\cdot, \cdot, \cdot)\sigma_{\mathcal{R}(X)},
$$

where $(\cdot, \cdot, \cdot)$ stands for an arbitrary triple of internal twists, and $\mathcal{R}(X = x_1 \ldots x_i \ldots x_n) = x_n \ldots x_i \ldots x_1$, the reversion operation of a crossing sequence. Definition D.2 also defines the inversion of a crossing sequence, namely $\mathcal{I}(X = x_1 \ldots x_i \ldots x_n) = x_1^{-1} \ldots x_i^{-1} \ldots x_n^{-1}$. Obviously, $\mathcal{I}\mathcal{R}(X) = X^{-1}$. Regarding the permutation induced by a crossing sequence, however, $\sigma_{\mathcal{R}(X)} = \sigma_{\mathcal{I}\mathcal{R}(X)}$, which means $\sigma_{\mathcal{R}(X)} = \sigma_{X^{-1}}$. Consequently, the equation above is extended to

$$
\sigma_X^{-1}(\cdot, \cdot, \cdot) = (\cdot, \cdot, \cdot)\sigma_{X^{-1}}.
\tag{7.11}
$$

Finally, in view of Eqs. 7.10 and 7.11, and all the relations we have in hand, it is easy to see that Eq. 7.9 is satisfied. That is, the triples of internal twists of B_1 and B_2 can be anything they can. Therefore, for $B_1 \vec{+}_e B_2$ and $B_1 \overset{\leftarrow}{+}_e B_2$ can be equal in certain way, we demand $B_1 = {}^{S_{1l}}[(T_{1a}, T_{1b}, T_{1c})\sigma_{X_1 X}]^S$ and $B_2 = {}^S[(T_{2a}, T_{2b}, T_{2c})\sigma_{X^{-1} X_2}]^{S_{2r}}$. For compactness, the following theorem concludes the discussion above.

Theorem 7.3. *Exchange interaction between two arbitrary braids $B_1, B_2 \in \mathfrak{B}^S$, if allowed, is asymmetric in general. The asymmetry of the first kind goes like $B_1 \vec{+}_e B_2 \neq B_2 \vec{+}_e B_1$ ($B_1 \overleftarrow{+}_e B_2 \neq B_2 \overleftarrow{+}_e B_1$), whereas the asymmetry of the second kind reads $B_1 \vec{+}_e B_2 \neq B_1 \overleftarrow{+}_e B_2$. But the following special cases exist.*

1. *Such that $B_1 \vec{+}_e B_2 = B_2 \vec{+}_e B_1$ ($B_1 \overleftarrow{+}_e B_2 = B_2 \overleftarrow{+}_e B_1$) in certain way, B_1 and B_2 must be in the form*

$$B_1 = B_2 = {}^S[(\cdot, \cdot, \cdot)\sigma_{XX'}]^S \quad (B_1 = B_2 = {}^S[(\cdot, \cdot, \cdot)\sigma_{X'X}]^S), \tag{7.12}$$

where $(\cdot, \cdot, \cdot)$ represents an arbitrary triple of internal twists, and X' is the chosen reducible crossing segment.

2. *Such that $B_1 \vec{+}_e B_2 = B_1 \overleftarrow{+}_e B_2$ in certain way, B_1 and B_2 must satisfy*

$$\begin{aligned} B_1 &= {}^{S_{1l}}[(\cdot, \cdot, \cdot)\sigma_{X_1 X}]^S \\ B_2 &= {}^S[(\cdot, \cdot, \cdot)\sigma_{X^{-1} X_2}]^{S_{2r}}, \end{aligned} \tag{7.13}$$

where X and X^{-1} are the specified reducible crossing segments of B_1 and B_2 respectively during the two interactions.

The existence of exchange interaction brings the braids and their dynamics closer to Quantum Field Theory. This is not to say that we already have a fundamental field theoretic formulation of our theory. Rather, we can have an effective field theory describing the dynamics of braids. To make this more transparent, we need first to show another dynamical process of braids.

7.3 Braid Decay

It is mentioned in Chapter 3 that there can be reversed processes of direct interactions: a braid may split into two braids. We may call a reversed direct interaction a decay. Hence, obviously through decay a braid always radiates at least one actively interacting braid. In a direct interaction, the actively interacting braid involved may interact with the other braid from the left or from the right. As a result, via a decay the braid may radiate an actively interacting braid to its right or to its left, depending on whether the braid is right-reducible or left-reducible. We thus differentiate a left-decay from a right-decay. The former is symbolized by $B \overset{\leftrightsquigarrow}{\to} B' + B''$, indicating that $B' \in \mathfrak{B}^b$, while the latter is denoted by $B \overset{\rightsquigarrow}{\to} B' + B''$ because $B'' \in \mathfrak{B}^b$.

Fig. 7.3 presents the defining process of right-decay. Fig. 7.3(a) shows a right-reducible braid, $B = {}^{S_l}[(T_a, T_b, T_c)\sigma_{XX'}]^{S_r}$, with a chosen reducible crossing segment X'. As in an exchange interaction X' can be a part of the maximal reducible crossing segment of B'. This indicates that generically a braid can also have different ways of decay, corresponding to each choice of the reducible segment. We thus need to specify this choice in a specific decay process.

Taking a $1 \to 4$ move on the right end-node of B leads to Fig. 7.3(b). One then translate the three nodes, one in state S_r and two in $-S_r$, along the red dashed loop in Fig. 7.3(b) to the left of
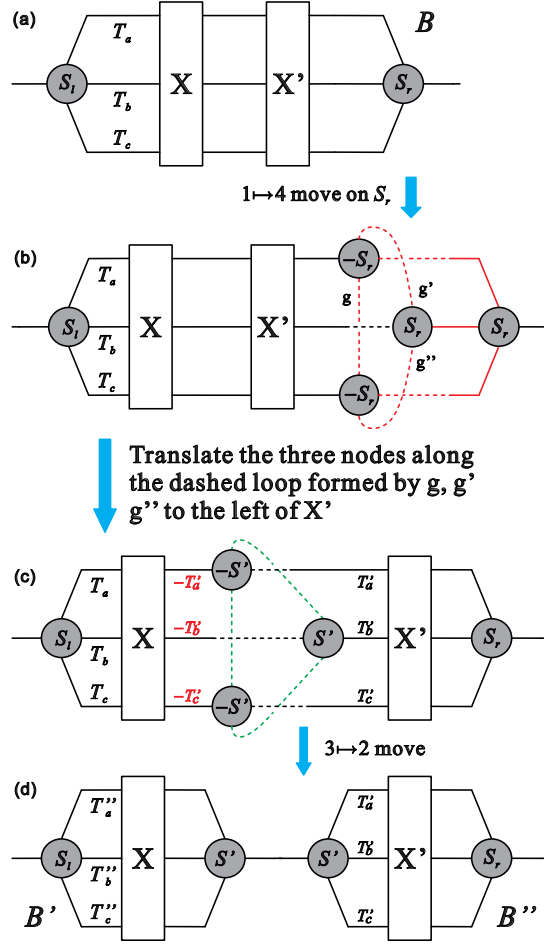
Figure 7.3: Definition of braid decay: $B \overset{\rightsquigarrow}{\rightarrow} B' + B''$, $B, B' \in \mathfrak{B}^S$, $B'' \in \mathfrak{B}^b$. In (c) and (d), $S' = (-)^{|X'|} S_r$. In (b) and (c), the dashed lines emphasize the dependence of their relative positions on the state S_r. In (d), (T''_a, T''_b, T''_c) is the triple of internal twists of B'.

X', and rearrange them in a proper configuration for a $3 \to 2$ move, as shown in Fig. 7.3(c). This produces the pair of opposite triples of twists in Fig. 7.3(c), namely $-(T'_a, T'_b, T'_c)$ and (T'_a, T'_b, T'_c). Note that the triple $-(T'_a, T'_b, T'_c)$, which is in red, should be understood to be added to (T_a, T_b, T_c), the original triple of internal twists of B, taking into account the permutation induced by X, i.e., $(T_a, T_b, T_c) - \sigma_X^{-1}(T'_a, T'_b, T'_c) = (T''_a, T''_b, T''_c)$. Finally, a $3 \to 2$ move results in Fig. 7.3(d), which depicts the two resulted adjacent braids, B' and B''. Thus, we have

$$B = {}^{S_l}[(T_a, T_b, T_c)\sigma_{XX'}]^{S_r} \overset{\rightsquigarrow}{\rightarrow} {}^{S_l}[((T_a, T_b, T_c) - \sigma_X^{-1}(T'_a, T'_b, T'_c))\sigma_X]^{S'} + {}^{S'}[(T'_a, T'_b, T'_c)\sigma_{X'}]^{S_r},$$
$$= B' + B''$$

(7.14)

where $S' = (-)^{|X'|} S_r$ and $B'' \in \mathfrak{B}^b$. Left-decay is defined similarly.

The notation of decay already implies that a decay is in general not symmetric. For a braid

$B \in \mathfrak{B}^f \sqcup \mathfrak{B}^b$ that is able to decay in both directions, say $B \overset{\sim}{\rightarrow} B_1 + B_2$ and $B \overset{\sim}{\rightarrow} B'_1 + B'_2$, $B_1 = B'_1$ and $B_2 = B'_2$ cannot be equal because we must have $B_1, B'_2 \in \mathfrak{B}^b$ but $B_2, B'_1 \in \mathfrak{B} \setminus \mathfrak{B}^b$. Even if B is an actively interacting braid, its left and right decays give rise to different results because both of its left and right decays have more than one ways to occur, as pointed out above. In some special cases, an actively interacting braid can have a left-decay that is the same as a right-decay. The conditions of this are similar to those for a direct interaction to be symmetric found in Section 5.3.2.

Because of the relation between decay and direct interaction, effective twist Θ and effective state χ must be respectively an additive conserved quantity and a multiplicative conserved quantity under a decay. By the same token, because direct interactions are invariant under C, P, T, and their combinations according to Section 6.2.3, so are decays. Decay and direct interaction of braids indicate that an actively interacting braid can be singly created and destroyed. This reinforces the implication that actively interacting braids are analogous to bosons.

7.4 Braid Feynman diagrams

Our study of braid excitations of embedded framed spin networks, in particular the discovery of the dynamics of these excitations, namely direct and exchange interactions, and decay of braids, makes it possible to describe the dynamics of braids by an effective theory based on Feynman diagrams. These diagrams are called braid Feynman diagrams. We remark that as a distinction from the usual QFT Feynman diagrams that do not have any internal structure, each braid Feynman diagram is an effective description of the whole dynamical process of an interaction of braids, its internal structure records how the braids and their neighborhood evolve.

We use $\bullet\!\!\longrightarrow\!\!-$ and $\longrightarrow\!\!\bullet$ for respectively outgoing and ingoing propagating braids in $\mathfrak{B}^f$, $\bullet\!\cdots\!\!\dashrightarrow\!\cdots$ and $\cdots\!\!\dashrightarrow\!\cdots\!\bullet$ for respectively outgoing and ingoing non-actively propagating braids[4] in $\mathfrak{B}^s$. Because it is implied that actively interacting braids are analogous to bosons, outgoing and ingoing braids in $\mathfrak{B}^b$ are better represented by $\overrightarrow{\sim\!\!\sim\!\!\sim}$ and $\overrightarrow{\sim\!\!\sim\!\!\sim}\!\bullet$ respectively.

In accordance with left and right-decay, we will henceforth denote left and right direct interactions by $\overset{\leftarrow}{+}_d$ and $\overset{\rightarrow}{+}_d$ respectively. Note that if the two braids being interacting are both actively interacting, the direction of the direct interaction is irrelevant because the result does not depend on which of the two braids plays the actual active role in the interaction. According to the algebraic structure of braids under direct interaction found in Theorem 5.4, namely $\mathfrak{B}^b \overset{\rightarrow}{+}_d \mathfrak{B}^b \subseteq \mathfrak{B}^b$ and $\mathfrak{B}^b \overset{\rightarrow}{+}_d (\mathfrak{B}^f \sqcup \mathfrak{B}^s) \subseteq \mathfrak{B}^f \sqcup \mathfrak{B}^s$, the only possible single vertices of right direct interactions are listed below. (Those corresponding to left direct interactions are left-right mirror images these.)

Similarly, right-decay have the possible basic single vertices in Fig. 7.5. (The left-decay vertices are left-right mirror images of these.)

The arrows over the wavy lines in Figs. 7.4 and 7.5 are important because they differentiate a left process from a right process. That said, one can flip the arrow over the braid B in each of the first four diagrams in Fig. 7.5 and obtain the diagram of the corresponding left direction

---

[4]These braids can still propagate in an induced way.
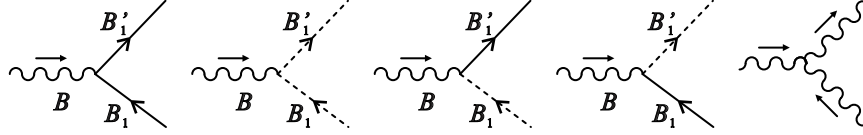
Figure 7.4: Possible right direct interaction vertices. Time flows up.
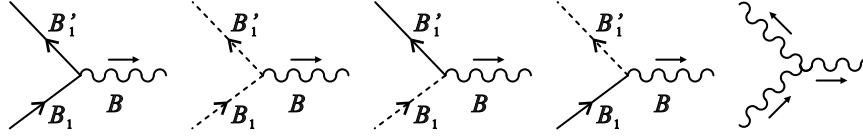
Figure 7.5: Possible right-decay interaction vertices. Time flows up.

interaction. One can also turn the fifth diagram in Fig. 7.5 upside down to get its corresponding direct interaction diagram.

The result of an exchange interaction of two braids, say $B_1 \vec{+}_e B_2 \rightarrow B_1' + B_2'$ by exchanging some virtual $B \in \mathfrak{B}^b$, is the same as that of the combined process of the decay, $B_1 \vec{\rightarrow} B_1' + B$, and the direct interaction $B \vec{+}_d B_2 \rightarrow B_2'$. Nonetheless, it is important to note that the former process and the latter combined process are two topologically and dynamically distinct processes; they only have the same in and out states topologically. Therefore, we obtain in Fig. 7.6 all possible basic 2-vertex diagrams for right exchange interaction.

The left-right mirror images of the diagrams in Fig. 7.6 are certainly the basic diagrams for left exchange interaction. In Fig. 7.6(e), (f), (h), (n), (s) and their left-right mirror images, if $B_1 \in \mathfrak{B}^s$ happens to be irreducible, $B_1 = B_1'$ and $B = B_0^+$ or $B = B_0^-$ are understood. Given all these it becomes manifest that exchange interaction is invariant under the C, P, T and their products, as in the case of direct interaction and decay.

Recalling Theorem 7.3, braid Feynman diagrams make it transparent to tell whether an exchange interaction can be symmetric. Regarding the asymmetry of the first kind, one simply needs to check if the diagram of an interaction looks the same as its left-right mirror with also the arrow over the virtual braid reversed. Fig. 7.6(c), (d), (h) through (o), and (q) through (t) depict exchange interactions that do not allow any violation of the asymmetry of the first kind, viz $B_1 \vec{+}_e B_2 \neq B_2 \vec{+}_e B_1$. The reason is that in each of these diagrams, the out-state contains two braids in two different divisions respectively. Their mirror images have the same kind of asymmetry with respect to left exchange interaction.

As to the asymmetry of the second kind, one should check if the arrow over the virtual braid in a diagram can be flipped. As can be seen, all the exchange interactions in Fig. 7.6 may have instances violating the asymmetry of the second kind if conditions in Theorem 7.3 are satisfied. As a result, the exchange interactions that can be fully symmetric when conditions in Theorem 7.3 are satisfied correspond respectively to the diagrams in Fig. 7.6(a), (b), (e), (f), (g), and (p).

The braid Feynman diagrams in Figs. 7.4, 7.5, and 7.6 manifests the analogy between actively

107
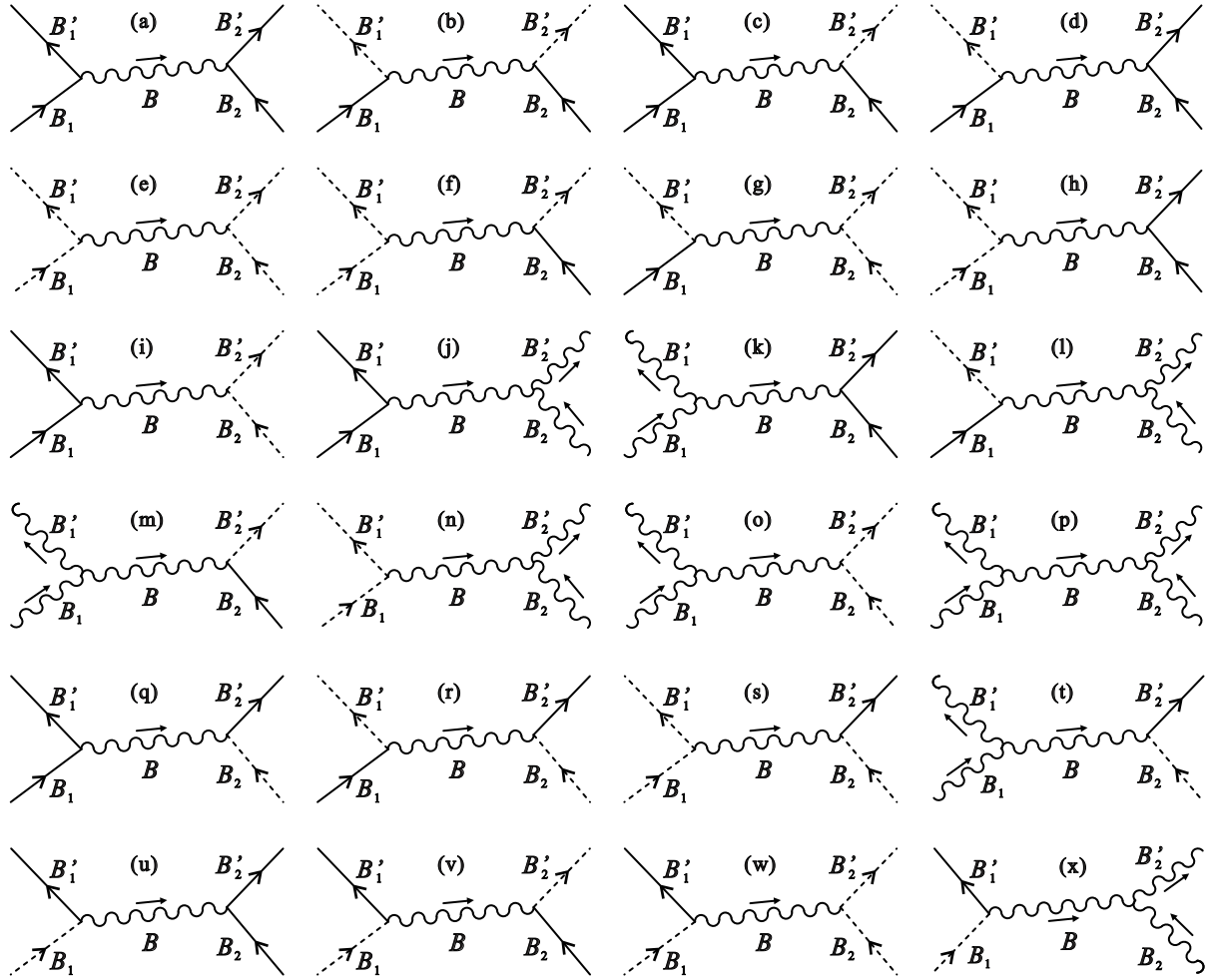
Figure 7.6: Possible right exchange interaction 2-vertices. Time flows up.

interacting braids and bosons. Fermionic degrees of freedom may correspond to those braids that are not actively interacting because their interactions are mediated by the actively interacting ones. They are more probably corresponding to braids in $\mathfrak{B}^f$, which are chiral propagating but not actively interacting.

More complicated braid Feynman diagrams including the loop ones can be constructed out of these basic vertices. As a result, there should exist an effective field theory based on these diagrams, in which the probability amplitudes of each diagram can be computed. For this one should figure out the terms evaluating external lines, vertices, and propagators of braids.

In a more complete sense, one may try to write down an action of the effective fields representing braids that can generate these braid Feynman diagrams. In such an effective theory, each line of a braid Feynman diagram represents an effective field characterizing a braid; it should be labeled by characterizing quantities of the braid represented by the line, which are elements of certain

groups or the corresponding representations of these groups. For a braid these quantities are its two end-node states that are elements of $\mathbb{Z}_2$, its crossing sequence, an element of the braid group B_3, its twists that are elements in $\mathbb{Z}$, and spin network labels when they are taken into account. Moreover, these group elements are constrained on the lines meeting at a vertex.

This is more difficult than just to find a way to compute the probability amplitude of each braid Feynman diagram. In any case, the very first challenge of fulfilling this task is to choose an appropriate mathematical language. In the next section we will briefly mention three possible formalisms.

Nevertheless, these braid Feynman diagrams put a constraint on defining the probability amplitudes regardless of the underlining mathematical language. We use an example to illustrate this point. Let us consider the braid Feynman diagram in Fig. 7.6(a) for some specific interaction. This diagram is the same as concatenating the first diagram in Fig. 7.5 with the first diagram in Fig. 7.4 from the left along the wavy line. That is, the exchange interaction, $B_1 \vec{+}_e B_2 \rightarrow B_1' + B_2'$ by exchanging some virtual $B \in \mathfrak{B}^b$, and the combined process of the decay, $B_1 \overset{\leadsto}{\rightarrow} B_1' + B$, and the direct interaction $B \vec{+}_d B_2 \rightarrow B_2'$, have identical in and out braid states at this tree level. We then expect the following equality at this level, which is only formal,

$$\mathcal{M}\left(B_1 \vec{+}_e B_2 \rightarrow B_1' + B_2'\right) = \sum_\alpha \mathcal{M}\left(B \vec{+}_d B_2 \rightarrow B_2' \,\middle|\, B_1 \overset{\leadsto}{\rightarrow} B_1' + B, \alpha\right) G_B(\alpha). \tag{7.15}$$

The LHS of Eq. 7.15 is the probability amplitude of the exchange interaction, which is independent of the virtual braid B being exchanged during the interaction but only determined by the evolution moves involved in the interaction and the external lines in Fig. 7.6(a), namely B_1, B_2, B_1' and B_2'. The first term on the RHS of this equation is the conditional probability amplitude of the direct interaction provided with the occurrence of the decay and the meeting of B and B_2. Besides B_1, B_2, B_1', B_2' and the corresponding evolution moves, this also certainly depends on the braid B, which is characterized by a set of parameters, denoted by α, including the end-node states, spin network labels, twists, and crossings of B. The second term on the RHS, i.e., $G_B(\alpha)$ represents the propagator (however it will be defined) of B, which is obviously also a function of α. α must be summed over to obtain a final result independent of B. This summation has analogies in usual quantum field theories, e.g., the integration over the momentum defining the propagator of the virtual particle in an interaction, and the summation over polarizations of gauge bosons.

Though derived with the help of a specific example, Eq. 7.15 is generic because one can simply replace the exchange interaction on the LHS with any other one and substitute the corresponding direct interaction and decay on the RHS simultaneously. No matter how the continuum limit of our theory is to be obtained, α should account for the momentum of braid B in this limit. Therefore, Eq. 7.15 can be used as a validity check of the theory's future possible developments that will be able to define the probability amplitudes of the dynamical processes of our braids.

7.5 Summary

In conclusion, we have found the exchange interaction of braids, which has two kinds of asymmetry. Conserved quantities under exchange interaction are discussed. We also discussed decay of

braids. The existence of exchange interaction and its relation with direct interaction and decay of braids imply the analogy between actively interacting braids and bosons. Braid Feynman diagrams are developed and used to represent the dynamics of braids. An effective theory describing braid dynamics can be based on these braid Feynman diagrams. We emphasize that an interaction of two braids is not point-like, although braid Feynman vertices are point-like. This is similar to the case of String Theory in which two strings do no interact at a point.

Despite the lack of a fully fundamental theory of quantum gravity with matter, an effective theory of topological excitations, such as our braids, of quantum geometry may be more relevant to the testable region of our physical world. The study of collective modes in condensed matter physics provides a great motivation to this. For example, in the current stage of the string-net condensation, all Standard Model gauge fields and fermionic fields but chiral fermions appear to be low energy effective fields emergent out of certain high energy lattice models[10, 11].

Another open issue is that we cannot justify for now whether the actively interacting braids are analogous to bosons or gauge bosons in particular. For the latter to be true, actively interacting braids should obey certain gauge symmetry. We would like to see gauge symmetries arise when we include spin network labels, which are normally gauge group representations, in our model. We hope our future work may find a solution of this.

Our next step is try to write down an effective field theory of these braid excitations in an algebraic way. Nonetheless, we would delay the discussion of possible approaches towards this goal but discuss all future work related issues collectively in the next chapter.

Chapter 8

Discussion and Outlook

The 4-valent formulation resolved many issues and limitations persisting in the 3-valent approach. In the first place, we obtain a $(3 + 1)$-dimensional evolution of quantum states of space-time, which has intrinsic dynamics of the braid excitations of these states. Because of the framing and embedding of spin networks, strands of a braid excitation admit twists only in units of 1/3. The twists of a braid is directly related to its electric charge, which naturally, rather than by hand, gives rise to charge quantization and fractional charges such as quark charges. The 4-valent theory also contains another natural selection: to identify discrete transformations of braids with analogues of C, P, T, and their products, braid dynamics picks out from the discrete group $S_3 \times \mathbb{Z}_3$ a subgroup of exactly eight elements, including identity.

Nevertheless, most open questions raised in the 3-valent approach still remain unanswered. Some of them have been discussed more or less in the thesis, e.g., Section 6.3 on CP-violation. In the next section, we will discuss some issues that bear on the interpretation of these results. In the last section, however, we shall introduce ideas, future work, and work in progress, which may remove these issues.

8.1   Discussion

Stability and locality

We argued that the stable braid excitations of embedded 4-valent spin networks may be considered local excitations because they are noiseless subsystems of the theory. Nevertheless, one may compare our topological excitations to topological field theories that do not bear any local degrees of freedom, and hence is skeptical about the locality of them. In fact, locality in the context of background independent theories of quantum gravity is very subtle; it is correlated with two other important issues, namely the problem of the concept of space-time and the problem of low energy limit. Moreover, the locality and stability of a braid are also related.

A background independent quantum gravity theory usually lacks a metric that directly measures locality in space. One may define locality on each individual spin network with respect to the graph metric of the network. In this sense, a stable braid is local because its state space is

intact under evolution moves. The problem is, however, that although a braid's braiding structure is protected under evolution, its locality can be destroyed by evolution moves because of the issue in the stability of the braid. Our stability condition only protects the braiding of a braid from being undone, but does not prevent the braid's end-nodes from being expanded by $1 \rightarrow 4$ moves. That is, the three strands of a braid may turn out to be attached to different nodes far from each other on the network. When this happens, a braid is nonlocal. A possible solution is to strengthen our stability condition by further forbidding the action of a $1 \rightarrow 4$ move on either end-node of a stable braid in our original definition. The consequence is the loss of braid decay because the decay of a braid begins by a $1 \rightarrow 4$ move on its reducible end-node. Either way seems to have a trade-off.

Apart from looking for finer stability conditions, nonetheless, we may not need to worry about the potential instability and non-locality of stable braids because what is physically relevant are the low energy effective degrees of freedom of the braids that survive the evolution of spin networks and certain limiting process. Thus, it is important to write down a physical effective theory of the braid excitations. We will discuss this shortly in the next section.

The locality discussed above is termed as micro-locality. Opposed to micro-locality is macro-locality, defined in the low energy end of the theory. Markopoulou and Smolin proposed these two notions of locality and found that they do not match in general[7]. Another work of the author of the thesis, [93], also illustrated this mismatch by studying Ising models. The quantum space-time in our context is pre-geometric, as it is a sum over quantum histories of superposed pre-geometric spin networks; it is conjectured that continuous space-time emerge as certain limit of this quantum space-time. It then makes no sense for the micro-locality defined on each spin network to match the macro-locality in continuous space-time.

Macro-locality is more relevant to the known physics; however, it is obtained from micro-locality. This goes back to the problem of low energy limit, to resolve which Markopoulou *et al.* adapted the idea of noiseless subsystems with micro-symmetries from Quantum Information. Therefore, we expect that the symmetry of the braid excitations will induce emergent symmetries, including time and space translation invariance, in the low energy effective description of the braids. Our work in progress, which will be introduced in the next section, indicates that this expectation is hopeful.

Particle identification and mass

The ultimate physical content of the 3-strand braids is not fully comprehended at this stage. As a work on the 3-valent approach, [39] proposed a tentative mapping between the 3-valent braids and Standard Model particles, with, however, the absence of dynamics. In the 4-valent approach, such a direct mapping, if not impossible, is at least still obscure. A reason is that the dynamics of 4-valent braids strongly constrains the possible set of twists, crossing sequence, and end-node states of an actively propagating or actively interacting braid. In addition, the closed form of this constraint is still missing. Consequently, one should not assign to a 4-valent braid any topological property just in order to make it a Standard Model particle. We need more study and maybe new mathematical tools to reveal whether the 4-valent braids can directly correspond to Standard Model particles.

In fact, braid excitations are more likely fundamental matter degrees of freedom whose low energy effective descriptions will correspond to the Standard Model particles. In any case, the issue is how mass will arise. Two possibilities are in order. First, a braid may acquire zero or nonzero mass from some of its intrinsic attributes. Second, mass is not well-defined at the level of spin networks but is emergent in the low energy effective action of the braid excitations, directly or via a breaking of certain emergent symmetry. The latter requires working out the effective action, which is our future work. As to the former, we have a hint. In the trivalent approach, [15, 90] conjectured that the mass of a capped braid should be constructed from topological invariants of the braid and is associated with the number of crossings of the braid. This has a problem: the number of crossings of a capped braid is not a topological invariant because all capped braids are equivalent to trivial braids without any crossing.

The situation in our 4-valent approach is more interesting, owing to the existence of both actively interacting and non-actively interacting braids. Actively interacting braids are equivalent to trivial braids too, whereas non-actively interacting ones are not. If we associate a braid's mass with its number of crossings, all actively interacting braids become massless, which seems consistent with their analogue with (gauge) bosons. On the other hand, although the number of crossings of an actively interacting braid is not invariant but representation dependent, its value in the unique representation of the braid is special, because it characterizes the CPT-multiplet the braid belongs to. As a result, this value cannot be the charge (which is already mapped to the braid's effective twists) or 3-momentum of the braid; however, it is possibly related to the energy of the braids in the multiplet in a way. Now that most non-actively interacting braids are not fully reducible, they may be massive.

The role of spin network labels

If our 4-valent braids are more fundamental than the Standard Model particles, then what do they correspond to, what do their interactions mean, and how do they eventually give rise to Standard Model particles? Nevertheless, our current understanding of 4-valent braids has not provided sufficient knowledge to give an answer. The realm of braids of spin networks is enormous, and a great deal of future work must be done.

For example, in our study we have yet not included spin network labels, which are normally representations of gauge groups, or of the quantum groups of the corresponding gauge groups. This may cause the misunderstanding that the properties of braids are independent of the spin network they live on. This is nevertheless not true. On the one hand, although that a braid is actively propagating and/or interacting depends on its topological setting, whether it can indeed propagate away from its location and/or interact with its adjacent braids depends on the structure of its neighborhood and hence of the whole spin network it is on. On the other hand, when spin network labels are taken into account, a braid becomes manifestly dependent of its spin network, with only its topological properties unchanged. Braids of the same topology but different set of spin network labels would be considered physically different, though maybe not different particles.

Since we mainly discuss framed spin networks whose edges are labeled by quantum groups, e.g., $SU_q(2)$, it will be interesting to see if we can incorporate the twists of edges into these labels,

in particular, into the label q.

Moreover, with spin network labels, a dynamical move, e.g., a $2 \rightarrow 3$ move, may have a superposition of outcomes in identical topological configuration but different set of spin network labels; each outcome has a certain probability amplitude. Nevertheless, the original set of topological quantities of a braid, which is essential for the braid to be actively propagating and/or interacting, is still valid even after spin network labels are considered. In Chapter 6, we also suggested that a braid's spin is associated with its spin network labels.

Other questions

Several other questions are as follows.

- Although we made an analogue between actively interacting braids and bosons, we are lack of a quantum statistics that can turn this analogue into an identification. In a low energy effective theory of the braids, there should be emergent spin statistics of the effective degrees of freedom; however, can we have such a statistics at the level of spin networks? Would there be anyonic braid states? We do not know the answers yet.

- In this thesis, the braid excitations naturally exist on embedded spin networks; however, the theory is lack of a mechanism to directly create a nontrivial 3-strand braid from a spin network state that is absent from any nontrivial topological structures, unless the 3-strand braid to be created is a trivial braid or a braid reducible to a trivial braid. We shall leave the discussion of a possible solution of this question to the next section, where we introduce our future work by using Group Field Theories.

- The number of relevant braid excitations, although strongly constrained by the braid dynamics, is still infinite; nevertheless, the number of elementary particles is small. Therefore, a natural question to ask is: does a selection rule exist to pick the right number of braid excitations to recover our known particle physics? We expect to see some new physics in our theory, along with recovering the known particles.

- That space-time is fundamentally discrete is one of our ansatz inspired by the area and volume operators, with a discrete spectrum, in Loop Quantum Gravity. Nevertheless, whether these area and volume operators are physical is still under discussion[94, 95]. On the one hand, these operators are not gauge invariant. On the other hand, the areas and volumes that we routinely measure are associated to spatial regions determined by matter[56, 96]. Loop Quantum Gravity was thought to be a theory of gravity only; hence, one may need to couple matter fields into the theory to write down a physical version of the area and volume operators. As we have shown, however, since matter degrees of freedom may be encoded in Loop Quantum Gravity as braid excitations of spin networks, the results of the thesis may shed new light on whether the area and volume operators in Loop Quantum Gravity are physical and what the physical version of these operators is.

8.2   Future directions

This thesis indicates the convergence of our work with other areas of Mathematical Physics such as Group Field Theory, Tensor Category, and so on. We expect to resolve the current issues in our approach and answer those open questions by reformulating our approach in one or more of these frameworks of Mathematical Physics. In below, we shall sketch our plan and work in progress.

Group Field Theories with braids

Group Field Theories[1] consider d-dimensional simplicies the fundamental building blocks of $(d + 1)$-dimensional space-time and treat them as fields whose variables are elements in the group defining the simplicies. That is, a Group Field Theory is a local, covariant quantum field theory of "universes" in terms of the fields associated with the fundamental building blocks. It would produce a transition amplitude between quantum "universes" by summing over the Feynman diagrams of this transition, i.e., summing over all triangulations and topologies as the histories built from the evolution of the fundamental d-simplicies. These Feynman diagrams can also be viewed as spin networks and dual to $(d + 1)$-simplicies. Group Field Theories do not even need to assume a space-time topology, unlike Loop Quantum Gravity and most Spin Foam models, and realize a larger background independence. Group Field Theories encompass most of the other approaches to non-perturbative quantum gravity, such as Loop Quantum Gravity and Spin Foam models, provide a link between them, and go beyond the limitations of them[100].

In Group Field Theories, spin networks are purely combinatoric and unembedded. Nevertheless, to reformulate our approach of braid excitations of embedded spin networks as a Group Field Theory, one may enlarge the configuration space of certain $(3 + 1)$ Group Field Theory by adding to its fundamental field extra group variables that characterize the 3-strand braids.

An even simpler strategy is to construct a composite group field for a braid out of a pair of fundamental group fields by identifying the group variables of these two fields in a braided way, and then integrate out the fundamental fields to obtain an effective theory of the composite field in certain background given by the fundamental fields. This is similar to constructing theories of collective modes in condensed matter physics.

Either way combines spin network labels automatically and is expected to result in a low energy effective theory of braid excitations in a background space-time, which may recover the known physics and produce more. The former seems more fundamental and should be able to solve the issue that nontrivial braids cannot be created from spin networks free of braids. The latter is what we are currently taking. In our work in progress[102], we construct a toy Group Field Theory with only trivial braids defined in Eq. 7.1, which are represented by composite fields built from fundamental fields. Surprisingly, we see that it is very likely to obtain a scalar ϕ^4 theory in a flat or

---

[1]The first Group Field Theory, known as the Boulatov model[97], originates as a generalization of Matrix Models of 2D gravity to 3D. As more Group Field Theory models in 3D and 4D coming out, they are realized as generating theories of Spin Foam models[98, 99]. Later, it is suggested that Group Field Theories are rather fundamental formulations of quantum gravity[100]. [101] presents an extensive review on the subject.

curved background if we can successfully integrate out the fundamental fields. The details are yet to be worked out.

As long as we have a meaningful effective theory of braid excitations, many open questions may be answered. These approaches, if successful, will bring us beyond Loop Quantum Gravity and Spin Foam Models.

Tensor Categorical methods

Tensor Category[103] appears to be another elegant and unified way to resolve many aforementioned issues once and for all. In particular, braided tensor categories with twists will be a suitable mathematical tool. In fact, the connection between LQG and Spin Foam Models and Tensor Categories has actually been realized for about two decades. It was first introduced by Crane[104] and elaborated by others, e.g., Kauffman[105]. One should also note that the string-net condensation due to Wen *et al*[106, 107] is an example that indicates that tensor category may be a proper underlying mathematical language toward a unification of gravity and matter. Same as the methods of Group Field Theory, a Tensor Category formulation of 4-valent braids would be purely algebraic, without any topological embedding, and is thus beyond the context of Loop Quantum Gravity too.

As explained in Section 6.3, a twist of a strand of a braid can be interpreted as characterizing a non-trivial isomorphism from $U(1)$ to $U(1)$. Nonetheless, the concept of twist can be generalized to vector spaces other than representation spaces of $U(1)$. This is the way how twists are defined in the language of tensor categories. In this manner, we may view spin network labels as if they represent generalized framing of spin networks other than the $U(1)$ framing we have just studied, such that generalized twists can arise. The consequence is our twists and spin network labels (the quantum group ones), as well as gauge symmetries and space-time symmetries, may be unified in this way.

Tensor categories naturally use isomorphisms between tensor products of vector spaces to account for braiding. This can be understood, for example, from the solutions of (Quantum) Yang-Baxter Equations. It is important, however, to note that our braids are special because each of them has two 4-valent end-nodes and two external edges. All these will exert further constraints on the possible tensor categories we can use, or motivate new types of tensor categories. Tensor-categorized 4-valent braids and evolution moves may be evaluated by the relevant techniques already defined in theories of tensor category or new techniques adapted to our case.

Other directions

The 4-valent approach can be advanced in other direction as well. Here, we give two examples. Firstly, we have shown that the set of stable braids has a rich algebraic structure given by braid interaction. In particular, the set of actively interacting braids form a noncommutative algebra under direct braid interaction. It is therefore possible to quantize the algebra of braids via the Gelfand-Naimark-Segal construction, which can establish a correspondence between representations of the algebra of braids and certain Hilbert space.

Secondly, [108] finds the speed of light[2] as a Lieb-Robinson bound[109] in models of a general theory of background independent quantum gravity based on graphs, namely Quantum Graphity[110, 111]. Our theory of braid excitations of spin networks can be viewed as a Quantum Graphity theory. Hence, one may borrow the idea and adopt the methods in [108] to study the Lieb-Robinson bound of braid propagation. An expectation is that actively interacting braids saturate the Lieb-Robinson bound of the system but non-actively interacting ones do not, such that they correspond to respectively massless and massive matter degrees of freedom.

8.3   Relation to Topological Quantum Computing

One should not be surprised to notice that our work described in this thesis is related to Topological Quantum Computing (TQC). TQC is a rapidly growing, fascinating research area, owing to its fault-tolerance. In fact, as aforementioned, being a concept rooted in Quantum Computing/Information and adapted to models of quantum gravity[7–9, 15], the notion of noiseless subsystems is a key underlying idea of this thesis. Furthermore, [8, 9] suggested that background independent quantum gravity is a quantum information processing system. On the other hand, in [10, 11, 112] topological quantum phase transitions have been shown giving rise to emergent gauge and (linearized) gravitational degrees of freedom. Therefore, it is interesting to study TQC from the viewpoint of a quantum gravitist and to see if TQC sheds any light on the development of quantum gravity.

The key entities in TQC are non-Abelian Anyons, quasi-particles as representations of braid groups. An obvious, though maybe superficial, connection between TQC and the work described in this thesis is the presence of braids and their algebra in both disciplines. A major difference is that our braid excitations are topological structures of embedded 4-valent spin networks, such that each braid has three strands and two end-nodes. Each end-node takes the three strands of the braid to an external strand connecting with the rest of the spin network. We observe that an end-node of a braid may be related to a fusion rule or thought as a quantum gate in TQC. An interesting phenomenon of the braids is that they can interact, namely in some cases two braids can merge into a new braid or scatter into two different braids and one braid can decay into two braids. Both additive and multiplicative conserved quantities exist under braid interactions. If this new feature was introduced to TQC, it would tells us how two quantum processes can join, how one quantum process can split, and when two sequences of quantum processes can be equivalent.

On the other hand, new results may be found by looking at the results in quantum gravity from the viewpoint of TQC or vise versa. For example, what do the twists of the strands of our braids mean in TQC? Moreover, findings in TQC may help to decode more information in our braid dynamics. For instance, what are the physical meanings of the conserved quantities of braids, and does a braid have other conserved quantities that may bring our braids closer to matter particles?

A limitation for now is that the 3-strand braids, apart from their end-nodes, are elements of the braid group B_3. This means they can only handle the action of the braid algebra of B_3 on three

---

[2]This is understood as the maximum speed, at which information can propagate in a system.

particles in TQC. Nonetheless, one can study more complex structures of the embedded 4-valent spin networks, or directly investigate higher-strand braids of higher-valent spin networks.

As mentioned before, a future direction of our work on emergent matter is to employ tensor categories. In particular, tangle and braided ribbon categories are mathematical tools that may be used to make an elegant reformulation of the whole approach. It is known that TQC is naturally described in the language of tensor category[113, 114]. This implies another possible joining of our work and TQC.

Appendix A

$2\pi/3$ and π Rotations

A.1 $2\pi/3$-Rotations

Two consecutive $\pi/3$ rotations certainly give rise to a $2\pi/3$ rotation. Nevertheless, it is intuitive to understand $2\pi/3$ rotations in a more topological way. Obviously, rotating a tetrahedron by $2\pi/3$ with respect to the normal of any of the four faces of the tetrahedron does not change the view of it. Therefore, by the local duality between a node and a tetrahedron, as long as an edge of a node is chosen, the other three edges of the node are on an equal footing. If we rotate a node with respect to any of its four edges by $2\pi/3$, the resulting diagram should be diffeomorphic to, or in our context equivalent to, the original one. In Fig. A.1 and Fig. A.2 we list all the $2\pi/3$-rotations.
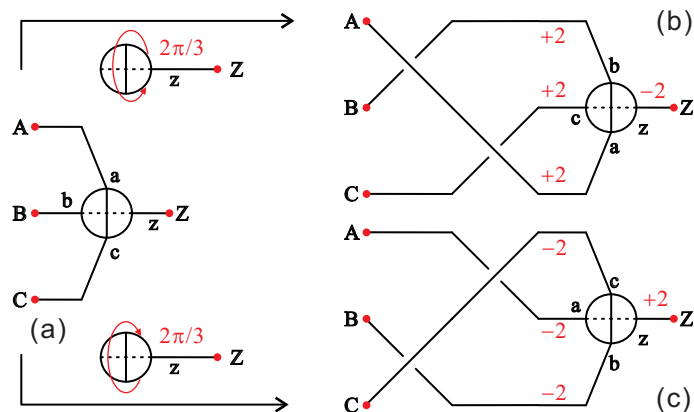
Figure A.1: (b) & (c) are results of (a) by rotating the $\oplus$-node in (a) w.r.t. edge z in two directions respectively. Points A, B, C, and Z are assumed to be connected somewhere else and are kept fixed during the rotation. All edges of the node gain the same amount of twist after rotation.

Each of such rotations generate two crossings and twists on all four edges. The twist number on the rotation axis of a node is always opposite to that of the other three edges of the node. Note that a $2\pi/3$ rotation does not change the state of a node with respect to the rotation axis, i.e., if a
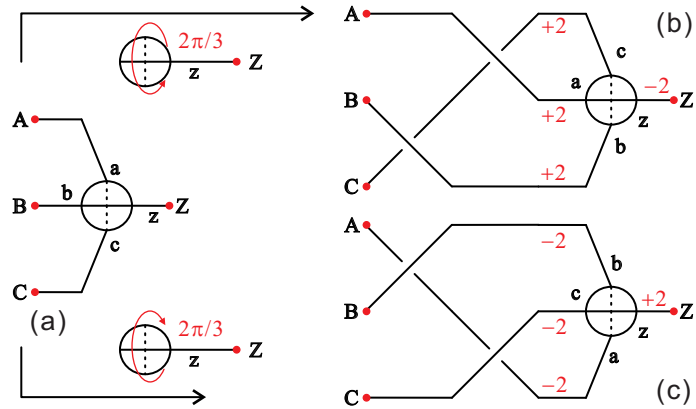
Figure A.2: (b) & (c) are results of (a) by rotating the $\ominus$-node in (a) w.r.t. edge z in two directions respectively. Points A, B, C, and Z are assumed to be connected somewhere else and are kept fixed during the rotation. All edges of the node gain the same amount of twist after rotation.

node is in state $\oplus$ with respect to z before the rotation, it is still a $\oplus$-node after the rotation.

A.2 π-Rotations

The $\pi/3$ and $2\pi/3$ rotations can be used to construct larger rotations, for example the π rotations, which also certainly do not change the diffeomorphism class a projection belongs to. For the convenience of future use, we depict these four possible rotations in Fig. A.3 and Fig. A.4.
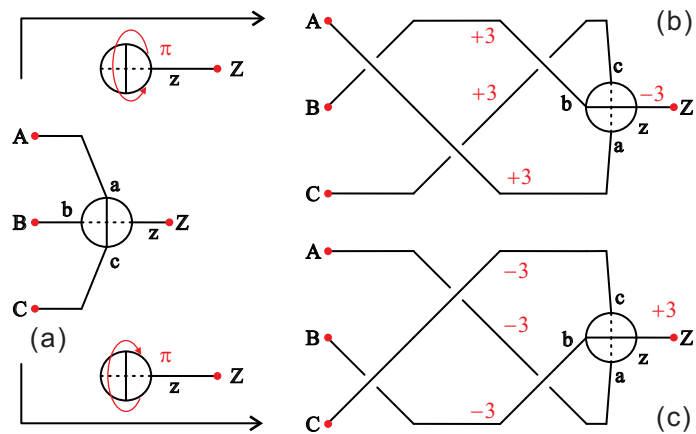
Figure A.3: (b) & (c) are results of (a) by rotating the $\oplus$-node in (a) w.r.t. edge z in two directions respectively. Points A, B, C, and Z are assumed to be connected somewhere else and are kept fixed during the rotation. All edges of the node gain the same amount of twist after the rotation.
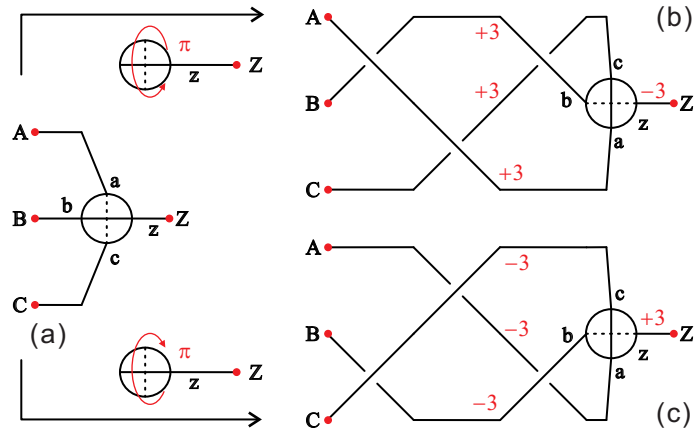
Figure A.4: (b) & (c) are results of (a) by rotating the ⊖-node in (a) w.r.t. edge z in two directions respectively. Points A, B, C, and Z are assumed to be connected somewhere else and are kept fixed during the rotation. All edges of the node gain the same amount of twist after the rotation.

Note that a π rotation changes the state of a node, i.e., if a node is in state $\oplus$ with respect to its rotation axis before the rotation, it becomes a ⊖-node with respect to the same axis after the rotation.

Appendix B

Classification of 3-Strand Braid diagrams

In this appendix, we classify 3-strand braid diagrams according to the properties of their end-nodes and crossing patterns. For a better illustration, we do not use conventional symbolic notation of ordinary 3-strand braid diagrams for crossing patterns; rather we invent a new notation for our 3-strand braid diagrams. This new notation is used in this appendix exclusively. The results, however, are used throughout the thesis, starting from Section 2.4. To classify our braid diagrams, we study them as if they are isolated regions in a graph. We also ignore all the twists because this classification does not depend on them. Hence, this classification applies to braids of unframed spin networks too.

Definition B.1. *A braid diagram is called **reducible**, if it is equivalent to a braid diagram with fewer crossings; otherwise, it is **irreducible**.*

The braid on the top part of Fig. 2.10 is an example of a reducible braid, whereas the one at the bottom of the figure is an irreducible braid. To classify the braid diagrams in a convenient way, we need a new notation and some auxiliary definitions. Since we have a way of assigning crossings integers $+1$ or -1, as in Fig. 2.5, we can use $2 \times N$ matrices with two end-nodes in either state $\oplus$ or $\ominus$ to denote a 3-strand braid with N crossings, as shown in Fig. B.1 and its caption, keeping in mind that the state of an end-node is and can only be with respect to its external edge. For calculational purposes, it is also convenient to associate crossings with one of the two end-nodes of a braid. For example, in Fig. B.1 the left end-node with its nearest crossing can be denoted by $\oplus \begin{pmatrix} -1 \\ 0 \end{pmatrix}$, and the right end-node with its nearest two crossings can be written as $\begin{pmatrix} 0 & 0 \\ +1 & +1 \end{pmatrix} \ominus$, which has $\begin{pmatrix} 0 \\ +1 \end{pmatrix} \ominus$ as its 1-crossing **sub end-node**. End-nodes represented in this way are called 1-crossing end-nodes, 2-crossing end-nodes, etc. An end-node without any crossing is termed a **bare end-node**.

A braid can be decomposed into or recombined from a left end-node, a right end-node, and a sequence of crossings represented by matrices. For instance,

$$\oplus \begin{pmatrix} -1 & 0 & -1 \\ 0 & +1 & 0 \end{pmatrix} \oplus \Longleftrightarrow \oplus \begin{pmatrix} -1 \\ 0 \end{pmatrix} + \begin{pmatrix} +1 \\ 0 \end{pmatrix} + \begin{pmatrix} -1 & 0 & -1 \\ 0 & +1 & 0 \end{pmatrix} \oplus,$$

122

where the "+" between two matrices on the RHS means direct sum or concatenation of two pieces of braids. One can see from the above equation that the first two crossings or the second and third crossings on the RHS are canceled. Given this, we have the following definition.

Definition B.2. *An N-crossing end-node is said to be a **reducible end-node**, if it is equivalent to a M-crossing end-node with M < N, by equivalence moves done on the node; otherwise, it is irreducible.*

The definition above gives rise to another definition of reducible braid diagram, which is equivalent to Definition B.1.

Definition B.3. *A braid diagram is said to be **reducible** if it has a reducible end-node. If a braid has a reducible left or right end-node, or both, it is called **left-**, or **right-,** or **two-way-reducible.***

For consistency we may also symbolize the rotation moves. Because rotations are exerted only on the end-nodes of a braid, we can denote all possible moves by rotation operators R_{LL}^{θ}, R_{LR}^{θ}, R_{RL}^{θ}, and R_{RR}^{θ}, where the superscript θ is the angle of rotation, the first subscript L (R) reads that the operation is on the left (right) end-node of a braid, and the second subscript L (R) indicates that the direction of rotation is left- (right-) handed. The left- (right-) handedness of the rotation is defined in such a way that if you grab the rotation axis of a node in your left (right) hand, with the thumb pointing to the node, your hand wraps up in the direction of rotation. Figs. 2.8, 2.9, and A.1 through A.4 present the results of the rotation operators. Here we show an example of the algebra in the following equation.

$$
R_{RR}^{\pi/3} \left[\oplus \begin{pmatrix} -1 & 0 & 0 \\ 0 & +1 & +1 \end{pmatrix} \ominus \right]
$$

$$
= \oplus \begin{pmatrix} -1 & 0 & 0 \\ 0 & +1 & +1 \end{pmatrix} R_{RR}^{\pi/3} (\ominus)
$$

$$
= \oplus \begin{pmatrix} -1 & 0 & 0 \\ 0 & +1 & +1 \end{pmatrix} + \begin{pmatrix} -1 \\ 0 \end{pmatrix} \oplus
$$

$$
= \oplus \begin{pmatrix} -1 & 0 & 0 & -1 \\ 0 & +1 & +1 & 0 \end{pmatrix} \oplus .
$$

Because a braid diagram can be reduced only from its end-nodes, we first classify the (ir)reducible end-nodes. We start from 1-crossing end-nodes; all the possible ones are listed in table B.1.

The following equations then show how all the reducible 1-crossing end-nodes are reduced to
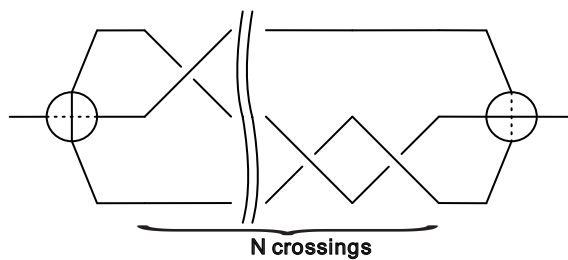
Figure B.1: This braid can be represented by $\oplus \begin{pmatrix} -1 & \cdots & \cdots & 0 & 0 \\ 0 & \cdots & \cdots & +1 & +1 \end{pmatrix} \ominus$.

Left end-nodes		Right end-nodes
$\oplus \begin{pmatrix} \pm 1 \\ 0 \end{pmatrix}$		$\begin{pmatrix} \pm 1 \\ 0 \end{pmatrix} \oplus$
$\oplus \begin{pmatrix} 0 \\ \pm 1 \end{pmatrix}$		$\begin{pmatrix} 0 \\ \pm 1 \end{pmatrix} \oplus$
$\ominus \begin{pmatrix} \pm 1 \\ 0 \end{pmatrix}$		$\begin{pmatrix} \pm 1 \\ 0 \end{pmatrix} \ominus$
$\ominus \begin{pmatrix} 0 \\ \pm 1 \end{pmatrix}$		$\begin{pmatrix} 0 \\ \pm 1 \end{pmatrix} \ominus$

Table B.1: Table of all possible 1-crossing end-nodes.

bare nodes.

$$R_{LR}^{\pi/3}\left[\oplus\begin{pmatrix}+1\\0\end{pmatrix}\right]=\ominus\begin{pmatrix}-1\\0\end{pmatrix}+\begin{pmatrix}+1\\0\end{pmatrix}=\ominus\begin{pmatrix}0\\0\end{pmatrix} \tag{B.1}$$

$$R_{LL}^{\pi/3}\left[\oplus\begin{pmatrix}0\\-1\end{pmatrix}\right]=\ominus\begin{pmatrix}0\\+1\end{pmatrix}+\begin{pmatrix}0\\-1\end{pmatrix}=\ominus\begin{pmatrix}0\\0\end{pmatrix}$$

$$R_{LL}^{\pi/3}\left[\ominus\begin{pmatrix}-1\\0\end{pmatrix}\right]=\oplus\begin{pmatrix}+1\\0\end{pmatrix}+\begin{pmatrix}-1\\0\end{pmatrix}=\oplus\begin{pmatrix}0\\0\end{pmatrix}$$

$$R_{LR}^{\pi/3}\left[\ominus\begin{pmatrix}0\\+1\end{pmatrix}\right]=\oplus\begin{pmatrix}0\\-1\end{pmatrix}+\begin{pmatrix}0\\+1\end{pmatrix}=\oplus\begin{pmatrix}0\\0\end{pmatrix}$$

$$R_{RL}^{\pi/3}\left[\begin{pmatrix}-1\\0\end{pmatrix}\oplus\right]=\begin{pmatrix}-1\\0\end{pmatrix}+\begin{pmatrix}+1\\0\end{pmatrix}\ominus=\begin{pmatrix}0\\0\end{pmatrix}\ominus$$

$$R_{RR}^{\pi/3}\left[\begin{pmatrix}0\\+1\end{pmatrix}\oplus\right]=\begin{pmatrix}0\\+1\end{pmatrix}+\begin{pmatrix}0\\-1\end{pmatrix}\ominus=\begin{pmatrix}0\\0\end{pmatrix}\ominus$$

$$R_{RR}^{\pi/3}\left[\begin{pmatrix}+1\\0\end{pmatrix}\ominus\right]=\begin{pmatrix}+1\\0\end{pmatrix}+\begin{pmatrix}-1\\0\end{pmatrix}\oplus=\begin{pmatrix}0\\0\end{pmatrix}\oplus$$

$$R_{RL}^{\pi/3}\left[\begin{pmatrix}0\\-1\end{pmatrix}\ominus\right]=\begin{pmatrix}0\\-1\end{pmatrix}+\begin{pmatrix}0\\+1\end{pmatrix}\oplus=\begin{pmatrix}0\\0\end{pmatrix}\oplus$$

With the help of the above calculations, we can easily list all the irreducible 1-crossing end-nodes in table B.2.

Left end-nodes		Right end-nodes
$\oplus\begin{pmatrix}-1\\0\end{pmatrix}$		$\begin{pmatrix}+1\\0\end{pmatrix}\oplus$
$\oplus\begin{pmatrix}0\\+1\end{pmatrix}$		$\begin{pmatrix}0\\-1\end{pmatrix}\oplus$
$\ominus\begin{pmatrix}+1\\0\end{pmatrix}$		$\begin{pmatrix}-1\\0\end{pmatrix}\ominus$
$\ominus\begin{pmatrix}0\\-1\end{pmatrix}$		$\begin{pmatrix}0\\+1\end{pmatrix}\ominus$

Table B.2: Table of irreducible 1-crossing end-nodes.

Now we consider 2-crossing end-nodes, forty-eight of them in total, including left and right end-nodes. To find all the irreducible 2-crossing end-nodes, we need only to think about those whose sub 1-crossing nodes are irreducible, since otherwise a 2-crossing end-node is already reducible; this excludes 24 2-crossing end-nodes. If a 2-crossing node has an irreducible sub 1-crossing node, its crossings can definitely not be reduced by $2\pi/3$-rotations, because a $2\pi/3$-rotation is made of two consecutive $\pi/3$-rotations that do not reduce any irreducible 1-crossing

125

node, and it does not flip the state of a bare node. Interestingly, however, a 2-crossing end-node with an irreducible sub 1-crossing end-node may still be reduced to an irreducible 1-crossing end-node by π-rotations, which can be seen from the following equations.

$$R_{LL}^{\pi}\left[\oplus\begin{pmatrix} -1 & 0 \\ 0 & -1 \end{pmatrix}\right] = \ominus\begin{pmatrix} +1 & 0 & +1 \\ 0 & +1 & 0 \end{pmatrix} + \begin{pmatrix} -1 & 0 \\ 0 & -1 \end{pmatrix} = \ominus\begin{pmatrix} +1 \\ 0 \end{pmatrix} \tag{B.2}$$

$$R_{LR}^{\pi}\left[\oplus\begin{pmatrix} 0 & +1 \\ +1 & 0 \end{pmatrix}\right] = \ominus\begin{pmatrix} 0 & -1 & 0 \\ -1 & 0 & -1 \end{pmatrix} + \begin{pmatrix} 0 & +1 \\ +1 & 0 \end{pmatrix} = \ominus\begin{pmatrix} 0 \\ -1 \end{pmatrix}$$

$$R_{LR}^{\pi}\left[\ominus\begin{pmatrix} +1 & 0 \\ 0 & +1 \end{pmatrix}\right] = \oplus\begin{pmatrix} -1 & 0 & -1 \\ 0 & -1 & 0 \end{pmatrix} + \begin{pmatrix} +1 & 0 \\ 0 & +1 \end{pmatrix} = \oplus\begin{pmatrix} -1 \\ 0 \end{pmatrix}$$

$$R_{LL}^{\pi}\left[\ominus\begin{pmatrix} 0 & -1 \\ -1 & 0 \end{pmatrix}\right] = \oplus\begin{pmatrix} 0 & +1 & 0 \\ +1 & 0 & +1 \end{pmatrix} + \begin{pmatrix} 0 & -1 \\ -1 & 0 \end{pmatrix} = \oplus\begin{pmatrix} 0 \\ +1 \end{pmatrix}$$

$$R_{RR}^{\pi}\left[\begin{pmatrix} 0 & +1 \\ +1 & 0 \end{pmatrix}\oplus\right] = \begin{pmatrix} 0 & +1 \\ +1 & 0 \end{pmatrix} + \begin{pmatrix} -1 & 0 & -1 \\ 0 & -1 & 0 \end{pmatrix}\ominus = \begin{pmatrix} -1 \\ 0 \end{pmatrix}\ominus$$

$$R_{RL}^{\pi}\left[\begin{pmatrix} -1 & 0 \\ 0 & -1 \end{pmatrix}\oplus\right] = \begin{pmatrix} -1 & 0 \\ 0 & -1 \end{pmatrix} + \begin{pmatrix} 0 & +1 & 0 \\ +1 & 0 & +1 \end{pmatrix}\ominus = \begin{pmatrix} 0 \\ +1 \end{pmatrix}\ominus$$

$$R_{LL}^{\pi}\left[\begin{pmatrix} 0 & -1 \\ -1 & 0 \end{pmatrix}\ominus\right] = \begin{pmatrix} 0 & -1 \\ -1 & 0 \end{pmatrix} + \begin{pmatrix} +1 & 0 & +1 \\ 0 & +1 & 0 \end{pmatrix}\oplus = \begin{pmatrix} +1 \\ 0 \end{pmatrix}\oplus$$

$$R_{LR}^{\pi}\left[\begin{pmatrix} +1 & 0 \\ 0 & +1 \end{pmatrix}\ominus\right] = \begin{pmatrix} +1 & 0 \\ 0 & +1 \end{pmatrix} + \begin{pmatrix} 0 & -1 & 0 \\ -1 & 0 & -1 \end{pmatrix}\oplus = \begin{pmatrix} 0 \\ -1 \end{pmatrix}\oplus$$

Consequently, we can list all the irreducible 2-crossing end-nodes in table B.3

Left end-nodes			Right end-nodes	
$\oplus\begin{pmatrix} -1 & 0 \\ 0 & +1 \end{pmatrix}$	$\oplus\begin{pmatrix} -1 & -1 \\ 0 & 0 \end{pmatrix}$		$\begin{pmatrix} 0 & +1 \\ -1 & 0 \end{pmatrix}\oplus$	$\begin{pmatrix} +1 & +1 \\ 0 & 0 \end{pmatrix}\oplus$
$\oplus\begin{pmatrix} 0 & -1 \\ +1 & 0 \end{pmatrix}$	$\oplus\begin{pmatrix} 0 & 0 \\ +1 & +1 \end{pmatrix}$		$\begin{pmatrix} +1 & 0 \\ 0 & -1 \end{pmatrix}\oplus$	$\begin{pmatrix} 0 & 0 \\ -1 & -1 \end{pmatrix}\oplus$
$\ominus\begin{pmatrix} +1 & 0 \\ 0 & -1 \end{pmatrix}$	$\ominus\begin{pmatrix} +1 & +1 \\ 0 & 0 \end{pmatrix}$		$\begin{pmatrix} 0 & -1 \\ +1 & 0 \end{pmatrix}\ominus$	$\begin{pmatrix} -1 & -1 \\ 0 & 0 \end{pmatrix}\ominus$
$\ominus\begin{pmatrix} 0 & +1 \\ -1 & 0 \end{pmatrix}$	$\ominus\begin{pmatrix} 0 & 0 \\ -1 & -1 \end{pmatrix}$		$\begin{pmatrix} -1 & 0 \\ 0 & +1 \end{pmatrix}\ominus$	$\begin{pmatrix} 0 & 0 \\ +1 & +1 \end{pmatrix}\ominus$

Table B.3: Table of irreducible 2-crossing end-nodes.

The following theorem states that it is unnecessary to investigate end-nodes with more crossings to see if they are irreducible.

Theorem B.1. *An N-crossing end-node, N > 2, which has an irreducible 2-crossing sub end-node, is irreducible.*

Proof. If the *N*-crossing end-node has a irreducible 2-crossing sub end-node, the two crossings nearest to the node are not reducible by either a single $\pi/3$- or a single $2\pi/3$-rotation on the node. We may consider π-rotations on its 3-crossing sub end-node. Nevertheless, if a 3-crossing end-node is reducible by a π-rotation, it must contain a reducible 2-crossing sub end-node according to Fig. A.3, Fig. A.4 and Eq. B.2, which is contradictory to the condition given in the theorem. Hence, this is true for all cases where $N > 3$ by simple induction. Therefore, the theorem holds. $\square$

Equipped with the knowledge of (ir)reducible end-nodes, we are ready to classify braids. The two end-nodes of a braid are either in the same states or in opposite states, we first look at braids whose end nodes are in the same states.

Theorem B.2. *All N-crossing braid diagrams in the form* $\oplus \begin{pmatrix} \cdots \\ \cdots \end{pmatrix} \oplus$ *and* $\ominus \begin{pmatrix} \cdots \\ \cdots \end{pmatrix} \ominus$ *are reducible for $N \le 3$.*

Proof. It suffices to prove the $\oplus\oplus$ case, the case of $\ominus\ominus$ follows similarly or by symmetry.

1) $N = 1$. Only four possibilities exist, namely $\oplus \begin{pmatrix} \pm 1 \\ 0 \end{pmatrix} \oplus$ and $\oplus \begin{pmatrix} 0 \\ \pm 1 \end{pmatrix} \oplus$; however, they are all reducible because they all contain one reducible 1-crossing end-node according to Eq. B.1.

2) $N = 2$. We first consider the braids formed by an irreducible 2-crossing end-node $\oplus_{irred}$ (2-crossing) or (2-crossing) $\oplus_{irred}$, and a bare end-node $\oplus_b$. We do the following decomposition

$$\oplus_{irred} (2\text{-crossing}) + \oplus_b = \oplus_{irred} (2\text{-crossing}) \oplus_b = \oplus_{irred} + (2\text{-crossing}) \oplus_b$$
$$\oplus_b + (2\text{-crossing}) \oplus_{irred} = \oplus_b (2\text{-crossing}) \oplus_{irred} = \oplus_b (2\text{-crossing}) + \oplus_{irred}.$$

Then from table B.3, it is readily seen that (2-crossing) $\oplus_b$ and $\oplus_b$ (2-crossing) are always reducible end-nodes for any choice of $\oplus_{irred}$ (2-crossing) and (2-crossing) $\oplus_{irred}$ respectively. That is, the braids formed this way are reducible. We then consider braids formed by two irreducible 1-crossing end-nodes. The first two rows in table B.2 and Eq. B.2 clearly shows that the result is either a trivial braid or one with a reducible 2-crossing end-node.

3) $N = 3$. We need only consider braid diagrams, each of which is formed by the direct sum of a 2-crossing irreducible end-node and a 1-crossing irreducible end-node. This can be done by taking the direct sum between the (right) left end-nodes in the first two rows of table B.2, and the (left) right end-nodes in the first two rows of table B.3. One can see that any resultant braid diagram has merely two possible forms: i) two neighboring crossings are canceled by the direct sum, which leads to 1-crossing braids that are proven to be reducible in the case of $N = 1$; and ii) a crossing in the irreducible 2-crossing end-node is combined with the irreducible 1-crossing end-node to form a reducible 2-crossing end-node, i.e., the braid is reducible. $\square$

Theorem B.2 does not cover the case where $N \ge 4$, which will be included in another theorem soon. Before that, let us consider the braids whose end-nodes are in opposite states.

Case B.1. *N-crossing braids in the form* $\oplus \begin{pmatrix} \cdots \\ \cdots \end{pmatrix} \ominus$ *and* $\ominus \begin{pmatrix} \cdots \\ \cdots \end{pmatrix} \oplus$, *for $N \le 3$. Note that according to TheoremB.2, the set of irreducible 1-crossing braid diagrams to be found here represents the full set of irreducible braids for $N \le 3$, regardless of the states of the end-nodes.*

1. $N = 1$. An irreducible braid diagram can consist of only an irreducible 1-crossing end-node and a bare node. From table B.2, we have only four options, which are indeed all irreducible; they are now listed in table B.4.

$$\oplus \begin{pmatrix} -1 \\ 0 \end{pmatrix} \ominus \qquad \ominus \begin{pmatrix} +1 \\ 0 \end{pmatrix} \oplus$$

$$\oplus \begin{pmatrix} 0 \\ +1 \end{pmatrix} \ominus \qquad \ominus \begin{pmatrix} 0 \\ -1 \end{pmatrix} \oplus$$

Table B.4: Table of irreducible 1-crossing braids.

2. $N = 2$. It is sufficient to consider the braids formed by an irreducible 2-crossing end-node and a bare end-node in the opposite state. The reason is that if a 2-crossing braid is irreducible, its two 2-crossing end-nodes must be irreducible as well; moreover, if a 2-crossing end-node is irreducible, its 1-crossing sub end-node is already irreducible. Therefore, one can simply add to each irreducible end-node in table B.3 a bare end-node in the opposite state to create an irreducible 2-crossing braid. Being a bit redundant, we list all the 16 irreducible 2-crossing braid diagrams in table B.5.

$$\oplus \begin{pmatrix} -1 & 0 \\ 0 & +1 \end{pmatrix} \ominus \quad \oplus \begin{pmatrix} -1 & -1 \\ 0 & 0 \end{pmatrix} \ominus \qquad \ominus \begin{pmatrix} 0 & +1 \\ -1 & 0 \end{pmatrix} \oplus \quad \ominus \begin{pmatrix} +1 & +1 \\ 0 & 0 \end{pmatrix} \oplus$$

$$\oplus \begin{pmatrix} 0 & -1 \\ +1 & 0 \end{pmatrix} \ominus \quad \oplus \begin{pmatrix} 0 & 0 \\ +1 & +1 \end{pmatrix} \ominus \qquad \ominus \begin{pmatrix} +1 & 0 \\ 0 & -1 \end{pmatrix} \oplus \quad \ominus \begin{pmatrix} 0 & 0 \\ -1 & -1 \end{pmatrix} \oplus$$

$$\ominus \begin{pmatrix} +1 & 0 \\ 0 & -1 \end{pmatrix} \oplus \quad \ominus \begin{pmatrix} +1 & +1 \\ 0 & 0 \end{pmatrix} \oplus \qquad \oplus \begin{pmatrix} 0 & -1 \\ +1 & 0 \end{pmatrix} \ominus \quad \oplus \begin{pmatrix} -1 & -1 \\ 0 & 0 \end{pmatrix} \ominus$$

$$\ominus \begin{pmatrix} 0 & +1 \\ -1 & 0 \end{pmatrix} \oplus \quad \ominus \begin{pmatrix} 0 & 0 \\ -1 & -1 \end{pmatrix} \oplus \qquad \oplus \begin{pmatrix} -1 & 0 \\ 0 & +1 \end{pmatrix} \ominus \quad \oplus \begin{pmatrix} 0 & 0 \\ +1 & +1 \end{pmatrix} \ominus$$

Table B.5: Table of irreducible 2-crossing braid diagrams.

3. $N = 3$. A 3-crossing braid diagram in this case is irreducible if and only if it admits the following two decompositions.

An irreducible 1-crossing end-node + An irreducible 2-crossing end-node

An irreducible 2-crossing end-node + An irreducible 1-crossing end-node,

where "+" is understood as the direct sum. The proof of this claim follows immediately from Theorem B.1.

It is time to summarize the case of $N \geq 4$ for N-crossing braid diagrams, regardless of the states of the end-nodes, by the following theorem.

Theorem B.3. *Let $N \geq 4$ and let B be an N-crossing braid diagram that has the minimal number of crossings possible using just the braid relations. Then B is irreducible if and only if it admits a decomposition:*

An irreducible 2-crossing end-node

+ Arbitrary sequence of crossings

+ An irreducible 2-crossing end-node,

where "+" is understood as the direct sum.

Proof. An irreducible 2-crossing end-node contains an irreducible 1-crossing end-node. By theorem B.1, if the above decomposition is admitted, the braid is not reducible on either end-node whatever the arbitrary sequence of crossings is up to the constraint. Therefore, the theorem holds. □

The braids that are interesting to us are those reducible ones, as seen in Chapter 3. Thus, we may make more detailed divisions in the type of reducible braids by the definition below.

Definition B.4. *Given a reducible braid diagram B, a braid diagram B′ obtained from B by doing as much reduction as possible is called an* **extremum** *of B; B may have more than one* **extrema***, but all the extrema have the same number of crossings. We then have the following.*

1. *If all extrema of B are trivial braid diagrams, i.e., braids without crossings, B is said to be* **completely reducible.**

2. *if an extremum of B can be reached by equivalence moves exerted only on its (left)right end-node, B is called* **extremely (left-)right-reducible;** *if B is also completely reducible, B is then said to be* **completely (left-)right-reducible.** *Note that completely (left-) right-reducible implies extremely (left-) right-reducible, but not vice versa in general.*

Appendix C

Active Propagation of Braids

Due to Conditions 2.1 and 2.2, we found that putting braids in their unique representations is most convenient to studying their dynamics by the graphic calculus we developed in the previous chapter. As a result, we stick to the unique representation in this chapter. That is, we study braids by their braid diagrams without external twists.

C.1 Definition of active propagation

We study here a simple example of propagation as follows. A braid is inserted in an edge of a graph as in Fig. C.1. We see a node to the right of the braid, with two structures growing out of it. By a series of local moves, the braid moves so that these structures are now attached to a node to the left of the braid, while the braid remains unchanged up to internal twists.

In more detail, an **active right-propagation** of a braid B involves its changing places through a series of evolution moves with a structure A on its right, which is composed of two sub-spinnets, S and S', which are connected by a node Y but not any other edge, as shown in Fig. C.1. S and S' are supposed not connected to elsewhere in the spin network. The right end-node X of the braid and node Y have one and only one common edge.

Begin with an initial condition as shown in Fig. C.1(a).

1. Make a $2 \rightarrow 3$ move on nodes X and Y if the move is legal (See Condition 2.1. The result is shown in Fig. C.1(b).

2. Translate nodes 2 and 3 together with their common edge g to the left, passing all crossings. This may not be possible because a tangle between edge g and any of the edges a, b, and c occur (see Fig. C.2).

3. Re-arrange nodes 1, 2, and 3 and their edges, by equivalence moves (e.g., rotations), into a proper configuration ready for a $3 \rightarrow 2$ move (see Condition 2.2).

4. Do the $3 \rightarrow 2$ move on nodes 1, 2, and 3; leading to Fig. C.1(c), in which the braid B and the structure A are both recovered but the braid B is now on the right of structure A.
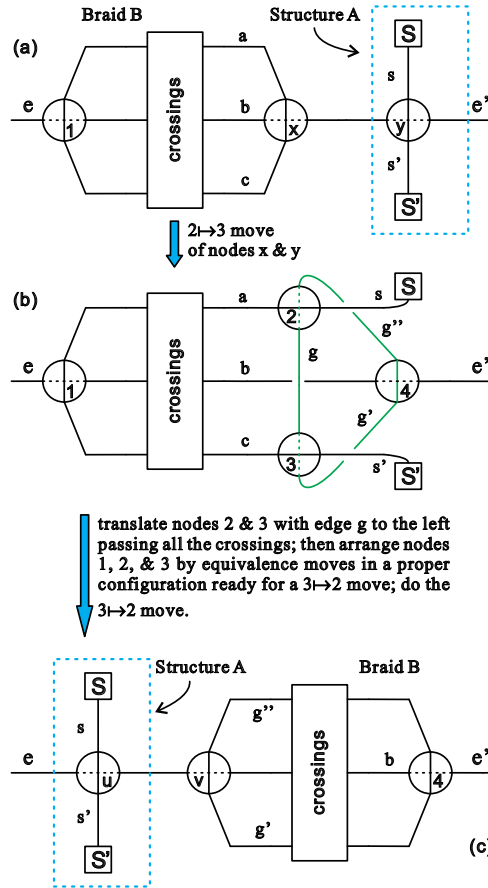
Figure C.1: Definition of right interaction. (a) shows a braid *B* on the left of an arbitrary structure *A*, composed of two sub-spinnets *S* & *S'* connected via a node *Y*. (b) is obtained from (a) by the $2 \to 3$ move on nodes *X* and *Y*. (c) is the result of the propagation, in which braid *B* and structure *A* switched positions.

We remark a potential issue in this setting. In above, we require that the sub-spinnets *S* and *S'* in Fig. C.1 are not directly connected and are not connected elsewhere; however, if our spin networks under study are closed networks, this requirement is impossible as each node is 4-valent unless one allows the *S* and *S'* to have nodes of mixed-valence, e.g., trivalent and 4-valent. A possible resolution to this issue is to allow *S* and *S'* to be open, whose free edges are subject to certain constraints. We would like to leave further study of the constraints, perhaps certain boundary conditions, and any potential problems to future work.

A **left-propagation** is defined similarly in that the unknown structure in a dashed blue square in Fig. (a) is initially on the left of the braid. A braid that can actively propagate is called actively propagating.

In fact, most braids do not actively propagate because their structures do not let them going through step 2 and/or 3 in Definition C.1. Braids that do not propagate actively are named non-
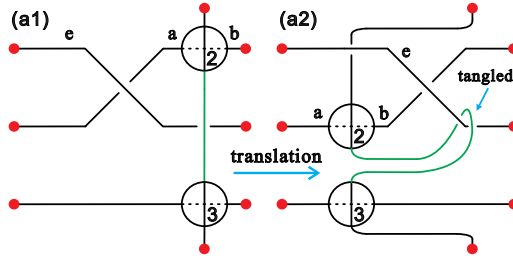
Figure C.2: (a2) is obtained from (a1) by translating nodes 2, 3, and their common edge to the left, passing the crossing. A tangle occurs between the edge e and the common edge of nodes 2 and 3.
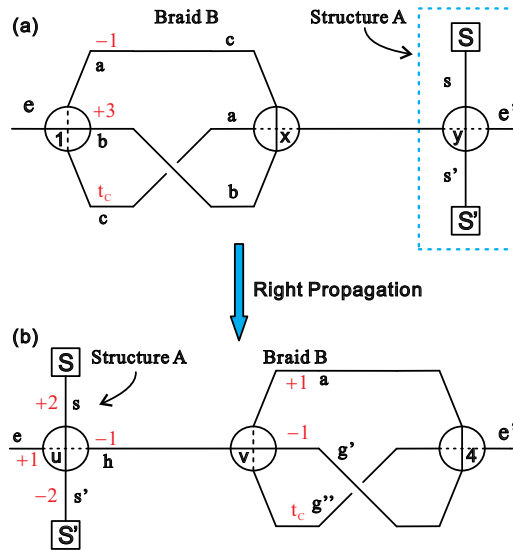
Figure C.3: Second example of right propagation. t_c is arbitrary but the total twist is unpreserved.

actively propagating braids.

C.2 Examples of propagation

We now give an example of right-propagation in Fig. C.3. The left-right mirror image of this example is an example of left-propagation. One can see that the braid in Fig. C.3 top turns into a braid with all the same structures but different set of internal twists. This nonconservation of internal twists does not rise in the unframed case. To understand the detailed procedure of a propagation, in Fig. C.4 we present all the necessary steps of an example in the unframed case for simplicity.

Since all the steps in a propagation of a braid are reversible, one can, for example, reverse the propagation in Fig. C.3 to obtain a left-propagation of the braid in Fig. C.3 bottom, which

leads to Fig. C.3 top. This is reasonable as it is in accordance with the time reversal of a particle propagation in particle physics.
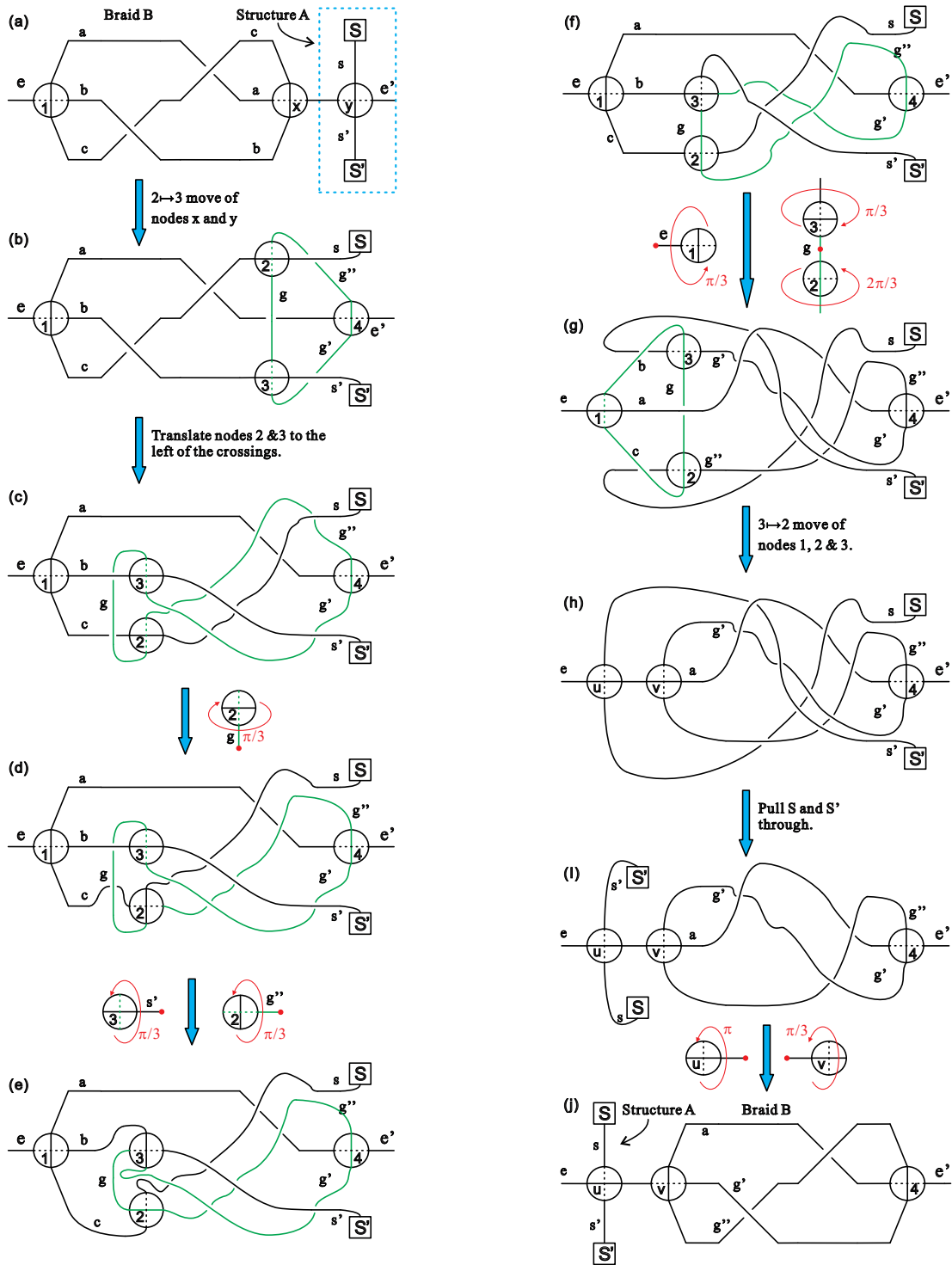
Figure C.4: The detail of a propagation in the unframed case.

Appendix D

Atomic Discrete Transformations of Braids

It is useful to represent a legal discrete transformation in an algebraic form. Nonetheless, a discrete transformation of a braid normally acts on all elements in the characterizing 8-tuple of the braid. Consequently, one can split an action of a discrete transformation to minimal sub-operations on components of the 8-tuple. These minimal sub-transformations are named **atomic discrete transformation**s, or atomic operations for short. An atomic operation can only act on one and only one type of component in the characterizing 8-tuple of a braid because otherwise it can be divided again and hence is not atomic.

Let us be precise. The characterizing 8-tuple of a braid, say $\{T_l, S_l, T_a, T_b, T_c, X, S_r, T_r\}$, consists of four types of components-to wit (T_l, T_r), the pair of external twists, (T_a, T_b, T_c), the triple of internal twists, the crossing sequence X, and the pair of end-node states, (S_l, S_r). In some cases, the external twists and internal twists can be considered together because they are transformed simultaneously in the same manner. An atomic operation is allowed to act only on one of these four types or on the set of all twists. In addition, if an atomic operation acts on an element in the 8-tuple it must also acts on all other elements of the same type in a similar way because otherwise Condition 6.1 would be violated. This will be clarified case by case. We now try to sort out all legal atomic operations.

Since twists, crossings, and end-node states can take both positive and negative values in our framework, it is natural to have discrete operations that flip their values. Three such atomic operations, namely inversions, exist.

Definition D.1. *The **inversion of the end-node states** of a braid, denoted by $\mathcal{I}_S$, is an atomic operation flipping the signs of both end-node states of the braid. That is,*

$$\mathcal{I}_S : (S_l, S_r) \mapsto (\bar{S}_l, \bar{S}_r).$$

Definition D.2. *The **inversion of the crossing sequence** X of a braid, denoted by $\mathcal{I}_X$, is an atomic operation taking each crossing in X to its inverse, namely*

$$\mathcal{I}_X : u \mapsto u^{-1}$$
$$d \mapsto d^{-1}$$
$$X = x_1 x_2 \cdots x_n \mapsto x_1^{-1} x_2^{-1} \cdots x_n^{-1}.$$

135

This operation negates the integral value of each crossing, and hence the crossing number of the braid. In addition, we clearly have $\sigma_X = \sigma_{I_X}$. The two atomic operations above must act on both end-nodes and on all crossings of X respectively. Otherwise, one cannot combine them to make a discrete transformation that is legal for arbitrary braids.

Definition D.3. *The **inversion of the twists** of a braid, denoted by $\mathcal{I}_T$, is an atomic operation that multiplies a -1 to every twist of the braid, i.e.,*

$$\mathcal{I}_T : \{T_l, T_a, T_b, T_c, T_r\} \mapsto \{-T_l, -T_a, -T_b, -T_c, -T_r\}.$$

That this atomic discrete transformation acts on all the twists, internal and external, of a braid is largely because of Condition 6.1. The reason is that if not all but one or several of its twists are flipped, to combine such an operation with other atomic operations is impossible, albeit all other operations are legal, to keep any actively-interacting braids active, since twists play a key role in the activity of a braid. X allows two more atomic operations.

Definition D.4. *The **reversion** is an atomic operation, denoted by $\mathcal{R}$, which reverses the order of the crossings in a crossing sequence X:*

$$\mathcal{R} : X = x_1 x_2 \cdots x_n \mapsto x_n x_{n-1} \cdots x_1.$$

It is also useful for calculation to define X^{-1} to be the combined result of $\mathcal{I}_X$ and $\mathcal{R}$ on X, i.e., $X^{-1} = \mathcal{I}_X \mathcal{R}(X)$. Note that for the permutation induced by X, $\sigma_X^{-1} \neq \sigma_{X^{-1}}$ in general. Nevertheless, it is quite clear that

$$\sigma_X \sigma_{\mathcal{R}(X)} = \sigma_{\mathcal{R}(X)}^{-1} \sigma_X^{-1} \equiv \mathbb{1} \tag{D.1}$$

The meaning of this equation must be understood from its action on triples of internal twists. That is,

$$(T_a, T_b, T_c) \sigma_X \sigma_{\mathcal{R}(X)} = (T_a, T_b, T_c).$$

Keeping in mind that σ_X^{-1} is a left-acting function, if we apply a σ_X^{-1} to the left of both sides of the above equation, we get

$$\sigma_X^{-1}(T_a, T_b, T_c) \sigma_X \sigma_{\mathcal{R}(X)} = \sigma_X^{-1}(T_a, T_b, T_c)$$
$$\overset{Eq.??}{\Longrightarrow} (T_a, T_b, T_c) \sigma_{\mathcal{R}(X)} = \sigma_X^{-1}(T_a, T_b, T_c). \tag{D.2}$$

Similarly, what follows is also true:

$$\sigma_{\mathcal{R}(X)}^{-1}(T_a, T_b, T_c) = (T_a, T_b, T_c) \sigma_X. \tag{D.3}$$

Definition D.5. *A **chain shift** is an atomic operation on X, denoted by $\mathcal{S}_c$, shifting every upper crossing in X to a lower one and a lower one to an upper one, with however, the crossing's chirality intact. That is,*

$$\mathcal{S}_c : \forall x_i \in X, x_i \mapsto \begin{cases} d, & \text{if } x_i = u \\ u, & \text{if } x_i = d \end{cases} , i = 1 \ldots n.$$

The above two atomic operations on X must apply to every crossing in X simultaneously because otherwise an alternating braid could be transformed into a non-alternating braid and vice versa, which certainly causes the violation of Condition 6.1 if they are part of a discrete transformation of a braid.

Actually, a braid's characterizing 8-tuple contains a hidden triple, namely the triple of internal twists on the right of the crossing sequence X, $(T_{a'}, T_{b'}, T_{c'})$. It is not explicitly included in the 8-tuple because is is related to the triple (T_a, T_b, T_c) by the induced permutation σ_X, as aforementioned. One can have a transformation that exchanges these two triples, however.

Definition D.6. *The **exchange of triples of internal twists** of a braid is an atomic operation, denoted by $\mathcal{E}_T$, doing the following:*

$$\mathcal{E}_T : (T_a, T_b, T_c) \mapsto (T_{a'}, T_{b'}, T_{c'})$$

and vice versa, where $(T_a, T_b, T_c)\sigma_X = (T_{a'}, T_{b'}, T_{c'})$.

An exchange of triples of internal twists is usually accompanied by an exchange of the two external twists of a braid.

Definition D.7. *The **exchange of external twists** of a braid, $\mathcal{E}_{T_e}$, is an atomic operation, such that*

$$\mathcal{E}_{T_e} : (T_l, T_r) \mapsto (T_r, T_l).$$

The last possible atomic discrete transformation on twists is defined as follows.

Definition D.8. *The **twist swap** is an atomic operation, denoted by $\mathcal{S}_T$, which swaps the top and bottom internal twists of a braid:*

$$\mathcal{S}_T : (T_a, T_b, T_c) \mapsto (T_c, T_b, T_a).$$

Finally, one can exchanges the two end-node states of a braid.

Definition D.9. *The **exchange of end-node states**, $\mathcal{E}_S$, is an atomic operation, such that*

$$\mathcal{E}_S : (S_l, S_r) \mapsto (S_r, S_l).$$

An important remark is that all above atomic operations in fact act on braids. For simplicity, nevertheless, we only show here their definitions and their effects on the relevant characterizing quantities of a braid. Another remark is that all atomic operations commute with each other, and hence their relative positions in a combination as a discrete transformation do not matter.

Appendix E

Examples of Braids under C, P, and T
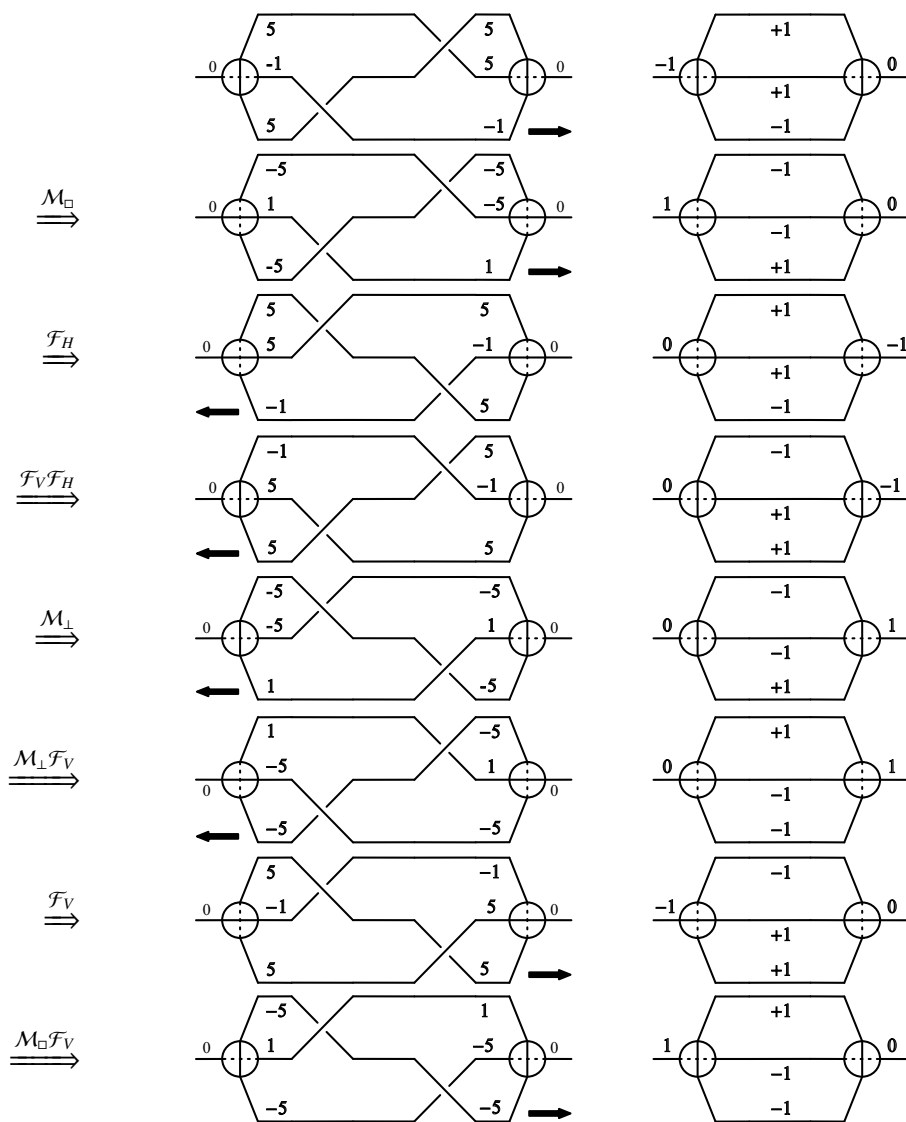
The figure above illustrates two examples of braids under the action of $G_\mathcal{D}$. The first row shows the two original braid diagrams: the left one is an actively propagating braid in zero external twist representation, and the right one is an actively interacting braid represented by a trivial braid diagram. The thick arrow on the lower left or right corner of a braid diagram indicates the propagation direction of the braid.

Bibliography

[1] W. Thompson (Lord Kelvin), Proc. Roy. Soc. Vol. 41, pp. 94–105, Edinburgh, 1987.

[2] J. A. Wheeler, Phys. Rev. 97 (1955) 511.

[3] D. Finkelstein and C. W. Misner, Annals of Physics 6 (1959) 230.

[4] D. R. Brill and J. B. Hartle, Phys. Rev. 135 (1964) B271.

[5] G. P. Perry and F. I. Cooperstock, Class. Quant. Grav. 16 (1999) 1889.

[6] H. F. Dowker and R. D. Sorkin, Class. Quant. Grav. 15 (1998) 1153, arXiv:gr-qc/9609064.

[7] F. Markopoulou and L. Smolin, Phys. Rev. D70 (2004) 124029.

[8] D. W. Kribs and F. Markopoulou, arXiv:gr-qc/0510052.

[9] F. Markopoulou, J. Phys. Conf. Ser. 67 (2007) 012019, arXiv:gr-qc/0703027.

[10] M. A. Levin and X. G. Wen, Rev. Mod. Phys. 77 (2005) 871, arXiv:cond-mat/0407140.

[11] Z. C. Gu and X. G. Wen, arXiv:gr-qc/0606100.

[12] S. Bilson-Thompson, arXiv:hep-ph/0503213.

[13] H. Harari, Phys. Lett. B86 (1979) 83.

[14] M. Shupe, Phys. Lett. B86 (1979) 87.

[15] S. Bilson-Thompson, F. Markopoulou and L. Smolin, Class. Quant. Grav. 24 (2007) 3975, arXiv:hep-th/0603022.

[16] P. Zanardi and M. Rasetti, Phys. Rev. Lett. 79 (1997) 3306, arXiv:quant-ph/9705044.

[17] J. Kempe et al., Phys. Rev. A63 (2001) 042307, arXiv:quant-ph/0004064.

[18] J. A. Holbrook, D. W. Kribs and R. Laflamme, Quant. Inf. Proc. 2 (2004) 381, arXiv:quant-ph/0402056.

[19] D. W. Kribs, R. Laflamme and D. Poulin, Phys. Rev. Lett. 94 (2005) 180501, arXiv:quant-ph/0412076.

[20] F. Markopoulou and . D.Poulin, Noiseless subsystems and the low energy limit of spin foam models.

[21] O. Dreyer, F. Markopoulou and L. Smolin, Nucl. Phys. B744 (2006) 1.

[22] L. Smolin, arXiv:hep-th/0507235.

[23] D. Benedetti, Quantum Gravity from Simplices: Analytical Investigations of Causal Dynamical Triangulations, PhD thesis, University of Utrecht, 2007.

[24] R. Sorkin, Notes for the Valdivia Summer School (2002), arXiv:gr-qc/0309009.

[25] F. Dowker, Causal Sets and the Deep Structure of Spacetime (World Scientific, 2005) , arXiv:gr-qc/0508109.

[26] G. T. Horowitz and J. Polchinski, Gauge/Gravity Duality (Cambridge University Press, 2007) , arXiv:gr-qc/0602037.

[27] M. Rozali, Adv. Sci. Lett (2009), arXiv:0809.3962.

[28] C. Rovelli, Living Rev. Rel. 11 (2008) 5.

[29] H. Sahlmann and T. Thiemann, Class. Quant. Grav. 23 (2006) 867, arXiv:gr-qc/0207030.

[30] A. Ashtekar, L. Bombelli and A. Corichi, Phys. Rev. D72 (2005) 02500, arXiv:gr-qc/0504052.

[31] B. Bahr and T. Thiemann, Class. Quant. Grav. 26 (2009) 045011, arXiv:0709.4619.

[32] T. Thiemann, (Cambridge University Press, 2007).

[33] E. Alesci and C. Rovelli, Phys. Rev. D76 (2007) 104012, arXiv:0708.0883.

[34] E. Alesci and C. Rovelli, Phys. Rev. D77 (2008) 044024, arXiv:0711.1284.

[35] C. Perini, C. Rovelli and S. Speziale, arXiv:0810.1714.

[36] E. Alesci, E. Bianchi and C. Rovelli, arXiv:0812.5018.

[37] J. D. Christensen, E. R. Livine and S. Speziale, Phys. Lett. B670 (2009) 403, arXiv:0710.0617.

[38] J. Hackett, Class. Quant. Grav. 24 (2007) 5757, arXiv:hep-th/0702198.

[39] S. Bilson-Thompson, J. Hackett and L. Kauffman, arXiv:0804.0037.

[40] Y. Wan, arXiv:0710.1312.

[41] L. Smolin and Y. Wan, Nucl. Phys. B796 (2008) 331, arXiv:0710.1548.

[42] J. Hackett and Y. Wan, to appear in Class. Quant. Grav. (2009), arXiv:0803.3203.

[43] S. He and Y. Wan, Nucl. Phys. B804 (2008), arXiv:0805.0453.

[44] S. He and Y. Wan, Nucl. Phys. B805 (2008) 1, arXiv:0805.1265.

[45] Y. Wan, Nucl. Phys. B814 (2009) 1, arXiv:0809.4464.

[46] R. Penrose, Angular monentum: an approach to combinatorial space-time (Cambridge University Press, 1971) .

[47] R. Penrose, On the nature of quantum geometry (Freeman, San Francisco, 1972) .

[48] C. Rovelli and L. Smolin, Phys. Rev. D52 (1995) 5743, arXiv:gr-qc/9505006.

[49] C. Rovelli, Quantum Gravity (Cambridge University Press, 2004).

[50] J. P. Moussouris, Quantum models as spacetime based on recoupling theory, PhD thesis, Oxford, 1983.

[51] A. Ashtekar, Lectures on Non-Perturbative Canonical Gravity (World Scientific, 1991).

[52] J. C. Baez, Gauge Fields, Knots and Gravity (World Scientific, 1994).

[53] L. Smolin, (2007), hep-th/0408048.

[54] L. Smolin, Generic Predictions of Quantum Theories of Gravity (Cambridge University Press, 2009) , arXiv:hep-th/0605052.

[55] R. Loll, Phys. Rev. Lett. 75 (1995) 3048.

[56] R. De Pietri and R. Rovelli, arXiv:gr-qc/9602023.

[57] F. Markopoulou, arXiv:gr-qc/9704013.

[58] T. Thiemann, Phys.Lett. B 380 (1996) 257, gr-qc/9606088.

[59] T. Thiemann, Class. Quant. Grav. 15 (1998) 839, gr-qc/9606089.

[60] T. Thiemann, Class. Quant. Grav. 15 (1998) 875, gr-qc/9606090.

[61] J.W. Barrett and L. Crane, J. Math. Phys. 39 (1998) 3296, gr-qc/9709028.

[62] L. Freidel and K. Krasnov, Class. Quant. Grav. 25 (2008) 125018, 0708.1595.

[63] Y. Wan and J. Hackett, under review in Phys. Rev. D. (2009), arXiv:0811.2161.

[64] J. C. Baez, Class. Quant. Grav. 15 (1998) 1827, arXiv:gr-qc/9709052.

[65] C. Rovelli, Living Rev. Rel. 1 (1998) 1, arXiv:gr-qc/9710008.

[66] J. C. Baez, Lect. Notes Phys. 543 (2000) 25, arXiv:gr-qc/9905087.

[67] U. Pachner, Ahb. Math. Sem. Univ. Hamburg 57 (1987) 69.

[68] R. De Pietri and C. Petronio, J. Math. Phys. 41 (2000) 6671, arXiv:gr-qc/0004045.

[69] F. Markopoulou and I. Prémont-Schwarz, Class. Quant. Grav. 25 (2008) 5015, arXiv:0805.3175.

[70] S. Major and L. Smolin, B473 (1996) 267, arXiv:gr-qc/9512020.

[71] R. Borissov, S. Major and L. Smolin, Class. Quant. Grav. 13 (1996) 3183, arXiv:gr-qc/9512043.

[72] S. Major, Q-Quantum Gravity, PhD thesis, The Pennsylvania State University, 1997.

[73] L. Smolin, arXiv:hep-th/0209079.

[74] P. Ehrenfest, Proceedings of the Amsterdam Academy 20 (1917) 200.

[75] J. Kogut and L. Susskind, Phys. Rev. D11 (1975) 395.

[76] W. Furmanski and A. Kowala, Nucl. Phys. B291 (1987) 594.

[77] J. Wade Cherrington, arXiv:0810.0546.

[78] J. Wade Cherrington and J. D. Christensen, Nucl. Phys. B813 (2009) 370.

[79] H. Ooguri, Mod. Phys. Lett. A7 (1992) 2799.

[80] V. Turaev and O. Viro, Topology 31 (1992) 865.

[81] L. Crane and I. B. Frenkel, J. Math. Phys. 35 (1994) 5136.

[82] T. J. Foxon, Class. Quant. Grav. 12 (1995) 951.

[83] L. Smolin, arXiv:gr-qc/9404010.

[84] H. A. Morales-Tecotl and C. Rovelli, Nucl. Phys. B451 (1995) 325.

[85] J. C. Baez and K. Krasnov, J. Math. Phys. 39 (1998) 1251, arXiv:hep-th/9703112.

[86] T. Thiemann, Class. Quant. Grav. 15 (1998) 1487, arXiv:gr-qc/9705021.

[87] L. Freidel, J. Kowalski-Glikman and A. Starodubtsev, Phys. Rev. D74 (2006) 084002, arXiv:gr-qc/0607014.

[88] M. Bojowald and R. Das, Phys. Rev. D78 (2008) 064009, arXiv:0710.5722.

[89] F. Markopoulou and L. Smolin, Phys. Rev. D58 (1998) 084032, arXiv:gr-qc/9712067.

[90] S. Bilson-Thompson et al., (2008), 0804.0037.

[91] S. Bilson-Thompson, J. Hackett and L. Kauffman, In progress .

[92] K. Reidemeister, Knot Theory (Chelsea, New York, 1948).

[93] Y. Wan, arXiv:hep-th/0512210.

[94] B. Dittrich and T. Thiemann, J. Math. Phys. 50 (2009) 012503, arXiv:0708.1721.

[95] C. Rovelli, arXiv:0708.2481.

[96] C. Rovelli and L. Smolin, Nucl. Phys. B442 (1995) 593.

[97] D. Boulatov, Mod. Phys. Lett. A 7 (1992) 1629, hep-th/9202074.

[98] L. Freidel, Int. J. Theor. Phys. 44 (2005) 1769, hep-th/0505016.

[99] D. Oriti, (2006), gr-qc/0512103.

[100] D. Oriti, arXiv:gr-qc/060703.

[101] D. Oriti, Spin Foam Models of Quantum Spacetime, PhD thesis, arXiv:gr-qc/0311066.

[102] M. Han, D. Oriti and Y. Wan.

[103] C. Kassel, Quantum GroupsGraduate Texts in Mathematics (Springer Verlag, 1995).

[104] L. Crane, Commun. Math. Phys. 135 (1991) 615.

[105] L. Kauffman.

[106] Z. C. Gu, M. A. Levin and X. G. Wen, Phys. Rev. B78 (2008) 205116, arXiv:0807.2010.

[107] Z. C. Gu et al., Phys. Rev. B79 (2009) 085118, arXiv:0809.2821.

[108] A. Hamma et al., Phys. Rev. Lett. 102 (2009) 017204, 0808.2495.

[109] E. H. Lieb and D. W. Robinson, Commun. Math. Phys. 28 (1972) 251.

[110] T. Konopka, F. Markopoulou and L. Smolin, (2006), hep-th/0611197.

[111] T. Konopka, F. Markopoulou and S. Severini, Phys. Rev. D77 (2008) 104029, 0801.0861.

144

[112] M. A. Levin and X. G. Wen, Phys. Rev. B71 (2005) 045110.

[113] Z. Wang, arXiv:cond-mat/0601285.

[114] E. C. Rowell, arXiv:0803.1258.